

Dissertation zur Erlangung des Doktorgrades der Fakultät für Chemie und Pharmazie
der Ludwig-Maximilians-Universität München



Oxidation of Modified DNA Nucleobases: Computational Study

von

Vasili Korotenko

aus

Togliatti, Russland

2023

Erklärung

Diese Dissertation wurde im Sinne von § 7 der Promotionsordnung vom 1. Januar 2019 von Herrn Prof. Dr. Hendrik Zipse betreut.

Eidesstattliche Versicherung

Diese Dissertation wurde selbständig, ohne unerlaubte Hilfe erarbeitet.
München, 15.01.2023

Vasilii Korotenko

Dissertation eingereicht am 15.02.2023

1. Gutachter: Prof. Dr. Hendrik Zipse
2. Gutachter: Prof. Dr. Christian Ochsenfeld

Mündliche Prüfung am 03.03.2023

List of Publications

F. Zott, V. Korotenko, H. Zipse «The pH-Dependence of the Hydration of 5-Formylcytosine-an Experimental and Theoretical Study» *ChemBioChem* 2021

V. Korotenko, H. Zipse « The Stability of Oxygen-Centered Radicals and its Response to Hydrogen Bonding Interactions» *J. Comp. Chem.* 2023

V. Korotenko, F. Zott, H. Zipse «The Acid-Base Equilibrium and C-H Bond Dissociation Energies of Modified Pyrimidine DNA Bases: The Influence of the Hydrate Form of 5fC» *J. Phys. Chem.* 2023

A. Kastrati, A. Kremsmair, A. S. Sunagatullina, V. Korotenko, Y. C. Guersoy, S. K. Rout, F. Lima, C. E. Brocklehurst, K. Karaghiosoff, H. Zipse, P. Knochel «Calculation-Assisted Regioselective Functionalization of the Imidazo[1,2-a]pyrazine Scaffold via Zinc and Magnesium Organometallic Intermediates» *Chem. Sci.* 2023

Acknowledgments

My deepest gratitude goes to Prof. Dr. Hendrik Zipse for the interesting and beautiful time in his research group, for support and for inspiration! Critical way of thinking, ideas, questions, comments, constructive discussions from Professor Zipse do help! I do appreciate everything that I have got from my Teacher and I will never forget. Vielen herzlichen Dank! I thank Prof. Dr. Christian Ochsenfeld for agreeing to be my Zweitgutachter!

I am extremely grateful to all present as well as former members of our research group, to all my teachers from the Mendeleev University in Moscow, and to all my friends in Germany, Russia and Ukraine! I thank Ludwig-Maximilians-Universität München and SFB1309 for financial support, and Leibniz-Rechenzentrum München for providing computational facilities.

Thank you very much to my family for the constant guidance, warmth and love!

«The laws of Nature are written
in the language of mathematics»

Galileo Galilei

«Truth is revealed in silence
to those who seek it»

Dmitri Mendeleev

«The most incomprehensible
thing about the universe
is that it is comprehensible»

Albert Einstein

«Shut up and calculate! »

David Mermin

«vi veri veniversum vivus vici»

VVVVV

Dedicated to
My Family

List of Abbreviations and Symbols

°C	Degree Celsius
‡	Transition state
Å	Ångström
a.u.	atomic units
aug-cc-pVXZ	Dunning's correlation consistent basis set (X = D (double), X = T (triple), X = Q (quadruple)) augmented (aug) with diffuse functions
B2-PLYP	double-hybrid density functional by Grimme
B3LYP	the hybrid density functional including Becke's three-parameter exchange functional and Lee-Yang-Parr's correlation functional
BSSE	basis set superposition error
calc.	calculated
CBS	complete basis set
CCSD(T)	coupled-cluster with single and double and perturbative triple excitations
DFT	density functional theory
eqn.	equation
E_{tot}	total energy
EWG	electron withdrawing group
exp.	experimental
G2	Gaussian-2 theory
G2(MP2)	cheaper variation of G2
G3	Gaussian-3 theory
G3B3	G3 with geometries and zero-point vibrational energies calculated at B3LYP/6-31G(d) level of theory
G3large	an extension of 6-311G(d,p) basis set with more flexible polarization functions (2df) and polarization of the core electrons (3d2f on Na-Ar). This basis set is used as the 'limiting HF' basis set in the G3 method.
G3MP2large	G3large basis set excluding core polarization functions.
h	Planck constant (6.62×10^{-34} J s)
HOMO	highest occupied molecular orbital
k	rate constant
k	kilo
k_B	Boltzmann constant (1.38×10^{-23} J K ⁻¹)
LUMO	lowest unoccupied molecular orbital
MAD	mean absolute deviation
MO	molecular orbital
mol	mole
MP2(FC)	second-order Møller–Plesset perturbation theory with frozen core approximation
MP2(FULL)	second-order Møller–Plesset perturbation theory; inner-core electrons are included
NBO	natural bond orbital
NMR	nuclear magnetic resonance
NPA	natural population analysis
PCM	polarizable continuum model
SMD	solvent model based on density
p <i>K</i> _a	negative lg of acid dissociation constant (<i>K</i> _a)
ppm	parts per million
R	common organic substituent or (<i>R</i>)-configured enantiomer or universal

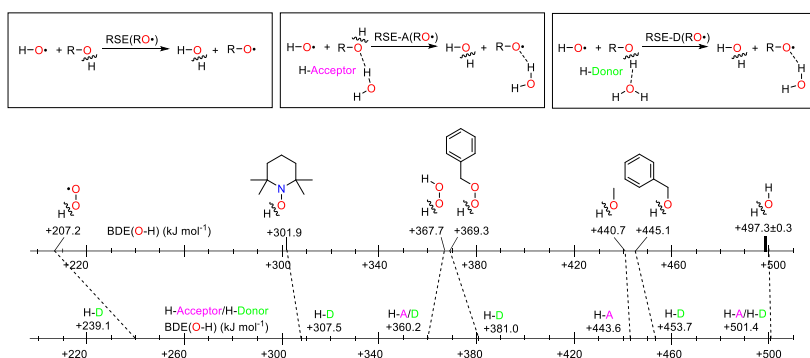
	gas constant (8.314510 J mol ⁻¹ K ⁻¹)
RHF	restricted Hartree-Fock
S	(S)-configured enantiomer or Entropy
SCF	self-consistent field
SCS-MP2	spin-component scaled second-order Møller–Plesset perturbation theory
T	Temperature
t_{1/2}	half-life time
TS	transition state
TZVP	Ahlrichs triple- ζ basis sets with one set of polarization functions
TZVPP	Ahlrichs triple- ζ basis sets with two sets of polarization functions
UAHF	United Atom for Hartree-Fock
UAKS	United atom Kohn-Sham
vs.	<i>Versus</i>
X-YZ+G(ndf,mpd)	valence-double- ζ basis set by Pople and coworkers supplemented by polarization (df,pd) and diffuse (+ or ++) functions, <i>e.g.</i> 6-31+G(2d,p)
X-YZW+G(ndf,mpd)	valence-triple- ζ basis set by Pople and coworkers supplemented by polarization (df,pd) and diffuse (+ or ++) functions, <i>e.g.</i> 6-311++G(2d,2p)
ZPE	zero-point energy
δ	chemical shift
ΔG_{298}	Gibbs free energy at 298K
ΔH_{298}	enthalpy at 298K
σ	shielding

Summary

In this work, the oxidizing properties of oxygen-centered radicals and the reducing properties of epigenetically modified DNA bases were studied. Special attention was paid to the equilibrium of the hydration reaction of 5-formylcytosine, because the corresponding hydrate product can be very easily oxidized. All this together allowed us to propose and thermodynamically evaluate the mechanism of the 1,5-Dimethylcytosine autoxidation reaction.

The Stability of Oxygen-Centered Radicals and its Response to Hydrogen Bonding Interactions

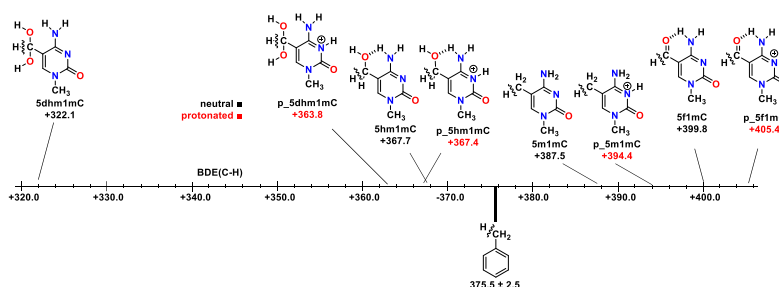
The radical stabilization energy (RSE) of various alkoxy/aryloxy/peroxy radicals, as well as TEMPO and triplet dioxygen ($^3\text{O}_2$) has been explored at a variety of theoretical levels. Good correlations between $\text{RSE}_{\text{theor}}$ and RSE_{exp} are found for hybrid DFT methods, for compound schemes such as G3B3-D3, and also for DLPNO-CCSD(T) calculations. The effects of hydrogen bonding interactions on the stability of oxygen-centered radicals have been probed



by addition of a single solvating water molecule. While this water molecule always acts as a H-bond donor to the oxygen-centered radical itself, it can act as a H-bond donor or acceptor to the respective closed-shell parent.

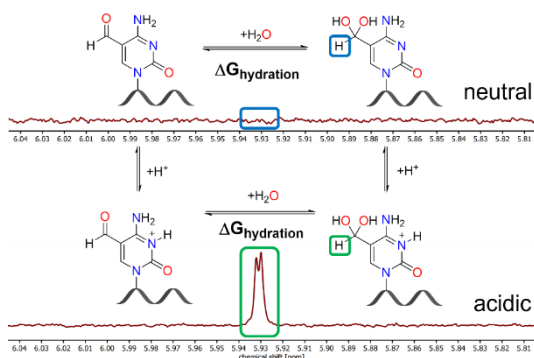
The Redox Properties of Modified DNA Bases: C-H Bond Dissociation Energies

The properties of the oxidation products of 5mC and 5mU in their protonated, neutral and deprotonated forms were studied. Radical stabilization energies (RSE) have been calculated at the SMD(H_2O)/(U)B3LYP-D3 and SMD(H_2O)/DLPNO-CCSD(T) levels of theory. In the derivatives of uracil and cytosine, among the substituents at the 5th position, the following trend in BDE values is observed: 5dhm- < 5hm- < 5m- < 5f- (where 5dhm is dihydroxymethyl, 5hm — hydroxymethyl, 5m — methyl, 5f — formyl). It has been established that the charge distribution will strongly affect the reactivity of both closed- and open-shell systems. Protonation increases the calculated BDE(C-H) values in cytosine derivatives, while deprotonation decreases them in uracil derivatives. Addition of one explicit water does not change the results notably. Attaching a complementary base increases the calculated BDE(C-H) value and does not change the observed trend.



The pH-Dependence of the Hydration of 5-Formylcytosine: An Experimental and Theoretical Study

5-Formylcytosine is an important nucleobase in epigenetic regulation, whose hydrate form has been implicated in the formation of 5-carboxycytosine as well as oligonucleotide binding events. The hydrate content of 5-formylcytosine and its uracil derivative has now been quantified using a combination of NMR and mass spectroscopic measurements as well as theoretical studies. Small amounts of hydrate can be identified for the protonated form of 5-formylcytosine and for neutral 5-formyluracil. For neutral 5-formylcytosine, however, direct detection of the hydrate was not possible due to its very low abundance. This is in full agreement with theoretical estimates.



Autoxidation of 1,5-Dimethylcytosine: Computational Study

The (aut)oxidation reaction of 1,5-dimethylcytosine (1,5-dmC) was studied using DFT and DLPNO-CCSD(T) levels of theory. The autoxidation of 5mC is unlikely to occur through initiation by triplet oxygen or through unimolecular decomposition of hydroperoxides. All endergonic bimolecular chain reactions between neutral closed-shell compounds and free radicals involve the transfer of a hydrogen atom to form a product with a higher BDE value. The thermodynamics of the presented mechanism, in principle, agrees with the experimental kinetics. We assume that the protonation ($\text{pH} < 7$) of oxidizable nucleic acids inhibits the oxidation process by increasing the BDE(C-H) values.

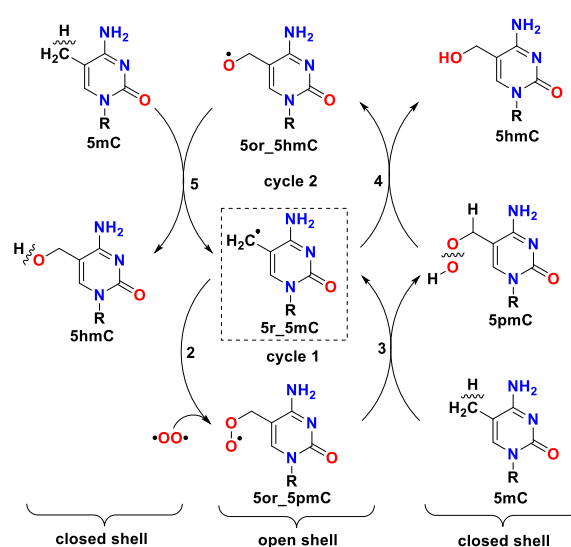


Table of Contents

1. Introduction	1
Molecular basis of epigenetics	1
DNA methylation	1
DNA damage and oxygen radical toxicity	2
2. The Stability of Oxygen-Centered Radicals and its Response to Hydrogen Bonding Interactions	4
2.1. Manuscript	5
Introduction	5
Methods	6
Methodological considerations	6
Theoretical methods	7
Conformational analysis	7
Experimental data	7
Results	8
Influence of theoretical methods	8
The stability of alkoxy radicals in the absence of intermolecular interactions	10
The effects of monosolvation	11
The effects of monosolvation on the stability of aryloxy radicals	14
The effects of monosolvation on the stability of peroxy radicals, triplet dioxygen and TEMPO	14
Acknowledgments	19
References and Notes	19
2.2. Supplementary information	23
·SI	23
1. Methodology	24
1.1. Computational methodology	25
1.2. Conformational search	27
1.3. General results	31
2. No explicit water	32
2.1. Calculated RSE values and correlation with experiment	33
2.2. Best structures and NBO charges	35
2.3. NBO charges difference - radical vs alcohol	39
2.4. RSE values and the raw data	40
2.5. G3B3-D3 wavefunction-states	98
3. One explicit water	100
3.1. Calculated RSE-A and RSE-D values	101
3.2. Enthalpies of complexation	103
3.3. Best structures	105
3.4. Selected data - H-donor and H-acceptor conformers only	115
3. The Redox Properties of Modified DNA Bases - CH Bond Dissociation Energies	150
3.1 Manuscript	151
Introduction	151
Computational details	152
Results and discussion	154
Calculated BDE(C-H) values	154
Effect of one explicit water on the calculated BDE(C-H) values	155
Effect of base pairing	156
Conclusions	157
References	157
3.2. Supplementary information	159
·SI	159
1. General results	160
1.1. Thermodynamic cycle	161
1.2. BDE scales	162
1.3. BDE values in C, U, 1mC, 1mU and their best by enthalpy structures	163
1.4. BDE values in G_C, 9mG_1mC and their best by enthalpy structures	165
1.5. BDE values in A_U, 9mA_1mU and their best by enthalpy structures	171
2. Detailed results	177
2.1. BDE values in C and 1mC	178
2.2. BDE values in U and 1mU	182

2.3. Effect of base pairing on BDE values	185
2.4. Base pairing enthalpies in G_C and 9mG_1mC	188
2.5. Base pairing enthalpies in A_U and 9mA_1mU	190
3. Boltzmann averaged data	192
3.1. Reference compound	193
3.2. C and 1mC	194
3.3. U and 1mU	197
3.4. G_C and 9mG_1mC	200
3.5. A_U and 9mA_1mU	202
4. The pH-Dependence of the Hydration of 5-Formylcytosine - an Experimental and Theoretical Study	204
4.1 Manuscript	205
Results and discussion	206
Isotopic exchange experiment	206
NMR identification and quantification	206
Theoretical determination of ΔG	207
Conclusion	209
Experimental section	209
Acknowledgements	210
Conflict of interest	210
Data availability statement	210
References	210
5. Autoxidation of 1,5-Dimethyl-Cytosine - Computational Study	213
5.1 Manuscript	214
Introduction	214
Computational details	219
Results	219
Conclusions	221
References	222
6. Appendix	223
6.1. Conformational Analysis Tools	224
Energy sorting script (ESS)	224
Centroid comparison script (CCS)	225
Full combinatoric comparison	227
Restricted combinatoric comparison based on geometry expansion	229
Restricted combinatoric comparison based on RMSD	230
Geometry expansion comparison	231
Sorted geometries comparison	232
Benchmark	233
Strategy of stochastic conformational search	236
7. CV	237

1. Introduction

Genetics (from the Greek γενητως – “generating, originating from someone”) is a branch of biology that studies genes, genetic variations and heredity in organisms.

Gene (ancient Greek γένος – genus – meaning generation or birth or gender) - in classical genetics - a hereditary factor that carries information about a certain trait or function of an organism, and which is a structural and functional unit of heredity. In this capacity, the term "gene" was introduced in 1905 by the Danish botanist, plant physiologist and geneticist Wilhelm Johannsen.¹ In nature and in living cells, a gene is presented as a sequence of nucleotides in DNA (in some viruses - RNA) that codes for the synthesis of a gene product, either RNA or protein.² Although this is not necessarily. For example, in the popular-science book by evolutionary biologist Richard Dawkins «The Selfish Gene», it is stated that any “replicator” molecule capable of self-copying or catalyzing the synthesis of its copies (autocatalysis) can be called a “gene”.³ Currently there is no universal definition of a gene that would satisfy all researchers.

Epigenetics (ancient Greek ἐπι- is a prefix denoting being on something or being placed on something) is a section of genetics. Epigenetics studies inherited changes in gene activity during cell growth and division (Epigenetic inheritance) - changes in protein synthesis caused by mechanisms that do not change the nucleotide sequence in DNA. Epigenetic changes persist in a number of mitotic divisions of somatic cells and can also be passed on to the next generations. Regulators of protein synthesis (activity of genetic sequences) - DNA methylation and demethylation, histone acetylation and deacetylation, phosphorylation and dephosphorylation of transcription factors and other intracellular mechanisms.⁴

Epigenome is a set of molecular markers that regulate the activity of genes, but do not change the primary structure of DNA.

Molecular basis of epigenetics

The molecular basis of epigenetics is complex, and it does not affect the primary structure of DNA, but changes the activity of certain genes.⁵ This explains why only the genes necessary for their specific activity are expressed in differentiated cells of a multicellular organism. A feature of epigenetic changes is that they are preserved during cell division. It is known that most epigenetic changes occur only within the lifetime of one organism. At the same time, if the change in DNA occurred in the sperm or egg, then some epigenetic manifestations can be transmitted from one generation to another.⁶

DNA methylation

The most well studied epigenetic mechanism to date is the methylation of DNA cytosine bases. Intensive studies of the role of methylation in the regulation of genetic expression, including during aging, began in the 1970s by the pioneering work of B. F. Vanyushin and G. D. Berdyshev et al. The process of DNA methylation consists in the addition of a methyl group to cytosine as part of a CpG dinucleotide at the C5 position of the cytosine ring. DNA methylation is mainly characteristic of eukaryotes. In humans, about 1% of genomic DNA is methylated. Three enzymes, called DNA methyltransferases 1, 3a and 3b (DNMT1, DNMT3a and DNMT3b), are responsible for the process of DNA methylation. (Figure 1) It is suggested that DNMT3a and DNMT3b are de novo methyltransferases that shape the DNA methylation

profile in the early stages of development, while DNMT1 maintains DNA methylation at later stages of an organism's life. The DNMT1 enzyme has a high affinity for 5-methylcytosine. When DNMT1 finds a "semi-methylated site" (a site where only one DNA strand has cytosine methylated), it methylates the cytosine on the second strand at the same site. The function of methylation is to activate/inactivate a gene. In most cases, methylation of the promoter regions of a gene results in suppression of gene activity. It has been shown that even minor changes in the degree of DNA methylation can significantly change the level of gene expression.⁷⁻¹⁰

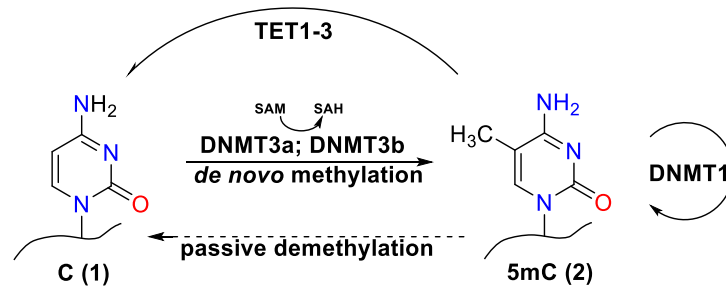


Figure 1. The mechanism of DNA methylation. DNA methylation is exerted by DNA methyltransferases (DNMTs). DNMTs at the 5'-position of cytosine residues in CpG dinucleotides transfers methyl groups from SAM (S-adenosylmethionine) to SAH (S-adenosylhomocysteine); thus, 5-methylcytosine is formed.

DNA damage and oxygen radical toxicity

DNA damage is a change in the chemical structure of DNA, such as a single-strand or double-strand break in the sugar-phosphate backbone of DNA, loss or chemical change of nitrogenous bases, cross-linking of DNA chains, cross-linking of DNA-protein. The structure of DNA in a cell is regularly disrupted due to the fact that during natural metabolism, compounds are formed that have the ability to damage DNA. These compounds include reactive oxygen species, reactive nitrogen species, reactive carbonyl groups, lipid peroxidation products, and alkylating agents.¹¹ The frequency of DNA damage caused by exposure to natural cellular metabolites reaches, according to some estimates, tens of thousands of events per day per cell.¹² DNA can also be damaged by external agents such as ionizing radiation or chemical mutagens.

DNA damage must be distinguished from mutations. DNA damages are abnormal chemical structures in DNA, while mutations are changes in the sequence of standard base pairs: A (adenosine), T (thymidine), G (guanosine), C (cytidine).

Most DNA damage can be repaired during DNA repair, but DNA repair, firstly, is not completely effective, and secondly, in some cases, DNA damage repair leads to errors and, as a result, to the occurrence of mutations. In addition, there is evidence that the process of repair of some DNA damages, namely DNA double-strand breaks, can lead to epigenetic changes in the form of methylation of the surrounding DNA and, as a result, silencing of gene expression.¹³

DNA damage can trigger programmed cell death, i.e., apoptosis.¹⁴ Uncorrected DNA damage can accumulate in non-dividing post-mitotic cells, such as brain cells or muscle cells in adult mammals, and may be the cause of aging.¹⁵ In dividing cells, such as intestinal epithelial cells or hematopoietic bone marrow cells, errors in DNA damage repair can lead to mutations that are passed on to subsequent generations of cells, and some of these mutations may have oncogenic potential.

In aerobic life forms, the energy necessary for the implementation of biological functions is produced by mitochondria along the electron transport chain. Reactive oxygen species (ROS), which have the potential to harm cells, are produced along with energy. ROS can damage lipids, DNA, RNA, and proteins, which in theory contribute to physiological changes during aging.

ROS occur as a normal product of cellular metabolism. Among them, the main instigator of oxidative damage is hydrogen peroxide (H₂O₂), which arises from superoxide secreted by mitochondria. Catalase and superoxide dismutase mitigate the damaging effects of hydrogen peroxide and superoxide, respectively, by converting these substances into oxygen and hydrogen peroxide (which later turns into water) - that is, they produce harmless molecules. However, these transformations are not 100% effective, and peroxide residues remain in the cells. Although ROS are a product of the normal functioning of cells, their excess leads to detrimental consequences.^{16,17}

References

- [1] W. Johannsen. *Arvelighedslærens elementer*, **1905**.
- [2] H. Pearson, *Nature* **2006**, *441*, 398.
- [3] R. Dawkins, N. Davis. *The selfish gene*; Macat Library, **2017**.
- [4] C. Dupont, D. R. Armant, C. A. Brenner. *Seminars in reproductive medicine*, 2009, pp 351.
- [5] A. Watanabe, Y. Yamada, S. Yamanaka, *Philos. Trans. R. Soc. Lond., B, Biol. Sci.* **2013**, *368*, 20120292.
- [6] V. L. Chandler, *Cell* **2007**, *128*, 641.
- [7] B. A. Buck-Koehntop, P.-A. Defossez, *Epigenetics* **2013**, *8*, 131.
- [8] S. Seisenberger, J. R. Peat, T. A. Hore, F. Santos, W. Dean, W. Reik, *Philos. Trans. R. Soc. Lond., B, Biol. Sci.* **2013**, *368*, 20110330.
- [9] G. Kelsey, R. Feil, *Philos. Trans. R. Soc. Lond., B, Biol. Sci.* **2013**, *368*, 20110336.
- [10] M. Ciechomska, L. Roszkowski, W. Maslinski, *Cells* **2019**, *8*, 953.
- [11] R. De Bont, N. Van Larebeke, *Mutagenesis* **2004**, *19*, 169.
- [12] C. Bernstein, A. Prasad, V. Nfonam, H. Bernstein, *Prof. Clark Chen (Ed.), InTech* **2013**.
- [13] H. M. O'Hagan, H. P. Mohammad, S. B. Baylin, *PLoS Genet.* **2008**, *4*, e1000155.
- [14] W. P. Roos, B. Kaina, *Cancer Lett.* **2013**, *332*, 237.
- [15] A. A. Freitas, J. P. De Magalhães, *Mutat. Res. - Rev. Mutat. Res.* **2011**, *728*, 12.
- [16] L. Packer. *Understanding the Process of Aging: The Roles of Mitochondria: Free Radicals, and Antioxidants*; CRC Press, **1999**.
- [17] J. A. Imlay, S. Linn, *Science* **1988**, *240*, 1302.

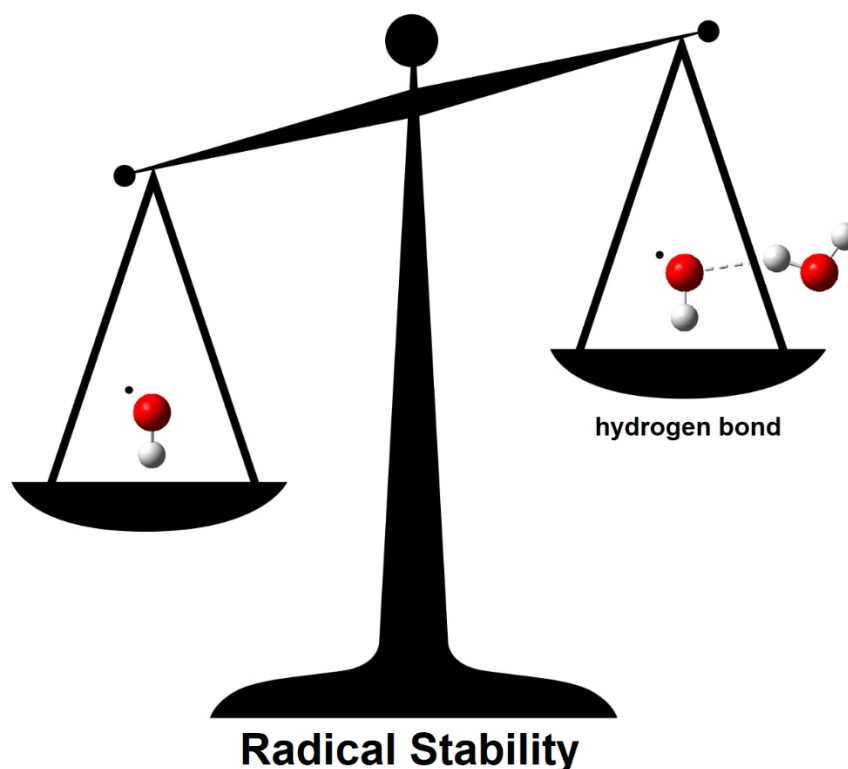
2. The Stability of Oxygen-Centered Radicals and its Response to Hydrogen Bonding Interactions

Vasily Korotenko and Hendrik Zipse*

Submitted manuscript.

Author contributions: The project was conceived by V.K. and H.Z. The computational study was performed by V.K. The manuscript was written by V.K.

The radical stabilization energy (RSE) of various alkoxy/aryloxy/peroxy radicals, as well as TEMPO and triplet dioxygen ($^3\text{O}_2$) has been explored at a variety of theoretical levels. Good correlations between $\text{RSE}_{\text{theor}}$ and RSE_{exp} are found for hybrid DFT methods, for compound schemes such as G3B3-D3, and also for DLPNO-CCSD(T) calculations. The effects of hydrogen bonding interactions on the stability of oxygen-centered radicals have been probed by addition of a single solvating water molecule. While this water molecule always acts as a H-bond donor to the oxygen-centered radical itself, it can act as a H-bond donor or acceptor to the respective closed-shell parent.



The Stability of Oxygen-Centered Radicals and its Response to Hydrogen Bonding Interactions

Vasily Korotenko¹, Hendrik Zipse²

Correspondence to: Hendrik Zipse (E-mail: zipse@cup.uni-muenchen.de)

^{1,2} Department of Chemistry, LMU München, Butenandtstrasse 5-13, 81377 München, Germany

ABSTRACT

The stability of various alkoxy/aryloxy/peroxy radicals, as well as TEMPO and triplet dioxygen (³O₂) has been explored at a variety of theoretical levels. Good correlations between RSE_{theor} and RSE_{exp} are found for hybrid DFT methods, for compound schemes such as G3B3-D3, and also for DLPNO-CCSD(T) calculations. The effects of hydrogen bonding interactions on the stability of oxygen-centered radicals have been probed by addition of a single solvating water molecule. While this water molecule always acts as a H-bond donor to the oxygen-centered radical itself, it can act as a H-bond donor or acceptor to the respective closed-shell parent.

KEYWORDS

radicals, thermodynamic stability, isodesmic equations, *ab initio* calculations, hydrogen abstraction, hydrogen bonding

Introduction

Oxygen-centered radicals play a central role in radical reactions as diverse as the autoxidation of lipids and its inhibition through antioxidants, the cumol hydroperoxide process for the production of acetone and phenol, or the reduction of ribonucleotides by class I ribonucleotide reductase.¹⁻⁸ The radicals involved in these reactions vary largely in terms of their kinetic and thermodynamic properties (Figure 1). On the high-activity end of the scale we may find the hydroxyl radical ($\bullet\text{OH}$, **1**), whose often very short lifetime in solution-phase experiments is tightly connected to its low thermochemical stability. Oxygen-centered radicals of intermediate stability are those derived from phenoxy radical (**2**), either in the context of the antioxidative activity of phenols such as α -tocopherol (**3**), or in enzyme-mediated reactions involving tyrosyl radicals (**4**).⁹⁻¹¹

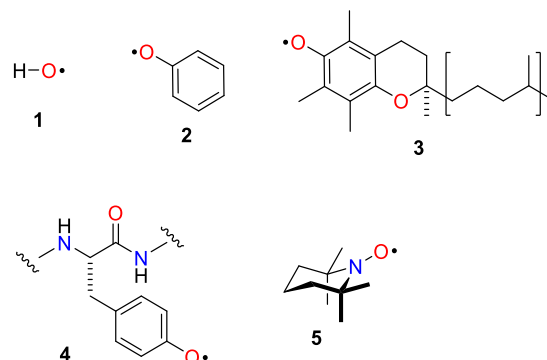
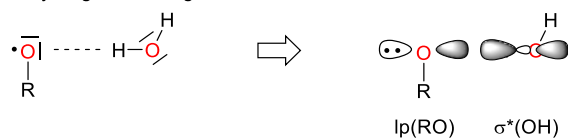


FIGURE 1 O-Centered radicals involved in common radical reactions: hydroxyl radical (**1**), phenoxy radical (**2**), α -tocopheryl radical (**3**), tyrosyl radical (**4**), and TEMPO radical (**5**).

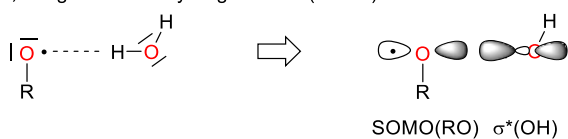
On the low-activity end we can find nitroxyl radicals such as (2,2,6,6-tetramethylpiperidin-1-yl)oxy radical (TEMPO, **5**), whose kinetic and thermochemical stability is high enough to allow

bottling and shipping at ambient temperature. The electronic structure of oxygen-centered radicals is typically characterized by the presence of two lone pairs at the spin-carrying oxygen atom as shown in Figure 2. Interactions between oxygen-centered radicals and their condensed-phase environments depends, among others, on specific interactions of these lone pair orbitals and the unpaired spin with suitable interaction partners. Three specific types of interaction have to be anticipated based on earlier precedent as shown in Figure 2 for water as a molecular probe. These include: (a) hydrogen bonding interactions, where one of the RO• radical lone pair orbitals acts as the hydrogen bond acceptor; (b) single-electron hydrogen bond (SEHB) interactions involving the RO• radical SOMO and the $\sigma^*(\text{OH})$ orbital of water; and (c) 2c3e "hemibond" interactions¹² between the RO• radical SOMO and one of the water lone pair orbitals. In the following we analyze the impact of these interactions on the thermodynamic stability of oxygen-centered radicals RO• as a function of the substituent R.

(a) Hydrogen bonding interactions



(b) Single-electron hydrogen bond (SEHB) interactions



(c) „Hemibond“ (2c3e) interactions

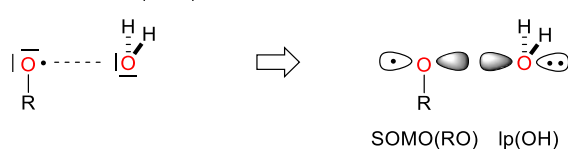


FIGURE 2 Possible interaction types between oxygen-centered radicals RO• and a water molecule.

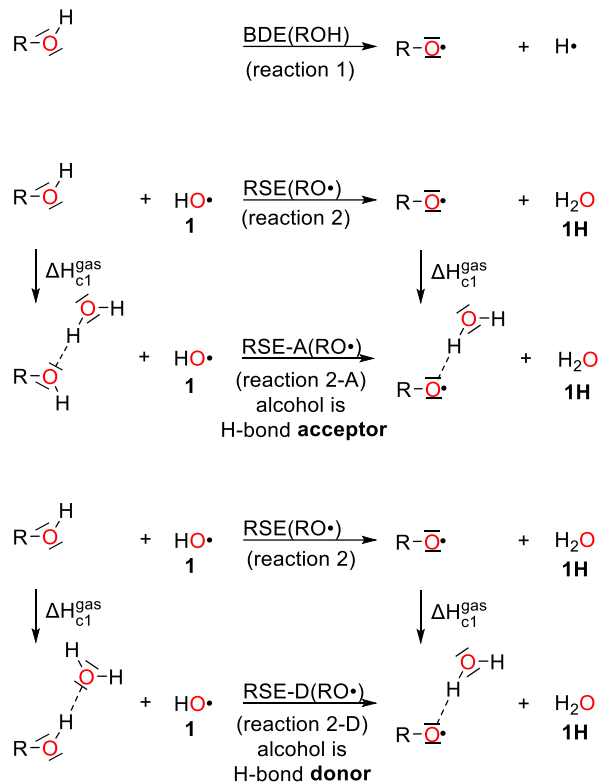


FIGURE 3 Interaction of an explicit water molecule with oxygen-centered radicals RO• and the respective parent alcohols ROH.

Methods

Methodological considerations

The thermodynamic stability of O-centered radicals can be characterized by the O-H bond dissociation energy (BDE(OH)) of the respective alcohols as defined in reaction 1 in Figure 3, larger values indicating thermochemically less stable radicals. Variations of BDE(OH) values can conveniently be expressed relative to a common reference system such as hydroxyl radical (**1**) through the formal hydrogen atom transfer reaction shown in reaction 2 in Figure 3. The reaction enthalpy at 298.15 K calculated for this isodesmic hydrogen transfer reaction is sometimes referred to as the radical stabilization energy (RSE) of radical RO• as it reflects, to a certain extent, the influence of substituent R on the properties of radical RO•. Combination of these RSE values with the experimentally determined BDE value of water¹³ of BDE(OH, **1H**)

= +497.3 ± 0.1 kJ mol⁻¹ as expressed in eq. 1 provides an indirect and accurate way for the determination of BDE(OH) values in alcohols ROH.¹⁴⁻²⁰

$$\text{BDE}(\text{RO-H}) = \text{RSE}(\text{RO} \bullet) + \text{BDE}_{\text{exp}}(\text{HO-H}) \quad (\text{eq. 1})$$

$$\begin{aligned} \Delta\text{RSE} &= \text{RSE-A/D}(\text{RO} \bullet) - \text{RSE}(\text{RO} \bullet) = \\ &= \Delta\text{H}_{\text{c1}}^{\text{gas}}(\text{RO} \bullet) - \Delta\text{H}_{\text{c1}}^{\text{gas}}(\text{ROH}) \quad (\text{eq. 2}) \end{aligned}$$

$$\text{BDE-A/D}(\text{RO-H}) = \text{BDE}(\text{RO-H}) + \Delta\text{RSE} \quad (\text{eq. 3})$$

Aside from serving as a general indicator of radical stability, the BDE(OH) values also provide the basis for assessing the thermodynamics of hydrogen transfer reactions between O-centered radicals and hydrogen atom donors. The experimental determination of BDE(OH) values has only in selected cases been possible with "chemical accuracy", which is often taken to be at the 1 kcal mol⁻¹ (or 4 kJ mol⁻¹) limit. In order to provide accurate values for a broader range of systems, efforts have in recent years been undertaken to identify theoretical methods for the accurate calculation of bond dissociation energies.

Theoretical methods

The theoretical methods used in these types of studies range from DFT-based methods (for extended systems),²¹⁻²⁴ wavefunction-based methods involving perturbation theory such as the ROMP2(FC)/6-311+G(3df,2p) approach,^{12,18} double-hybrid functionals such as B2-PLYP,^{25,26} all the way to highly elaborate compound schemes such as G3(MP2)-RAD,^{14-20,27-32} G3B3,^{33,34} CBS-QB3,³⁵ or the Weizmann-family³⁶ of methods. More recently the DLPNO-CCSD(T) method for open-shell systems has emerged as an additional tool for the accurate description of larger radicals, in particular when combined with the complete basis set (CBS) extrapolation scheme.³⁷⁻³⁹ The underlying geometries employed in the above-mentioned theoretical approaches are often optimized using hybrid DFT methods. The compound G3B3 method, for example, employs geometries optimized at the (U)B3LYP/6-31G(d)⁴⁰⁻⁴² level of theory.

Particularly for larger molecular systems, the geometries optimized with or without corrective terms for London dispersion interactions (e.g. the D3 corrections parameterized by Grimme et al.)^{43,44} may differ considerably. Preliminary calculations of selected RO• radicals furthermore indicated that consistent structural data require a basis set at least as large as 6-31+G(d,p) (see SI for further details). The subsequent results are therefore based on geometries optimized at the (U)B3LYP-D3/6-31+G(d,p) level of theory.

Conformational analysis

The initial structures of molecular complexes were generated randomly using the «kick» algorithm.^{45,46} Geometry optimizations have been performed using the (U)B3LYP hybrid functional, either alone or complemented by the D3 dispersion correction.⁴⁴ The 6-31G(d) and 6-31+G(d,p) all electron basis sets have been used for all elements. Frequency calculations have been carried out to verify that the optimized structures are true minima. Thermochemical corrections to H^{gas} and G^{gas} at 298.15 K were calculated using the rigid rotor/harmonic oscillator model.⁴⁷ The symbol (^{gas}) denotes a gas phase standard state of 1 atm. The individuality of the found conformers was confirmed using an energy criterion ΔE_{tot} > 10⁻⁷ Hartree⁴⁸ and comparing geometries by distances between each atom and the centroid point.⁴⁹ A detailed description of both algorithms can be found in the SI.

Experimental data

Table 1 contains RSE and BDE(OH) values for systems selected such that they represent the three most relevant classes of substituents in O-centered radicals: (a) radicals with alkyl substituents attached to the spin-bearing oxygen atom such as methoxy radical (**6**); (b) radicals with π-systems attached to the radical center as is the case in phenoxy radical (**2**) or formyloxy radical (**20**); and (c) radicals with lone-pair donors attached to the radical oxygen as is found in peroxy radicals or in nitroxyl radicals such as TEMPO (**5**). The last column in Table 1 collects

experimentally determined BDE(OH) values together with the respective RSE(RO•) values obtained according to reaction 2 in Figure 3. In several cases data from different experimental sources have been considered, and the currently most accurate recommended value is labeled in bold. Wherever available, data from the *Active Thermochemical Tables* (ATcT) have been employed.¹³ The O-H bond enthalpy in water of BDE(OH) = 497.3±0.3 kJ mol⁻¹ represents the upper bond enthalpy limit and thus an important reference for all other systems considered here.^{13,51} For the O-H bond enthalpy in *t*-BuOH (**7H**) photoelectron spectroscopy measurements⁵⁰ yield a value of 444.9 kJ mol⁻¹, while thermochemical measurements yield a slightly larger value of 446.8 kJ mol⁻¹.⁵¹ The BDE(OH) for methanol (**6H**) has an ATcT value of 440.4 kJ mol⁻¹, which is closely matched by data from photoelectron spectroscopy.⁵⁰ The O-H bond enthalpy in ethanol (**9H**) at BDE(OH) = 440.4±0.5 kJ mol⁻¹ is practically identical to that in methanol, which implies only a minor effect through the different alkyl substituents.^{13,53} Stabilizing effects through further elongations in the alkyl chain remain moderate as can be seen from BDE(OH) = 432.3 kJ mol⁻¹ for *n*-butanol (**11H**),⁵² as are the effects of benzylic substituents as in benzyl alcohol (**8H**) with BDE(OH) = 442.7 kJ mol⁻¹⁵³ or in cumyl alcohol PhC(CH₃)₂OH (**10H**) with BDE(OH) = 438.2 kJ mol⁻¹.⁵⁴ The most accurate gas phase measurements for phenol (**2H**) have been reported by Ashfold and coworkers at 0 K.⁵⁵ As stated previously,¹⁵ the addition of thermal corrections (0.6 kJ mol⁻¹) to the experimentally determined RSE values yields the most accurate values of BDE(OH) = 365.0 kJ mol⁻¹ for phenol (**2H**) and BDE(OH) = 356.6 kJ mol⁻¹ for *para*-methylphenol (**14H**). Combination of the value for **2H** with known substituent effects^{56,57} we obtain reference BDE(OH) values for substituted phenols X-PhOH with X = NH₂ (324±13) and X = NO₂ (390±8). The O-H bond energies in hydroperoxides are quite similar to those in phenols, the value for the parent hydrogen peroxide (H₂O₂, **13H**) amounting to BDE(OH) = 365.7±0.2 kJ mol⁻¹ and

that for methylhydroperoxide **15H** being only slightly lower at BDE(OH) = 358.4±0.7 kJ mol⁻¹. This latter value is closely similar to a recent comparative analysis of alkylhydroperoxides,⁵⁸ but somewhat lower than earlier estimates based on gas phase kinetics measurements.^{59,60} The currently available BDE(OH) data for PhCH₂OOH (**16H**) of BDE(OH) = 365 kJ mol⁻¹ and *t*-BuOOH (**17H**) of BDE(OH) = 352.3±8.8 kJ mol⁻¹ are somewhat less accurate and have also seen less attention than most other systems in Table 1.^{60,61} For TEMPO-H (**5H**) we adopt the currently recommended BDE(OH) value in heptane solution of 293.2 kJ mol⁻¹.^{62,63} Triplet dioxygen (³O₂, **19**) is also included here as an important oxygen-based radical, despite the fact that it carries a triplet ground state and thus differs from all other systems in Table 1. It is nevertheless included here due to its frequent involvement in oxidation reactions and its debatable role in direct hydrogen atom abstractions from hydrocarbon substrates. The rather low value of BDE(OH) = 205.8 kJ mol⁻¹ in radical HOO• (**13**) already implies that direct hydrogen atom abstractions from hydrocarbon substrates by ³O₂ are thermochemically rather unfavorable.

Results

Influence of theoretical methods

Basis set effects were studied for (U)B2PLYP and DLPNO-CCSD(T) calculations using (U)B3LYP-D3/6-31+G(d,p) optimized geometries. The two-point (cc-pVTZ and cc-pVQZ) extrapolation strategy was employed for DLPNO-CCSD(T) calculations to estimate the complete basis set limit.^{38,64} In general, changing the basis set from cc-pVTZ to cc-pVQZ in case of both (U)B2PLYP and DLPNO-CCSD(T) makes the radical stabilization energy as defined by reaction 2 in Figure 3 slightly more negative and also leads to a small improvement of the correlation coefficient with experimental values *R*² (Table 1). The rather moderate magnitude of these effects suggests that calculations with basis sets of

TABLE 1 RSE(RO•) values for selected O-centered radicals (in kJ mol⁻¹) calculated at various levels of theory together with available experimental data (and the associated BDE(O-H) data) ordered by experimental BDE(RO•) values.

Radical	RSE(RO•)								BDE(RO•)	
	DFT ^[a]	(U)B2PLYP ^[b,c]		DLPNO-CCSD(T) ^[b,c]			G3B3-D3		exp.	exp.
		TZ	QZ	TZ	QZ	CBS	^[b]	^[d]		
HO• (1)	0.0	0.0	0.0	0.0	0.0	0.0	0.0	0.0	0.0	+497.3±0.1 ^[13] +497.1±0.3 ^[65]
HC(O)O• (20)	-35.2	-40.0	-43.3	-14.3	-18.6	-20.9	-30.2	-27.6	-28.4±0.6	+468.89±0.56 ^[13]
<i>t</i> -Bu-O• (7)	-57.7	-49.9	-52.3	-42.8	-45.4	-46.7	-47.2	-47.7	-52.4±2.8	+444.9±2.8 ^[50,66] +446.8±4.2 ^[51]
PhCH ₂ O• (8)	-65.0	-57.3	-59.2	-48.4	-50.8	-52.2	-54.8	-55.5	-54.6±8.8	+442.7±8.8 ^[53,66]
CH ₃ O• (6)	-65.3	-58.6	-60.3	-53.4	-55.5	-56.6	-55.3	-55.8	-56.9±0.3	+440.4±0.3 ^[13] +440.2±3.0 ^[51,66] +437.7±2.8 ^[50]
CH ₃ CH ₂ O• (9)	-66.6	-58.7	-60.4	-52.5	-54.6	-55.7	-57.5	-54.8	-56.9±0.5	+440.4±0.5 ^[13] +441.0±5.9 ^[51, 66] +438.1±3.3 ^[50]
PhC(CH ₃) ₂ O• (10)	-58.1	-50.5	-53.2	-40.9	-43.7	-45.1	-45.9	-47.8	-59.1±1.0	+438.2±1.0 ^[54, 66]
<i>n</i> -Bu-O• (11)	-66.8	-59.1	-61.1	-52.2	-54.5	-55.7	-52.9	-55.3	-65.0	+432.3 ^[52]
<i>p</i> -nitro-PhO• (12)	-114.5	-97.7	-100.8	-100.8	-104.3	-106.1	-113.4	-106.0	-107±8	+390±8 ^[56, 15] +396±8 ^[56]
HOO• (13)	-134.4	-133.7	-135.8	-124.9	-128.1	-129.6	-129.2	-129.6	-131.6±0.2	+365.7±0.2 ^[13]
PhO• (2)	-132.9	-114.2	-117.7	-116.3	-121.0	-123.6	-121.1	-121.6	-132.3±0.5	+365±0.5 ^[15] +371.3±2.3 ^[56] +367.1±0.9 ^[13] +362.7±3.0 ^[67]
PhCH ₂ -OO• (16)	-139.0	-136.4	-140.4	-122.1	-125.9	-128.0	-126.5	-131.5	-132.3	+365 ^[61]
CH ₃ OO• (15)	-141.8	-139.4	-142.4	-128.9	-132.8	-134.7	-133.0	-135.8	-138.9±0.7	+358.4±0.7 ^[13] +370.3±2.1 ^[59, 66] +367.3±4 ^[60] +357±5 ^[58]
<i>p</i> -methyl-PhO• (14)	-141.3	-122.5	-126.3	-122.5	-127.6	-130.5	-128.8	-129.3	-140.7±0.6	+356.6±0.6 ^[15] +363±4 ^[67]
<i>t</i> -Bu-OO• (17)	-148.5	-145.6	-149.1	-132.7	-136.8	-138.7	-140.8	-141.5	-145±8.8	+352.3±8.8 ^[60, 66]
<i>p</i> -amino-PhO• (18)	-168.8	-152.2	-156.1	-143.9	-149.3	-152.4	-153.3	-153.8	-173±13	+324±13 ^[67, 15] +331±13 ^[67]
TEMPO (5)	-208.0	-206.4	-210.9	-185.1	-191.7	-195.4	-198.0	-198.4	-204.1±0.4	+293.2±0.4 ^[62] +291.2 ^[63]
³ O ₂ (19)	-274.6	-291.7	-294.4	-283.8	-288.0	-290.1	-289.1	-289.2	-291.5±0.2	+205.8±0.27 ^[13]
MSE	-2.8	3.3	0.4	12.1	8.3	6.4	5.4	5.2		
MUE	5.5	6.6	7.0	12.1	8.3	6.4	5.4	5.3		
R ²	0.9956	0.9823	0.9830	0.9906	0.9926	0.9936	0.9938	0.9935		

[a] "DFT" - (U)B3LYP-D3/6-31+G(d,p); [b] Using (U)B3LYP-D3/6-31+G(d,p) optimized geometries; [c] "TZ, QZ" - cc-pVTZ, cc-pVQZ; [d] Using (U)B3LYP-D3/6-31G(d) optimized geometries.

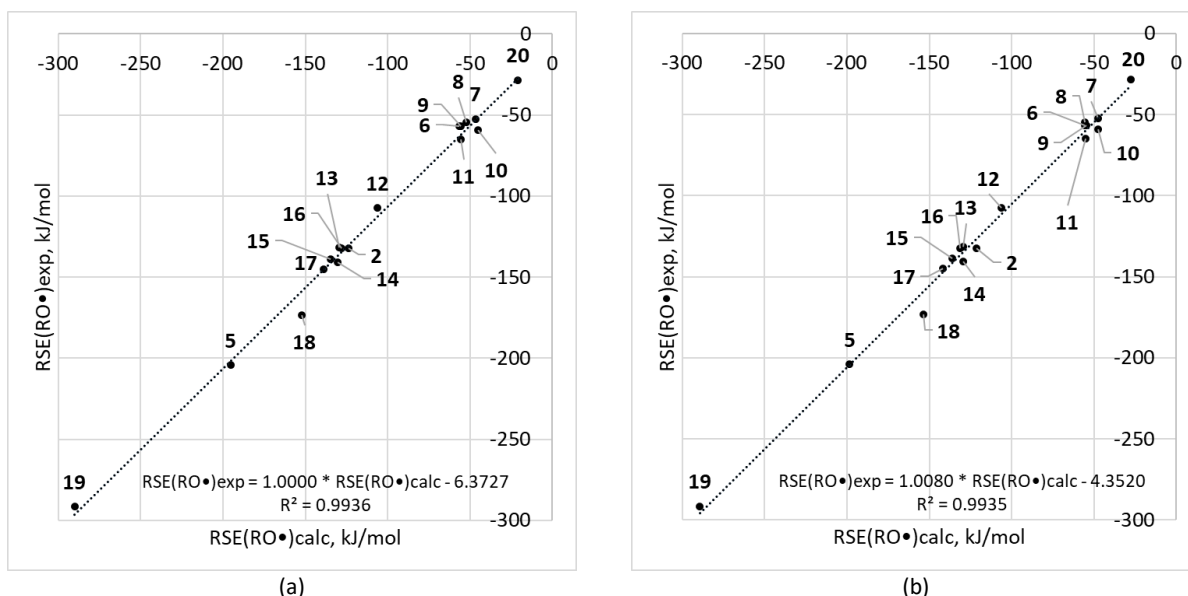


FIGURE 4 Correlation plots for (a) DLPNO-CCSD(T)/CBS//(U)B3LYP-D3/6-31+G(d,p) and (b) G3B3-D3.

quadruple zeta quality may only be required in exceptional cases. In Table 1 it can be seen that DLPNO-CCSD(T)/CBS and G3B3-D3 results are quite similar for most systems, the largest difference (-20.9 vs. -27.7 kJ/mol) being that for formyloxy radical (**20**). Correlations for the RSE values calculated at G3B3-D3 and DLPNO-CCSD(T)/CBS levels with the corresponding experimental data is shown in Figure 4. Both have positive mean signed errors (MSE) and mean unsigned errors (MUE) of almost identical magnitude, which implies that the calculated radical stabilities are systematically smaller than experimental values. Perusal of Table 1 indicates this to result mainly from the values for the four phenoxy radicals **2**, **12**, **14**, and **18**. The economical (U)B3LYP-D3/6-31+G(d,p) method employed for geometry optimization shows, in comparison, an impressively good correlation.

The stability of alkoxy radicals in the absence of intermolecular interactions

The stabilities of oxygen-centered radicals as collected in Table 1 and shown graphically in Figure 4 depend significantly more on the attached substituents than carbon- or nitrogen-centered radicals. The underlying mechanisms for these substituent effects have been

discussed earlier and will therefore be reiterated here only briefly.^{68,69} Alkyl substituents are moderately stabilizing with RSE values around -62 ± 5 kJ mol⁻¹ through hyperconjugative interactions between the oxygen-based SOMO and the neighboring C-C and C-H bonds. The latter appear somewhat more effective as can be seen from the stability difference between the methoxy and *tert*-butoxy radicals (**6** vs. **7**). The stability of aryl- and acyloxy radicals varies widely as a function of the structure of the attached π -system. On the low stability side this includes the formyloxy radical (**20**) with $RSE(\mathbf{20}) = -28.4$ kJ mol⁻¹, whose delicate electronic structure has been noted in earlier theoretical studies.⁷⁰ The phenoxy radical **2** is, in comparison, much more stable at $RSE(\mathbf{2}) = -132.3$ kJ mol⁻¹, and displays an impressive stability variation of more than 50 kJ mol⁻¹ between its 4-nitro- and 4-amino-substituted variants (**12** vs. **18**). Peroxy radicals are similarly stable as phenoxy radical **2**. For the alkyl-substituted cases **15**, **16**, and **17** included here we note that their stability is only moderately higher as compared to the parent HOO• radical at $RSE(\mathbf{13}) = -131.6$ kJ mol⁻¹. Nitroxyl radicals such as TEMPO are, in comparison, significantly more stable at $RSE(\mathbf{5}) = -204$ kJ mol⁻¹, which illustrates the superior

ability of amino- as compared to alkoxy-groups to act as electron donors. The even higher stability of triplet dioxygen at $RSE(\mathbf{19}) = -291.5 \text{ kJ mol}^{-1}$ simply documents the unique electronic structure of this system,⁷¹ that cannot (and should not) be compared directly with all other O-centered (doublet state) radicals in this study.

The effects of monosolvation

The principal interaction modes of explicit water molecules with oxygen-centered radicals $RO\bullet$ have already been detailed in Figure 2. When assessing the impact of these interactions on radical stability as defined earlier in reaction 2 in Figure 3, we also have to decide on the interaction of water with the parent alcohols. One obvious interaction scheme is shown in reaction 2-A in Figure 3, where the parent alcohols act as hydrogen-bond acceptors in very much the same way as the oxygen-centered radicals. Radical stabilization energies calculated with these interaction types will be designated "RSE-A" and reflect, in addition to the influences of substituent R, the change in hydrogen bond strength to the alcohol oxygen on radical formation. Alternatively, the parent alcohols may also act as a hydrogen-bond donor to the water molecule probe, while the oxygen-centered radical remains to act as a hydrogen-bond acceptor as expressed in reaction 2-D in Figure 3. Radical stabilization energies calculated according to this latter definition will be designated "RSE-D". In the following we will first analyze how RSE-A values differ from the gas phase values presented before in Table 1.

The smallest system, where the influence of water complexation can be explored, is the $H_2O/HO\bullet$ radical reference system itself (that is, $R = H$ in Figure 2). This involves the water dimer on the reactant side, whose hydrogen-bound structure has been studied in large detail experimentally as well as theoretically.⁷²⁻⁷⁴ Whether or not minima other than the structure shown in Figure 5 exist on the potential energy surface depends largely on the theoretical method.⁷⁵ At the B3LYP-D3/6-31+G(d,p) level employed here only one true minimum can be

located on the PES. This minimum is characterized by a hydrogen bonding distance of 191.2 pm. Three true minima are found for the complex of hydroxyl radical **1** with water at the UB3LYP-D3/6-31+G(d,p) level.⁷⁶ In the energetically most favorable structure the $HO\bullet$ radical acts as hydrogen bond donor, while the roles are reversed in the second-best structure **1a_2** located 8.0 kJ mol^{-1} higher in energy (DLPNO-CCSD(T)/CBS results).⁷⁷⁻⁸¹ This latter structure corresponds to the hydrogen bonding situation shown in Figure 2a and is characterized by a hydrogen bonding distance of 203.2 pm. The energetically least stable minimum corresponds to a "hemibond" structure **1a_3** best described by the orbital interaction described before in Figure 2c and is located 13.0 kJ mol^{-1} higher. Concentrating on water complex **1a_2** with the hydrogen-bonding pattern shown in Figure 2a, a radical stabilization energy of $RSE-A(\mathbf{1a}) = +4.1 \text{ kJ mol}^{-1}$ is obtained at the DLPNO-CCSD(T)/CBS level of theory. By definition, the corresponding RSE value in the absence of hydrogen bonding interactions with water is 0.0 kJ mol^{-1} , and we may thus conclude that hydrogen-bond formation to the oxygen atom of the $HO\bullet$ radical is destabilizing by $+4.1 \text{ kJ mol}^{-1}$. From the geometrical data and the ESP plots for the water complexes **1Ha** and **1a_2**, as well as the SD plot for **1a_2** we can see that the underlying hydrogen bonding interactions correspond to those expected from the principal interaction types presented in Figure 2.

Analysis of the energetically best water complexes of all other radicals studied here shows that the hydrogen-bonding pattern described by Figure 2a is present in all of these. Interactions of types (b) and (c) can also be identified for some of the radicals, but these are systematically less stable and thus have a comparatively low Boltzmann population with little impact on the calculated RSE values. Further structural analysis of the water complexes of O-radicals and their parent alcohols indicates that more than one contact typically exists between the complexation partners. These can be $C-H\cdots O_w$,^{80,82,83} $Ar\cdots H_w$

^{80,84} and other weak «secondary» intermolecular interactions,⁸⁵ or a second hydrogen bond (as in the case of peroxy radicals and the corresponding peroxide parents, see below). These additional interactions are stabilizing in nature and thus influence both the water/substrate complexation energies and their structural characteristics. As a consequence, the water/substrate complexation energies show only poor correlations with single structural parameters such as hydrogen bond distances.

The molecular orbitals of phenoxy radical **2** shown as an example in Figure 6 allow, in combination with the associated molecular electrostatic potential (ESP), for a better understanding of the intermolecular interactions. The 24α and 24β (HOMO) orbitals have a similar shape and contribute to the electron density on the oxygen atom along the aromatic ring plane, to which the 25α (SOMO) and 25β (LUMO) orbitals show a perpendicular orientation.

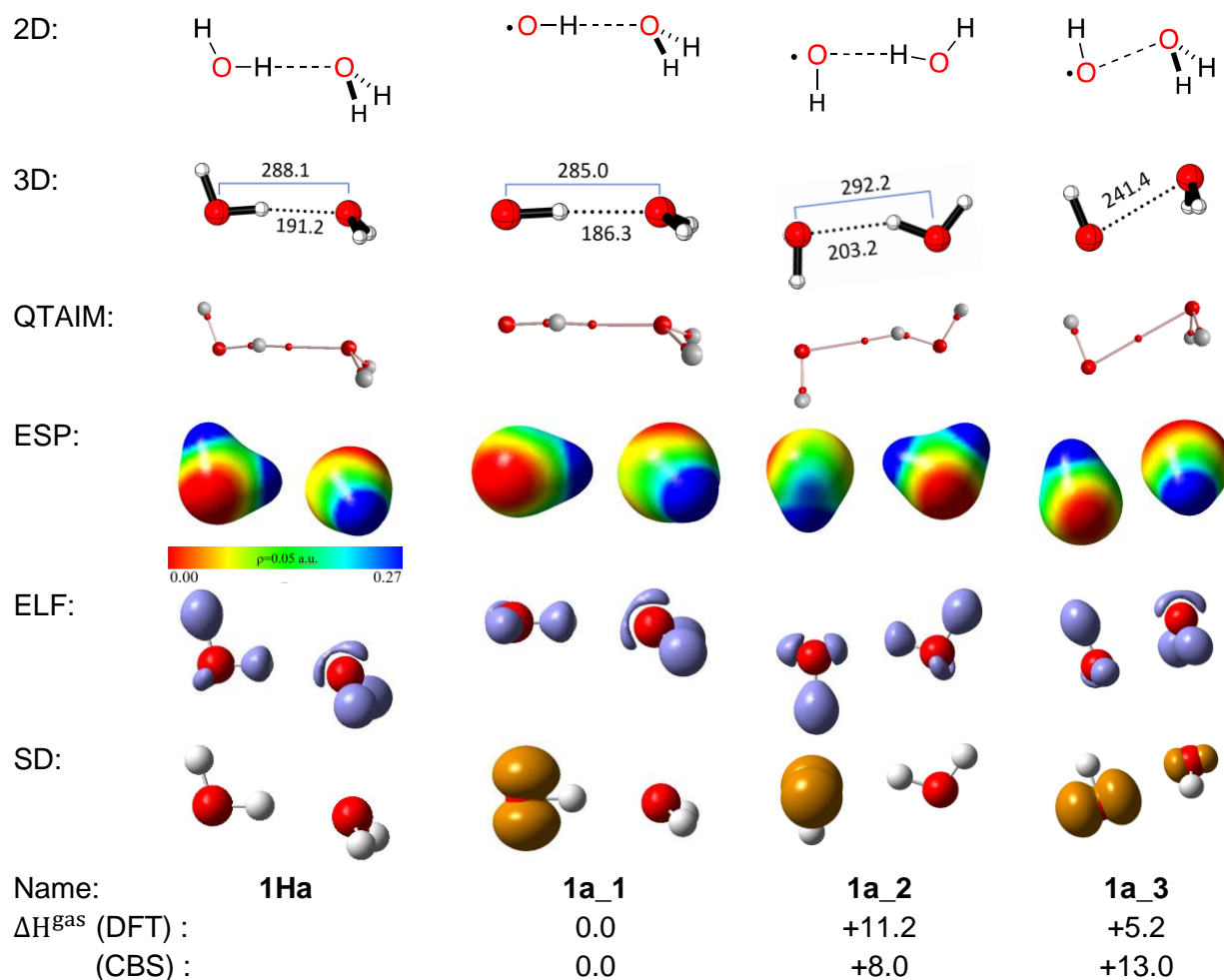


FIGURE 5 2D- and 3D-structures, quantum theory of atoms in molecules (QAIM), electrostatic potential (ESP), electron localization function (ELF=0.90 a.u.), spin density (SD=0.01 a.u.) for water dimer **1Ha** and the water complexes of hydroxyl radical **1a_1** - **1a_3**. For the latter three complexes relative enthalpies ΔH^{gas} (kJ mol^{-1}) calculated at the (U)B3LYP-D3/6-31+G(d,p) (DFT) and DLPNO-CCSD(T)/CBS (CBS) levels are also given.

TABLE 2 RSE-A and RSE-D values (kJ mol⁻¹) calculated for selected O-centered radicals (ordered according to Table 1).

Radical	RSE(RO•)					
	Alcohol			Alcohol		
	DFT ^[a]	CBS ^[b]	G3B3-D3 ^[c]	DFT ^[a]	CBS ^[b]	G3B3-D3 ^[c]
HO• (1)	+6.1	+4.1	+4.1 ^[d]	+6.1	+4.1	+4.1 ^[d]
HC(O)O• (20)	-39.4	-10.3	-23.9	-9.0	+16.4	+3.1
			-15.0 ^[d]			+11.5 ^[d]
<i>t</i> -Bu-O• (7)	-55.1	-44.3	-44.6	-62.9	-49.5	-52.7
PhCH ₂ O• (8)	-56.6	-45.2	-45.0	-56.5	-43.6	-44.8
CH ₃ O• (6)	-60.6	-53.7	-51.6	-63.4	-55.3	-55.7
CH ₃ CH ₂ O• (9)	-60.1	-51.5	-50.2	-65.7	-55.1	-56.1
PhC(CH ₃) ₂ O• (10)	-55.1	-41.5	-44.3	-53.5	-38.8	-40.1
<i>n</i> -Bu-O• (11)	-62.7	-53.1	-52.2	-68.5	-57.1	-57.5
<i>p</i> -nitro-PhO• (12)	-125.3	-115.3	-114.8	-104.7	-98.1	-95.6
HOO• (13)	-142.9	-137.1	-137.6	-142.9	-137.1	-137.6
PhO• (2)	-144.0	-132.5	-130.4	-133.4	-124.0	-118.9
PhCH ₂ OO• (16)	-137.5	-126.8	-129.3	-127.5	-116.3	-118.7
CH ₃ OO• (15)	-143.5	-136.0	-137.3	-132.3	-124.9	-126.1
<i>p</i> -methyl-PhO• (14)	-153.1	-140.0	-138.5	-143.8	-132.7	-128.3
<i>t</i> -Bu-OO• (17)	-149.6	-139.5	-144.5	-137.1	-127.8	-131.8
<i>p</i> -amino-PhO• (18)	-183.2	-163.9	-165.7	-176.3	-158.2	-160.9
TEMPO• (5)	-215.5	-203.4	-208.8	-198.6	-189.8	-191.4
•OO• (19)				-236.4	-258.2	-257.6

[a] (U)B3LYP-D3/6-31+G(d,p) level of theory
 [b] DLPNO-CCSD(T)/CBS using (U)B3LYP-D3/6-31+G(d,p) optimized geometries
 [c] Using (U)B3LYP-D3/6-31G(d) optimized geometries
 [d] Using (U)B3LYP-D3/6-31+G(d,p) optimized geometries

Since there is no electron in the LUMO, this leads to the formation of two more negative ESP-regions on oxygen favorable for hydrogen bonding interactions. All oxygen-centered radicals studied here have a similar electronic structure at the radical center. The second effect, which can affect the charge distribution on the radical center, is based on the concept of σ -holes as reported previously for sulphur-,⁸⁶ nitrogen-,⁸⁷ and halogen-containing compounds.⁸⁸ The electron density of the oxygen atom is slightly shifted towards the covalent bond along the C-O• (or O-O•) axis, the effect being most visible for peroxy radicals.

The effects of monosolvation on the stability of alkoxy radicals

The RSE-A values of alkoxy radicals listed in Table 2 are somewhat less negative than the RSE values in Table 1. These radicals are thus

destabilized through mono-complexation with water, the destabilization varying between 2.6 kJ mol⁻¹ for *n*-BuO• (**11**) and 7.0 kJ mol⁻¹ for PhCH₂O• (**8**). These changes imply that the complexation energies for the parent alcohols (acting as H-bond acceptors) are larger than those for the respective radicals. This may, at least in part, differences in the oxygen atom partial charges (NBO), which are significantly smaller on the radical oxygen as compared to those in the parent alcohols (see SI). Changing the role of the parent alcohol to that of the H-bond donor yields the alkoxy radical RSE-D values in Table 2, which are closely similar to the RSE values of uncomplexed alkoxy radicals in Table 1. Only for the benzyloxy-type radicals **8** and **19** are the RSE-D values similarly less negative than already found for the RSE-A values, the largest change being that for benzyloxy radical **8** with a $\Delta\Delta\text{RSE} = +8.6$ kJ/mol.

The effects of monosolvation on the stability of aryloxy radicals

The monosolvation enthalpy $\Delta H_{c1}^{gas}(ArO\bullet)$ increases systematically when moving from acceptor- to donor-substituted phenoxy radicals, the lowest value being found for radical *p*-NO₂-PhO• ($\Delta H_{c1}^{gas}(\mathbf{12}) = -20.1 \text{ kJ mol}^{-1}$) and the highest for *p*-NH₂-PhO• ($\Delta H_{c1}^{gas}(\mathbf{18}) = -25.5 \text{ kJ mol}^{-1}$) at DLPNO-CCSD(T)/CBS level. This is accompanied by a decrease in the hydrogen bonding distances $r(O\cdots H)$ of 195.2 pm for radical **12** and 183.3 pm for **18**, and an increase in the partial charge of the radical oxygen atom of -0.46 in radical **12** and -0.55 in radical **18**. It should be added that the NBO charge of the radical oxygen atom in aryloxy radicals amounts to only 70% of the charge of the same atom in the parent phenols. From a structural point of view, the aryloxy radical water complexes are largely similar in that the water is located in the aryl group ring plane. That this type of orientation provides the most effective interaction with the oxygen lone pair electron density is easily seen in Figure 6.

Comparing the RSE-A and RSE-D values for aryloxy radicals in Table 2 we note that these are actually quite different. In a very general sense, these differences result from phenols being much better hydrogen bond donors as compared to acceptors. Focusing first on the RSE-A values, we note that these are systematically larger (more negative) by approx. 10 kJ mol⁻¹ as compared to the RSE values for aryloxy radicals in Table 1. This shift results from differences in complexation energies $\Delta H_{c1}^{gas}(ArOH)$ for the parent phenols, which are approx. 10 kJ mol⁻¹ smaller than for the resulting phenoxy radicals. Taking the parent phenol system as an example, we have $\Delta H_{c1}^{gas}(\mathbf{2H}) = -13.1 \text{ kJ mol}^{-1}$ vs. $\Delta H_{c1}^{gas}(\mathbf{2}) = -21.7 \text{ kJ mol}^{-1}$. The difference of these values of $\Delta\Delta H_{c1}^{gas} = -8.6 \text{ kJ mol}^{-1}$ is closely similar to the difference in RSE(**2**) and RSE-A(**2**) values (-123.6 vs. -132.5 kJ mol⁻¹). The range of RSE-D values listed for aryloxy radicals in Table 2 (-98.1 for radical **12** to -158.2 for radical **18**) is somewhat larger than the range

of RSE values in Table 1 (from -106.1 for radical **12** to -152.4 for radical **18**). This is due to the fact that *p*-NO₂-PhOH is a much better H-bond donor as compared to the donor-substituted phenols **14H** and **18H**. As a result, we find that *p*-NO₂-PhO• is destabilized and *p*-NH₂-PhO• is (weakly) stabilized when their respective parent phenols act as H-bond donors. For the parent phenol (**2H**) system we find that RSE and RSE-D values are almost identical (-123.6 vs. -124.0 kJ mol⁻¹).

The effects of monosolvation on the stability of peroxy radicals, triplet dioxygen and TEMPO

The monosolvation enthalpies $\Delta H_{c1}^{gas}(ROO\bullet)$ for the radicals CH₃OO•, *t*-BuOO• and PhCH₂OO• are -13.6, -13.8, -17.0 kJ mol⁻¹, respectively. While for peroxides such as CH₃OOH, *t*-BuOOH and PhCH₂OOH interacting with water as a H-acceptor $\Delta H_{c1}^{gas}(ROOH)$, these values are -13.9, -13.0 and -18.1 kJ mol⁻¹. These closely similar complexation energies of alkylperoxy radicals and alkylhydroperoxides imply that their RSE and RSE-A values are almost identical. Alkylhydroperoxides are, however, much better hydrogen bond donors than acceptors. As a consequence, the RSE-D values for alkylperoxy radicals are much smaller (less stabilizing) than the respective RSE values. For methylperoxy radical (CH₃OO•, **15**) as the smallest system in this group, the difference amounts to RSE-D = -124.9 kJ mol⁻¹ vs. RSE = -134.7 kJ mol⁻¹.

For HOO• (**13**) as the smallest possible peroxy radical the situation is much more complicated due to multiple interactions between the solvating water molecules and the HOO•/(H₂O₂) interaction partners. The minima identified for these systems at the DLPNO-CCSD(T)/CBS// (U)B3LYP-D3/6-31+G(d,p) level of theory are shown in Figure 9 together with the respective relative stabilities. The best conformer of the HOOH⋯H₂O complex is of cyclic type (Figure 9a) with two H-bonds, in which the HOOH molecule can be considered as both a H-accepting ($r(O_{alk}\cdots HOH) = 227.5 \text{ pm}$) and a H-donating ($r(OH_{alk}\cdots OH_2) = 190.1 \text{ pm}$) system at the same time. The presence of two H-bonds

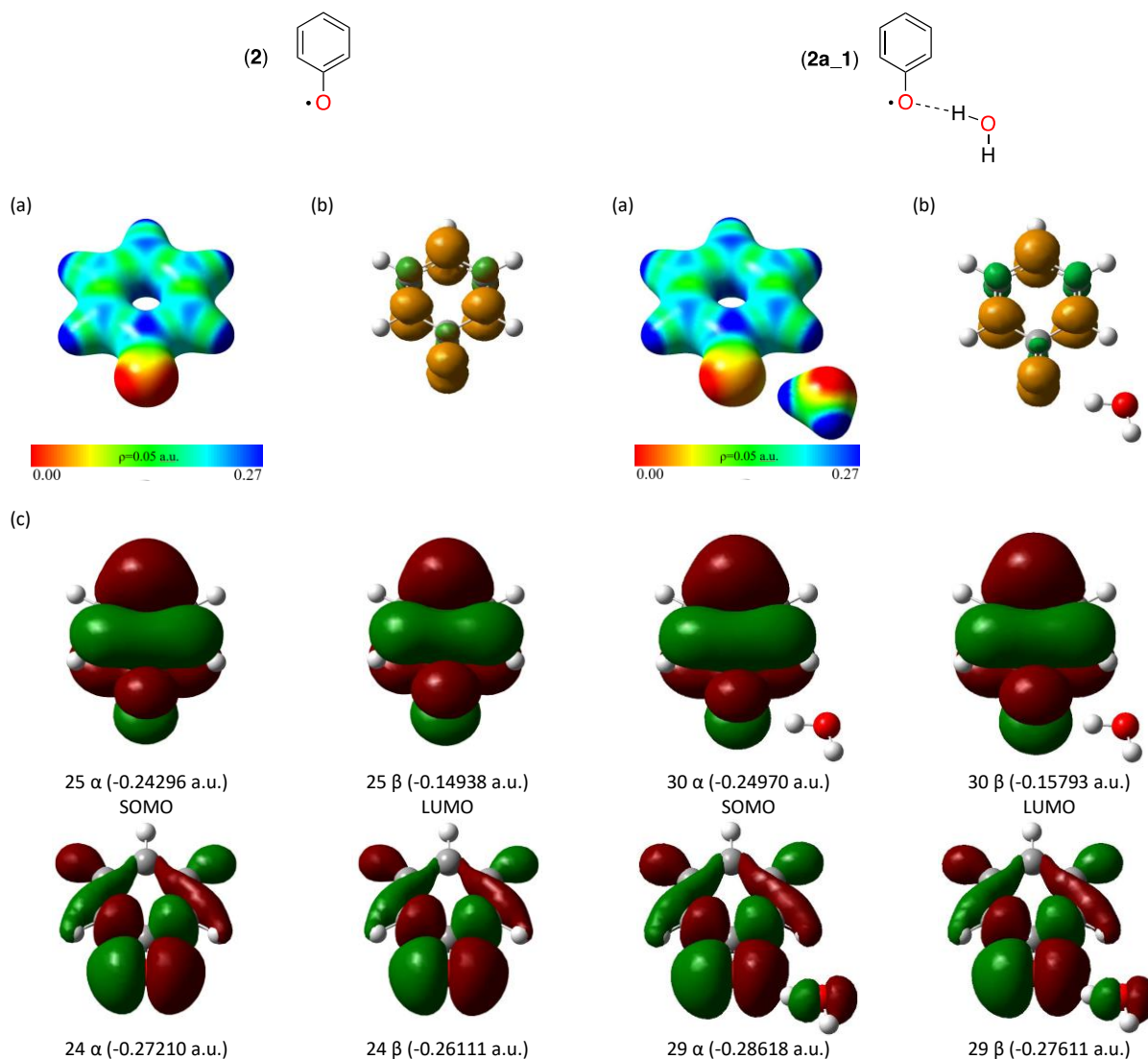


FIGURE 6. Orbital analysis for phenoxy radical (**2**) and the best conformation of its complex with one water molecule (**2a_1**). Electrostatic potential (a), spin density (SD=0.005 a.u.) (b), and molecular orbitals (c) calculated at the UB3LYP-D3/6-31+G(d,p) level of theory.

gives this complex a rather low monosolvation enthalpy of $\Delta H_{c1}^{\text{gas}}(\mathbf{13H}) = -22.5 \text{ kJ mol}^{-1}$. This type of structure was established experimentally by matrix isolation infrared spectroscopy.⁸⁹ For the $\text{HOO}\cdots\text{H}_2\text{O}$ complex we identify the three conformations shown in Figure 9e-g. The most stable conformation is also of cyclic type (Figure 9e) and is very similar to the best conformer of the $\text{HOOH}\cdots\text{H}_2\text{O}$ complex. In this structure, the $\text{HOO}\cdot$ radical is interacting with water as both a

H-acceptor and a H-donor through two H-bonds: 1) between the hydrogen of water and the spin-bearing oxygen with $r(\text{O}\cdots\text{HOH}) = 246.9 \text{ pm}$; and 2) between the hydrogen of the $\text{HOO}\cdot$ radical and the oxygen of water with $r(\text{OH}_{\text{alk}}\cdots\text{OH}_2) = 177 \text{ pm}$. This structure has been described already in earlier theoretical⁹⁰ and experimental^{91,92} studies. The other two conformers of the $\text{HOO}\cdots\text{H}_2\text{O}$ complex are more than 20 kJ mol^{-1} less stable because they

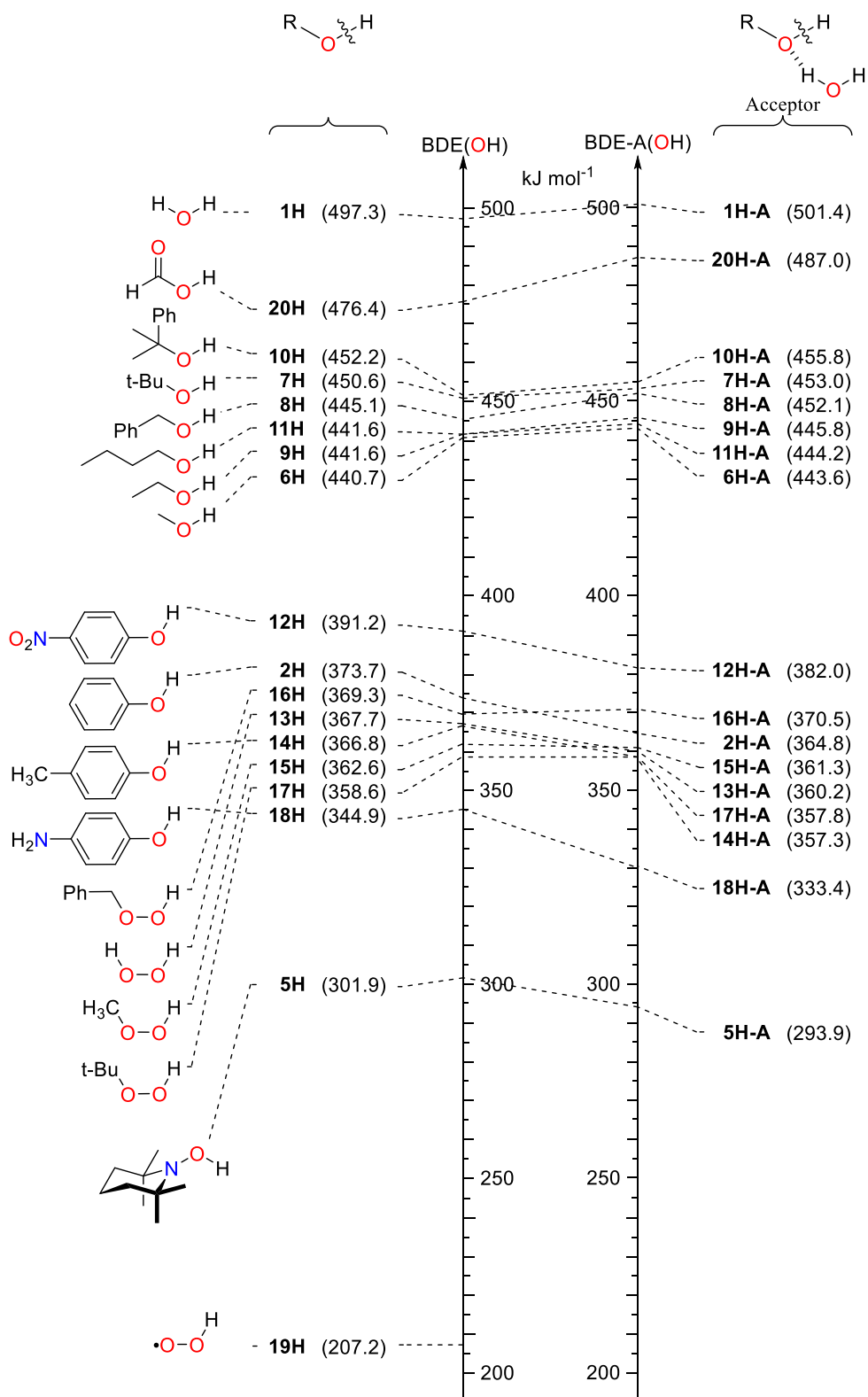


FIGURE 7. BDE(OH) and BDE-A(OH) values (DLPNO-CCSD(T)/CBS//(U)B3LYP-D3/6-31+G(d,p) results).

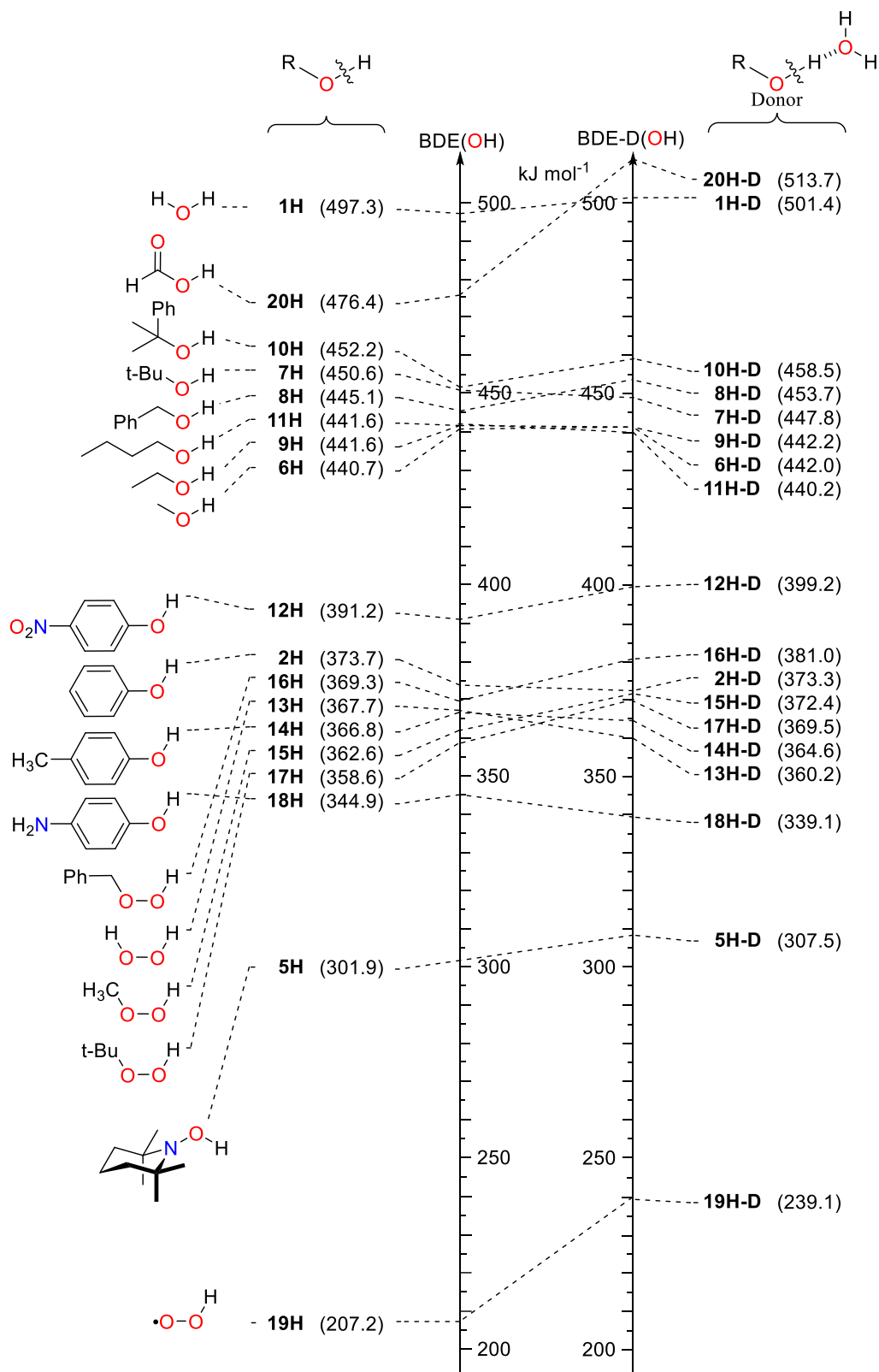


FIGURE 8. BDE(OH) and BDE-D(OH) values (DLPNO-CCSD(T)/CBS//(U)B3LYP-D3/6-31+G(d,p) results).

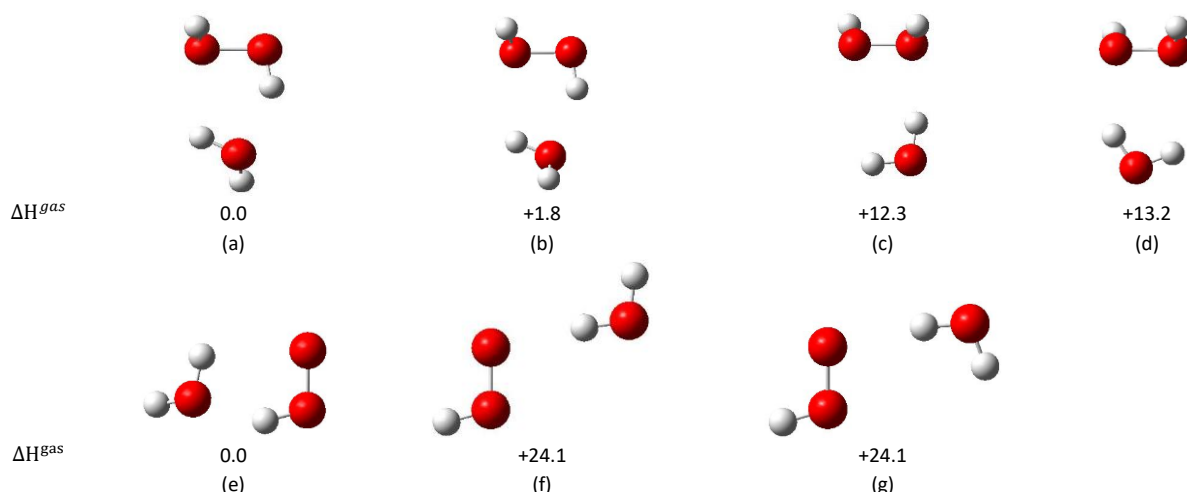


FIGURE 9. Relative ΔH^{gas} values (in kJ mol^{-1}) for the $\text{HOOH}\cdots\text{H}_2\text{O}$ (a - d) and $\text{HOO}\cdots\text{H}_2\text{O}$ (e - g) complexes (DLPNO-CCSD(T)/CBS//(U)B3LYP-D3/6-31+G(d,p) results).

contain only one H-bond with $r(\text{O}\cdots\text{HOH})$ distances of 204.6 to 206.4 pm as shown in Figure 9. Although the water complexes of radical **13** and its parent **13H** share large structural similarities, the complexation energy of radical **13** is significantly more favorable at $\Delta H_{\text{c1}}^{\text{gas}}(\mathbf{13}) = -29.7 \text{ kJ mol}^{-1}$. This difference of 7.5 kJ mol^{-1} translates into a significant stabilization of radical **13** and the associated values of $\text{RSE}(\mathbf{13}) = -129.6 \text{ kJ mol}^{-1}$ and $\text{RSE-A}(\mathbf{13}) = -137.1 \text{ kJ mol}^{-1}$. Given the simultaneous presence of multiple H-bonding interactions in the water complexes in Figure 9, RSE-A and RSE-D values are taken to be identical for this system. For triplet oxygen ($^3\text{O}_2$, **19**) the $\text{HOO}\bullet$ radical represents (formally) the parent alcohol. The list of conformers presented in Figure 9 for the $\text{HOO}\cdots\text{H}_2\text{O}$ complex lacks a structure where the HO group oxygen interacts with water as the H-bond acceptor, and calculation of an RSE-A values is therefore not possible. Acting as a H-bond donor as in Figure 9e, radical **13** forms a much more stable water complex as compared to triplet oxygen. This leads to a very substantial difference between $\text{RSE}(\mathbf{19}) = -290.1 \text{ kJ mol}^{-1}$ and $\text{RSE-D}(\mathbf{19}) = -258.1 \text{ kJ mol}^{-1}$. The TEMPO radical (**5**) as the most stable (doublet) system considered here forms a water complex characterized by a comparatively short H-bond of $r(\text{O}\cdots\text{HOH}) = 182.7 \text{ pm}$ and a

complexation energy of $\Delta H_{\text{c1}}^{\text{gas}} = -22.8 \text{ kJ mol}^{-1}$. This value is larger as compared to that for the closed-shell TEMPOL parent acting as a H-bond acceptor ($\Delta H_{\text{c1}}^{\text{gas}} = -15.1 \text{ kJ mol}^{-1}$), which implies that $\text{RSE-A}(\mathbf{5}) = -212.2 \text{ kJ mol}^{-1}$ is more negative (more stabilizing) than $\text{RSE}(\mathbf{5}) = -195.4 \text{ kJ mol}^{-1}$. However, TEMPOL is a much better H-bond donor (than acceptor), which is also reflected in $\text{RSE-D}(\mathbf{5}) = -189.8 \text{ kJ mol}^{-1}$.

The final system considered here is $\text{HC(O)O}\bullet$ radical **20**, whose electronic structure varies significantly as a function of the level of theory. This is also the reason for the largely different RSE values obtained from DFT, DLPNO-CCSD(T)/CBS, and G3B3-D3 calculations (Table 1). The water complexes of formic acid (**20H**) are more stable as compared to the water complex of radical **20**, and the RSE-A and RSE-D values are thus less negative (less stabilizing) as compared to $\text{RSE}(\mathbf{20}) = -20.9 \text{ kJ mol}^{-1}$. Formic acid is a particularly good H-bond donor, which leads to $\text{RSE-D}(\mathbf{20}) = +16.4 \text{ kJ mol}^{-1}$.

Conclusions

The range of (formally) oxygen-centered radicals considered here ranges from the comparatively unstable hydroxyl radical (**1**), alkoxy radicals such as $\text{CH}_3\text{O}\bullet$ (**6**), aryloxy radicals such as $\text{PhO}\bullet$

(2), peroxy radicals such as $\text{CH}_3\text{OO}\cdot$ (15) and nitroxy radicals such as TEMPO (5). The most favorable water complexes identified for these systems all correspond to type (a) shown in Figure 2. The alternative interaction modes described as the SEHB or 2c3e hemibond are found only in (some) higher energy conformers of the water/radical complexes. The influence of water complexation on the respective RSE values is smallest for the group of alkoxy radicals and largest for the group of aryloxy radicals. The parent alcohol system can act as H-bond donor or acceptor in almost all systems, which gives rise to the associated RSE-A and RSE-D values. The difference between BDE-A and BDE-D simply reflects the difference in hydrogen bonding in the closed shell parent. Selecting the thermochemically most stable alcohol/water complex leads to the smaller (less negative) of the RSE-A or RSE-D values. For most of the systems considered here, this is the RSE-D values, the exceptions being the alkoxy radicals $\text{CH}_3\text{O}\cdot$, $\text{CH}_3\text{CH}_2\text{O}\cdot$, *n*-Bu-O \cdot and *t*-Bu-O \cdot .

Acknowledgments

We thank the Deutsche Forschungsgemeinschaft (DFG, German Research Foundation) for financial support via SFB1309 (PID 325871075).

((Additional Supporting Information may be found in the online version of this article.))

References and Notes

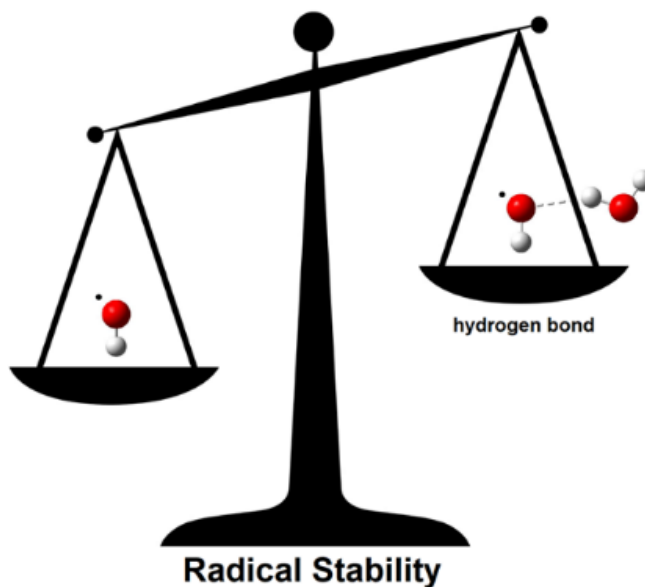
- [1] J. Stubbe, W. A. van Der Donk, *Chem. Rev.* **1998**, *98*, 2661.
- [2] H. Eklund, U. Uhlin, M. Färnegårdh, D. T. Logan, P. Nordlund, *Prog. Biophys. Mol. Biol.* **2001**, *77*, 177.
- [3] J. Stubbe, D. G. Nocera, C. S. Yee, M. C. Chang, *Chem. Rev.* **2003**, *103*, 2167.
- [4] M. Kolberg, K. R. Strand, P. Graff, K. K. Andersson, *Biochim Biophys Acta Proteins Proteom* **2004**, *1699*, 1.
- [5] M. Bennati, F. Lenzian, M. Schmittel, H. Zipse, *Biol. Chem.* **2005**, *386*, 1007.
- [6] J. Fritscher, E. Artin, S. Wnuk, G. Bar, J. H. Robblee, S. Kacprzak, M. Kaupp, R. G. Griffin, M. Bennati, J. Stubbe, *J. Am. Chem. Soc.* **2005**, *127*, 7729.
- [7] P. Nordlund, P. Reichard, *Annu. Rev. Biochem.* **2006**, *75*, 681.
- [8] H. Zipse, E. Artin, S. Wnuk, G. J. Lohman, D. Martino, R. G. Griffin, S. Kacprzak, M. Kaupp, B. Hoffman, M. Bennati, *J. Am. Chem. Soc.* **2009**, *131*, 200.
- [9] A. Benjdia, K. Heil, T. R. Barends, T. Carell, I. Schlichting, *Nucleic Acids Res.* **2012**, *40*, 9308.
- [10] A. C. Kneuttinger, K. Heil, G. Kashiwazaki, T. Carell, *Chem. Commun.* **2013**, *49*, 722.
- [11] J. Hioe, H. Zipse, *Chem. Eur. J.* **2012**, *18*, 16463.
- [12] D. M. Chipman, *J. Phys. Chem. A* **2011**, *115*, 1161.
- [13] ATcT, <http://atct.anl.gov/>.
- [14] J. Hioe, H. Zipse, *Org. Biomol. Chem.* **2010**, *8*, 3609.
- [15] J. Hioe, H. Zipse, *Faraday Discuss.* **2010**, *145*, 301.
- [16] K. Condić-Jurkić, H. Zipse, D. M. Smith, *J. Comput. Chem.* **2010**, *31*, 1024.
- [17] K. Čondić-Jurkić, V. T. Perchyonok, H. Zipse, D. M. Smith, *J. Comput. Chem.* **2008**, *29*, 2425.
- [18] W. Tantawy, H. Zipse. Wiley Online Library, **2007**.
- [19] J. Hioe, A. Karton, J. L. Martin, H. Zipse, *Chem. Eur. J.* **2010**, *16*, 6861.
- [20] M. Coote, C. Lin, H. Zipse. Wiley, New Jersey, **2010**.
- [21] E. I. Izgorodina, D. R. Brittain, J. L. Hodgson, E. H. Krenske, C. Y. Lin, M. Namazian, M. L. Coote, *J. Phys. Chem. A* **2007**, *111*, 10754.
- [22] D. Moran, R. Jacob, G. P. Wood, M. L. Coote, M. J. Davies, R. A. O'Hair, C. J. Easton, L. Radom, *Helv. Chim. Acta* **2006**, *89*, 2254.
- [23] Y. Zhao, D. G. Truhlar, *J. Phys. Chem. A* **2008**, *112*, 1095.
- [24] J. Zheng, Y. Zhao, D. G. Truhlar, *J. Phys. Chem. A* **2007**, *111*, 4632.
- [25] S. Grimme, *J. Chem. Phys.* **2006**, *124*, 034108.
- [26] D. C. Graham, A. S. Menon, L. Goerigk, S. Grimme, L. Radom, *J. Phys. Chem. A* **2009**, *113*, 9861.
- [27] D. J. Henry, C. J. Parkinson, L. Radom, *J. Phys. Chem. A* **2002**, *106*, 7927.

- [28] D. J. Henry, M. B. Sullivan, L. Radom, *J. Chem. Phys.* **2003**, *118*, 4849.
- [29] S. D. Wetmore, D. M. Smith, J. T. Bennett, L. Radom, *J. Am. Chem. Soc.* **2002**, *124*, 14054.
- [30] S. D. Wetmore, D. M. Smith, B. T. Golding, L. Radom, *J. Am. Chem. Soc.* **2001**, *123*, 7963.
- [31] D. M. Smith, W. Buckel, H. Zipse, *Angew. Chem. Int. Ed.* **2003**, *42*, 1867.
- [32] L. Curtis, K. Raghavachari, J. Pople, *J. Chem. Phys.* **1993**, *98*, 1293.
- [33] A. G. Baboul, L. A. Curtiss, P. C. Redfern, K. Raghavachari, *J. Chem. Phys.* **1999**, *110*, 7650.
- [34] L. A. Curtiss, P. C. Redfern, K. Raghavachari, *J. Chem. Phys.* **2007**, *126*, 084108.
- [35] J. A. Montgomery Jr, M. J. Frisch, J. W. Ochterski, G. A. Petersson, *J. Chem. Phys.* **2000**, *112*, 6532.
- [36] J. M. Martin, G. de Oliveira, *J. Chem. Phys.* **1999**, *111*, 1843.
- [37] A. Altun, F. Neese, G. Bistoni, *Beilstein J. Org. Chem.* **2018**, *14*, 919.
- [38] F. Neese, E. F. Valeev, *J. Chem. Theory Comput.* **2011**, *7*, 33.
- [39] M. Saitow, U. Becker, C. Riplinger, E. F. Valeev, *J. Chem. Phys.* **2017**, *146*, 164105.
- [40] A. D. Beck, *J. Chem. Phys.* **1993**, *98*, 5648.
- [41] C. Lee, W. Yang, R. G. Parr, *Phys. Rev. B* **1988**, *37*, 785.
- [42] W. J. Hehre, R. Ditchfield, J. A. Pople, *J. Chem. Phys.* **1972**, *56*, 2257.
- [43] S. Grimme, S. Ehrlich, L. Goerigk, *J. Comput. Chem.* **2011**, *32*, 1456.
- [44] S. Grimme, J. Antony, S. Ehrlich, H. Krieg, *J. Chem. Phys.* **2010**, *132*, 154104.
- [45] D. Šakić, M. Hanževački, D. M. Smith, V. Vrček, *Org. Biomol. Chem.* **2015**, *13*, 11740.
- [46] D. Šakić, <https://kick.science/KICK.html>.
- [47] E. Suarez, N. Diaz, D. Suarez, *J. Chem. Theory Comput.* **2011**, *7*, 2638.
- [48] V. Korotenko, <https://github.com/vnkorotenko/ess>.
- [49] V. Korotenko, <https://github.com/vnkorotenko/ccs>.
- [50] K. M. Ervin, V. F. DeTuri, *J. Phys. Chem. A* **2002**, *106*, 9947.
- [51] D. R. Reed, M. C. Hare, A. Fattahi, G. Chung, M. S. Gordon, S. R. Kass, *J. Am. Chem. Soc.* **2003**, *125*, 4643.
- [52] E. T. Denisov, V. Tumanov, *Russ. Chem. Rev.* **2005**, *74*, 825.
- [53] A. Fattahi, S. R. Kass, *J. Org. Chem.* **2004**, *69*, 9176.
- [54] T. Denisova, E. Denisov, *Kinet. Catal.* **2006**, *47*, 121.
- [55] M. G. Nix, A. L. Devine, B. Cronin, R. N. Dixon, M. N. Ashfold, *J. Chem. Phys.* **2006**, *125*, 133318.
- [56] R. M. Borges dos Santos, J. A. Martinho Simões, *J. Phys. Chem. Ref. Data* **1998**, *27*, 707.
- [57] M. Lucarini, P. Pedrielli, G. F. Pedulli, S. Cabiddu, C. Fattuoni, *J. Org. Chem.* **1996**, *61*, 9259.
- [58] H. Wang, J. W. Bozzelli, *J. Chem. Eng. Data* **2016**, *61*, 1836.
- [59] O. Kondo, S. W. Benson, *J. Phys. Chem.* **1984**, *88*, 6675.
- [60] S. J. Blanksby, T. M. Ramond, G. E. Davico, M. R. Nimlos, S. Kato, V. M. Bierbaum, W. C. Lineberger, G. B. Ellison, M. Okumura, *J. Am. Chem. Soc.* **2001**, *123*, 9585.
- [61] M. Jonsson, *J. Phys. Chem.* **1996**, *100*, 6814.
- [62] P. S. Billone, P. A. Johnson, S. Lin, J. Scaiano, G. A. DiLabio, K. Ingold, *J. Org. Chem.* **2011**, *76*, 631.
- [63] L. Mahoney, G. Mendenhall, K. Ingold, *J. Am. Chem. Soc.* **1973**, *95*, 8610.
- [64] A. Altun, F. Neese, G. Bistoni, *J. Org. Chem.* **2018**, *14*, 919.
- [65] B. Ruscic, A. F. Wagner, L. B. Harding, R. L. Asher, D. Feller, D. A. Dixon, K. A. Peterson, Y. Song, X. Qian, C.-Y. Ng, *J. Phys. Chem. A* **2002**, *106*, 2727.
- [66] Y.-R. Luo. Comprehensive handbook of chemical bond energies; CRC press, **2007**.
- [67] P. Mulder, H.-G. Korth, D. A. Pratt, G. A. DiLabio, L. Valgimigli, G. Pedulli, K. Ingold, *J. Phys. Chem. A* **2005**, *109*, 2647.
- [68] H. Zipse, *Radicals in Synthesis I* **2006**, 163.
- [69] J. Hioe, H. Zipse, *Encyclopedia of Radicals in Chemistry, Biology and Materials* **2012**.
- [70] W. M. Fabian, R. Janoschek, *J. Mol. Struct. Theochem* **2005**, *713*, 227.

- [71] W. T. Borden, R. Hoffmann, T. Stuyver, B. Chen, *J. Am. Chem. Soc.* **2017**, *139*, 9010.
- [72] A. Mukhopadhyay, W. T. Cole, R. J. Saykally, *Chem. Phys. Lett.* **2015**, *633*, 13.
- [73] A. Mukhopadhyay, S. S. Xantheas, R. J. Saykally, *Chem. Phys. Lett.* **2018**, *700*, 163.
- [74] A. Engdahl, G. Karlström, B. Nelander, *J. Chem. Phys.* **2003**, *118*, 7797.
- [75] J. A. Plumley, J. Dannenberg, *J. Comput. Chem.* **2011**, *32*, 1519.
- [76] P. Cabral do Couto, R. Guedes, B. Costa Cabral, J. Martinho Simoes, *J. Chem. Phys.* **2003**, *119*, 7344.
- [77] Y. Ohshima, K. Sato, Y. Sumiyoshi, Y. Endo, *J. Am. Chem. Soc.* **2005**, *127*, 1108.
- [78] S. Aloisio, J. S. Francisco, *Acc. Chem. Res.* **2000**, *33*, 825.
- [79] D. P. Schofield, H. G. Kjaergaard, *J. Chem. Phys.* **2004**, *120*, 6930.
- [80] Z. Zhou, Y. Qu, A. Fu, B. Du, F. He, H. Gao, *Int. J. Quantum Chem* **2002**, *89*, 550.
- [81] M. P. DeMatteo, J. S. Poole, X. Shi, R. Sachdeva, P. G. Hatcher, C. M. Hadad, M. S. Platz, *J. Am. Chem. Soc.* **2005**, *127*, 7094.
- [82] M. A. Allodi, M. E. Dunn, J. Livada, K. N. Kirschner, G. C. Shields, *J. Phys. Chem. A* **2006**, *110*, 13283.
- [83] U. Koch, P. L. Popelier, *J. Phys. Chem.* **1995**, *99*, 9747.
- [84] S. Tsuzuki, K. Honda, T. Uchimaru, M. Mikami, K. Tanabe, *J. Am. Chem. Soc.* **2000**, *122*, 11450.
- [85] M. J. Calhorda, *Chem. Commun.* **2000**, 801.
- [86] M. R. Koebel, A. Cooper, G. Schmadeke, S. Jeon, M. Narayan, S. Sirimulla, *J. Chem. Inf. Model* **2016**, *56*, 2298.
- [87] R. Shukla, D. Chopra, *Physical Chemistry Chemical Physics* **2016**, *18*, 29946.
- [88] A. Priimagi, G. Cavallo, P. Metrangolo, G. Resnati, *Acc. Chem. Res.* **2013**, *46*, 2686.
- [89] A. Engdahl, B. Nelander, *Physical Chemistry Chemical Physics* **2000**, *2*, 3967.
- [90] S. Aloisio, J. Francisco, *J. Phys. Chem. A* **1998**, *102*, 1899.
- [91] S. Aloisio, J. S. Francisco, R. R. Friedl, *J. Phys. Chem. A* **2000**, *104*, 6597.
- [92] B. Nelander, *J. Phys. Chem. A* **1997**, *101*, 9092.

GRAPHICAL ABSTRACT

The thermodynamic stability of various alkoxy/aryloxy/peroxy radicals, as well as TEMPO and triplet dioxygen has been explored at a variety of theoretical levels. The effects of hydrogen bonding interactions on the stability of oxygen-centered radicals have been probed by addition of a single solvating water molecule.



2.2

Supplementary Information

The Stability of Oxygen-Centered Radicals
and its Response to Hydrogen Bonding
Interactions

1. Methodology

Computational Methodology

Theoretical methods

Geometry optimizations have been performed using the B3LYP hybrid functional, complemented by the D3 dispersion correction. Geometry optimizations have been performed with the 6-31+G(d,p) basis set. Geometry optimizations have also been performed with the smaller 6-31G(d) basis set for selected cases. Thermal corrections to enthalpies at 298.15 K have been calculated at the same level as the geometry optimizations using the rigid rotor/harmonic oscillator model using unscaled frequencies. We note in passing, that the C_{2v} structure of formyloxy radical **20** is a transition state at UB3LYP-D3/6-31G(d) level, but a true minimum at the UB3LYP-D3/6-31+G(d,p) level. If not stated otherwise, all results reported on the following pages refer to (U)B3LYP-D3/6-31+G(d,p) geometries.

The generation of initial random structures with explicit water (intermolecular dimers) was done using the “kick” algorithm.^{1,2} The individuality (lack of repetition) of the found conformers was confirmed using an energy criterion ($\Delta E_{\text{tot}} > 10^{-7}$ Hartree)³ and comparing geometries by distances between each atom and the centroid point.⁴

Single point calculations have been performed for all geometries optimized at the UB3LYP-D3/6-31+G(d,p) level at the double-hybrid (U)B2PLYP/cc-pVTZ and (U)B2PLYP/cc-pVQZ levels, then also for the coupled cluster DLPNO-CCSD(T)/cc-pVTZ, DLPNO-CCSD(T)/cc-pVQZ theories implemented in ORCA, and finally for the composite method G3B3-D3. One water molecule was added to the resulting geometries in a random position, followed by optimization at the (U)B3LYP-D3/6-31+G(d,p) level of theory in the gas phase and followed by the same single point calculations as before. All calculations have been performed with *Gaussian 09, rev. D.01*, except for DLPNO-CCSD(T) calculations, which were performed with *ORCA 4.0.2*.

DLPNO-CCSD(T)/CBS

The energies were calculated for a temperature of 298.15 K in the gas phase and the thermal corrections to the enthalpy and Gibb’s free energy were obtained at the (U)B3LYP-D3/6-31+G(d,p) level of theory using unscaled frequencies. DLPNO-CCSD(T) calculations have been performed with the cc-pVTZ (n=3) and cc-pVQZ (m=4) basis sets using “TightSCF” and “TightPNO” settings. The complete basis set (CBS) limits of the reference energies E_{HF} and correlation energies E_{c} were calculated according to:

$$E_{\text{HF}}^{\text{CBS}} = \frac{E_{\text{HF}}^{(n)} \times e^{-\alpha\sqrt{m}} - E_{\text{HF}}^{(m)} \times e^{-\alpha\sqrt{n}}}{e^{-\alpha\sqrt{m}} - e^{-\alpha\sqrt{n}}} \quad (1)$$

$$E_{\text{corr}}^{\text{CBS}} = \frac{n^{\beta} E_{\text{corr}}^{(n)} - m^{\beta} E_{\text{corr}}^{(m)}}{n^{\beta} - m^{\beta}} \quad (2)$$

$$E_{\text{DLPNO}}^{\text{CBS}} = E_{\text{HF}}^{\text{CBS}} + E_{\text{corr}}^{\text{CBS}} \quad (3)$$

For the given pair of basis set, cc-pVTZ and cc-pVQZ i.e for the 3/4 extrapolation (n=3 and m=4) the values of constants $\alpha = 5.46$, and $\beta = 3.05$ were used.^{5,6} The final DLPNO-CCSD(T)/CBS total energies were then obtained as the sum of individual terms: $E_{\text{HF}}^{\text{CBS}}$ and $E_{\text{corr}}^{\text{CBS}}$. Finally, the thermal corrections obtained from the optimized geometries were added to $E_{\text{tot}}(\text{DLPNO-CCSD(T)/CBS})$ to yield the respective enthalpies H_{298} .

G3B3-D3 scheme

According to the G3B3-D3 scheme, enthalpies were calculated as follows:

$H_{298}(\text{G3B3-D3}) =$	$E_{\text{tot}}(\text{QCISD}/6-31\text{G(d)}/\text{B3LYP-D3}/\text{BASIS}) + \Delta E(+) + \Delta E(2\text{df,p}) + \Delta E(\text{G3large}) + \Delta E(\text{HLC}) + \Delta H_{\text{therm}}$																																																																																																																																																														
$\Delta E(+) =$	$E_{\text{tot}}(\text{MP4}/6-31+\text{G(d)}/\text{B3LYP-D3}/\text{BASIS}) - E_{\text{tot}}(\text{MP4}/6-31\text{G(d)}/\text{B3LYP-D3}/\text{BASIS})$																																																																																																																																																														
$\Delta E(2\text{df,p}) =$	$E_{\text{tot}}(\text{MP4}/6-31\text{G}(2\text{df,p})/\text{B3LYP-D3}/\text{BASIS}) - E_{\text{tot}}(\text{MP4}/6-31\text{G(d)}/\text{B3LYP-D3}/\text{BASIS})$																																																																																																																																																														
$\Delta E(\text{G3large}) =$	$E_{\text{tot}}(\text{MP2}/\text{G3large}/\text{B3LYP-D3}/\text{BASIS}) - E_{\text{tot}}(\text{MP2}/6-31\text{G}(2\text{df,p})/\text{B3LYP-D3}/\text{BASIS}) - E_{\text{tot}}(\text{MP2}/6-31+\text{G(d)}/\text{B3LYP-D3}/\text{BASIS}) + E_{\text{tot}}(\text{MP2}/6-31\text{G(d)}/\text{B3LYP-D3}/\text{BASIS})$																																																																																																																																																														
ΔH_{therm}	thermal corrections to enthalpies at standard state conditions (Scaling factor = 0.96, B3LYP-D3/BASIS)																																																																																																																																																														
BASIS	6-31G(d) 6-31+G(d,p)																																																																																																																																																														
$\Delta E(\text{HLC}) =$	$-A*\text{beta} - B*(\text{alpha} - \text{beta})$																																																																																																																																																														
<p>A = 6.760 mHartrees B = 3.233 mHartrees alpha = No. of alpha valence electrons beta = No. of beta valence electrons</p>																																																																																																																																																															
<table border="1"> <thead> <tr> <th>Radical</th> <th>alpha</th> <th>beta</th> <th>$\Delta E(\text{HLC})$</th> <th>Alcohol</th> <th>alpha</th> <th>beta</th> <th>$\Delta E(\text{HLC})$</th> </tr> </thead> <tbody> <tr> <td>HO•</td> <td>4</td> <td>3</td> <td>-0.023513</td> <td>HOH</td> <td>4</td> <td>4</td> <td>-0.027040</td> </tr> <tr> <td>CH3O•</td> <td>7</td> <td>6</td> <td>-0.043793</td> <td>CH3OH</td> <td>7</td> <td>7</td> <td>-0.047320</td> </tr> <tr> <td>CH3CH2O•</td> <td>10</td> <td>9</td> <td>-0.064073</td> <td>CH3CH2OH</td> <td>10</td> <td>10</td> <td>-0.067600</td> </tr> <tr> <td>BuO•</td> <td>16</td> <td>15</td> <td>-0.104633</td> <td>BuOH</td> <td>16</td> <td>16</td> <td>-0.108160</td> </tr> <tr> <td>t-BuO•</td> <td>16</td> <td>15</td> <td>-0.104633</td> <td>t-BuOH</td> <td>16</td> <td>16</td> <td>-0.108160</td> </tr> <tr> <td>PhCH2O•</td> <td>21</td> <td>20</td> <td>-0.138433</td> <td>PhCH2OH</td> <td>21</td> <td>21</td> <td>-0.141960</td> </tr> <tr> <td>PhC(CH3)2O•</td> <td>27</td> <td>26</td> <td>-0.178993</td> <td>PhC(CH3)2OH</td> <td>27</td> <td>27</td> <td>-0.182520</td> </tr> <tr> <td>PhO•</td> <td>18</td> <td>17</td> <td>-0.118153</td> <td>PhOH</td> <td>18</td> <td>18</td> <td>-0.121680</td> </tr> <tr> <td>p-nitro-PhO•</td> <td>26</td> <td>25</td> <td>-0.172233</td> <td>p-nitro-PhOH</td> <td>26</td> <td>26</td> <td>-0.175760</td> </tr> <tr> <td>p-methyl-PhO•</td> <td>21</td> <td>20</td> <td>-0.138433</td> <td>p-methyl-PhOH</td> <td>21</td> <td>21</td> <td>-0.141960</td> </tr> <tr> <td>p-amino-PhO•</td> <td>21</td> <td>20</td> <td>-0.138433</td> <td>p-amino-PhOH</td> <td>21</td> <td>21</td> <td>-0.141960</td> </tr> <tr> <td>HOO•</td> <td>7</td> <td>6</td> <td>-0.043793</td> <td>HOOH</td> <td>7</td> <td>7</td> <td>-0.047320</td> </tr> <tr> <td>CH3OO•</td> <td>10</td> <td>9</td> <td>-0.064073</td> <td>CH3OOH</td> <td>10</td> <td>10</td> <td>-0.067600</td> </tr> <tr> <td>t-BuOO•</td> <td>19</td> <td>18</td> <td>-0.124913</td> <td>t-BuOOH</td> <td>19</td> <td>19</td> <td>-0.128440</td> </tr> <tr> <td>PhCH2OO•</td> <td>24</td> <td>23</td> <td>-0.158713</td> <td>PhCH2OOH</td> <td>24</td> <td>24</td> <td>-0.162240</td> </tr> <tr> <td>TEMPO•</td> <td>33</td> <td>32</td> <td>-0.219553</td> <td>TEMPOH</td> <td>33</td> <td>33</td> <td>-0.223080</td> </tr> <tr> <td>•OO•</td> <td>7</td> <td>5</td> <td>-0.040266</td> <td>HOO•</td> <td>7</td> <td>6</td> <td>-0.043793</td> </tr> <tr> <td>HCO2•</td> <td>9</td> <td>8</td> <td>-0.057313</td> <td>HCO2H</td> <td>9</td> <td>9</td> <td>-0.060840</td> </tr> </tbody> </table>								Radical	alpha	beta	$\Delta E(\text{HLC})$	Alcohol	alpha	beta	$\Delta E(\text{HLC})$	HO•	4	3	-0.023513	HOH	4	4	-0.027040	CH3O•	7	6	-0.043793	CH3OH	7	7	-0.047320	CH3CH2O•	10	9	-0.064073	CH3CH2OH	10	10	-0.067600	BuO•	16	15	-0.104633	BuOH	16	16	-0.108160	t-BuO•	16	15	-0.104633	t-BuOH	16	16	-0.108160	PhCH2O•	21	20	-0.138433	PhCH2OH	21	21	-0.141960	PhC(CH3)2O•	27	26	-0.178993	PhC(CH3)2OH	27	27	-0.182520	PhO•	18	17	-0.118153	PhOH	18	18	-0.121680	p-nitro-PhO•	26	25	-0.172233	p-nitro-PhOH	26	26	-0.175760	p-methyl-PhO•	21	20	-0.138433	p-methyl-PhOH	21	21	-0.141960	p-amino-PhO•	21	20	-0.138433	p-amino-PhOH	21	21	-0.141960	HOO•	7	6	-0.043793	HOOH	7	7	-0.047320	CH3OO•	10	9	-0.064073	CH3OOH	10	10	-0.067600	t-BuOO•	19	18	-0.124913	t-BuOOH	19	19	-0.128440	PhCH2OO•	24	23	-0.158713	PhCH2OOH	24	24	-0.162240	TEMPO•	33	32	-0.219553	TEMPOH	33	33	-0.223080	•OO•	7	5	-0.040266	HOO•	7	6	-0.043793	HCO2•	9	8	-0.057313	HCO2H	9	9	-0.060840
Radical	alpha	beta	$\Delta E(\text{HLC})$	Alcohol	alpha	beta	$\Delta E(\text{HLC})$																																																																																																																																																								
HO•	4	3	-0.023513	HOH	4	4	-0.027040																																																																																																																																																								
CH3O•	7	6	-0.043793	CH3OH	7	7	-0.047320																																																																																																																																																								
CH3CH2O•	10	9	-0.064073	CH3CH2OH	10	10	-0.067600																																																																																																																																																								
BuO•	16	15	-0.104633	BuOH	16	16	-0.108160																																																																																																																																																								
t-BuO•	16	15	-0.104633	t-BuOH	16	16	-0.108160																																																																																																																																																								
PhCH2O•	21	20	-0.138433	PhCH2OH	21	21	-0.141960																																																																																																																																																								
PhC(CH3)2O•	27	26	-0.178993	PhC(CH3)2OH	27	27	-0.182520																																																																																																																																																								
PhO•	18	17	-0.118153	PhOH	18	18	-0.121680																																																																																																																																																								
p-nitro-PhO•	26	25	-0.172233	p-nitro-PhOH	26	26	-0.175760																																																																																																																																																								
p-methyl-PhO•	21	20	-0.138433	p-methyl-PhOH	21	21	-0.141960																																																																																																																																																								
p-amino-PhO•	21	20	-0.138433	p-amino-PhOH	21	21	-0.141960																																																																																																																																																								
HOO•	7	6	-0.043793	HOOH	7	7	-0.047320																																																																																																																																																								
CH3OO•	10	9	-0.064073	CH3OOH	10	10	-0.067600																																																																																																																																																								
t-BuOO•	19	18	-0.124913	t-BuOOH	19	19	-0.128440																																																																																																																																																								
PhCH2OO•	24	23	-0.158713	PhCH2OOH	24	24	-0.162240																																																																																																																																																								
TEMPO•	33	32	-0.219553	TEMPOH	33	33	-0.223080																																																																																																																																																								
•OO•	7	5	-0.040266	HOO•	7	6	-0.043793																																																																																																																																																								
HCO2•	9	8	-0.057313	HCO2H	9	9	-0.060840																																																																																																																																																								

The energies were calculated for a temperature of 298.15 K in the gas phase and the thermal corrections to the enthalpy and Gibb's free energy were obtained at the (U)B3LYP-D3/BASIS level of theory using a scaling factor of 0.960.

References

- [1] D. Šakić, <https://kick.science/KICK.html>.
- [2] "A computational study of the chlorination and hydroxylation of amines by hypochlorous acid", D. Šakić, M. Hanževački, D. M. Smith, V. Vrčec, *Org. Biomol. Chem.* **2015**, *13*, 11740 - 11752.
- [3] V. Korotenko, <https://github.com/vnkorotenko/ess>.
- [4] V. Korotenko, <https://github.com/vnkorotenko/ccs>.
- [5] A. Altun, F. Neese and G. Bistoni, *Beilstein J. Org. Chem.* **2018**, *14*, 919.
- [6] F. Neese and E. F. Valeev *J. Chem. Theory Comput.* **2011**, *7*, 33

Conformational Search

Energy Sorting Script (ESS)

The «Energy Sorting Script» allows you to discard unnecessary calculation results, **possibly** containing repeating structures using energy criterion ($\Delta E_{\text{tot}} > 10^{-7}$ a.u. by default).

Options	
-7	Etot criterion 0.0000001
-6	Etot criterion 0.000001
-5	Etot criterion 0.00001
-4	Etot criterion 0.0001
-3	Etot criterion 0.001
-z	zero criterion (criterion 0 a.u.)
-c	to enter your Etot criterion manually (0.000001 a.u. by default)
-s	to enforce singlet output: $\langle S^2 \rangle = 0.0000$
-lm	Search for local minima (by default)
-ts	Search for transitional states
-a	you need all files in the list (without any exclusion)

The general algorithm of ESS includes the following steps

- 1) Extraction of the most important data from a list of Gaussian-log files: filename, ZPE1, $\delta H.1$, $\delta G.1$, E_{tot} , $\langle S^2 \rangle$, 1-st frequency. Check, if 1-st frequency > 0 .
- 2) Sorting the list of extracted data in ascending order of E_{tot} .
- 3) Comparison by E_{tot} . Each log-file will be compared with the previous one by E_{tot} using the following criterion: If $\Delta E_{\text{tot}} > 10^{-7}$ Hartree (by default) then it makes sense to consider this file. Otherwise: the current file is most likely a “replicant/duplicate”, **possibly** containing the same structure as in previous file.

Benefits:

- Allows you to reduce the number of conformers in the list quickly

Disadvantages:

- The “replicant” structures can still be presented in the list, because this analysis does not take into account geometry:

First example: Geometries can be almost the same, but have slightly different energies due to the difference in the number of geometry-convergence steps or in the number of SCF steps. The second example: a radical particle with the same geometry can have two different wave functions that differ greatly in energy.

- Loss of structures (which is very rare, but possible) with a high conformational lability of the molecule, two different conformers can have almost the same energy (with a difference of less than ΔE_{tot} criterion). In this case, the structure will be eliminated from the list.

Centroid Comparison Script (CCS)

The analysis of certain interatomic distances and visualization of geometry is widely used by chemists all over the world. However, when it comes to a large number of structures and the search for individual conformations among them, "manual" methods take a lot of time and do not exclude human error.

The «Centroid Comparison Script» allows you to discard unnecessary xyz-files or Gaussian log-files, **possibly** containing repeating structures comparing geometries by distances between each atom and centroid point. CCS is applicable only in chemistry, but wherever it comes to searching for individual geometries (just need to change the length units and criterion). (Figure S1 and Figure S2)

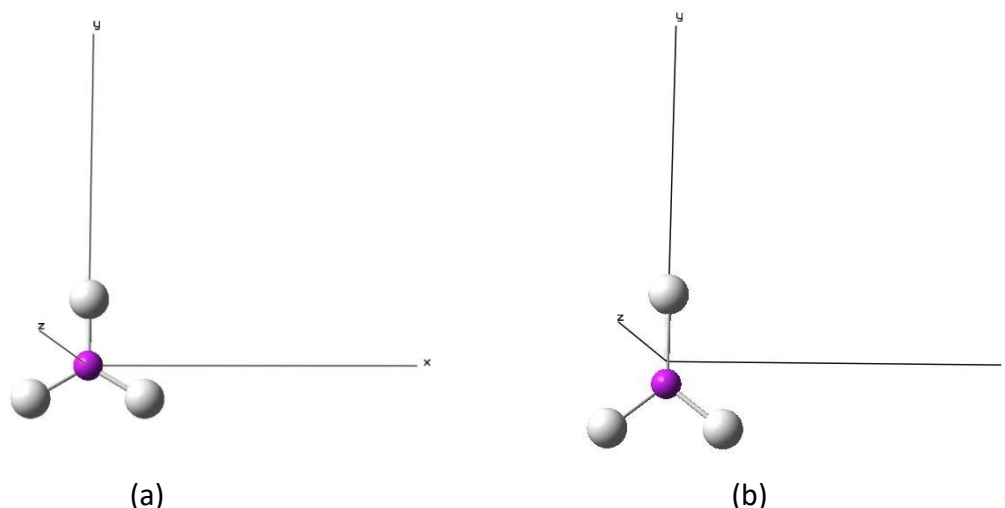


Figure S1. Equilateral (a) and Isosceles triangles (b). The lines correspond distances between triangle-vertices (gray points) and centroid (purple point).

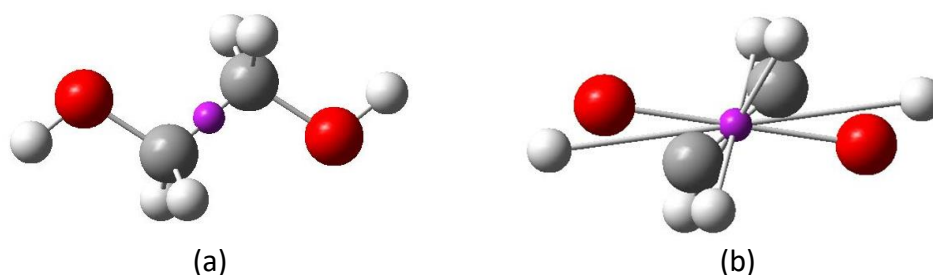


Figure S2. ethylene glycol molecule. The lines correspond to (a) covalent bonds and (b) distances between atoms and centroid (purple point).

Algorithm/Principle	General options:
Sorted Geometries Comparison	<p>1) xyz/log files: create your own “.ccs” input-list file, where the geometries are sorted as you want (by any property). Each geometry will be compared to the previous one ccs ccs -s</p> <p>2) log files: comparison of energy-neighboring geometries (just a special case). In this case, ESS will generate an input-list ess;ccs ess -(option);ccs -(option)</p>

Sorted Geometries Comparison

To start, you need to create a “.ccs” input-list file, where the geometries are sorted as you want (by any property). If you want to make a comparison of energy-neighboring geometries, you need a special input-list, where the geometries are sorted by energy. Such a list can be created using ESS.

In this cases, the algorithm of CCS includes the following steps

1) Reading of the Geometry from each xyz/log file (**G** - matrix). The number of atoms **n** must be the same in all files

$$\mathbf{G} = \begin{bmatrix} x_1 & y_1 & z_1 \\ \dots & \dots & \dots \\ x_i & y_i & z_i \\ x_n & y_n & z_n \end{bmatrix}$$

2) Calculation of Centroid point $C(x_c; y_c; z_c)$ for each geometry:

$$x_c = \frac{\sum_{i=0}^n x_i}{n}$$

$$y_c = \frac{\sum_{i=0}^n y_i}{n}$$

$$z_c = \frac{\sum_{i=0}^n z_i}{n}$$

and definition of **C** – matrix with **n** lines for each geometry:

$$\mathbf{C} = \begin{bmatrix} x_c & y_c & z_c \\ \dots & \dots & \dots \\ x_c & y_c & z_c \\ x_c & y_c & z_c \end{bmatrix}$$

3) Calculation of **L** – matrix for each geometry, which contains «xyz-components of the absolute distance l_i from i th atom to the C_{xyz} point ($i = 1$ to n):

$$\mathbf{L} = |\mathbf{C} - \mathbf{G}| = \begin{bmatrix} x_c & y_c & z_c \\ \dots & \dots & \dots \\ x_c & y_c & z_c \\ x_c & y_c & z_c \end{bmatrix} - \begin{bmatrix} x_1 & y_1 & z_1 \\ \dots & \dots & \dots \\ x_i & y_i & z_i \\ x_n & y_n & z_n \end{bmatrix} = \begin{bmatrix} l_1^x & l_1^y & l_1^z \\ \dots & \dots & \dots \\ l_i^x & l_i^y & l_i^z \\ l_n^x & l_n^y & l_n^z \end{bmatrix}$$

In other words, \mathbf{L} – matrix contains the modulus of the difference in the coordinates of each atom l_i^x, l_i^y, l_i^z ($i = 1$ to n) and coordinates the C_{xyz} point:

$$\begin{aligned} l_i^x &= |x_c - x_i| \\ l_i^y &= |y_c - y_i| \\ l_i^z &= |z_c - z_i| \end{aligned}$$

Which is needed to calculate the distances

$$l_i = \sqrt{(l_i^x)^2 + (l_i^y)^2 + (l_i^z)^2}$$

And to define the \mathbf{l} – column-matrix

$$\mathbf{l} = \begin{bmatrix} l_1 \\ \dots \\ l_i \\ l_n \end{bmatrix}$$

4) Calculation of $\Delta\mathbf{l}$ – column-matrices: $\Delta\mathbf{l}_j = |\mathbf{l}_j - \mathbf{l}_{j-1}|$, where j is the geometry number ($j = 2$ to N , N is the number of geometries). $\Delta\mathbf{l}_j$ – column-matrices will be computed sequentially for $(N - 1)$ geometries.

5) Geometry-individuality criterion. Each considered j -th geometry will be compared with the previous one j -th geometry using the following criterion: If at least one element of $\Delta\mathbf{l}_j$ is > 0.02 Angström, then the j -th geometry can be considered different from the previous one and, therefore, “individual”. Otherwise: the j -th geometry is a “replicant” of previous geometry.

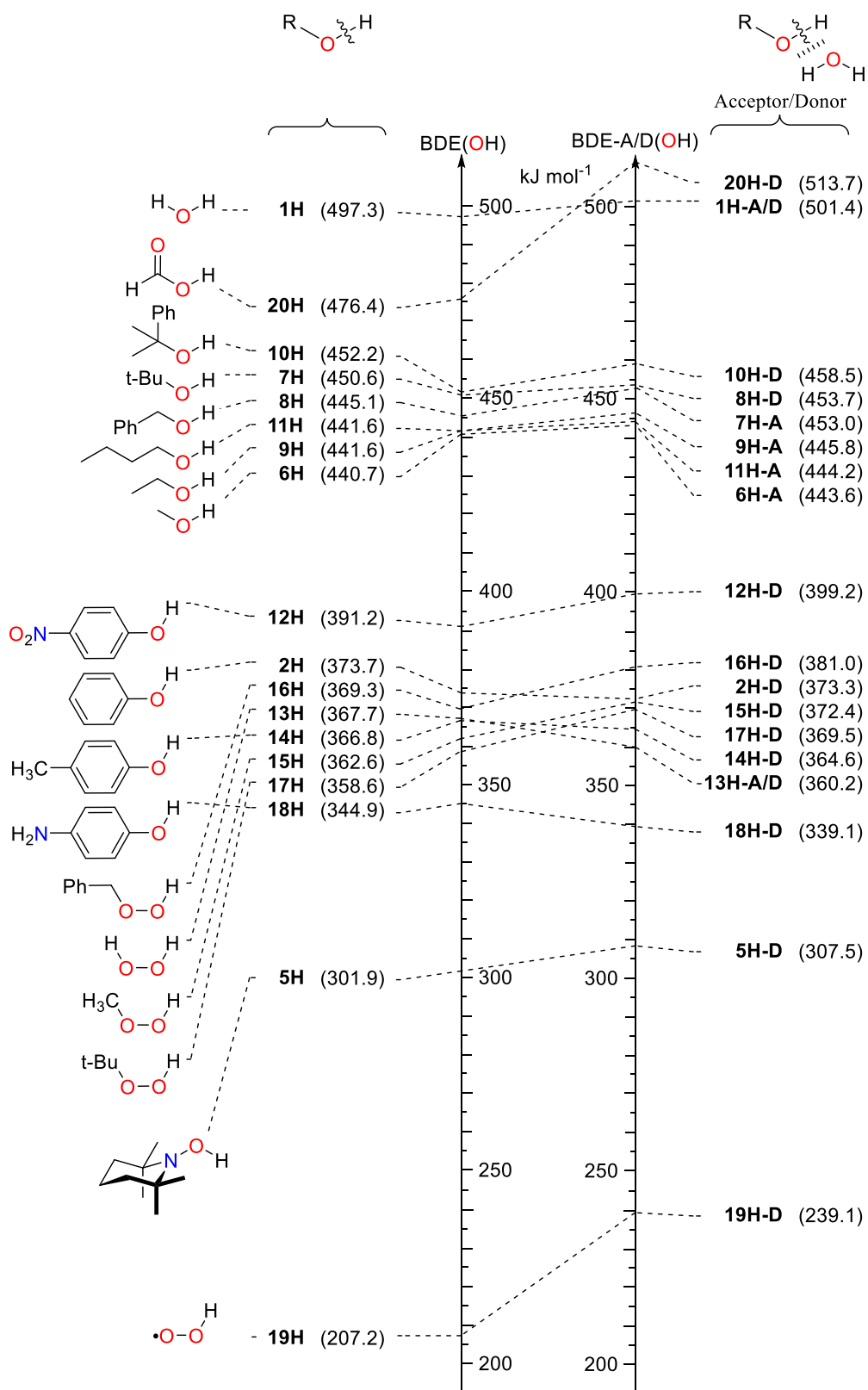


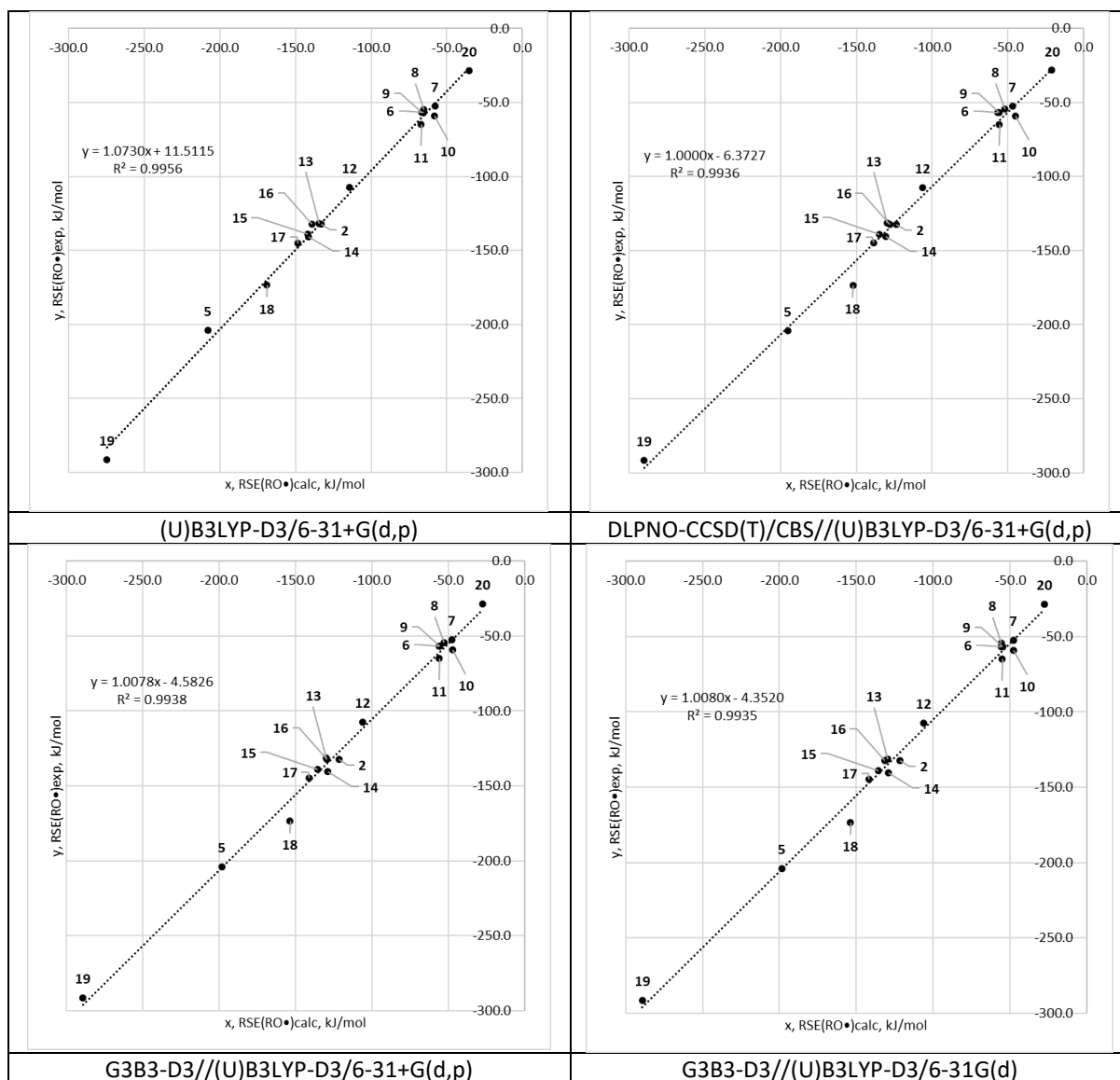
Figure S1.3.1. The calculated BDE(OH) values and the highest BDE-A(OH)/BDE-D(OH) value. (DLPNO-CCSD(T)/CBS)

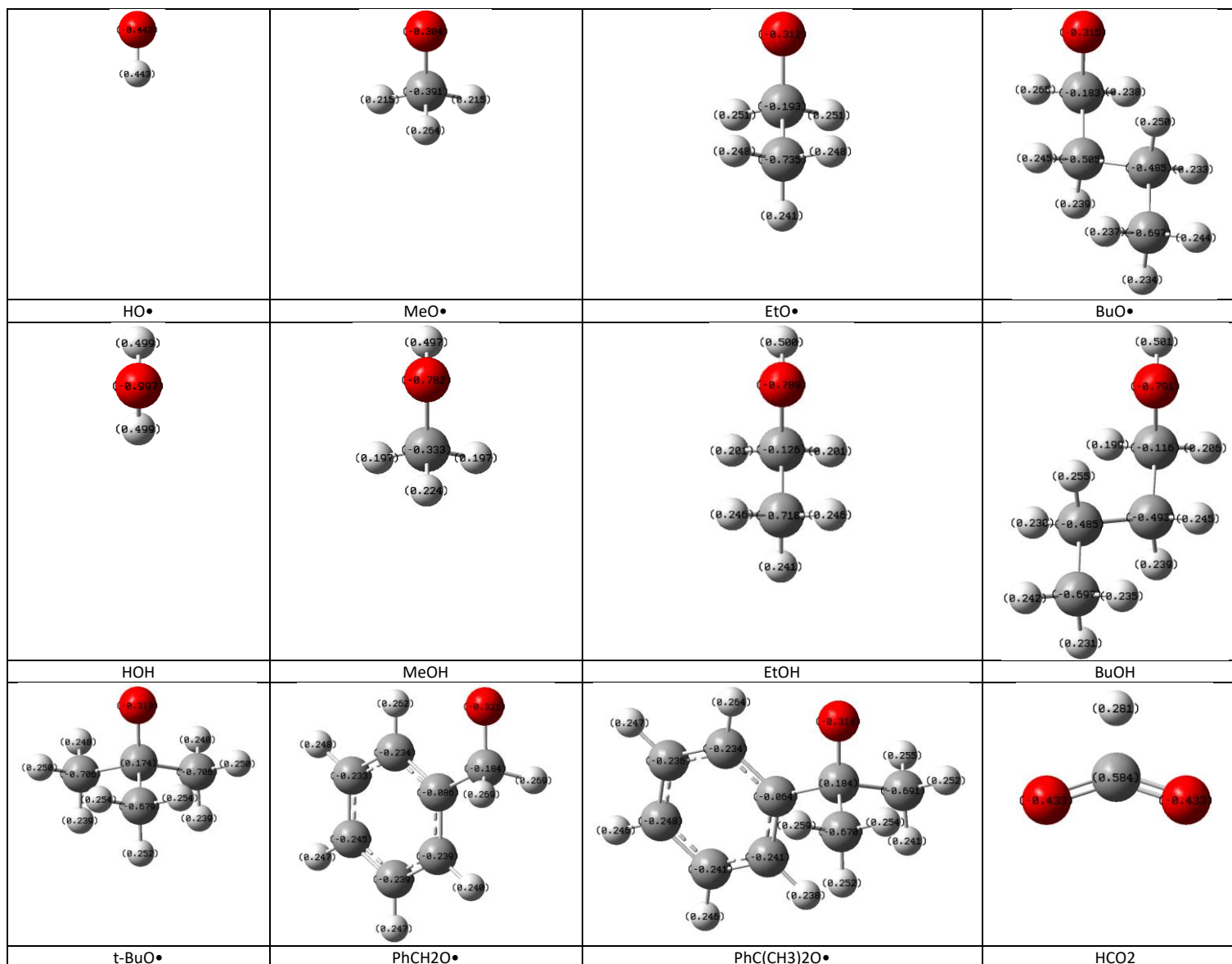
2. No explicit water

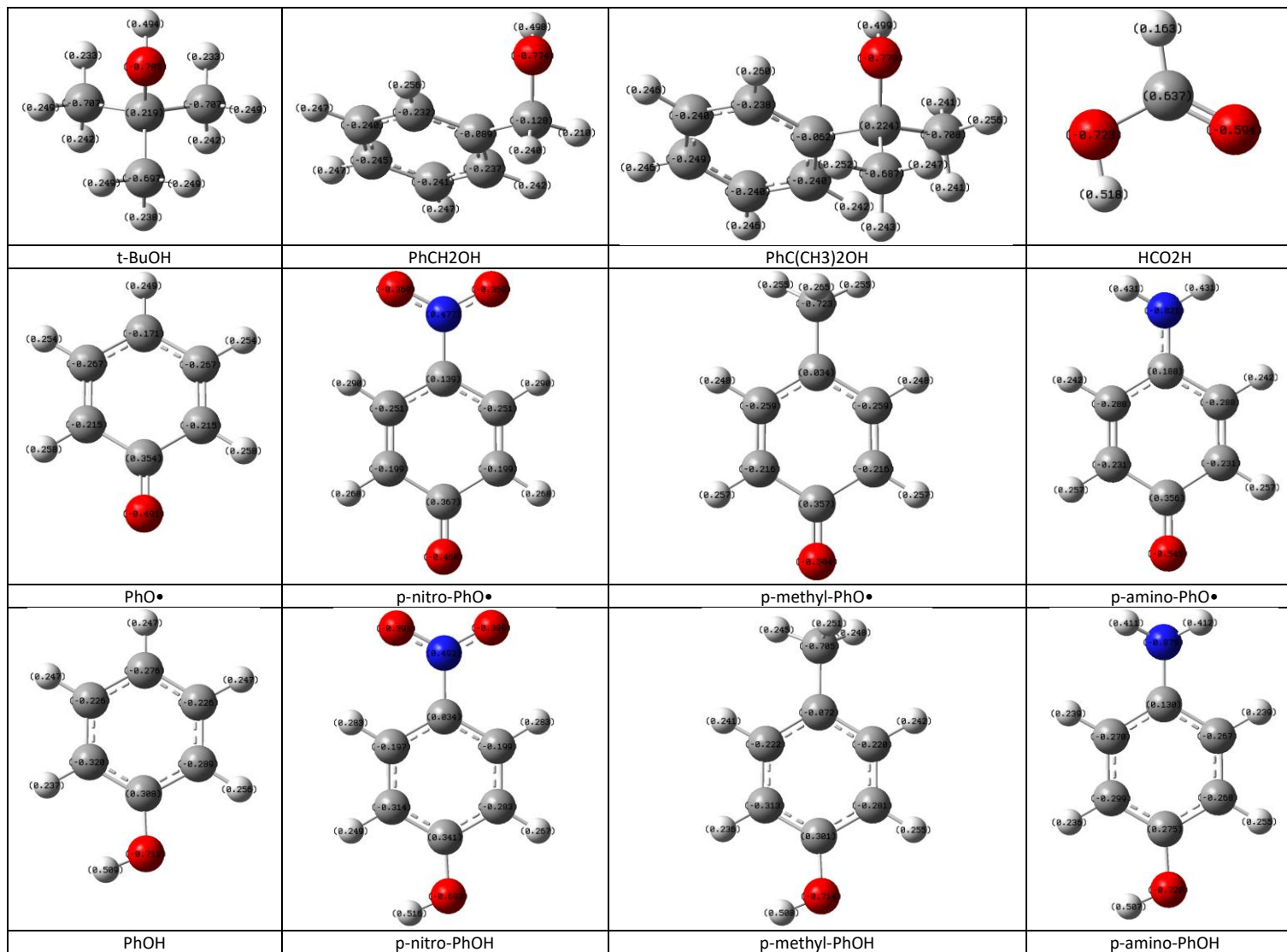
TABLE 2.1.1 RSE(RO•) values for selected O-centered radicals (in kJ mol⁻¹) calculated at various levels of theory together with available experimental data (and the associated BDE(O-H) data) ordered by experimental BDE(RO•) values.

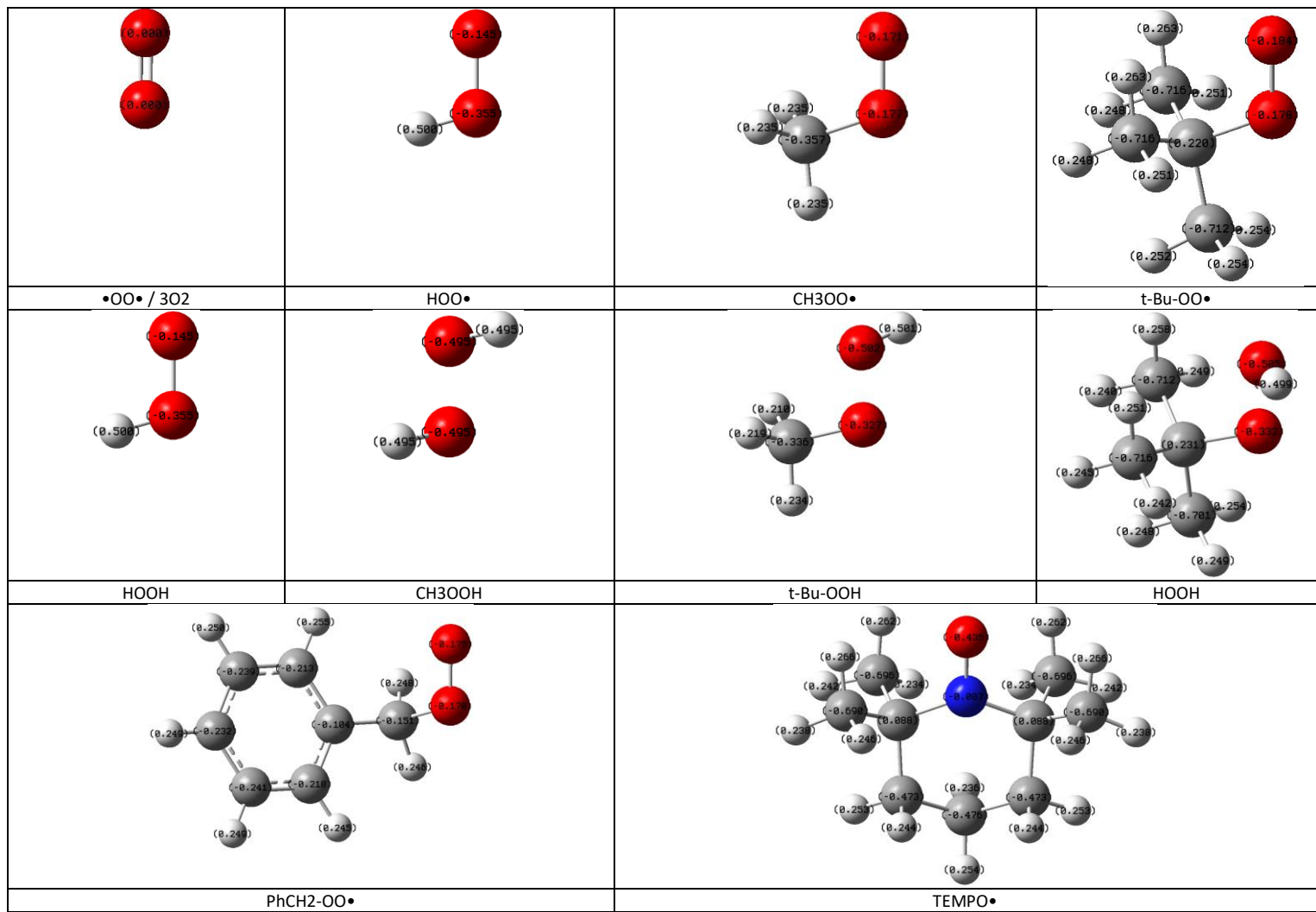
Radical	RSE(RO•)								exp.	BDE(RO•) exp.
	DFT ^[a]	(U)B2PLYP ^[b,c]		DLPNO-CCSD(T) ^[b,c]			G3B3-D3			
		TZ	QZ	TZ	QZ	CBS	^[b]	^[d]		
HO• (1)	0.0	0.0	0.0	0.0	0.0	0.0	0.0	0.0	0.0	+497.3±0.1 ^[13] +497.1±0.3 ^[65]
HC(O)O• (20)	-35.2	-40.0	-43.3	-14.3	-18.6	-20.9	-30.2	-27.6	-28.4±0.6	+468.89±0.56 ^[13]
<i>t</i> -Bu-O• (7)	-57.7	-49.9	-52.3	-42.8	-45.4	-46.7	-47.2	-47.7	-52.4±2.8	+444.9±2.8 ^[50,66] +446.8±4.2 ^[51]
PhCH ₂ O• (8)	-65.0	-57.3	-59.2	-48.4	-50.8	-52.2	-54.8	-55.5	-54.6±8.8	+442.7±8.8 ^[53,66]
CH ₃ O• (6)	-65.3	-58.6	-60.3	-53.4	-55.5	-56.6	-55.3	-55.8	-56.9±0.3	+440.4±0.3 ^[13] +440.2±3.0 ^[51,66] +437.7±2.8 ^[50]
CH ₃ CH ₂ O• (9)	-66.6	-58.7	-60.4	-52.5	-54.6	-55.7	-57.5	-54.8	-56.9±0.5	+440.4±0.5 ^[13] +441.0±5.9 ^[51,66] +438.1±3.3 ^[50]
PhC(CH ₃) ₂ O• (10)	-58.1	-50.5	-53.2	-40.9	-43.7	-45.1	-45.9	-47.8	-59.1±1.0	+438.2±1.0 ^[54,66]
<i>n</i> -Bu-O• (11)	-66.8	-59.1	-61.1	-52.2	-54.5	-55.7	-52.9	-55.3	-65.0	+432.3 ^[52]
<i>p</i> -nitro-PhO• (12)	-114.5	-97.7	-100.8	-100.8	-104.3	-106.1	-113.4	-106.0	-107±8	+390±8 ^[56,15] +396±8 ^[56]
HOO• (13)	-134.4	-133.7	-135.8	-124.9	-128.1	-129.6	-129.2	-129.6	-131.6±0.2	+365.7±0.2 ^[13]
PhO• (2)	-132.9	-114.2	-117.7	-116.3	-121.0	-123.6	-121.1	-121.6	-132.3±0.5	+365±0.5 ^[15] +371.3±2.3 ^[56] +367.1±0.9 ^[13] +362.7±3.0 ^[67]
PhCH ₂ -OO• (16)	-139.0	-136.4	-140.4	-122.1	-125.9	-128.0	-126.5	-131.5	-132.3	+365 ^[61]
CH ₃ OO• (15)	-141.8	-139.4	-142.4	-128.9	-132.8	-134.7	-133.0	-135.8	-138.9±0.7	+358.4±0.7 ^[13] +370.3±2.1 ^[59,66] +367.3±4 ^[60] +357±5 ^[58]
<i>p</i> -methyl-PhO• (14)	-141.3	-122.5	-126.3	-122.5	-127.6	-130.5	-128.8	-129.3	-140.7±0.6	+356.6±0.6 ^[15] +363±4 ^[67]
<i>t</i> -Bu-OO• (17)	-148.5	-145.6	-149.1	-132.7	-136.8	-138.7	-140.8	-141.5	-145±8.8	+352.3±8.8 ^[60,66]
<i>p</i> -amino-PhO• (18)	-168.8	-152.2	-156.1	-143.9	-149.3	-152.4	-153.3	-153.8	-173±13	+324±13 ^[67,15] +331±13 ^[67]
TEMPO (5)	-208.0	-206.4	-210.9	-185.1	-191.7	-195.4	-198.0	-198.4	-204.1±0.4	+293.2±0.4 ^[62] +291.2 ^[63]
³ O ₂ (19)	-274.6	-291.7	-294.4	-283.8	-288.0	-290.1	-289.1	-289.2	-291.5±0.2	+205.8±0.27 ^[13]
MSE	-2.8	3.3	0.4	12.1	8.3	6.4	5.4	5.2		
MUE	5.5	6.6	7.0	12.1	8.3	6.4	5.4	5.3		
R ²	0.9956	0.9823	0.9830	0.9906	0.9926	0.9936	0.9938	0.9935		

[a] "DFT" - (U)B3LYP-D3/6-31+G(d,p); [b] Using (U)B3LYP-D3/6-31+G(d,p) optimized geometries; [c] "TZ, QZ" - cc-pVTZ, cc-pVQZ; [d] Using (U)B3LYP-D3/6-31G(d) optimized geometries.









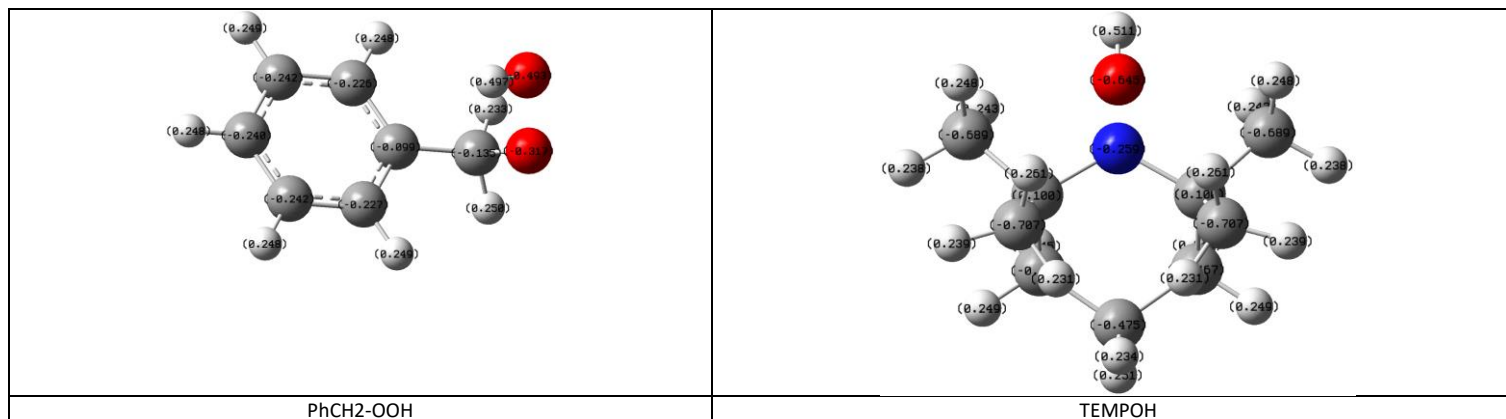


Figure S2.2.1. Calculated at the (U)B3LYP-D3/6-31+G(d,p) level of theory NBO charges (in a.u.). Best by enthalpy structures.

Table S2.3.1. The calculated NBO charges (a.u.) at the (U)B3LYP-D3/6-31+G(d,p) level of theory

$\begin{array}{c} \text{H} \\ \\ \text{R}-\text{O} \\ \text{Alcohol} \end{array}$				$\begin{array}{c} \text{R}-\text{O}\cdot \\ \text{Radical} \end{array}$				$\begin{array}{c} \text{R}-\text{O}\cdot \\ \Delta = \text{Radical} \end{array}$		$\begin{array}{c} \text{H} \\ \\ \text{R}-\text{O} \\ \text{Alcohol} \end{array}$		$\begin{array}{c} \text{H} \\ \\ \text{R}-\text{O} \\ \text{Alcohol} \end{array}$	
								Δ		Δ rel. to HO•		Δ rel. to HOH	
Name	att. atom	O	H	att. atom	O•	H	att. atom	O•/O	O•/O	H			
HOH	(1H)	0.499	-0.997	0.499	0.443	-0.443	-	-0.056	0.554	0.000	0.000		
CH ₃ OH	(6H)	-0.333	-0.782	0.497	-0.391	-0.304	-	-0.058	0.478	-0.076	-0.002		
CH ₃ CH ₂ OH	(9H)	-0.125	-0.789	0.500	-0.193	-0.312	-	-0.068	0.477	-0.077	0.001		
<i>n</i> -Bu-OH	(11H)	-0.116	-0.791	0.501	-0.183	-0.315	-	-0.067	0.476	-0.078	0.002		
<i>t</i> -Bu-OH	(7H)	0.219	-0.785	0.494	0.174	-0.319	-	-0.045	0.466	-0.088	-0.005		
PhCH ₂ OH	(8H)	-0.128	-0.774	0.498	-0.184	-0.321	-	-0.056	0.453	-0.101	-0.001		
PhC(CH ₃) ₂ OH	(10H)	0.224	-0.779	0.499	0.184	-0.314	-	-0.040	0.465	-0.089	0.000		
PhOH	(2H)	0.308	-0.712	0.509	0.354	-0.491	-	0.046	0.221	-0.333	0.010		
<i>p</i> -nitro-PhOH	(12H)	0.341	-0.693	0.516	0.367	-0.460	-	0.026	0.233	-0.321	0.017		
<i>p</i> -methyl-PhOH	(14H)	0.301	-0.714	0.508	0.357	-0.504	-	0.056	0.210	-0.344	0.009		
<i>p</i> -amino-PhOH	(18H)	0.275	-0.720	0.507	0.356	-0.545	-	0.081	0.175	-0.379	0.008		
HOOH	(13H)	-0.495	-0.495	0.495	-0.355	-0.145	-	0.140	0.350	-0.204	-0.004		
CH ₃ OOH	(15H)	-0.327	-0.502	0.501	-0.177	-0.171	-	0.150	0.331	-0.223	0.002		
<i>t</i> -Bu-OOH	(17H)	-0.332	-0.505	0.499	-0.178	-0.184	-	0.154	0.321	-0.233	0.000		
PhCH ₂ OOH	(16H)	-0.317	-0.493	0.497	-0.170	-0.175	-	0.147	0.318	-0.236	-0.002		
TEMPOH	(5H)	-0.259	-0.645	0.511	-0.007	-0.435	-	0.252	0.210	-0.344	0.012		
HOO•	(19H)	-0.145	-0.355	0.500	0.000	0.000	-	0.145	0.355	-0.199	0.001		
HC(O)OH	(20H)	0.637	-0.723	0.518	0.584	-0.433	-	-0.053	0.290	-0.264	0.019		
							Type:	Average values					
							Alkoxy	-0.056	0.469	-0.085	-0.001		
							Aroma	0.052	0.210	-0.344	0.011		
							Peroxy	0.148	0.330	-0.224	-0.001		

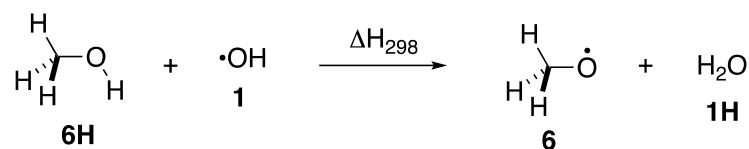


Figure 2.4.06. Reaction of hydroxyl radical (**1**) with methanol (**6H**).

Table S2.4.06a. Radical stabilization energies (RSE values) calculated for the systems shown in Fig. S06.

level of theory	RSE (E_{tot})	RSE (H_{298})	RSE (G_{298})
(U)B3LYP/6-31G(d)	-56.59	-60.86	-63.80
(U)B3LYP-D3/6-31G(d)	-55.41	-59.76	-62.73
(U)B3LYP/6-31+G(d,p)	-61.59	-66.46	-69.27
(U)B3LYP-D3/6-31+G(d,p)	-60.39	-65.35	-68.18
(U)B2PLYP/cc-pVTZ//(U)B3LYP-D3/6-31+G(d,p)	-53.64	-58.60	-61.43
(U)B2PLYP/cc-pVQZ//(U)B3LYP-D3/6-31+G(d,p)	-55.34	-60.30	-63.13
ROB2PLYP/cc-pVTZ//(U)B3LYP-D3/6-31+G(d,p)	-53.04	-57.99	-60.82
ROB2PLYP/cc-pVQZ//(U)B3LYP-D3/6-31+G(d,p)	-54.75	-59.71	-62.54
DLPNO-CCSD(T)/cc-pVTZ//(U)B3LYP-D3/6-31+G(d,p)	-48.42	-53.38	-56.21
DLPNO-CCSD(T)/cc-pVQZ//(U)B3LYP-D3/6-31+G(d,p)	-50.53	-55.49	-58.32
DLPNO-CCSD(T)/CBS//(U)B3LYP-D3/6-31+G(d,p)	-51.67	-56.63	-59.46
G3B3-D3//(U)B3LYP-D3/6-31+G(d,p)	-51.43	-56.19	-58.97
G3B3-D3//(U)B3LYP-D3/6-31G(d)	-51.60	-55.77	-58.70
DLPNO-CCSD(T)/aug-cc-pVTZ//(U)B3LYP-D3/6-31+G(d,p)	-50.47	-55.43	-58.25
DLPNO-CCSD(T)/aug-cc-pVQZ//(U)B3LYP-D3/6-31+G(d,p)	-51.53	-56.49	-59.32
DLPNO-CCSD(T)/CBS//(U)B3LYP-D3/6-31+G(d,p)	-52.19	-57.15	-59.98
exp.^a		-56.96±0.29	

^a Data from ATcT, version 1.122p, **2020**: BDE(O-H,**8H**) = +440.36±0.29 kJ/mol and BDE(O-H,**1H**) = +497.32±0.26 kJ/mol.

Table S2.4.06b. Energy values for all systems shown in Figure 2.4.06.

system	E _{tot} (U)B3LYP/ 6-31G(d)	H ₂₉₈ (U)B3LYP/ 6-31G(d)	G ₂₉₈ (U)B3LYP/ 6-31G(d)	E _{tot} (U)B3LYP-D3/ 6-31G(d)	H ₂₉₈ (U)B3LYP-D3/ 6-31G(d)	G ₂₉₈ (U)B3LYP-D3/ 6-31G(d)	E _{tot} G3B3-D3 ^(a)	H ₂₉₈ G3B3-D3 ^(a)
1H								
HOH	-76.4089533	-76.3840103	-76.4054563	-76.4089616	-76.3840216	-76.4054676	-76.4089616	-76.3840216
6								
CH3O1 (Cs, 2A')	-115.0504625	-115.0097145	-115.0365955	-115.0511257	-115.0104527	-115.0373377	-115.0511257	-115.0104527
1								
HO	-75.7234548	-75.7118458	-75.7320928	-75.7234554	-75.7118464	-75.7320934	-75.7234554	-75.7118464
6H								
CH3OH	-115.7144073	-115.6587003	-115.6856603	-115.7155275	-115.6598675	-115.6868175	-115.7155275	-115.6598675

^(a) Using structures and thermal corrections from gas phase (U)B3LYP-D3/6-31G(d) calculations.**Table S2.4.06c.** Energy values for all systems shown in Figure 2.4.06.

system	E _{tot} (U)B3LYP/ 6-31+G(d,p)	H ₂₉₈ (U)B3LYP/ 6-31+G(d,p)	G ₂₉₈ (U)B3LYP/ 6-31+G(d,p)	E _{tot} (U)B3LYP-D3/ 6-31+G(d,p)	H ₂₉₈ (U)B3LYP-D3/ 6-31+G(d,p)	G ₂₉₈ (U)B3LYP-D3/ 6-31+G(d,p)
1H						
HOH	-76.4340477	-76.4089807	-76.4304097	-76.4340566	-76.4089926	-76.4304206
6						
CH3O1 (Cs, 2A')	-115.0632984	-115.0229614	-115.0498824	-115.0639558	-115.0236958	-115.0506198
1						
HO	-75.7390146	-75.7272716	-75.7475126	-75.7390151	-75.7272721	-75.7475131
6H						
CH3OH	-115.7348716	-115.6793556	-115.7063976	-115.7359964	-115.6805264	-115.7075604

Table S2.4.06d. Energy values for all systems shown in Figure 2.4.06.

system	E_{tot} (U)B2PLYP/ cc-pVTZ ^(a)	E_{tot} (U)B2PLYP/ cc-pVQZ ^(a)	E_{tot} ROB2PLYP/ cc-pVTZ ^(a)	E_{tot} ROB2PLYP/ cc-pVQZ ^(a)	E_{tot} G3B3-D3 ^(a)	H_{298} G3B3-D3 ^(a)
1H						
HOH	-76.4068145	-76.4221036	-76.4068145	-76.4221036	-76.4040880	-76.3798740
6						
CH3O1 (Cs, 2A')	-115.0039947	-115.0220418	-115.0019654	-115.0199688	-115.0011447	-114.9623067
1						
HO	-75.7137796	-75.7266444	-75.7119819	-75.7247971	-75.7044006	-75.6929956
6H						
CH3OH (Cs)	-115.6765979	-115.6964227	-115.6765979	-115.6964227	-115.6812416	-115.6277836

^(a) Using structures and thermal corrections from gas phase (U)B3LYP-D3/6-31+G(d,p) calculations.**Table S2.4.06e.** Energy values for all systems shown in Figure 2.4.06.

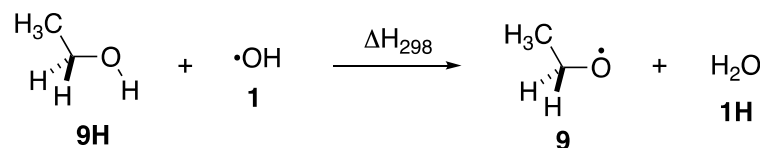
system	E_{tot} DLPNO- CCSD(T)/ cc-pVTZ ^(a)	H_{298} DLPNO- CCSD(T)/ cc-pVTZ ^(a)	E_{tot} DLPNO- CCSD(T)/ cc-pVQZ ^(a)	H_{298} DLPNO- CCSD(T)/ cc-pVQZ ^(a)	E_{tot} DLPNO- CCSD(T)/ CBS ^(a)	H_{298} DLPNO- CCSD(T)/ CBS ^(a)
1H						
HOH	-76.3319273	-76.3068633	-76.3594799	-76.3344159	-76.3759529	-76.3508889
6						
CH3O1 (C2v, 2A1)	-114.8744982	-114.8342382	-114.9095010	-114.8692410	-114.9308974	-114.8906374
1						
HO	-75.6376446	-75.6259016	-75.6612830	-75.6495400	-75.6754790	-75.6637360
6H						
CH3OH_a (Cs)	-115.5503371	-115.4948671	-115.5884523	-115.5329823	-115.6116900	-115.5562200

^(a) Using structures and thermal corrections from gas phase (U)B3LYP-D3/6-31+G(d,p) calculations.

Table S2.4.06f. Energy values for all systems shown in Figure 2.4.06.

system	E_{tot} DLPNO- CCSD(T)/ aug-cc-pVTZ ^(a)	H_{298} DLPNO- CCSD(T)/ aug-cc-pVTZ ^(a)	E_{tot} DLPNO- CCSD(T)/ aug-cc-pVQZ ^(a)	H_{298} DLPNO- CCSD(T)/ aug-cc-pVQZ ^(a)	E_{tot} DLPNO- CCSD(T)/ CBS ^(a)	H_{298} DLPNO- CCSD(T)/ CBS ^(a)
1H						
HOH	-76.3421010	-76.3170370	-76.3633066	-76.3382426	-76.3762075	-76.3511435
6						
CH3O1 (C2v, 2A1)	-114.8845740	-114.8443140	-114.9132689	-114.8730089	-114.9307765	-114.8905165
1						
HO	-75.6455007	-75.6337577	-75.6642373	-75.6524943	-75.6755624	-75.6638194
6H						
CH3OH_a (Cs)	-115.5619522	-115.5064822	-115.5927114	-115.5372414	-115.6115434	-115.5560734

^(a) Using structures and thermal corrections from gas phase (U)B3LYP-D3/6-31+G(d,p) calculations.

**Figure 2.4.09.** Reaction of hydroxyl radical (**1**) with ethanol (**9H**).**Table S2.4.09a.** Radical stabilization energies (RSE values) calculated for the systems shown in Fig. S09.

level of theory	RSE (E_{tot})	RSE (H_{298})	RSE (G_{298})
(U)B3LYP/6-31G(d)	-56.98	-61.65	-66.16
(U)B3LYP-D3/6-31G(d)	-55.05	-59.75	-64.19
(U)B3LYP/6-31+G(d,p)	-62.57	-68.06	-74.83
(U)B3LYP-D3/6-31+G(d,p)	-60.93	-66.59	-75.08

(U)B2PLYP/cc-pVTZ//(U)B3LYP-D3/6-31+G(d,p)	-53.09	-58.74	-67.24
(U)B2PLYP/cc-pVQZ//(U)B3LYP-D3/6-31+G(d,p)	-54.76	-60.41	-68.91
ROB2PLYP/cc-pVTZ//(U)B3LYP-D3/6-31+G(d,p)	-52.44	-58.10	-66.59
ROB2PLYP/cc-pVQZ//(U)B3LYP-D3/6-31+G(d,p)	-54.12	-59.78	-68.28
DLPNO-CCSD(T)/cc-pVTZ//(U)B3LYP-D3/6-31+G(d,p)	-46.89	-52.54	-61.04
DLPNO-CCSD(T)/cc-pVQZ//(U)B3LYP-D3/6-31+G(d,p)	-48.98	-54.63	-63.13
DLPNO-CCSD(T)/CBS//(U)B3LYP-D3/6-31+G(d,p)	-50.09	-55.75	-64.24
G3B3-D3//(U)B3LYP-D3/6-31+G(d,p)	-50.25	-55.63	-64.13
G3B3-D3//(U)B3LYP-D3/6-31G(d)	-50.41	-54.82	-59.02
exp.^a		-56.90±0.47	

^a Data from ATcT, version 1.122p, **2020**: BDE(O-H,**9H**) = +440.4±0.47 kJ/mol and BDE(O-H,**1H**) = +497.3±0.26 kJ/mol.

Table S2.4.09b. Energy values for all systems shown in Figure 2.4.09.

system	E _{tot} (U)B3LYP/ 6-31G(d)	H ₂₉₈ (U)B3LYP/ 6-31G(d)	G ₂₉₈ (U)B3LYP/ 6-31G(d)	E _{tot} (U)B3LYP-D3/ 6-31G(d)	H ₂₉₈ (U)B3LYP-D3/ 6-31G(d)	G ₂₉₈ (U)B3LYP-D3/ 6-31G(d)	E _{tot} G3B3-D3 ^(a)	H ₂₉₈ G3B3-D3 ^(a)
1H								
HOH	-76.4089533	-76.3840103	-76.4054563	-76.4089616	-76.3840216	-76.4054676	-76.4089616	-76.3840216
6								
CH3CH2O1	-154.3704925	-154.3000375	-154.3310565	-154.3730829	-154.3026259	-154.3335789	-154.3730829	-154.3026259
1								
HO	-75.7234548	-75.7118458	-75.7320928	-75.7234554	-75.7118464	-75.7320934	-75.7234554	-75.7118464
6H								
CH3CH2OH2	-155.0342872	-154.9487212	-154.9792212	-155.0376201	-154.9520431	-154.9825051	-155.0376201	-154.9520431
CH3CH2OH1	-155.0338010	-154.9482710	-154.9788490	-155.0370190	-154.9514750	-154.9820180	-155.0370190	-154.9514750

^(a) Using structures and thermal corrections from gas phase (U)B3LYP-D3/6-31G(d) calculations.**Table S2.4.09c.** Energy values for all systems shown in Figure 2.4.09.

system	E _{tot} (U)B3LYP/ 6-31+G(d,p)	H ₂₉₈ (U)B3LYP/ 6-31+G(d,p)	G ₂₉₈ (U)B3LYP/ 6-31+G(d,p)	E _{tot} (U)B3LYP-D3/ 6-31+G(d,p)	H ₂₉₈ (U)B3LYP-D3/ 6-31+G(d,p)	G ₂₉₈ (U)B3LYP-D3/ 6-31+G(d,p)
1H						
HOH	-76.4340477	-76.4089807	-76.4304097	-76.4340566	-76.4089926	-76.4304206
9						
CH3CH2O1 (Cs, 2A'')	-154.3867795	-154.3170895	-154.3491505	-154.3893563	-154.3197153	-154.3523993
aco_046 (C1)	-154.3867916	-154.318040 (imag=-32 cm ⁻¹)	-154.348421	-154.3893683	-154.320652 (imag=-94 cm ⁻¹)	-154.351032
aco_048 (Cs, 2A')	-154.3851784	-154.314233	-154.344918	-154.3879434	-154.316939	-154.347572
1						
HO	-75.7390146	-75.7272716	-75.7475126	-75.7390151	-75.7272721	-75.7475131
9H						
CH3CH2OH2	-155.0579793	-154.9728763	-155.0035473	-155.0611896	-154.9760736	-155.0067086
CH3CH2OH1	-155.0578617	-154.9727427	-155.0033617	-155.0611891	-154.9760591	-155.0066361

Table S2.4.09d. Energy values for all systems shown in Figure 2.4.09.

system	E_{tot} (U)B2PLYP/ cc-pVTZ ^(a)	E_{tot} (U)B2PLYP/ cc-pVQZ ^(a)	E_{tot} ROB2PLYP/ cc-pVTZ ^(a)	E_{tot} ROB2PLYP/ cc-pVQZ ^(a)	E_{tot} G3B3-D3 ^(a)	H_{298} G3B3-D3 ^(a)
1H						
HOH	-76.4068145	-76.4221036	-76.4068145	-76.4221036	-76.4040880	-76.3798740
9						
CH3CH2O1 (Cs, 2A'')	-154.2971560	-154.3207632	-154.2951120	-154.3186759	-154.3047057	-154.2375537
1						
HO	-75.7137796	-75.7266444	-75.7119819	-75.7247971	-75.7044006	-75.6929956
9H						
CH3CH2OH2	-154.9699707	-154.9953673	-154.9699707	-154.9953673	-154.9852549	-154.9032439
CH3CH2OH1	-154.9699405	-154.9951846	-154.9699405	-154.9951846	-154.9850646	-154.9030416

^(a) Using structures and thermal corrections from gas phase (U)B3LYP-D3/6-31+G(d,p) calculations.

Table S2.4.09e. Energy values for all systems shown in Figure 2.4.09.

system	E_{tot} DLPNO- CCSD(T)/ cc-pVTZ ^(a)	H_{298} DLPNO- CCSD(T)/ cc-pVTZ ^(a)	E_{tot} DLPNO- CCSD(T)/ cc-pVQZ ^(a)	H_{298} DLPNO- CCSD(T)/ cc-pVQZ ^(a)	E_{tot} DLPNO- CCSD(T)/ CBS ^(a)	H_{298} DLPNO- CCSD(T)/ CBS ^(a)
1H						
HOH	-76.3319273	-76.3068633	-76.3594799	-76.3344159	-76.3759529	-76.3508889
9						
CH3CH2O1	-154.1182432	-154.0486022	-154.1647101	-154.0950691	-154.1933252	-154.1236842
1						
HO	-75.6376446	-75.6259016	-75.6612830	-75.6495400	-75.6754790	-75.6637360
9H						
CH3CH2OH2	-154.7946678	-154.7095518	-154.8442520	-154.7591360	-154.8747197	-154.7896037
CH3CH2OH1	-154.7946648	-154.7095348	-154.8441048	-154.7589748	-154.8744933	-154.7893633

^(a) Using structures and thermal corrections from gas phase (U)B3LYP-D3/6-31+G(d,p) calculations.

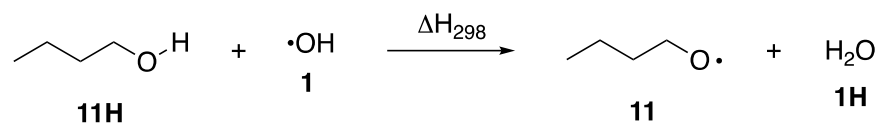


Figure 2.4.11. Reaction of hydroxyl radical (**1**) with butan-1-ol (**11H**).

Table S2.4.11a. Radical stabilization energies (RSE values) calculated for the systems shown in Fig. S11.

level of theory	RSE (E_{tot})	RSE (H_{298})	RSE (G_{298})
(U)B3LYP/6-31G(d)	-58.13	-62.37	-66.29
(U)B3LYP-D3/6-31G(d)	-55.81	-60.05	-63.91
(U)B3LYP/6-31+G(d,p)	-63.76	-68.53	-72.76
(U)B3LYP-D3/6-31+G(d,p)	-61.86	-66.82	-70.90
(U)B2PLYP/cc-pVTZ//(U)B3LYP-D3/6-31+G(d,p)	-54.16	-59.08	-63.14
(U)B2PLYP/cc-pVQZ//(U)B3LYP-D3/6-31+G(d,p)	-56.12	-61.09	-65.17
ROB2PLYP/cc-pVTZ//(U)B3LYP-D3/6-31+G(d,p)	-53.50	-58.42	-62.48
ROB2PLYP/cc-pVQZ//(U)B3LYP-D3/6-31+G(d,p)	-55.48	-60.44	-64.52
DLPNO-CCSD(T)/cc-pVTZ//(U)B3LYP-D3/6-31+G(d,p)	-47.26	-52.18	-56.24
DLPNO-CCSD(T)/cc-pVQZ//(U)B3LYP-D3/6-31+G(d,p)	-49.57	-54.53	-58.61
DLPNO-CCSD(T)/CBS//(U)B3LYP-D3/6-31+G(d,p)	-50.69	-55.65	-59.73
G3B3-D3//(U)B3LYP-D3/6-31+G(d,p)	-51.32	-56.06	-60.12
G3B3-D3//(U)B3LYP-D3/6-31G(d)	-51.33	-55.29	-58.85
exp.^a		-65.0	

^a Data from Luo: BDE(O-H,**10H**) = 432.3 kJ/mol and BDE(O-H,**1H**) = +497.3±0.26 kJ/mol.

Table S2.4.11b. Energy values for all systems shown in Figure 2.4.11.

system	E _{tot} (U)B3LYP/ 6-31G(d)	H ₂₉₈ (U)B3LYP/ 6-31G(d)	G ₂₉₈ (U)B3LYP/ 6-31G(d)	E _{tot} (U)B3LYP-D3/ 6-31G(d)	H ₂₉₈ (U)B3LYP-D3/ 6-31G(d)	G ₂₉₈ (U)B3LYP-D3/ 6-31G(d)	E _{tot} G3B3-D3 ^(a)	H ₂₉₈ G3B3-D3 ^(a)
1H								
HOH	-76.4089533	-76.3840103	-76.4054563	-76.4089616	-76.3840216	-76.4054676	-76.4089616	-76.3840216
6								
BuO2	-232.9987830	-232.8681760	-232.9059800	-233.0069065	-232.8761235	-232.9137135	-233.0069065	-232.8761235
BuO1	-232.9980840	-232.8675370	-232.9056420	-233.0065627	-232.8755107	-232.9126417	-233.0065627	-232.8755107
BuO3	-232.9977243	-232.8668453	-232.9046183	-233.0062990	-232.8752520	-232.9129010	-233.0062990	-232.8752520
BuO4	-232.9977207	-232.8668297	-232.9042277	-233.0059762	-232.8752722	-232.9131782	-233.0059762	-232.8752722
BuO5	-232.9969602	-232.8660772	-232.9039222	-233.0052939	-232.8742469	-232.9118869	-233.0052939	-232.8742469
1								
HO	-75.7234548	-75.7118458	-75.7320928	-75.7234554	-75.7118464	-75.7320934	-75.7234554	-75.7118464
6H								
BuOH1a	-233.6621392	-233.5165842	-233.5540952	-233.6711543	-233.5254253	-233.5627453	-233.6711543	-233.5254253
BuOH3a	-233.6617267	-233.5161497	-233.5539047	-233.6708159	-233.5250509	-233.5625299	-233.6708159	-233.5250509
BuOH4d	-233.6617348	-233.5161358	-233.5537578	-233.6706388	-233.5247928	-233.5622398	-233.6706388	-233.5247928
BuOH8b	-233.6614778	-233.5159728	-233.5535948	-233.6704040	-233.5246490	-233.5622080	-233.6704040	-233.5246490
BuOH7b	-233.6610820	-233.5155740	-233.5534160	-233.6702934	-233.5246134	-233.5620404	-233.6702934	-233.5246134
BuOH5c	-233.6611277	-233.5155037	-233.5531677	-233.6701375	-233.5243535	-233.5614555	-233.6701375	-233.5243535
BuOH2b	-233.6604354	-233.5148584	-233.5522204	-233.6700435	-233.5242295	-233.5615375	-233.6700435	-233.5242295
BuOH6b	-233.6604228	-233.5148118	-233.5525458	-233.6696355	-233.5239465	-233.5615925	-233.6696355	-233.5239465
BuOH9b	-233.6603463	-233.5147843	-233.5527183	-233.6696134	-233.5238694	-233.5615234	-233.6696134	-233.5238694
BuOH11d	-233.6603144	-233.5147744	-233.5526024	-233.6695075	-233.5237015	-233.5612005	-233.6695075	-233.5237015
BuOH10d	-233.6602097	-233.5146347	-233.5525017	-233.6692881	-233.5235221	-233.5611611	-233.6692881	-233.5235221
BuOH13c	-233.6596674	-233.5141594	-233.5520504	-233.6687985	-233.5231165	-233.5605805	-233.6687985	-233.5231165
BuOH12c	-233.6594432	-233.5139442	-233.5516212	-233.6686221	-233.5229191	-233.5605821	-233.6686221	-233.5229191
BuOH14b	-233.6588521	-233.5132181	-233.5506531	-233.6685382	-233.5227432	-233.5599272	-233.6685382	-233.5227432

^(a) Using structures and thermal corrections from gas phase (U)B3LYP-D3/6-31G(d) calculations.

Table S2.4.11c. Energy values for all systems shown in Figure 2.4.11.

system	E _{tot} (U)B3LYP/	H ₂₉₈ (U)B3LYP/	G ₂₉₈ (U)B3LYP/	E _{tot} (U)B3LYP-D3/	H ₂₉₈ (U)B3LYP-D3/	G ₂₉₈ (U)B3LYP-D3/
--------	-------------------------------	-------------------------------	-------------------------------	----------------------------------	----------------------------------	----------------------------------

	6-31+G(d,p)	6-31+G(d,p)	6-31+G(d,p)	6-31+G(d,p)	6-31+G(d,p)	6-31+G(d,p)
1H						
HOH	-76.4340477	-76.4089807	-76.4304097	-76.4340566	-76.4089926	-76.4304206
11						
BuO2	-233.0217124	-232.8921674	-232.9302304	-233.0297641	-232.9001131	-232.9380521
BuO1	-233.0214397	-232.8919897	-232.9305047	-233.0293178	-232.8997018	-232.9379428
BuO3	-233.0204473	-232.8907043	-232.9286873	-233.0291945	-232.8990965	-232.9362975
BuO4	-233.0203871	-232.8904551	-232.9279411	-233.0289513	-232.8990383	-232.9368183
BuO5	-233.0201910	-232.8903140	-232.9282720	-233.0285104	-232.8984694	-232.9362054
1						
HO	-75.7390146	-75.7272716	-75.7475126	-75.7390151	-75.7272721	-75.7475131
11H						
BuOH1a	-233.6924589	-233.5477729	-233.5855489	-233.7012452	-233.5563822	-233.5939542
BuOH3a	-233.6924131	-233.5476431	-233.5855601	-233.7011493	-233.5563023	-233.5938833
BuOH4d	-233.6923781	-233.5476731	-233.5856881	-233.7011378	-233.5562348	-233.5938448
BuOH8b	-233.6922101	-233.5475401	-233.5853211	-233.7010850	-233.5561360	-233.5938480
BuOH7b	-233.6920950	-233.5473680	-233.5851510	-233.7009170	-233.5560300	-233.5938400
BuOH5c	-233.6911913	-233.5464723	-233.5843093	-233.7004921	-233.5555171	-233.5931101
BuOH2b	-233.6910875	-233.5463215	-233.5842075	-233.7004379	-233.5555169	-233.5931219
BuOH6b	-233.6909736	-233.5461846	-233.5841036	-233.7002095	-233.5552895	-233.5929505
BuOH9b	-233.6908362	-233.5461362	-233.5842032	-233.7000503	-233.5550603	-233.5927253
BuOH11d	-233.6907994	-233.5460374	-233.5840814	-233.6998676	-233.5549106	-233.5927036
BuOH10d	-233.6906130	-233.5459200	-233.5838340	-233.6997775	-233.5548785	-233.5926975
BuOH13c	-233.6898427	-233.5451917	-233.5830827	-233.6993142	-233.5544542	-233.5919492
BuOH12c	-233.6897395	-233.5450705	-233.5828115	-233.6991397	-233.5543017	-233.5919787
BuOH14b	-233.6889250	-233.5441750	-233.5817330	-233.6985592	-233.5536582	-233.5910272

^(a) Using structures and thermal corrections from gas phase (U)B3LYP-D3/6-31+G(d,p) calculations.

Table S2.4.11d. Energy values for all systems shown in Figure 2.4.11.

system	E _{tot} (U)B2PLYP/ cc-pVTZ ^(a)	E _{tot} (U)B2PLYP/ cc-pVQZ ^(a)	E _{tot} ROB2PLYP/ cc-pVTZ ^(a)	E _{tot} ROB2PLYP/ cc-pVQZ ^(a)	E _{tot} G3B3-D3 ^(a)	H ₂₉₈ G3B3-D3 ^(a)
1H						
HOH	-76.4068145	-76.4221036	-76.4068145	-76.4221036	-76.4040880	-76.3798740
11						
BuO2	-232.8733134	-232.9081892	-232.8712630	-232.9060968	-232.9035794	-232.7786424
BuO1	-232.8727876	-232.9077365	-232.8707404	-232.9056479	-232.9030192	-232.7781122
BuO4	-232.8723463	-232.9071420	-232.8702949	-232.9050508	-232.9028292	-232.7776482
BuO3	-232.8721355	-232.9069549	-232.8700752	-232.9048532	-232.9028110	-232.7774600
BuO5	-232.8716952	-232.9066543	-232.8696505	-232.9045687	-232.9022632	-232.7769612
1						
HO	-75.7137796	-75.7266444	-75.7119819	-75.7247971	-75.7044006	-75.6929956
11H						
BuOH3a	-233.5457192	-233.5820935	-233.5457192	-233.5820935	-233.5837189	-233.4441669
BuOH1a	-233.5456783	-233.5822729	-233.5456783	-233.5822729	-233.5834397	-233.4439037
BuOH8b	-233.5454449	-233.5820545	-233.5454449	-233.5820545	-233.5833682	-233.4437772
BuOH7b	-233.5453002	-233.5820542	-233.5453002	-233.5820542	-233.5832980	-233.4437210
BuOH5c	-233.5448676	-233.5812089	-233.5448676	-233.5812089	-233.5833293	-233.4436923
BuOH2b	-233.5447033	-233.5812766	-233.5447033	-233.5812766	-233.5831367	-233.4435297
BuOH6b	-233.5442216	-233.5807083	-233.5442216	-233.5807083	-233.5829271	-233.4432701
BuOH9b	-233.5441709	-233.5807769	-233.5441709	-233.5807769	-233.5825409	-233.4429349
BuOH11d	-233.5439692	-233.5805607	-233.5439692	-233.5805607	-233.5823455	-233.4426705
BuOH10d	-233.5439524	-233.5806799	-233.5439524	-233.5806799	-233.5822416	-233.4426536
BuOH13c	-233.5436734	-233.5797188	-233.5436734	-233.5797188	-233.5821199	-233.4424759
BuOH12c	-233.5434557	-233.5797732	-233.5434557	-233.5797732	-233.5813472	-233.4418192
BuOH14b	-233.5425506	-233.5789423	-233.5425506	-233.5789423	-233.5812418	-233.4416938
BuOH4d	-233.5454460	-233.5819698	-233.5454460	-233.5819698	-233.5806613	-233.4410733

^(a) Using structures and thermal corrections from gas phase (U)B3LYP-D3/6-31+G(d,p) calculations.

Table S2.4.11e. Energy values for all systems shown in Figure 2.4.11.

system	E _{tot} DLPNO- CCSD(T)/ cc-pVTZ ^(a)	H ₂₉₈ DLPNO- CCSD(T)/ cc-pVTZ ^(a)	E _{tot} DLPNO- CCSD(T)/ cc-pVQZ ^(a)	H ₂₉₈ DLPNO- CCSD(T)/ cc-pVQZ ^(a)	E _{tot} DLPNO- CCSD(T)/ CBS ^(a)	H ₂₉₈ DLPNO- CCSD(T)/ CBS ^(a)
1H						
HOH	-76.3319273	-76.3068633	-76.3594799	-76.3344159	-76.3759529	-76.3508889
11						
BuO2	-232.5974867	-232.4678357	-232.6668970	-232.5372460	-232.7099355	-232.5802845
BuO1	-232.5968699	-232.4672539	-232.6663850	-232.5367690	-232.7094682	-232.5798522
BuO4	-232.5967538	-232.4668408	-232.6661280	-232.5362150	-232.7091664	-232.5792534
BuO3	-232.5964513	-232.4663533	-232.6659109	-232.5358129	-232.7090021	-232.5789041
BuO5	-232.5960289	-232.4659879	-232.6655576	-232.5355166	-232.7086471	-232.5786061
1						
HO	-75.6376446	-75.6259016	-75.6612830	-75.6495400	-75.6754790	-75.6637360
11H						
BuOH3a	-233.2737701	-233.1289231	-233.3460570	-233.2012100	-233.3908444	-233.2459974
BuOH1a	-233.2737260	-233.1288630	-233.3462147	-233.2013517	-233.3911029	-233.2462399
BuOH4d	-233.2735506	-233.1286476	-233.3459832	-233.2010802	-233.3908254	-233.2459224
BuOH8b	-233.2734356	-233.1284866	-233.3459396	-233.2009906	-233.3908047	-233.2458557
BuOH7b	-233.2732629	-233.1283759	-233.3459134	-233.2010264	-233.3908625	-233.2459755
BuOH5c	-233.2732046	-233.1282296	-233.3454552	-233.2004802	-233.3902274	-233.2452524
BuOH2b	-233.2730703	-233.1281493	-233.3455324	-233.2006114	-233.3904093	-233.2454883
BuOH6b	-233.2726810	-233.1277610	-233.3450941	-233.2001741	-233.3899345	-233.2450145
BuOH9b	-233.2724105	-233.1274205	-233.3449075	-233.1999175	-233.3897679	-233.2447779
BuOH11d	-233.2721929	-233.1272359	-233.3446828	-233.1997258	-233.3895435	-233.2445865
BuOH10d	-233.2721762	-233.1272772	-233.3447944	-233.1998954	-233.3897273	-233.2448283
BuOH13c	-233.2719398	-233.1270798	-233.3439269	-233.1990669	-233.3885970	-233.2437370
BuOH12c	-233.2716520	-233.1268140	-233.3438979	-233.1990599	-233.3886942	-233.2438562
BuOH14b	-233.2709413	-233.1260403	-233.3432681	-233.1983671	-233.3880658	-233.2431648

^(a) Using structures and thermal corrections from gas phase (U)B3LYP-D3/6-31+G(d,p) calculations.

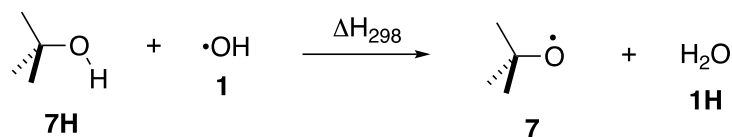


Figure 2.4.07. Reaction of hydroxyl radical (1) with *tert*-butanol (7H).

Table S2.4.07a. Radical stabilization energies (RSE values) calculated for the systems shown in Fig. S07.

level of theory	RSE (E_{tot})	RSE (H_{298})	RSE (G_{298})
(U)B3LYP/6-31G(d)	-54.34	-54.46	-58.70
(U)B3LYP-D3/6-31G(d)	-51.81	-52.05	-56.28
(U)B3LYP/6-31+G(d,p)	-59.78	-60.10	-64.09
(U)B3LYP-D3/6-31+G(d,p)	-57.25	-57.69	-61.71
(U)B2PLYP/cc-pVTZ//((U)B3LYP-D3/6-31+G(d,p)	-49.48	-49.92	-53.93
(U)B2PLYP/cc-pVQZ//((U)B3LYP-D3/6-31+G(d,p)	-51.82	-52.26	-56.28
ROB2PLYP/cc-pVTZ//((U)B3LYP-D3/6-31+G(d,p)	-49.02	-49.46	-53.48
ROB2PLYP/cc-pVQZ//((U)B3LYP-D3/6-31+G(d,p)	-51.40	-51.83	-55.85
DLPNO-CCSD(T)/cc-pVTZ//((U)B3LYP-D3/6-31+G(d,p)	-42.34	-42.78	-46.80
DLPNO-CCSD(T)/cc-pVQZ//((U)B3LYP-D3/6-31+G(d,p)	-44.98	-45.41	-49.43
DLPNO-CCSD(T)/CBS//((U)B3LYP-D3/6-31+G(d,p)	-46.31	-46.75	-50.77
G3B3-D3//((U)B3LYP-D3/6-31+G(d,p)	-47.41	-47.83	-51.80
G3B3-D3//((U)B3LYP-D3/6-31G(d)	-47.49	-47.72	-51.90
exp.^a		-52.4±2.8	

^a Data from Y. R. Luo, *Comprehensive Handbook of Chemical Bond Energies*, CRC Press, 2007: BDE(O-H, **7H**) = +444.9±2.8 kJ/mol, and BDE(O-H, **1H**) = +497.3±0.26 kJ/mol from ATcT, version 1.122p, 2020.

Table S2.4.07b. Energy values for all systems shown in Figure 2.4.07.

system	E _{tot} (U)B3LYP/ 6-31G(d)	H ₂₉₈ (U)B3LYP/ 6-31G(d)	G ₂₉₈ (U)B3LYP/ 6-31G(d)	E _{tot} (U)B3LYP-D3/ 6-31G(d)	H ₂₉₈ (U)B3LYP-D3/ 6-31G(d)	G ₂₉₈ (U)B3LYP-D3/ 6-31G(d)	E _{tot} G3B3-D3 ^(a)	H ₂₉₈ G3B3-D3 ^(a)
1H								
HOH	-76.4089533	-76.3840103	-76.4054563	-76.4089616	-76.3840216	-76.4054676	-76.4089616	-76.3840216
6								
t-BuO2	-233.0061692	-232.8756412	-232.9126312	-233.0157245	-232.8849935	-232.9217565	-233.0157245	-232.8849935
1								
HO	-75.7234548	-75.7118458	-75.7320928	-75.7234554	-75.7118464	-75.7320934	-75.7234554	-75.7118464
6H								
t-BuOH	-233.6709712	-233.5270612	-233.5636382	-233.6814959	-233.5373449	-233.5736929	-233.6814959	-233.5373449

^(a) Using structures and thermal corrections from gas phase (U)B3LYP-D3/6-31G(d) calculations.**Table S2.4.07c.** Energy values for all systems shown in Figure 2.4.07.

system	E _{tot} (U)B3LYP/ 6-31+G(d,p)	H ₂₉₈ (U)B3LYP/ 6-31+G(d,p)	G ₂₉₈ (U)B3LYP/ 6-31+G(d,p)	E _{tot} (U)B3LYP-D3/ 6-31+G(d,p)	H ₂₉₈ (U)B3LYP-D3/ 6-31+G(d,p)	G ₂₉₈ (U)B3LYP-D3/ 6-31+G(d,p)
1H						
HOH	-76.4340477	-76.4089807	-76.4304097	-76.4340566	-76.4089926	-76.4304206
7						
t-BuO2 (Cs, 2A')	-233.0294718	-232.8998388	-232.9368568	-233.0390287	-232.9091897	-232.9459787
aco_025 (Cs, 2A'')	-233.0290142	-232.900906 (imag=-541 cm ⁻¹)	-232.937476	-233.0385699	-232.910266 (imag=-545 cm ⁻¹)	-232.946618
1						
HO	-75.7390146	-75.7272716	-75.7475126	-75.7390151	-75.7272721	-75.7475131
7H						
t-BuOH (Cs)	-233.7017358	-233.5586568	-233.5953428	-233.7122651	-233.5689381	-233.6053831

Table S2.4.07d. Energy values for all systems shown in Figure 2.4.07.

system	E_{tot} (U)B2PLYP/ cc-pVTZ ^(a)	E_{tot} (U)B2PLYP/ cc-pVQZ ^(a)	E_{tot} ROB2PLYP/ cc-pVTZ ^(a)	E_{tot} ROB2PLYP/ cc-pVQZ ^(a)	E_{tot} G3B3-D3 ^(a)	H_{298} G3B3-D3 ^(a)
1H						
HOH	-76.4068145	-76.4221036	-76.4068145	-76.4221036	-76.4040880	-76.3798740
7						
t-BuO2 (C2v, 2A')	-232.8818521	-232.9168271	-232.8798819	-232.9148179	-232.9151268	-232.7899888
1						
HO	-75.7137796	-75.7266444	-75.7119819	-75.7247971	-75.7044006	-75.6929956
7H						
t-BuOH (Cs)	-233.5560423	-233.5925489	-233.5560423	-233.5925489	-233.5967583	-233.4586483

^(a) Using structures and thermal corrections from gas phase (U)B3LYP-D3/6-31+G(d,p) calculations.

Table S2.4.07e. Energy values for all systems shown in Figure 2.4.07.

system	E_{tot} DLPNO- CCSD(T)/ cc-pVTZ ^(a)	H_{298} DLPNO- CCSD(T)/ cc-pVTZ ^(a)	E_{tot} DLPNO- CCSD(T)/ cc-pVQZ ^(a)	H_{298} DLPNO- CCSD(T)/ cc-pVQZ ^(a)	E_{tot} DLPNO- CCSD(T)/ CBS ^(a)	H_{298} DLPNO- CCSD(T)/ CBS ^(a)
1H						
HOH	-76.3319273	-76.3068633	-76.3594799	-76.3344159	-76.3759529	-76.3508889
7						
t-BuO2	-232.6073098	-232.4774708	-232.6768785	-232.5470395	-232.7200341	-232.5901951
1						
HO	-75.6376446	-75.6259016	-75.6612830	-75.6495400	-75.6754790	-75.6637360
7H						
t-BuOH	-233.2854644	-233.1421374	-233.3579451	-233.2146181	-233.4028691	-233.2595421

^(a) Using structures and thermal corrections from gas phase (U)B3LYP-D3/6-31+G(d,p) calculations.

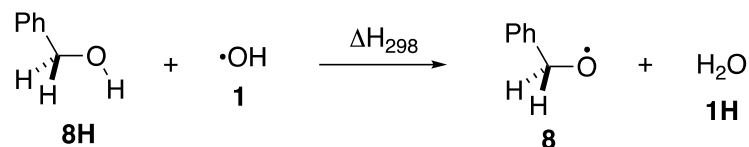


Figure 2.4.08. Reaction of hydroxyl radical (**1**) with benzyl alcohol (**8H**).

Table S2.4.08a. Radical stabilization energies (RSE values) calculated for the systems shown in Fig. S08.

level of theory	RSE (E_{tot})	RSE (H_{298})	RSE (G_{298})
(U)B3LYP/6-31G(d)	-56.11	-60.71	-66.08
(U)B3LYP-D3/6-31G(d)	-53.49	-58.21	-63.88
(U)B3LYP/6-31+G(d,p)	-62.01	-67.22	-74.55
(U)B3LYP-D3/6-31+G(d,p)	-59.79	-65.03	-71.37
(U)B2PLYP/cc-pVTZ//((U)B3LYP-D3/6-31+G(d,p)	-52.05	-57.29	-63.62
(U)B2PLYP/cc-pVQZ//((U)B3LYP-D3/6-31+G(d,p)	-54.01	-59.25	-65.58
ROB2PLYP/cc-pVTZ//((U)B3LYP-D3/6-31+G(d,p)	-51.24	-56.48	-62.81
ROB2PLYP/cc-pVQZ//((U)B3LYP-D3/6-31+G(d,p)	-53.21	-58.45	-64.79
DLPNO-CCSD(T)/cc-pVTZ//((U)B3LYP-D3/6-31+G(d,p)	-43.15	-48.39	-54.72
DLPNO-CCSD(T)/cc-pVQZ//((U)B3LYP-D3/6-31+G(d,p)	-45.60	-50.84	-57.17
DLPNO-CCSD(T)/CBS//((U)B3LYP-D3/6-31+G(d,p)	-46.93	-52.17	-58.50
G3B3-D3//((U)B3LYP-D3/6-31+G(d,p)	-47.90	-52.91	-59.21
G3B3-D3//((U)B3LYP-D3/6-31G(d)	-50.98	-55.49	-61.13
exp.^a		-54.6±8.8	

^a Data from Y. R. Luo, *Comprehensive Handbook of Chemical Bond Energies*, CRC Press, **2007**: BDE(O-H,**8H**) = +442.7±8.8 kJ/mol, and BDE(O-H,**1H**) = +497.3±0.26 kJ/mol from ATcT, version 1.122p, **2020**.

Table S2.4.08b. Energy values for all systems shown in Figure 2.4.08.

system	E _{tot} (U)B3LYP/ 6-31G(d)	H ₂₉₈ (U)B3LYP/ 6-31G(d)	G ₂₉₈ (U)B3LYP/ 6-31G(d)	E _{tot} (U)B3LYP-D3/ 6-31G(d)	H ₂₉₈ (U)B3LYP-D3/ 6-31G(d)	G ₂₉₈ (U)B3LYP-D3/ 6-31G(d)	E _{tot} G3B3-D3 ^(a)	H ₂₉₈ G3B3-D3 ^(a)
1H								
HOH	-76.4089533	-76.3840103	-76.4054563	-76.4089616	-76.3840216	-76.4054676	-76.4089616	-76.3840216
6								
PhCH2O2	-346.1064815	-345.9798925	-346.0201305	-346.1154124	-345.9888184	-346.0290204	-346.1154124	-345.9888184
PhCH2O3	-346.1036245	-345.9754945	-346.0158025	-346.1126664	-345.9844814	-346.0246234	-346.1126664	-345.9844814
1								
HO	-75.7234548	-75.7118458	-75.7320928	-75.7234554	-75.7118464	-75.7320934	-75.7234554	-75.7118464
6H								
PhCH2OH2	-346.7706079	-346.6289339	-346.6683239	-346.7805436	-346.6388216	-346.6780636	-346.7805436	-346.6388216
PhCH2OH1	-346.7676339	-346.6262269	-346.6662869	-346.7771928	-346.6357488	-346.6757048	-346.7771928	-346.6357488

^(a) Using structures and thermal corrections from gas phase (U)B3LYP-D3/6-31G(d) calculations.**Table S2.4.08c.** Energy values for all systems shown in Figure 2.4.08.

system	E _{tot} (U)B3LYP/ 6-31+G(d,p)	H ₂₉₈ (U)B3LYP/ 6-31+G(d,p)	G ₂₉₈ (U)B3LYP/ 6-31+G(d,p)	E _{tot} (U)B3LYP-D3/ 6-31+G(d,p)	H ₂₉₈ (U)B3LYP-D3/ 6-31+G(d,p)	G ₂₉₈ (U)B3LYP-D3/ 6-31+G(d,p)
1H						
HOH	-76.4340477	-76.4089807	-76.4304097	-76.4340566	-76.4089926	-76.4304206
8						
PhCH2O2	-346.1329494	-346.0070054	-346.0488394	-346.1418805	-346.0159255	-346.0571055
PhCH2O3	-346.1309376	-346.0032836	-346.0431956	-346.1399605	-346.0122495	-346.0520855
1						
HO	-75.7390146	-75.7272716	-75.7475126	-75.7390151	-75.7272721	-75.7475131
8H						
PhCH2OH2	-346.8043660	-346.6631100	-346.7033420	-346.8141481	-346.6728761	-346.7128311

PhCH2OH1	-346.8024913	-346.6614553	-346.7019423	-346.8120519	-346.6709759	-346.7113019
----------	--------------	--------------	--------------	--------------	--------------	--------------

Table S2.4.08d. Energy values for all systems shown in Figure 2.4.08.

system	E_{tot} (U)B2PLYP/ cc-pVTZ ^(a)	E_{tot} (U)B2PLYP/ cc-pVQZ ^(a)	E_{tot} ROB2PLYP/ cc-pVTZ ^(a)	E_{tot} ROB2PLYP/ cc-pVQZ ^(a)	E_{tot} G3B3-D3 ^(a)	H_{298} G3B3-D3 ^(a)
1H						
HOH	-76.4068145	-76.4221036	-76.4068145	-76.4221036	-76.4040880	-76.3798740
8						
PhCH2O2	-345.9318607	-345.9809661	-345.9276395	-345.9772125	-345.9630602	-345.8416012
PhCH2O3	-345.9295758	-345.9791939	-345.9297530	-345.9788164	-345.9615045	-345.8383745
1						
HO	-75.7137796	-75.7266444	-75.7119819	-75.7247971	-75.7044006	-75.6929956
8H						
PhCH2OH2	-346.6050709	-346.6558554	-346.6050709	-346.6558554	-346.6445051	-346.5083291
PhCH2OH1	-346.6031632	-346.6541702	-346.6031632	-346.6541702	-346.6428540	-346.5068630

^(a) Using structures and thermal corrections from gas phase (U)B3LYP-D3/6-31+G(d,p) calculations.

Table S2.4.08e. Energy values for all systems shown in Figure 2.4.08.

system	E_{tot} DLPNO- CCSD(T)/ cc-pVTZ ^(a)	H_{298} DLPNO- CCSD(T)/ cc-pVTZ ^(a)	E_{tot} DLPNO- CCSD(T)/ cc-pVQZ ^(a)	H_{298} DLPNO- CCSD(T)/ cc-pVQZ ^(a)	E_{tot} DLPNO- CCSD(T)/ CBS ^(a)	H_{298} DLPNO- CCSD(T)/ CBS ^(a)
1H						
HOH	-76.3319273	-76.3068633	-76.3594799	-76.3344159	-76.3759529	-76.3508889
8						
PhCH2O2	-345.4882378	-345.3622828	-345.5872641	-345.4613091	-345.6488115	-345.5228565
PhCH2O3	-345.4862255	-345.3585145	-345.5855293	-345.4578183	-345.6471397	-345.5194287
1						
HO	-75.6376446	-75.6259016	-75.6612830	-75.6495400	-75.6754790	-75.6637360
8H						

PhCH2OH2	-346.1660865	-346.0248145	-346.2680938	-346.1268218	-346.3314114	-346.1901394
PhCH2OH1	-346.1642151	-346.0231391	-346.2664407	-346.1253647	-346.3298593	-346.1887833

^(a) Using structures and thermal corrections from gas phase (U)B3LYP-D3/6-31+G(d,p) calculations.

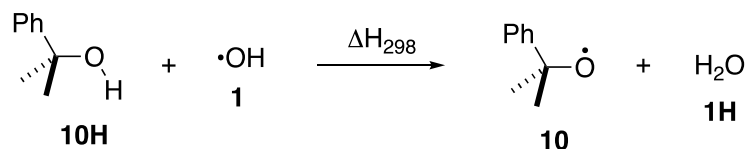


Figure 2.4.10. Reaction of hydroxyl radical (**1**) with 1-methyl-1-phenylethanol (**10H**).

Table S2.4.10a. Radical stabilization energies (RSE values) calculated for the systems shown in Fig. S10.

level of theory	RSE (E_{tot})	RSE (H_{298})	RSE (G_{298})
(U)B3LYP/6-31G(d)	-54.76	-55.33	-59.46
(U)B3LYP-D3/6-31G(d)	-51.46	-52.12	-56.07
(U)B3LYP/6-31+G(d,p)	-60.65	-61.43	-64.51
(U)B3LYP-D3/6-31+G(d,p)	-57.39	-58.14	-61.26
(U)B2PLYP/cc-pVTZ//((U)B3LYP-D3/6-31+G(d,p)	-49.76	-50.52	-53.64
(U)B2PLYP/cc-pVQZ//((U)B3LYP-D3/6-31+G(d,p)	-52.47	-53.23	-56.35
ROB2PLYP/cc-pVTZ//((U)B3LYP-D3/6-31+G(d,p)	-49.27	-50.03	-53.14
ROB2PLYP/cc-pVQZ//((U)B3LYP-D3/6-31+G(d,p)	-52.02	-52.77	-55.89
DLPNO-CCSD(T)/cc-pVTZ//((U)B3LYP-D3/6-31+G(d,p)	-40.12	-40.87	-43.99
DLPNO-CCSD(T)/cc-pVQZ//((U)B3LYP-D3/6-31+G(d,p)	-42.96	-43.72	-46.84
DLPNO-CCSD(T)/CBS//((U)B3LYP-D3/6-31+G(d,p)	-44.32	-45.08	-48.20
G3B3-D3//((U)B3LYP-D3/6-31+G(d,p)	-46.54	-47.27	-50.34
G3B3-D3//((U)B3LYP-D3/6-31G(d)	-47.14	-47.75	-51.66
exp.^a		-59.1±1.0	

^a Data from Luo: BDE(O-H,**10H**) = 438.2±1.0 kJ/mol and BDE(O-H,**1H**) = +497.32±0.26 kJ/mol.

Table S2.4.10b. Energy values for all systems shown in Figure 2.4.10.

system	E _{tot} (U)B3LYP/ 6-31G(d)	H ₂₉₈ (U)B3LYP/ 6-31G(d)	G ₂₉₈ (U)B3LYP/ 6-31G(d)	E _{tot} (U)B3LYP-D3/ 6-31G(d)	H ₂₉₈ (U)B3LYP-D3/ 6-31G(d)	G ₂₉₈ (U)B3LYP-D3/ 6-31G(d)	E _{tot} G3B3-D3 ^(a)	H ₂₉₈ G3B3-D3 ^(a)
1H								
HOH	-76.4089533	-76.3840103	-76.4054563	-76.4089616	-76.3840216	-76.4054676	-76.4089616	-76.3840216
6								
PhCCH32O3	-424.7402226	-424.5535866	-424.5992576	-424.7574653	-424.5705623	-424.6159603	-424.7574653	-424.5705623
1								
HO	-75.7234548	-75.7118458	-75.7320928	-75.7234554	-75.7118464	-75.7320934	-75.7234554	-75.7118464
6H								
PhCCH32OH2	-425.4048644	-425.2046754	-425.2499734	-425.4233696	-425.2228876	-425.2679796	-425.4233696	-425.2228876
PhCCH32OH3	-425.4036179	-425.2035569	-425.2486589	-425.4218145	-425.2214955	-425.2663825	-425.4218145	-425.2214955
PhCCH32OH1	-425.4004136	-425.2003086	-425.2456136	-425.4188141	-425.2184151	-425.2634991	-425.4188141	-425.2184151

^(a) Using structures and thermal corrections from gas phase (U)B3LYP-D3/6-31G(d) calculations.

Table S2.4.10c. Energy values for all systems shown in Figure 2.4.10.

system	E _{tot} (U)B3LYP/ 6-31+G(d,p)	H ₂₉₈ (U)B3LYP/ 6-31+G(d,p)	G ₂₉₈ (U)B3LYP/ 6-31+G(d,p)	E _{tot} (U)B3LYP-D3/ 6-31+G(d,p)	H ₂₉₈ (U)B3LYP-D3/ 6-31+G(d,p)	G ₂₉₈ (U)B3LYP-D3/ 6-31+G(d,p)
1H						
HOH	-76.4340477	-76.4089807	-76.4304097	-76.4340566	-76.4089926	-76.4304206
10						
PhCCH32O3	-424.7729961	-424.5872501	-424.6330391	-424.7902359	-424.6042189	-424.6497179
PhCCH32O2_a	-424.7713547	-424.5852387	-424.6304687	-424.7884533	-424.6021313	-424.6471403
1						
HO	-75.7390146	-75.7272716	-75.7475126	-75.7390151	-75.7272721	-75.7475131

10H						
PhCCH32OH2	-425.4449289	-425.2455609	-425.2913669	-425.4634197	-425.2637937	-425.3092917
PhCCH32OH3	-425.4442997	-425.2450797	-425.2904917	-425.4625048	-425.2630198	-425.3081938
PhCCH32OH1	-425.4416282	-425.2423312	-425.2878762	-425.4600159	-425.2604259	-425.3056789

Table S2.4.10d. Energy values for all systems shown in Figure 2.4.10.

system	E_{tot} (U)B2PLYP/ cc-pVTZ ^(a)	E_{tot} (U)B2PLYP/ cc-pVQZ ^(a)	E_{tot} ROB2PLYP/ cc-pVTZ ^(a)	E_{tot} ROB2PLYP/ cc-pVQZ ^(a)	E_{tot} G3B3-D3 ^(a)	H_{298} G3B3-D3 ^(a)
1H						
HOH	-76.4068145	-76.4221036	-76.4068145	-76.4221036	-76.4040880	-76.3798740
10						
PhCCH32O2_a	-424.5128475	-424.5735088	-424.5108970	-424.5715188	-424.5737640	-424.3944330
PhCCH32O3	-424.5149930	-424.5753891	-424.5130078	-424.5733688	-424.5716634	-424.3920444
1						
HO	-75.7137796	-75.7266444	-75.7119819	-75.7247971	-75.7044006	-75.6929956
10H						
PhCCH32OH2	-425.1890748	-425.2508629	-425.1890748	-425.2508629	-425.2557235	-425.0633075
PhCCH32OH3	-425.1882979	-425.2502678	-425.1882979	-425.2502678	-425.2549421	-425.0626581
PhCCH32OH1	-425.1855216	-425.2478144	-425.1855216	-425.2478144	-425.2528812	-425.0604962

^(a) Using structures and thermal corrections from gas phase (U)B3LYP-D3/6-31+G(d,p) calculations.

Table S2.4.10e. Energy values for all systems shown in Figure 2.4.10.

system	E_{tot} DLPNO- CCSD(T)/ cc-pVTZ ^(a)	H_{298} DLPNO- CCSD(T)/ cc-pVTZ ^(a)	E_{tot} DLPNO- CCSD(T)/ cc-pVQZ ^(a)	H_{298} DLPNO- CCSD(T)/ cc-pVQZ ^(a)	E_{tot} DLPNO- CCSD(T)/ CBS ^(a)	H_{298} DLPNO- CCSD(T)/ CBS ^(a)
1H						
HOH	-76.3319273	-76.3068633	-76.3594799	-76.3344159	-76.3759529	-76.3508889
10						
PhCCH32O3	-423.9769476	-423.7909306	-424.0987877	-423.9127707	-424.1746592	-423.9886422

PhCCH32O2_a	-423.9747497	-423.7884277	-424.0967353	-423.9104133	-424.1726537	-423.9863317
1						
HO	-75.6376446	-75.6259016	-75.6612830	-75.6495400	-75.6754790	-75.6637360
10H						
PhCCH32OH2	-424.6559510	-424.4563250	-424.7806203	-424.5809943	-424.8582514	-424.6586254
PhCCH32OH3	-424.6550229	-424.4555379	-424.7799400	-424.5804550	-424.8576901	-424.6582051
PhCCH32OH1	-424.6525200	-424.4529300	-424.7776556	-424.5780656	-424.8554775	-424.6558875

^(a) Using structures and thermal corrections from gas phase (U)B3LYP-D3/6-31+G(d,p) calculations.

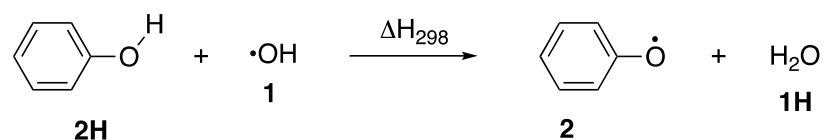


Figure 2.4.2. Reaction of hydroxyl radical (1) with phenol (2H).

Table S2.4.2a. Radical stabilization energies (RSE values) calculated for the systems shown in Fig. S2.

level of theory	RSE (E_{tot})	RSE (H_{298})	RSE (G_{298})
(U)B3LYP/6-31G(d)	-126.73	-126.54	-128.81
(U)B3LYP-D3/6-31G(d)	-125.38	-125.18	-129.13
(U)B3LYP/6-31+G(d,p)	-134.32	-134.27	-136.39
(U)B3LYP-D3/6-31+G(d,p)	-132.94	-132.91	-134.98
(U)B2PLYP/cc-pVTZ//((U)B3LYP-D3/6-31+G(d,p)	-114.21	-114.17	-116.25
(U)B2PLYP/cc-pVQZ//((U)B3LYP-D3/6-31+G(d,p)	-117.73	-117.69	-119.77
ROB2PLYP/cc-pVTZ//((U)B3LYP-D3/6-31+G(d,p)	-123.27	-123.23	-125.31
ROB2PLYP/cc-pVQZ//((U)B3LYP-D3/6-31+G(d,p)	-127.36	-127.32	-129.40
DLPNO-CCSD(T)/cc-pVTZ//((U)B3LYP-D3/6-31+G(d,p)	-116.37	-116.34	-118.41
DLPNO-CCSD(T)/cc-pVQZ//((U)B3LYP-D3/6-31+G(d,p)	-121.02	-120.98	-123.06
DLPNO-CCSD(T)/CBS//((U)B3LYP-D3/6-31+G(d,p)	-123.59	-123.55	-125.63
G3B3-D3//((U)B3LYP-D3/6-31+G(d,p)	-121.54	-121.52	-123.53
G3B3-D3//((U)B3LYP-D3/6-31G(d)	-121.74	-121.61	-123.80
DLPNO-CCSD(T)/aug-cc-pVTZ//((U)B3LYP-D3/6-31+G(d,p)	-120.82	-120.78	-122.86
DLPNO-CCSD(T)/aug-cc-pVQZ//((U)B3LYP-D3/6-31+G(d,p)	-122.84	-122.80	-124.88
DLPNO-CCSD(T)/CBS//((U)B3LYP-D3/6-31+G(d,p)	-124.17	-124.13	-126.21
exp.^a		-130.2±1	

^a Data from ATcT, version 1.122p, **2020**: BDE(O-H,**2H**) = +367.06±0.88 kJ/mol and BDE(O-H,**1H**) = +497.32±0.26 kJ/mol.

Table S2.4.2b. Energy values for all systems shown in Figure 2.4.2.

system	E _{tot} (U)B3LYP/ 6-31G(d)	H ₂₉₈ (U)B3LYP/ 6-31G(d)	G ₂₉₈ (U)B3LYP/ 6-31G(d)	E _{tot} (U)B3LYP-D3/ 6-31G(d)	H ₂₉₈ (U)B3LYP-D3/ 6-31G(d)	G ₂₉₈ (U)B3LYP-D3/ 6-31G(d)	E _{tot} G3B3-D3 ^(a)	H ₂₉₈ G3B3-D3 ^(a)
1H								
HOH	-76.4089533	-76.3840103	-76.4054563	-76.4089616	-76.3840216	-76.4054676	-76.4089616	-76.3840216
6								
PhO	-306.8276418	-306.7296468	-306.7647298	-306.8336783	-306.7356833	-306.7714233	-306.8336783	-306.7356833
1								
HO	-75.7234548	-75.7118458	-75.7320928	-75.7234554	-75.7118464	-75.7320934	-75.7234554	-75.7118464
6H								
PhOH	-307.4648705	-307.3536155	-307.3890335	-307.4714286	-307.3601816	-307.3956126	-307.4714286	-307.3601816

^(a) Using structures and thermal corrections from gas phase (U)B3LYP-D3/6-31G(d) calculations.

Table S2.4.2c. Energy values for all systems shown in Figure 2.4.2.

system	E _{tot} (U)B3LYP/ 6-31+G(d,p)	H ₂₉₈ (U)B3LYP/ 6-31+G(d,p)	G ₂₉₈ (U)B3LYP/ 6-31+G(d,p)	E _{tot} (U)B3LYP-D3/ 6-31+G(d,p)	H ₂₉₈ (U)B3LYP-D3/ 6-31+G(d,p)	G ₂₉₈ (U)B3LYP-D3/ 6-31+G(d,p)
1H						
HOH	-76.4340477	-76.4089807	-76.4304097	-76.4340566	-76.4089926	-76.4304206
2						
PhO	-306.8501209	-306.7524479	-306.7875909	-306.8561593	-306.7584873	-306.7936333
1						
HO	-75.7390146	-75.7272716	-75.7475126	-75.7390151	-75.7272721	-75.7475131
2H						
PhOH	-307.4939951	-307.3830151	-307.4185411	-307.5005653	-307.3895863	-307.4251283

Table S2.4.02d. Energy values for all systems shown in Figure 2.4.02.

system	E _{tot}	E _{tot}	E _{tot}	E _{tot}	E _{tot}	H ₂₉₈
--------	------------------	------------------	------------------	------------------	------------------	------------------

	(U)B2PLYP/ cc-pVTZ ^(a)	(U)B2PLYP/ cc-pVQZ ^(a)	ROB2PLYP/ cc-pVTZ ^(a)	ROB2PLYP/ cc-pVQZ ^(a)	G3B3-D3 ^(a)	G3B3-D3 ^(a)
1H						
HOH	-76.4068145	-76.4221036	-76.4068145	-76.4221036	-76.4040880	-76.3798740
2						
PhO	-306.6751109	-306.7188728	-306.6767639	-306.7206944	-306.6979178	-306.6037158
1						
HO	-75.7137796	-75.7266444	-75.7119819	-75.7247971	-75.7044006	-75.6929956
2H						
PhOH	-307.3246457	-307.3694926	-307.3246457	-307.3694926	-307.3513146	-307.2443096

^(a) Using structures and thermal corrections from gas phase (U)B3LYP-D3/6-31+G(d,p) calculations.

Table S2.4.02e. Energy values for all systems shown in Figure 2.4.02.

system	E _{tot} DLPNO- CCSD(T)/ cc-pVTZ ^(a)	H ₂₉₈ DLPNO- CCSD(T)/ cc-pVTZ ^(a)	E _{tot} DLPNO- CCSD(T)/ cc-pVQZ ^(a)	H ₂₉₈ DLPNO- CCSD(T)/ cc-pVQZ ^(a)	E _{tot} DLPNO- CCSD(T)/ CBS ^(a)	H ₂₉₈ DLPNO- CCSD(T)/ CBS ^(a)
1H						
HOH	-76.3319273	-76.3068633	-76.3594799	-76.3344159	-76.3759529	-76.3508889
2						
PhO	-306.2831089	-306.1854369	-306.3712242	-306.2735522	-306.4258729	-306.3282009
1						
HO	-75.6376446	-75.6259016	-75.6612830	-75.6495400	-75.6754790	-75.6637360
2H						
PhOH	-306.9330674	-306.8220884	-307.0233275	-306.9123485	-307.0792747	-306.9682957

^(a) Using structures and thermal corrections from gas phase (U)B3LYP-D3/6-31+G(d,p) calculations.

Table S2.4.02f. Energy values for all systems shown in Figure 2.4.02.

system	E_{tot} DLPNO- CCSD(T)/ aug-cc-pVTZ ^(a)	H_{298} DLPNO- CCSD(T)/ aug-cc-pVTZ ^(a)	E_{tot} DLPNO- CCSD(T)/ aug-cc-pVQZ ^(a)	H_{298} DLPNO- CCSD(T)/ aug-cc-pVQZ ^(a)	E_{tot} DLPNO- CCSD(T)/ CBS ^(a)	H_{298} DLPNO- CCSD(T)/ CBS ^(a)
1H						
HOH	-76.3421010	-76.3170370	-76.3633066	-76.3382426	-76.3762075	-76.3511435
2						
PhO	-306.3043704	-306.2066984	-306.3796221	-306.2819501	-306.4259593	-306.3282873
1						
HO	-75.6455007	-75.6337577	-75.6642373	-75.6524943	-75.6755624	-75.6638194
2H						
PhOH	-306.9549525	-306.8439735	-307.0319049	-306.9209259	-307.0793106	-306.9683316

^(a) Using structures and thermal corrections from gas phase (U)B3LYP-D3/6-31+G(d,p) calculations.

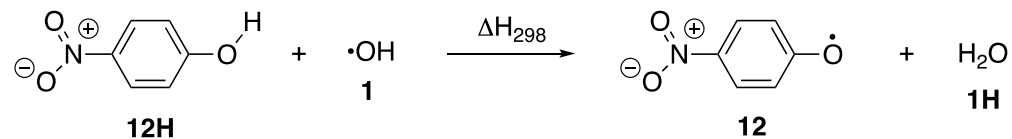


Figure 2.4.12. Reaction of hydroxyl radical (1) with *para*-nitrophenol (12H).

Table S2.4.12a. Radical stabilization energies (RSE values) calculated for the systems shown in Fig. S12.

level of theory	RSE (E_{tot})	RSE (H_{298})	RSE (G_{298})

(U)B3LYP/6-31G(d)	-108.01	-108.75	-114.01
(U)B3LYP-D3/6-31G(d)	-106.62	-107.38	-112.73
(U)B3LYP/6-31+G(d,p)	-115.03	-115.86	-119.43
(U)B3LYP-D3/6-31+G(d,p)	-113.62	-114.48	-118.18
(U)B2PLYP/cc-pVTZ//((U)B3LYP-D3/6-31+G(d,p)	-96.85	-97.71	-101.41
(U)B2PLYP/cc-pVQZ//((U)B3LYP-D3/6-31+G(d,p)	-99.95	-100.80	-104.50
ROB2PLYP/cc-pVTZ//((U)B3LYP-D3/6-31+G(d,p)	-107.86	-108.72	-112.42
ROB2PLYP/cc-pVQZ//((U)B3LYP-D3/6-31+G(d,p)	-111.59	-112.45	-116.14
DLPNO-CCSD(T)/cc-pVTZ//((U)B3LYP-D3/6-31+G(d,p)	-99.90	-100.75	-104.45
DLPNO-CCSD(T)/cc-pVQZ//((U)B3LYP-D3/6-31+G(d,p)	-103.47	-104.33	-108.03
DLPNO-CCSD(T)/CBS//((U)B3LYP-D3/6-31+G(d,p)	-105.28	-106.14	-109.84
G3B3-D3//((U)B3LYP-D3/6-31+G(d,p)	-105.10	-105.94	-109.58
G3B3-D3//((U)B3LYP-D3/6-31G(d)	-105.29	-106.03	-109.60
exp.^a		-107±8	

^a Data from BDE(phenol) + differences: BDE(O-H,**12H**) = +390 kJ/mol and BDE(O-H,**1H**) = +497.3±0.26 kJ/mol.

Table S2.4.12b. Energy values for all systems shown in Figure 2.4.12.

system	E _{tot} (U)B3LYP/ 6-31G(d)	H ₂₉₈ (U)B3LYP/ 6-31G(d)	G ₂₉₈ (U)B3LYP/ 6-31G(d)	E _{tot} (U)B3LYP-D3/ 6-31G(d)	H ₂₉₈ (U)B3LYP-D3/ 6-31G(d)	G ₂₉₈ (U)B3LYP-D3/ 6-31G(d)	E _{tot} G3B3-D3 ^(a)	H ₂₉₈ G3B3-D3 ^(a)
1H								
HOH	-76.4089533	-76.3840103	-76.4054563	-76.4089616	-76.3840216	-76.4054676	-76.4089616	-76.3840216
6								
p-nitro-PhO	-511.3246544	-511.2217224	-511.2644874	-511.3343591	-511.2313801	-511.2741841	-511.3343591	-511.2313801
1								
HO	-75.7234548	-75.7118458	-75.7320928	-75.7234554	-75.7118464	-75.7320934	-75.7234554	-75.7118464
6H								
p-nitro-PhOH	-511.9690131	-511.8524651	-511.8944281	-511.9792564	-511.8626564	-511.9046234	-511.9792564	-511.8626564

^(a) Using structures and thermal corrections from gas phase (U)B3LYP-D3/6-31G(d) calculations.**Table S2.4.12c.** Energy values for all systems shown in Figure 2.4.12.

system	E _{tot} (U)B3LYP/ 6-31+G(d,p)	H ₂₉₈ (U)B3LYP/ 6-31+G(d,p)	G ₂₉₈ (U)B3LYP/ 6-31+G(d,p)	E _{tot} (U)B3LYP-D3/ 6-31+G(d,p)	H ₂₉₈ (U)B3LYP-D3/ 6-31+G(d,p)	G ₂₉₈ (U)B3LYP-D3/ 6-31+G(d,p)
1H						
HOH	-76.4340477	-76.4089807	-76.4304097	-76.4340566	-76.4089926	-76.4304206
12						
p-nitro-PhO	-511.3543582	-511.2519102	-511.2942482	-511.3640726	-511.2615766	-511.3039696
1						
HO	-75.7390146	-75.7272716	-75.7475126	-75.7390151	-75.7272721	-75.7475131
12H						
p-nitro-PhOH	-512.0055779	-511.8894909	-511.9316579	-512.0158385	-511.8996945	-511.9418665

Table S2.4.12d. Energy values for all systems shown in Figure 2.4.12.

system	E _{tot} (U)B2PLYP/ cc-pVTZ ^(a)	E _{tot} (U)B2PLYP/ cc-pVQZ ^(a)	E _{tot} ROB2PLYP/ cc-pVTZ ^(a)	E _{tot} ROB2PLYP/ cc-pVQZ ^(a)	E _{tot} G3B3-D3 ^(a)	H ₂₉₈ G3B3-D3 ^(a)
--------	--	--	---	---	--	--

1H						
HOH	-76.4068145	-76.4221036	-76.4068145	-76.4221036	-76.4040880	-76.3798740
12						
p-nitro-PhO	-511.1293617	-511.2042454	-511.1317579	-511.2068325	-511.1188068	-511.0198088
1						
HO	-75.7137796	-75.7266444	-75.7119819	-75.7247971	-75.7044006	-75.6929956
12H						
p-nitro-PhOH	-511.7855079	-511.8616374	-511.7855079	-511.8616374	-511.7784629	-511.6663379

^(a) Using structures and thermal corrections from gas phase (U)B3LYP-D3/6-31+G(d,p) calculations.

Table S2.4.12e. Energy values for all systems shown in Figure 2.4.12.

system	E _{tot} DLPNO- CCSD(T)/ cc-pVTZ ^(a)	H ₂₉₈ DLPNO- CCSD(T)/ cc-pVTZ ^(a)	E _{tot} DLPNO- CCSD(T)/ cc-pVQZ ^(a)	H ₂₉₈ DLPNO- CCSD(T)/ cc-pVQZ ^(a)	E _{tot} DLPNO- CCSD(T)/ CBS ^(a)	H ₂₉₈ DLPNO- CCSD(T)/ CBS ^(a)
1H						
HOH	-76.3319273	-76.3068633	-76.3594799	-76.3344159	-76.3759529	-76.3508889
12						
p-nitro-PhO	-510.5070854	-510.4045894	-510.6579347	-510.5554387	-510.7509593	-510.6484633
1						
HO	-75.6376446	-75.6259016	-75.6612830	-75.6495400	-75.6754790	-75.6637360
12H						
p-nitro-PhOH	-511.1633196	-511.0471756	-511.3167213	-511.2005773	-511.4113329	-511.2951889

^(a) Using structures and thermal corrections from gas phase (U)B3LYP-D3/6-31+G(d,p) calculations.

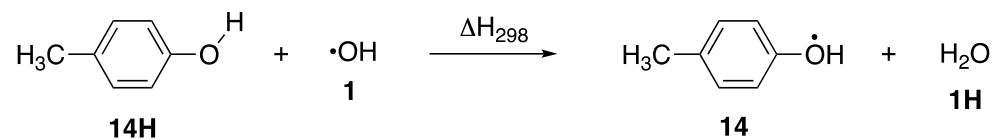


Figure 2.4.14. Reaction of hydroxyl radical (**1**) with *para*-methylphenol (**14H**).

Table S2.4.14a. Radical stabilization energies (RSE values) calculated for the systems shown in Fig. S14.

level of theory	RSE (E_{tot})	RSE (H_{298})	RSE (G_{298})
(U)B3LYP/6-31G(d)	-134.00	-133.65	-138.84
(U)B3LYP-D3/6-31G(d)	-132.69	-132.32	-137.34
(U)B3LYP/6-31+G(d,p)	-142.94	-142.62	-147.81
(U)B3LYP-D3/6-31+G(d,p)	-141.62	-141.31	-146.92
(U)B2PLYP/cc-pVTZ//(U)B3LYP-D3/6-31+G(d,p)	-122.83	-122.52	-128.13
(U)B2PLYP/cc-pVQZ//(U)B3LYP-D3/6-31+G(d,p)	-126.64	-126.32	-131.93
ROB2PLYP/cc-pVTZ//(U)B3LYP-D3/6-31+G(d,p)	-132.29	-131.97	-137.59
ROB2PLYP/cc-pVQZ//(U)B3LYP-D3/6-31+G(d,p)	-136.63	-136.31	-141.93
DLPNO-CCSD(T)/cc-pVTZ//(U)B3LYP-D3/6-31+G(d,p)	-122.82	-122.51	-128.12
DLPNO-CCSD(T)/cc-pVQZ//(U)B3LYP-D3/6-31+G(d,p)	-127.94	-127.63	-133.24
DLPNO-CCSD(T)/CBS//(U)B3LYP-D3/6-31+G(d,p)	-130.77	-130.46	-136.07
G3B3-D3//(U)B3LYP-D3/6-31+G(d,p)	-129.41	-129.13	-134.67
G3B3-D3//(U)B3LYP-D3/6-31G(d)	-129.66	-129.33	-134.27
exp.^a		-140.7±0.6	

^a Data from Ashfold + therm. corr. = +356.6±0.6 kJ/mol and BDE(O-H,**1H**) = +497.3±0.3 kJ/mol.

Table S2.4.14b. Energy values for all systems shown in Figure 2.4.14.

system	E _{tot} (U)B3LYP/ 6-31G(d)	H ₂₉₈ (U)B3LYP/ 6-31G(d)	G ₂₉₈ (U)B3LYP/ 6-31G(d)	E _{tot} (U)B3LYP-D3/ 6-31G(d)	H ₂₉₈ (U)B3LYP-D3/ 6-31G(d)	G ₂₉₈ (U)B3LYP-D3/ 6-31G(d)	E _{tot} G3B3-D3 ^(a)	H ₂₉₈ G3B3-D3 ^(a)
1H								
HOH	-76.4089533	-76.3840103	-76.4054563	-76.4089616	-76.3840216	-76.4054676	-76.4089616	-76.3840216
6								
p-methyl-PhO	-346.1477847	-346.0203167	-346.0614857	-346.1565726	-346.0290566	-346.0699926	-346.1565726	-346.0290566
1								
HO	-75.7234548	-75.7118458	-75.7320928	-75.7234554	-75.7118464	-75.7320934	-75.7234554	-75.7118464
6H								
p-methyl-PhOH	-346.7822458	-346.6415768	-346.6819678	-346.7915385	-346.6508335	-346.6910575	-346.7915385	-346.6508335

^(a) Using structures and thermal corrections from gas phase (U)B3LYP-D3/6-31G(d) calculations.**Table S2.4.14c.** Energy values for all systems shown in Figure 2.4.14.

system	E _{tot} (U)B3LYP/ 6-31+G(d,p)	H ₂₉₈ (U)B3LYP/ 6-31+G(d,p)	G ₂₉₈ (U)B3LYP/ 6-31+G(d,p)	E _{tot} (U)B3LYP-D3/ 6-31+G(d,p)	H ₂₉₈ (U)B3LYP-D3/ 6-31+G(d,p)	G ₂₉₈ (U)B3LYP-D3/ 6-31+G(d,p)
1H						
HOH	-76.4340477	-76.4089807	-76.4304097	-76.4340566	-76.4089926	-76.4304206
14						
p-methyl-PhO	-346.1734913	-346.0466003	-346.0885413	-346.1822805	-346.0553415	-346.0966435
1						
HO	-75.7390146	-75.7272716	-75.7475126	-75.7390151	-75.7272721	-75.7475131
14H						
p-methyl-PhOH	-346.8140799	-346.6739899	-346.7151419	-346.8233808	-346.6832408	-346.7235918

Table S2.4.14d. Energy values for all systems shown in Figure 2.4.14.

system	E _{tot}	E _{tot}	E _{tot}	E _{tot}	E _{tot}	H ₂₉₈
--------	------------------	------------------	------------------	------------------	------------------	------------------

	(U)B2PLYP/ cc-pVTZ ^(a)	(U)B2PLYP/ cc-pVQZ ^(a)	ROB2PLYP/ cc-pVTZ ^(a)	ROB2PLYP/ cc-pVQZ ^(a)	G3B3-D3 ^(a)	G3B3-D3 ^(a)
1H						
HOH	-76.4068145	-76.4221036	-76.4068145	-76.4221036	-76.4040880	-76.3798740
14						
p-methyl-PhO	-345.9690763	-346.0186311	-345.9708795	-346.0205899	-346.0035663	-345.8811533
1						
HO	-75.7137796	-75.7266444	-75.7119819	-75.7247971	-75.7044006	-75.6929956
14H						
p-methyl-PhOH	-346.6153264	-346.6658572	-346.6153264	-346.6658572	-346.6539630	-346.5188470

^(a) Using structures and thermal corrections from gas phase (U)B3LYP-D3/6-31+G(d,p) calculations.

Table S2.4.14e. Energy values for all systems shown in Figure 2.4.14.

system	E _{tot} DLPNO- CCSD(T)/ cc-pVTZ ^(a)	H ₂₉₈ DLPNO- CCSD(T)/ cc-pVTZ ^(a)	E _{tot} DLPNO- CCSD(T)/ cc-pVQZ ^(a)	H ₂₉₈ DLPNO- CCSD(T)/ cc-pVQZ ^(a)	E _{tot} DLPNO- CCSD(T)/ CBS ^(a)	H ₂₉₈ DLPNO- CCSD(T)/ CBS ^(a)
1H						
HOH	-76.3319273	-76.3068633	-76.3594799	-76.3344159	-76.3759529	-76.3508889
14						
p-methyl-PhO	-345.5276291	-345.4006901	-345.6274476	-345.5005086	-345.6894405	-345.5625015
1						
HO	-75.6376446	-75.6259016	-75.6612830	-75.6495400	-75.6754790	-75.6637360
14H						
p-methyl-PhOH	-346.1751319	-346.0349919	-346.2769142	-346.1367742	-346.3401060	-346.1999660

^(a) Using structures and thermal corrections from gas phase (U)B3LYP-D3/6-31+G(d,p) calculations.

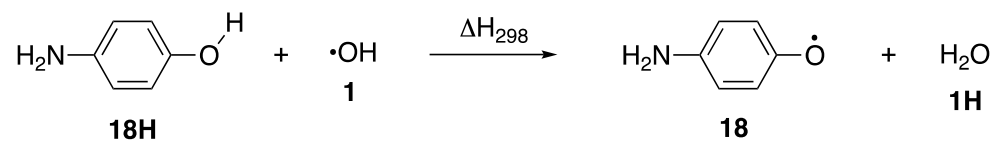


Figure 2.4.18. Reaction of hydroxyl radical (**1**) with *para*-aminophenol (**18H**).

Table S2.4.18a. Radical stabilization energies (RSE values) calculated for the systems shown in Fig. S18.

level of theory	RSE (E_{tot})	RSE (H_{298})	RSE (G_{298})
(U)B3LYP/6-31G(d)	-162.12	-160.56	-163.75
(U)B3LYP-D3/6-31G(d)	-160.75	-159.19	-162.33
(U)B3LYP/6-31+G(d,p)	-171.55	-170.17	-173.87
(U)B3LYP-D3/6-31+G(d,p)	-170.16	-168.79	-172.43
(U)B2PLYP/cc-pVTZ//(U)B3LYP-D3/6-31+G(d,p)	-153.57	-152.20	-155.84
(U)B2PLYP/cc-pVQZ//(U)B3LYP-D3/6-31+G(d,p)	-157.47	-156.10	-159.73
ROB2PLYP/cc-pVTZ//(U)B3LYP-D3/6-31+G(d,p)	-162.43	-161.06	-164.69
ROB2PLYP/cc-pVQZ//(U)B3LYP-D3/6-31+G(d,p)	-166.73	-165.36	-169.00
DLPNO-CCSD(T)/cc-pVTZ//(U)B3LYP-D3/6-31+G(d,p)	-145.23	-143.86	-147.50
DLPNO-CCSD(T)/cc-pVQZ//(U)B3LYP-D3/6-31+G(d,p)	-150.71	-149.34	-152.98
DLPNO-CCSD(T)/CBS//(U)B3LYP-D3/6-31+G(d,p)	-153.72	-152.35	-155.99
G3B3-D3//(U)B3LYP-D3/6-31+G(d,p)	-154.90	-153.60	-157.17
G3B3-D3//(U)B3LYP-D3/6-31G(d)	-155.26	-153.79	-156.86
exp.		-173.3±13	

^a Data from BDE(phenol) + differences: BDE(O-H,**18H**) = +324±13 kJ/mol and BDE(O-H,**1H**) = +497.3±0.26 kJ/mol.

Table S2.4.18b. Energy values for all systems shown in Figure 2.4.18.

system	E _{tot} (U)B3LYP/ 6-31G(d)	H ₂₉₈ (U)B3LYP/ 6-31G(d)	G ₂₉₈ (U)B3LYP/ 6-31G(d)	E _{tot} (U)B3LYP-D3/ 6-31G(d)	H ₂₉₈ (U)B3LYP-D3/ 6-31G(d)	G ₂₉₈ (U)B3LYP-D3/ 6-31G(d)	E _{tot} G3B3-D3 ^(a)	H ₂₉₈ G3B3-D3 ^(a)
1H								
HOH	-76.4089533	-76.3840103	-76.4054563	-76.4089616	-76.3840216	-76.4054676	-76.4089616	-76.3840216
6								
p-amino-PhO	-362.1909425	-362.0744315	-362.1132415	-362.1990804	-362.0825174	-362.1213144	-362.1990804	-362.0825174
1								
HO	-75.7234548	-75.7118458	-75.7320928	-75.7234554	-75.7118464	-75.7320934	-75.7234554	-75.7118464
6H								
p-amino-PhOH	-362.8146946	-362.6854416	-362.7242356	-362.8233617	-362.6940607	-362.7328587	-362.8233617	-362.6940607

^(a) Using structures and thermal corrections from gas phase (U)B3LYP-D3/6-31G(d) calculations.**Table S2.4.18c.** Energy values for all systems shown in Figure 2.4.18.

system	E _{tot} (U)B3LYP/ 6-31+G(d,p)	H ₂₉₈ (U)B3LYP/ 6-31+G(d,p)	G ₂₉₈ (U)B3LYP/ 6-31+G(d,p)	E _{tot} (U)B3LYP-D3/ 6-31+G(d,p)	H ₂₉₈ (U)B3LYP-D3/ 6-31+G(d,p)	G ₂₉₈ (U)B3LYP-D3/ 6-31+G(d,p)
1H						
HOH	-76.4340477	-76.4089807	-76.4304097	-76.4340566	-76.4089926	-76.4304206
18						
p-amino-PhO	-362.2234108	-362.1073228	-362.1465658	-362.2315504	-362.1154094	-362.1546404
1						
HO	-75.7390146	-75.7272716	-75.7475126	-75.7390151	-75.7272721	-75.7475131
18H						
p-amino-PhOH	-362.8531025	-362.7242165	-362.7632395	-362.8617811	-362.7328411	-362.7718741

Table S2.4.18d. Energy values for all systems shown in Figure 2.4.18.

system	E _{tot} (U)B2PLYP/ cc-pVTZ ^(a)	E _{tot} (U)B2PLYP/ cc-pVQZ ^(a)	E _{tot} ROB2PLYP/ cc-pVTZ ^(a)	E _{tot} ROB2PLYP/ cc-pVQZ ^(a)	E _{tot} G3B3-D3 ^(a)	H ₂₉₈ G3B3-D3 ^(a)
--------	--	--	---	---	--	--

1H						
HOH	-76.4068145	-76.4221036	-76.4068145	-76.4221036	-76.4040880	-76.3798740
18						
p-amino-PhO	-362.0246647	-362.0779902	-362.0262405	-362.0796717	-362.0479265	-361.9358735
1						
HO	-75.7137796	-75.7266444	-75.7119819	-75.7247971	-75.7044006	-75.6929956
18H						
p-amino-PhOH	-362.6592078	-362.7134726	-362.6592078	-362.7134726	-362.6886165	-362.5642495

^(a) Using structures and thermal corrections from gas phase (U)B3LYP-D3/6-31+G(d,p) calculations.

Table S2.4.18e. Energy values for all systems shown in Figure 2.4.18.

system	E _{tot} DLPNO- CCSD(T)/ cc-pVTZ ^(a)	H ₂₉₈ DLPNO- CCSD(T)/ cc-pVTZ ^(a)	E _{tot} DLPNO- CCSD(T)/ cc-pVQZ ^(a)	H ₂₉₈ DLPNO- CCSD(T)/ cc-pVQZ ^(a)	E _{tot} DLPNO- CCSD(T)/ CBS ^(a)	H ₂₉₈ DLPNO- CCSD(T)/ CBS ^(a)
1H						
HOH	-76.3319273	-76.3068633	-76.3594799	-76.3344159	-76.3759529	-76.3508889
18						
p-amino-PhO	-361.5657277	-361.4495867	-361.6723153	-361.5561743	-361.7382645	-361.6221235
1						
HO	-75.6376446	-75.6259016	-75.6612830	-75.6495400	-75.6754790	-75.6637360
18H						
p-amino-PhOH	-362.2046941	-362.0757541	-362.3131096	-362.1841696	-362.3801877	-362.2512477

^(a) Using structures and thermal corrections from gas phase (U)B3LYP-D3/6-31+G(d,p) calculations.

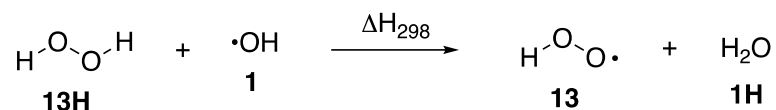


Figure 2.4.13. Reaction of hydroxyl radical (1) with H₂O₂ (13H).

Table S2.4.13a. Radical stabilization energies (RSE values) calculated for the systems shown in Fig. S13.

level of theory	RSE (E_{tot})	RSE (H_{298})	RSE (G_{298})
(U)B3LYP/6-31G(d)	-135.06	-133.19	-136.64
(U)B3LYP-D3/6-31G(d)	-134.39	-132.54	-136.00
(U)B3LYP/6-31+G(d,p)	-136.72	-135.11	-138.63
(U)B3LYP-D3/6-31+G(d,p)	-136.04	-134.44	-137.97
(U)B2PLYP/cc-pVTZ//(U)B3LYP-D3/6-31+G(d,p)	-135.35	-133.74	-137.27
(U)B2PLYP/cc-pVQZ//(U)B3LYP-D3/6-31+G(d,p)	-137.42	-135.81	-139.34
ROB2PLYP/cc-pVTZ//(U)B3LYP-D3/6-31+G(d,p)	-134.94	-133.33	-136.86
ROB2PLYP/cc-pVQZ//(U)B3LYP-D3/6-31+G(d,p)	-136.94	-135.34	-138.87
DLPNO-CCSD(T)/cc-pVTZ//(U)B3LYP-D3/6-31+G(d,p)	-126.53	-124.93	-128.46
DLPNO-CCSD(T)/cc-pVQZ//(U)B3LYP-D3/6-31+G(d,p)	-129.74	-128.13	-131.66
DLPNO-CCSD(T)/CBS//(U)B3LYP-D3/6-31+G(d,p)	-131.22	-129.61	-133.14
G3B3-D3//(U)B3LYP-D3/6-31+G(d,p)	-131.22	-129.72	-133.16
G3B3-D3//(U)B3LYP-D3/6-31G(d)	-131.32	-129.58	-132.95
exp. ^a		-131.6±0.3	

^a Data from ATcT, version 1.122p, 2020: BDE(O-H,20H) = +365.7±0.2 kJ/mol, and BDE(O-H,1H) = +497.3±0.26 kJ/mol.

Table S2.4.13b. Energy values for all systems shown in Figure 2.4.13.

system	E _{tot} (U)B3LYP/ 6-31G(d)	H ₂₉₈ (U)B3LYP/ 6-31G(d)	G ₂₉₈ (U)B3LYP/ 6-31G(d)	E _{tot} (U)B3LYP-D3/ 6-31G(d)	H ₂₉₈ (U)B3LYP-D3/ 6-31G(d)	G ₂₉₈ (U)B3LYP-D3/ 6-31G(d)	E _{tot} G3B3-D3 ^(a)	H ₂₉₈ G3B3-D3 ^(a)
1H								
HOH	-76.4089533	-76.3840103	-76.4054563	-76.4089616	-76.3840216	-76.4054676	-76.4089616	-76.3840216
6								
HOO	-150.8991566	-150.8813206	-150.9073126	-150.8992506	-150.8814286	-150.9074216	-150.8992506	-150.8814286
1								
HO	-75.7234548	-75.7118458	-75.7320928	-75.7234554	-75.7118464	-75.7320934	-75.7234554	-75.7118464
6H								
HOOH	-151.5332131	-151.5027541	-151.5286321	-151.5335686	-151.5031236	-151.5289966	-151.5335686	-151.5031236

^(a) Using structures and thermal corrections from gas phase (U)B3LYP-D3/6-31G(d) calculations.**Table S2.4.13c.** Energy values for all systems shown in Figure 2.4.13.

system	E _{tot} (U)B3LYP/ 6-31+G(d,p)	H ₂₉₈ (U)B3LYP/ 6-31+G(d,p)	G ₂₉₈ (U)B3LYP/ 6-31+G(d,p)	E _{tot} (U)B3LYP-D3/ 6-31+G(d,p)	H ₂₉₈ (U)B3LYP-D3/ 6-31+G(d,p)	G ₂₉₈ (U)B3LYP-D3/ 6-31+G(d,p)
1H						
HOH	-76.4340477	-76.4089807	-76.4304097	-76.4340566	-76.4089926	-76.4304206
13						
HOO	-150.9154499	-150.8975419	-150.9235339	-150.9155454	-150.8976514	-150.9236434
1						
HO	-75.7390146	-75.7272716	-75.7475126	-75.7390151	-75.7272721	-75.7475131
13H						
HOOH	-151.5584082	-151.5277912	-151.5536292	-151.5587701	-151.5281671	-151.5540011

Table S2.4.13d. Energy values for all systems shown in Figure 2.4.13.

system	E _{tot} (U)B2PLYP/ cc-pVTZ ^(a)	E _{tot} (U)B2PLYP/ cc-pVQZ ^(a)	E _{tot} ROB2PLYP/ cc-pVTZ ^(a)	E _{tot} ROB2PLYP/ cc-pVQZ ^(a)	E _{tot} G3B3-D3 ^(a)	H ₂₉₈ G3B3-D3 ^(a)
--------	--	--	---	---	--	--

1H						
HOH	-76.4068145	-76.4221036	-76.4068145	-76.4221036	-76.4040880	-76.3798740
13						
HOO	-150.8703607	-150.8942711	-150.8684061	-150.8922435	-150.8434495	-150.8261135
1						
HO	-75.7137796	-75.7266444	-75.7119819	-75.7247971	-75.7044006	-75.6929956
13H						
HOOH	-151.5118436	-151.5373906	-151.5118436	-151.5373906	-151.4931587	-151.4635857

^(a) Using structures and thermal corrections from gas phase (U)B3LYP-D3/6-31+G(d,p) calculations.

Table S2.4.13e. Energy values for all systems shown in Figure 2.4.13.

system	E _{tot} DLPNO- CCSD(T)/ cc-pVTZ ^(a)	H ₂₉₈ DLPNO- CCSD(T)/ cc-pVTZ ^(a)	E _{tot} DLPNO- CCSD(T)/ cc-pVQZ ^(a)	H ₂₉₈ DLPNO- CCSD(T)/ cc-pVQZ ^(a)	E _{tot} DLPNO- CCSD(T)/ CBS ^(a)	H ₂₉₈ DLPNO- CCSD(T)/ CBS ^(a)
1H						
HOH	-76.3319273	-76.3068633	-76.3594799	-76.3344159	-76.3759529	-76.3508889
13						
HOO	-150.7118999	-150.6940059	-150.7586317	-150.7407377	-150.7870706	-150.7691766
1						
HO	-75.6376446	-75.6259016	-75.6612830	-75.6495400	-75.6754790	-75.6637360
13H						
HOOH	-151.3579884	-151.3273854	-151.4074133	-151.3768103	-151.4375673	-151.4069643

^(a) Using structures and thermal corrections from gas phase (U)B3LYP-D3/6-31+G(d,p) calculations.

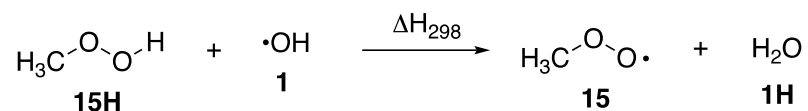


Figure 2.4.15. Reaction of hydroxyl radical (1) with methylhydroperoxide (15H).

Table S2.4.15a. Radical stabilization energies (RSE values) calculated for the systems shown in Fig. S15.

level of theory	RSE (E_{tot})	RSE (H_{298})	RSE (G_{298})
(U)B3LYP/6-31G(d)	-140.35	-137.05	-139.77
(U)B3LYP-D3/6-31G(d)	-139.33	-136.00	-138.67
(U)B3LYP/6-31+G(d,p)	-145.83	-142.76	-145.03
(U)B3LYP-D3/6-31+G(d,p)	-144.91	-141.81	-144.08
(U)B2PLYP/cc-pVTZ//(U)B3LYP-D3/6-31+G(d,p)	-142.50	-139.40	-141.66
(U)B2PLYP/cc-pVQZ//(U)B3LYP-D3/6-31+G(d,p)	-145.47	-142.37	-144.63
ROB2PLYP/cc-pVTZ//(U)B3LYP-D3/6-31+G(d,p)	-142.25	-139.15	-141.41
ROB2PLYP/cc-pVQZ//(U)B3LYP-D3/6-31+G(d,p)	-145.17	-142.07	-144.34
DLPNO-CCSD(T)/cc-pVTZ//(U)B3LYP-D3/6-31+G(d,p)	-131.98	-128.88	-131.14
DLPNO-CCSD(T)/cc-pVQZ//(U)B3LYP-D3/6-31+G(d,p)	-135.92	-132.82	-135.08
DLPNO-CCSD(T)/CBS//(U)B3LYP-D3/6-31+G(d,p)	-137.84	-134.74	-137.00
G3B3-D3//(U)B3LYP-D3/6-31+G(d,p)	-138.68	-135.76	-137.92
G3B3-D3//(U)B3LYP-D3/6-31G(d)	-138.97	-135.83	-138.39
exp.^a		-138.9±0.7	

^a Data from ATcT, version 1.122p, 2020: BDE(O-H,**20H**) = +358.4±0.7 kJ/mol, and BDE(O-H,**1H**) = +497.3±0.26 kJ/mol.

Table S2.4.15b. Energy values for all systems shown in Figure 2.4.15.

system	E _{tot} (U)B3LYP/ 6-31G(d)	H ₂₉₈ (U)B3LYP/ 6-31G(d)	G ₂₉₈ (U)B3LYP/ 6-31G(d)	E _{tot} (U)B3LYP-D3/ 6-31G(d)	H ₂₉₈ (U)B3LYP-D3/ 6-31G(d)	G ₂₉₈ (U)B3LYP-D3/ 6-31G(d)	E _{tot} G3B3-D3 ^(a)	H ₂₉₈ G3B3-D3 ^(a)
1H								
HOH	-76.4089533	-76.3840103	-76.4054563	-76.4089616	-76.3840216	-76.4054676	-76.4089616	-76.3840216
6								
CH3OO	-190.2152309	-190.1671729	-190.1976739	-190.2169841	-190.1689551	-190.1993841	-190.2169841	-190.1689551
1								
HO	-75.7234548	-75.7118458	-75.7320928	-75.7234554	-75.7118464	-75.7320934	-75.7234554	-75.7118464
6H								
CH3OOH	-190.8472716	-190.7871376	-190.8178026	-190.8494226	-190.7893316	-190.8199416	-190.8494226	-190.7893316

^(a) Using structures and thermal corrections from gas phase (U)B3LYP-D3/6-31G(d) calculations.**Table S2.4.15c.** Energy values for all systems shown in Figure 2.4.15.

system	E _{tot} (U)B3LYP/ 6-31+G(d,p)	H ₂₉₈ (U)B3LYP/ 6-31+G(d,p)	G ₂₉₈ (U)B3LYP/ 6-31+G(d,p)	E _{tot} (U)B3LYP-D3/ 6-31+G(d,p)	H ₂₉₈ (U)B3LYP-D3/ 6-31+G(d,p)	G ₂₉₈ (U)B3LYP-D3/ 6-31+G(d,p)
1H						
HOH	-76.4340477	-76.4089807	-76.4304097	-76.4340566	-76.4089926	-76.4304206
15						
CH3OO	-190.2302571	-190.1825091	-190.2130471	-190.2320066	-190.1842896	-190.2147596
1						
HO	-75.7390146	-75.7272716	-75.7475126	-75.7390151	-75.7272721	-75.7475131
15H						
CH3OOH	-190.8697446	-190.8098426	-190.8407066	-190.8718538	-190.8119958	-190.8427918

Table S2.4.15d. Energy values for all systems shown in Figure 2.4.15.

system	E _{tot} (U)B2PLYP/ cc-pVTZ ^(a)	E _{tot} (U)B2PLYP/ cc-pVQZ ^(a)	E _{tot} ROB2PLYP/ cc-pVTZ ^(a)	E _{tot} ROB2PLYP/ cc-pVQZ ^(a)	E _{tot} G3B3-D3 ^(a)	H ₂₉₈ G3B3-D3 ^(a)
--------	--	--	---	---	--	--

1H						
HOH	-76.4068145	-76.4221036	-76.4068145	-76.4221036	-76.4040880	-76.3798740
15						
CH3OO	-190.1531043	-190.1823439	-190.1512118	-190.1803841	-190.1352199	-190.0891709
1						
HO	-75.7137796	-75.7266444	-75.7119819	-75.7247971	-75.7044006	-75.6929956
15H						
CH3OOH	-190.7918641	-190.8223973	-190.7918641	-190.8223973	-190.7820853	-190.7243413

^(a) Using structures and thermal corrections from gas phase (U)B3LYP-D3/6-31+G(d,p) calculations.

Table S2.4.15e. Energy values for all systems shown in Figure 2.4.15.

system	E _{tot} DLPNO- CCSD(T)/ cc-pVTZ ^(a)	H ₂₉₈ DLPNO- CCSD(T)/ cc-pVTZ ^(a)	E _{tot} DLPNO- CCSD(T)/ cc-pVQZ ^(a)	H ₂₉₈ DLPNO- CCSD(T)/ cc-pVQZ ^(a)	E _{tot} DLPNO- CCSD(T)/ CBS ^(a)	H ₂₉₈ DLPNO- CCSD(T)/ CBS ^(a)
1H						
HOH	-76.3319273	-76.3068633	-76.3594799	-76.3344159	-76.3759529	-76.3508889
15						
CH3OO	-189.9426161	-189.8948991	-190.0006686	-189.9529516	-190.0362578	-189.9885408
1						
HO	-75.6376446	-75.6259016	-75.6612830	-75.6495400	-75.6754790	-75.6637360
15H						
CH3OOH	-190.5866319	-190.5267739	-190.6470982	-190.5872402	-190.6842307	-190.6243727

^(a) Using structures and thermal corrections from gas phase (U)B3LYP-D3/6-31+G(d,p) calculations.

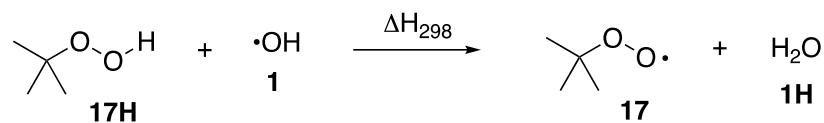


Figure 2.4.17. Reaction of hydroxyl radical (**1**) with *tert*-butylhydroperoxide (**17H**).

Table S2.4.17a. Radical stabilization energies (RSE values) calculated for the systems shown in Fig. S17.

level of theory	RSE (E_{tot})	RSE (H_{298})	RSE (G_{298})
(U)B3LYP/6-31G(d)	-147.64	-144.46	-147.57
(U)B3LYP-D3/6-31G(d)	-145.53	-142.46	-145.82
(U)B3LYP/6-31+G(d,p)	-153.37	-150.38	-153.31
(U)B3LYP-D3/6-31+G(d,p)	-151.51	-148.53	-151.52
(U)B2PLYP/cc-pVTZ//(U)B3LYP-D3/6-31+G(d,p)	-148.61	-145.62	-148.62
(U)B2PLYP/cc-pVQZ//(U)B3LYP-D3/6-31+G(d,p)	-152.03	-149.05	-152.04
ROB2PLYP/cc-pVTZ//(U)B3LYP-D3/6-31+G(d,p)	-148.35	-145.36	-148.36
ROB2PLYP/cc-pVQZ//(U)B3LYP-D3/6-31+G(d,p)	-151.76	-148.78	-151.77
DLPNO-CCSD(T)/cc-pVTZ//(U)B3LYP-D3/6-31+G(d,p)	-135.65	-132.67	-135.66
DLPNO-CCSD(T)/cc-pVQZ//(U)B3LYP-D3/6-31+G(d,p)	-139.76	-136.77	-139.77
DLPNO-CCSD(T)/CBS//(U)B3LYP-D3/6-31+G(d,p)	-141.68	-138.70	-141.69
G3B3-D3//(U)B3LYP-D3/6-31+G(d,p)	-144.05	-141.23	-144.13
G3B3-D3//(U)B3LYP-D3/6-31G(d)	-144.44	-141.54	-144.80
exp.^a		-145.0±8.8	

^a Data from Y. R. Luo, *Comprehensive Handbook of Chemical Bond Energies*, CRC Press, **2007**: BDE(O-H,**17H**) = +352.3±8.8 kJ/mol, and BDE(O-H,**1H**) = +497.32±0.26 kJ/mol from ATcT, version 1.122p, **2020**.

Table S2.4.17b. Energy values for all systems shown in Figure 2.4.17.

system	E _{tot} (U)B3LYP/ 6-31G(d)	H ₂₉₈ (U)B3LYP/ 6-31G(d)	G ₂₉₈ (U)B3LYP/ 6-31G(d)	E _{tot} (U)B3LYP-D3/ 6-31G(d)	H ₂₉₈ (U)B3LYP-D3/ 6-31G(d)	G ₂₉₈ (U)B3LYP-D3/ 6-31G(d)	E _{tot} G3B3-D3 ^(a)	H ₂₉₈ G3B3-D3 ^(a)
1H								
HOH	-76.4089533	-76.3840103	-76.4054563	-76.4089616	-76.3840216	-76.4054676	-76.4089616	-76.3840216
6								
t-BuOO	-308.1728880	-308.0365530	-308.0763790	-308.1846740	-308.0480870	-308.0875810	-308.1846740	-308.0480870
1								
HO	-75.7234548	-75.7118458	-75.7320928	-75.7234554	-75.7118464	-75.7320934	-75.7234554	-75.7118464
6H								
t-BuOOH	-308.8021547	-308.6536937	-308.6935347	-308.8147520	-308.6660010	-308.7054170	-308.8147520	-308.6660010

^(a) Using structures and thermal corrections from gas phase (U)B3LYP-D3/6-31G(d) calculations.**Table S2.4.17c.** Energy values for all systems shown in Figure 2.4.17.

system	E _{tot} (U)B3LYP/ 6-31+G(d,p)	H ₂₉₈ (U)B3LYP/ 6-31+G(d,p)	G ₂₉₈ (U)B3LYP/ 6-31+G(d,p)	E _{tot} (U)B3LYP-D3/ 6-31+G(d,p)	H ₂₉₈ (U)B3LYP-D3/ 6-31+G(d,p)	G ₂₉₈ (U)B3LYP-D3/ 6-31+G(d,p)
1H						
HOH	-76.4340477	-76.4089807	-76.4304097	-76.4340566	-76.4089926	-76.4304206
17						
t-BuOO	-308.1980644	-308.0626394	-308.1025574	-308.2098349	-308.0741619	-308.1137439
1						
HO	-75.7390146	-75.7272716	-75.7475126	-75.7390151	-75.7272721	-75.7475131
17H						
t-BuOOH	-308.8346817	-308.6870727	-308.7270627	-308.8471683	-308.6993103	-308.7389393

Table S2.4.17d. Energy values for all systems shown in Figure 2.4.17.

system	E _{tot} (U)B2PLYP/ (U)B2PLYP/ ROB2PLYP/ ROB2PLYP/ E _{tot} G3B3-D3 ^(a)	E _{tot} (U)B2PLYP/ (U)B2PLYP/ ROB2PLYP/ ROB2PLYP/ E _{tot} G3B3-D3 ^(a)	E _{tot} (U)B2PLYP/ (U)B2PLYP/ ROB2PLYP/ ROB2PLYP/ E _{tot} G3B3-D3 ^(a)	E _{tot} (U)B2PLYP/ (U)B2PLYP/ ROB2PLYP/ ROB2PLYP/ E _{tot} G3B3-D3 ^(a)	E _{tot} (U)B2PLYP/ (U)B2PLYP/ ROB2PLYP/ ROB2PLYP/ E _{tot} G3B3-D3 ^(a)	H ₂₉₈ G3B3-D3 ^(a)
--------	--	--	--	--	--	--

	cc-pVTZ ^(a)	cc-pVQZ ^(a)	cc-pVTZ ^(a)	cc-pVQZ ^(a)		
1H						
HOH	-76.4068145	-76.4221036	-76.4068145	-76.4221036	-76.4040880	-76.3798740
17						
t-BuOO	-308.0336903	-308.0797199	-308.0317937	-308.0777678	-308.0527741	-307.9219711
1						
HO	-75.7137796	-75.7266444	-75.7119819	-75.7247971	-75.7044006	-75.6929956
17H						
t-BuOOH	-308.6701245	-308.7172723	-308.6701245	-308.7172723	-308.6975953	-308.5550563

^(a) Using structures and thermal corrections from gas phase (U)B3LYP-D3/6-31+G(d,p) calculations.

Table S2.4.17e. Energy values for all systems shown in Figure 2.4.17.

system	E _{tot} DLPNO- CCSD(T)/ cc-pVTZ ^(a)	H ₂₉₈ DLPNO- CCSD(T)/ cc-pVTZ ^(a)	E _{tot} DLPNO- CCSD(T)/ cc-pVQZ ^(a)	H ₂₉₈ DLPNO- CCSD(T)/ cc-pVQZ ^(a)	E _{tot} DLPNO- CCSD(T)/ CBS ^(a)	H ₂₉₈ DLPNO- CCSD(T)/ CBS ^(a)
1H						
HOH	-76.3319273	-76.3068633	-76.3594799	-76.3344159	-76.3759529	-76.3508889
17						
t-BuOO	-307.6785042	-307.5428312	-307.7709584	-307.6352854	-307.8282657	-307.6925927
1						
HO	-75.6376446	-75.6259016	-75.6612830	-75.6495400	-75.6754790	-75.6637360
17H						
t-BuOOH	-308.3211194	-308.1732614	-308.4159253	-308.2680673	-308.4747768	-308.3269188

^(a) Using structures and thermal corrections from gas phase (U)B3LYP-D3/6-31+G(d,p) calculations.

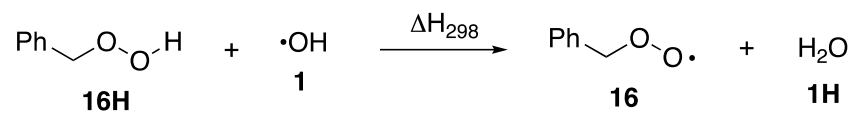


Figure 2.4.16. Reaction of hydroxyl radical (**1**) with benzylhydroperoxide (**16H**).

Table S2.4.16a. Radical stabilization energies (RSE values) calculated for the systems shown in Fig. S16.

level of theory	RSE (E_{tot})	RSE (H_{298})	RSE (G_{298})
(U)B3LYP/6-31G(d)	-137.96	-134.65	-140.54
(U)B3LYP-D3/6-31G(d)	-135.12	-131.78	-137.00
(U)B3LYP/6-31+G(d,p)	-145.60	-142.80	-146.77
(U)B3LYP-D3/6-31+G(d,p)	-141.84	-138.96	-141.51
(U)B2PLYP/cc-pVTZ//(U)B3LYP-D3/6-31+G(d,p)	-139.26	-136.38	-138.93
(U)B2PLYP/cc-pVQZ//(U)B3LYP-D3/6-31+G(d,p)	-143.26	-140.39	-142.94
ROB2PLYP/cc-pVTZ//(U)B3LYP-D3/6-31+G(d,p)	-139.02	-136.15	-138.70
ROB2PLYP/cc-pVQZ//(U)B3LYP-D3/6-31+G(d,p)	-142.99	-140.12	-142.67
DLPNO-CCSD(T)/cc-pVTZ//(U)B3LYP-D3/6-31+G(d,p)	-125.17	-122.11	-123.95
DLPNO-CCSD(T)/cc-pVQZ//(U)B3LYP-D3/6-31+G(d,p)	-128.98	-125.94	-128.49
DLPNO-CCSD(T)/CBS//(U)B3LYP-D3/6-31+G(d,p)	-130.85	-127.98	-130.53
G3B3-D3//(U)B3LYP-D3/6-31+G(d,p)	-132.30	-129.41	-131.69
G3B3-D3//(U)B3LYP-D3/6-31G(d)	-134.46	-131.54	-139.18
exp.		-132.3±0.3	

Table S2.4.16b. Energy values for all systems shown in Figure 2.4.16.

system	E _{tot} (U)B3LYP/ 6-31G(d)	H ₂₉₈ (U)B3LYP/ 6-31G(d)	G ₂₉₈ (U)B3LYP/ 6-31G(d)	E _{tot} (U)B3LYP-D3/ 6-31G(d)	H ₂₉₈ (U)B3LYP-D3/ 6-31G(d)	G ₂₉₈ (U)B3LYP-D3/ 6-31G(d)	E _{tot} G3B3-D3 ^(a)	H ₂₉₈ G3B3-D3 ^(a)
1H								
HOH	-76.4089533	-76.3840103	-76.4054563	-76.4089616	-76.3840216	-76.4054676	-76.4089616	-76.3840216
6								
PhCH2OO2	-421.2692892	-421.1353372	-421.1781722	-421.2801031	-421.1460881	-421.1887191	-421.2801031	-421.1460881
1								
HO	-75.7234548	-75.7118458	-75.7320928	-75.7234554	-75.7118464	-75.7320934	-75.7234554	-75.7118464
6H								
PhCH2OOH2	-421.9022409	-421.7562149	-421.7990289	-421.9141460	-421.7680700	-421.8104730	-421.9141460	-421.7680700
PhCH2OOH1	-421.9004122	-421.7545342	-421.7977782	-421.9117365	-421.7658185	-421.8088525	-421.9117365	-421.7658185
PhCH2OOH3	-421.9003551	-421.7543561	-421.7980481	-421.9110300	-421.7649900	-421.8085820	-421.9110300	-421.7649900

^(a) Using structures and thermal corrections from gas phase (U)B3LYP-D3/6-31G(d) calculations.**Table S2.4.16c.** Energy values for all systems shown in Figure 2.4.16.

system	E _{tot} (U)B3LYP/ 6-31+G(d,p)	H ₂₉₈ (U)B3LYP/ 6-31+G(d,p)	G ₂₉₈ (U)B3LYP/ 6-31+G(d,p)	E _{tot} (U)B3LYP-D3/ 6-31+G(d,p)	H ₂₉₈ (U)B3LYP-D3/ 6-31+G(d,p)	G ₂₉₈ (U)B3LYP-D3/ 6-31+G(d,p)
1H						
HOH	-76.4340477	-76.4089807	-76.4304097	-76.4340566	-76.4089926	-76.4304206
16						
PhCH2OO2	-421.2988378	-421.1655038	-421.2091178	-421.3089740	-421.1754890	-421.2184210
PhCH2OO1	-421.2983249	-421.1649089	-421.2080809	-421.3089690	-421.1755570	-421.2191140
1						
HO	-75.7390146	-75.7272716	-75.7475126	-75.7390151	-75.7272721	-75.7475131
16H						
PhCH2OOH2	-421.9384143	-421.7928243	-421.8361113	-421.9499920	-421.8043500	-421.8481240
PhCH2OOH1	-421.9375716	-421.7919936	-421.8357956	-421.9481777	-421.8025387	-421.8462557
PhCH2OOH3	-421.9368591	-421.7913811	-421.8355861	-421.9480209	-421.8025659	-421.8461189

Table S2.4.16d. Energy values for all systems shown in Figure 2.4.16.

system	E _{tot} (U)B2PLYP/ cc-pVTZ ^(a)	E _{tot} (U)B2PLYP/ cc-pVQZ ^(a)	E _{tot} ROB2PLYP/ cc-pVTZ ^(a)	E _{tot} ROB2PLYP/ cc-pVQZ ^(a)	E _{tot} G3B3-D3 ^(a)	H ₂₉₈ G3B3-D3 ^(a)
1H						
HOH	-76.4068145	-76.4221036	-76.4068145	-76.4221036	-76.4040880	-76.3798740
16						
PhCH2OO2	-421.0799534	-421.1404838	-421.0780505	-421.1385181	-421.0971400	-420.9684030
PhCH2OO1	-421.0799473	-421.1407249	-421.0780623	-421.1387748	-421.0970035	-420.9683345
1						
HO	-75.7137796	-75.7266444	-75.7119819	-75.7247971	-75.7044006	-75.6929956
16H						
PhCH2OOH2	-421.7199465	-421.7816211	-421.7199465	-421.7816211	-421.7464354	-421.6059904
PhCH2OOH1	-421.7185023	-421.7805234	-421.7185023	-421.7805234	-421.7444901	-421.6042201
PhCH2OOH3	-421.7180897	-421.7798046	-421.7180897	-421.7798046	-421.7445778	-421.6041308

^(a) Using structures and thermal corrections from gas phase (U)B3LYP-D3/6-31+G(d,p) calculations.

Table S2.4.16e. Energy values for all systems shown in Figure 2.4.16.

system	E _{tot} DLPNO- CCSD(T)/ cc-pVTZ ^(a)	H ₂₉₈ DLPNO- CCSD(T)/ cc-pVTZ ^(a)	E _{tot} DLPNO- CCSD(T)/ cc-pVQZ ^(a)	H ₂₉₈ DLPNO- CCSD(T)/ cc-pVQZ ^(a)	E _{tot} DLPNO- CCSD(T)/ CBS ^(a)	H ₂₉₈ DLPNO- CCSD(T)/ CBS ^(a)
1H						
HOH	-76.3319273	-76.3068633	-76.3594799	-76.3344159	-76.3759529	-76.3508889
16						
PhCH2OO2	-420.5560187	-420.4225337	-420.6780395	-420.5445545	-420.7536764	-420.6201914
PhCH2OO1	-420.5556774	-420.4222654	-420.6779711	-420.5445591	-420.7537359	-420.6203239
1						
HO	-75.6376446	-75.6259016	-75.6612830	-75.6495400	-75.6754790	-75.6637360
16H						

PhCH ₂ OOH ₂	-421.2026278	-421.0569858	-421.3271089	-421.1814669	-421.4043728	-421.2587308
PhCH ₂ OOH ₃	-421.2006539	-421.0551989	-421.3251306	-421.1796756	-421.4023864	-421.2569314
PhCH ₂ OOH ₁	-421.2006098	-421.0549708	-421.3253563	-421.1797173	-421.4027087	-421.2570697

^(a) Using structures and thermal corrections from gas phase (U)B3LYP-D3/6-31+G(d,p) calculations.

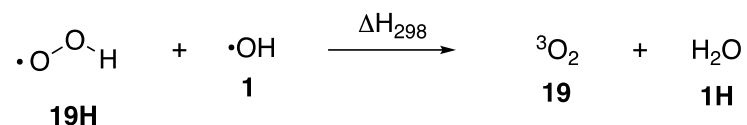


Figure 2.4.19. Reaction of hydroxyl radical (**1**) with hydroperoxy radical (**19H**).

Table S2.4.19a. Radical stabilization energies (RSE values) calculated for the systems shown in Fig. S19.

level of theory	RSE (E_{tot})	RSE (H_{298})	RSE (G_{298})
(U)B3LYP/6-31G(d)	-279.31	-272.52	-268.57
(U)B3LYP-D3/6-31G(d)	-279.09	-272.27	-268.31
(U)B3LYP/6-31+G(d,p)	-281.35	-274.89	-270.90
(U)B3LYP-D3/6-31+G(d,p)	-281.12	-274.63	-270.64
(U)B2PLYP/cc-pVTZ//((U)B3LYP-D3/6-31+G(d,p)	-298.15	-291.66	-287.68
(U)B2PLYP/cc-pVQZ//((U)B3LYP-D3/6-31+G(d,p)	-300.85	-294.36	-290.38
ROB2PLYP/cc-pVTZ//((U)B3LYP-D3/6-31+G(d,p)	-302.11	-295.61	-291.63
ROB2PLYP/cc-pVQZ//((U)B3LYP-D3/6-31+G(d,p)	-305.11	-298.62	-294.63
DLPNO-CCSD(T)/cc-pVTZ//((U)B3LYP-D3/6-31+G(d,p)	-290.27	-283.78	-279.79
DLPNO-CCSD(T)/cc-pVQZ//((U)B3LYP-D3/6-31+G(d,p)	-294.46	-287.97	-283.98
DLPNO-CCSD(T)/CBS//((U)B3LYP-D3/6-31+G(d,p)	-296.59	-290.10	-286.12
G3B3-D3//((U)B3LYP-D3/6-31+G(d,p)	-295.60	-289.38	-285.38
G3B3-D3//((U)B3LYP-D3/6-31G(d)	-295.76	-289.23	-285.26
exp. ^a		-291.54±0.26	

^a Data from ATcT, version 1.122p, 2020: BDE(O-H,**19H**) = +205.78±0.15 kJ/mol and BDE(O-H,**1H**) = +497.32±0.26 kJ/mol.

Table S2.4.19b. Energy values for all systems shown in Figure 2.4.19.

system	E _{tot} (U)B3LYP/ 6-31G(d)	H ₂₉₈ (U)B3LYP/ 6-31G(d)	G ₂₉₈ (U)B3LYP/ 6-31G(d)	E _{tot} (U)B3LYP-D3/ 6-31G(d)	H ₂₉₈ (U)B3LYP-D3/ 6-31G(d)	G ₂₉₈ (U)B3LYP-D3/ 6-31G(d)	E _{tot} G3B3-D3 ^(a)	H ₂₉₈ G3B3-D3 ^(a)
1H								
HOH	-76.4089533	-76.3840103	-76.4054563	-76.4089616	-76.3840216	-76.4054676	-76.4089616	-76.3840216
6								
3O2	-150.3200421	-150.3129551	-150.3362411	-150.3200431	-150.3129561	-150.3362421	-150.3200431	-150.3129561
1								
HO	-75.7234548	-75.7118458	-75.7320928	-75.7234554	-75.7118464	-75.7320934	-75.7234554	-75.7118464
6H								
HOO	-150.8991566	-150.8813206	-150.9073126	-150.8992506	-150.8814286	-150.9074216	-150.8992506	-150.8814286

^(a) Using structures and thermal corrections from gas phase (U)B3LYP-D3/6-31G(d) calculations.**Table S2.4.19c.** Energy values for all systems shown in Figure 2.4.19.

system	E _{tot} (U)B3LYP/ 6-31+G(d,p)	H ₂₉₈ (U)B3LYP/ 6-31+G(d,p)	G ₂₉₈ (U)B3LYP/ 6-31+G(d,p)	E _{tot} (U)B3LYP-D3/ 6-31+G(d,p)	H ₂₉₈ (U)B3LYP-D3/ 6-31+G(d,p)	G ₂₉₈ (U)B3LYP-D3/ 6-31+G(d,p)
1H						
HOH	-76.4340477	-76.4089807	-76.4304097	-76.4340566	-76.4089926	-76.4304206
19						
3O2	-150.3275770	-150.3205310	-150.3438180	-150.3275780	-150.3205320	-150.3438190
1						
HO	-75.7390146	-75.7272716	-75.7475126	-75.7390151	-75.7272721	-75.7475131
19H = 13						
HOO	-150.9154499	-150.8975419	-150.9235339	-150.9155454	-150.8976514	-150.9236434

Table S2.4.19d. Energy values for all systems shown in Figure 2.4.19.

system	E _{tot} (U)B2PLYP/ cc-pVTZ ^(a)	E _{tot} (U)B2PLYP/ cc-pVQZ ^(a)	E _{tot} ROB2PLYP/ cc-pVTZ ^(a)	E _{tot} ROB2PLYP/ cc-pVQZ ^(a)	E _{tot} G3B3-D3 ^(a)	H ₂₉₈ G3B3-D3 ^(a)
--------	--	--	---	---	--	--

1H						
HOH	-76.4068145	-76.4221036	-76.4068145	-76.4221036	-76.4040880	-76.3798740
19						
3O2	-150.2908867	-150.3134009	-150.2886401	-150.3111485	-150.2563506	-150.2494526
1						
HO	-75.7137796	-75.7266444	-75.7119819	-75.7247971	-75.7044006	-75.6929956
19H						
HOO	-150.8703607	-150.8942711	-150.8684061	-150.8922435	-150.8434495	-150.8261135

^(a) Using structures and thermal corrections from gas phase (U)B3LYP-D3/6-31+G(d,p) calculations.

Table S2.4.19e. Energy values for all systems shown in Figure 2.4.19.

system	E _{tot} DLPNO- CCSD(T)/ cc-pVTZ ^(a)	H ₂₉₈ DLPNO- CCSD(T)/ cc-pVTZ ^(a)	E _{tot} DLPNO- CCSD(T)/ cc-pVQZ ^(a)	H ₂₉₈ DLPNO- CCSD(T)/ cc-pVQZ ^(a)	E _{tot} DLPNO- CCSD(T)/ CBS ^(a)	H ₂₉₈ DLPNO- CCSD(T)/ CBS ^(a)
1H						
HOH	-76.3319273	-76.3068633	-76.3594799	-76.3344159	-76.3759529	-76.3508889
19						
3O2	-150.1281765	-150.1211305	-150.1725887	-150.1655427	-150.1995636	-150.1925176
1						
HO	-75.6376446	-75.6259016	-75.6612830	-75.6495400	-75.6754790	-75.6637360
19H						
HOO	-150.7118999	-150.6940059	-150.7586317	-150.7407377	-150.7870706	-150.7691766

^(a) Using structures and thermal corrections from gas phase (U)B3LYP-D3/6-31+G(d,p) calculations.

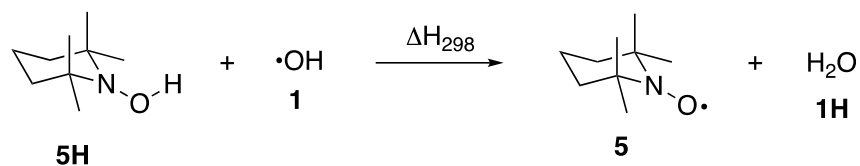


Figure 2.4.5. Reaction of hydroxyl radical (**1**) with TEMPOL (**5H**).

Table S2.4.5a. Radical stabilization energies (RSE values) calculated for the systems shown in Fig. S5.

level of theory	RSE (E_{tot})	RSE (H_{298})	RSE (G_{298})
(U)B3LYP/6-31G(d)	-208.08	-204.52	-210.10
(U)B3LYP-D3/6-31G(d)	-203.51	-199.91	-205.07
(U)B3LYP/6-31+G(d,p)	-216.05	-212.62	-218.14
(U)B3LYP-D3/6-31+G(d,p)	-211.51	-208.04	-213.20
(U)B2PLYP/cc-pVTZ//((U)B3LYP-D3/6-31+G(d,p)	-209.85	-206.37	-211.54
(U)B2PLYP/cc-pVQZ//((U)B3LYP-D3/6-31+G(d,p)	-214.41	-210.93	-216.10
ROB2PLYP/cc-pVTZ//((U)B3LYP-D3/6-31+G(d,p)	-211.42	-207.94	-213.11
ROB2PLYP/cc-pVQZ//((U)B3LYP-D3/6-31+G(d,p)	-216.13	-212.65	-217.82
DLPNO-CCSD(T)/cc-pVTZ//((U)B3LYP-D3/6-31+G(d,p)	-188.61	-185.13	-190.30
DLPNO-CCSD(T)/cc-pVQZ//((U)B3LYP-D3/6-31+G(d,p)	-195.20	-191.72	-196.88
DLPNO-CCSD(T)/CBS//((U)B3LYP-D3/6-31+G(d,p)	-198.87	-195.39	-200.56
G3B3-D3//((U)B3LYP-D3/6-31+G(d,p)	-201.62	-198.45	-203.80
G3B3-D3//((U)B3LYP-D3/6-31G(d)	-201.80	-198.39	-203.49
exp.^a		-204.1±0.1	

^a Data from P. S. Billone et al., *J. Org. Chem.* **2011**, 76, 631: BDE(OH,**5H**) = +293.2±0.1 kJ/mol, and BDE(O-H,**1H**) = +497.3±0.26 kJ/mol from ATcT, version 1.122p, **2020**.

Table S2.4.5b. Energy values for all systems shown in Figure 2.4.5.

system	E _{tot} (U)B3LYP/ 6-31G(d)	H ₂₉₈ (U)B3LYP/ 6-31G(d)	G ₂₉₈ (U)B3LYP/ 6-31G(d)	E _{tot} (U)B3LYP-D3/ 6-31G(d)	H ₂₉₈ (U)B3LYP-D3/ 6-31G(d)	G ₂₉₈ (U)B3LYP-D3/ 6-31G(d)	E _{tot} G3B3-D3 ^(a)	H ₂₉₈ G3B3-D3 ^(a)
1H								
HOH	-76.4089533	-76.3840103	-76.4054563	-76.4089616	-76.3840216	-76.4054676	-76.4089616	-76.3840216
6								
TEMPO	-483.7197701	-483.4434671	-483.4931981	-483.7522734	-483.4751944	-483.5241904	-483.7522734	-483.4751944
1								
HO	-75.7234548	-75.7118458	-75.7320928	-75.7234554	-75.7118464	-75.7320934	-75.7234554	-75.7118464
6H								
TEMPOH	-484.3260144	-484.0377324	-484.0865404	-484.3602668	-484.0712278	-484.1194568	-484.3602668	-484.0712278
TEMPOHa	-484.3211407	-484.0330287	-484.0818167	-484.3553775	-484.0665905	-484.1148865	-484.3553775	-484.0665905

^(a) Using structures and thermal corrections from gas phase (U)B3LYP-D3/6-31G(d) calculations.

Table S2.4.5c. Energy values for all systems shown in Figure 2.4.5.

system	E _{tot} (U)B3LYP/ 6-31+G(d,p)	H ₂₉₈ (U)B3LYP/ 6-31+G(d,p)	G ₂₉₈ (U)B3LYP/ 6-31+G(d,p)	E _{tot} (U)B3LYP-D3/ 6-31+G(d,p)	H ₂₉₈ (U)B3LYP-D3/ 6-31+G(d,p)	G ₂₉₈ (U)B3LYP-D3/ 6-31+G(d,p)
1H						
HOH	-76.4340477	-76.4089807	-76.4304097	-76.4340566	-76.4089926	-76.4304206
5						
TEMPO	-483.7593238	-483.4848158	-483.5346488	-483.7917897	-483.5165127	-483.5656387
1						
HO	-75.7390146	-75.7272716	-75.7475126	-75.7390151	-75.7272721	-75.7475131
5H						
TEMPOH	-484.3720665	-484.0855425	-484.1344615	-484.4062695	-484.1189965	-484.1673425
TEMPOHa	-484.3664172	-484.0801492	-484.1292272	-484.4006378	-484.1136918	-484.1622828

Table S2.4.05d. Energy values for all systems shown in Figure 2.4.05.

system	E _{tot}	E _{tot}	E _{tot}	E _{tot}	E _{tot}	H ₂₉₈
--------	------------------	------------------	------------------	------------------	------------------	------------------

	(U)B2PLYP/ cc-pVTZ ^(a)	(U)B2PLYP/ cc-pVQZ ^(a)	ROB2PLYP/ cc-pVTZ ^(a)	ROB2PLYP/ cc-pVQZ ^(a)	G3B3-D3 ^(a)	G3B3-D3 ^(a)
1H						
HOH	-76.4068145	-76.4221036	-76.4068145	-76.4221036	-76.4040880	-76.3798740
5						
TEMPO	-483.4551278	-483.5261475	-483.4539279	-483.5249550	-483.5500125	-483.2847835
1						
HO	-75.7137796	-75.7266444	-75.7119819	-75.7247971	-75.7044006	-75.6929956
5H						
TEMPOH	-484.0682342	-484.1399418	-484.0682342	-484.1399418	-484.1729051	-483.8960771
TEMPOHa	-484.0631096	-484.1348510	-484.0631096	-484.1348510	-484.1673548	-483.8908888

^(a) Using structures and thermal corrections from gas phase (U)B3LYP-D3/6-31+G(d,p) calculations.

Table S2.4.05e. Energy values for all systems shown in Figure 2.4.05.

system	E _{tot} DLPNO- CCSD(T)/ cc-pVTZ ^(a)	H ₂₉₈ DLPNO- CCSD(T)/ cc-pVTZ ^(a)	E _{tot} DLPNO- CCSD(T)/ cc-pVQZ ^(a)	H ₂₉₈ DLPNO- CCSD(T)/ cc-pVQZ ^(a)	E _{tot} DLPNO- CCSD(T)/ CBS ^(a)	H ₂₉₈ DLPNO- CCSD(T)/ CBS ^(a)
1H						
HOH	-76.3319273	-76.3068633	-76.3594799	-76.3344159	-76.3759529	-76.3508889
5						
TEMPO	-482.8768639	-482.6015869	-483.0199279	-482.7446509	-483.1092606	-482.8339836
1						
HO	-75.6376446	-75.6259016	-75.6612830	-75.6495400	-75.6754790	-75.6637360
5H						
TEMPOH	-483.4993076	-483.2120346	-483.6437777	-483.3565047	-483.7339877	-483.4467147
TEMPOHa	-483.4939624	-483.2070164	-483.6384003	-483.3514543	-483.7285490	-483.4416030

^(a) Using structures and thermal corrections from gas phase (U)B3LYP-D3/6-31+G(d,p) calculations.

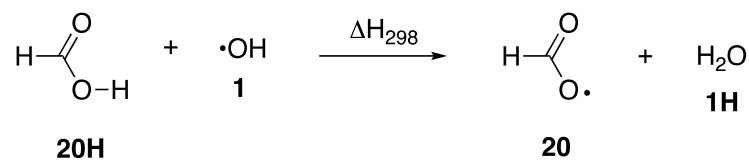


Figure 2.4.20. Reaction of hydroxyl radical (**1**) with formic acid (**20H**).

Table S2.4.20a. Radical stabilization energies (RSE values) calculated for the systems shown in Fig. S20.

level of theory	RSE (E_{tot})	RSE (H_{298})	RSE (G_{298})
(U)B3LYP/6-31G(d)	-20.27	-31.00	-37.30
(U)B3LYP-D3/6-31G(d)	-18.79	-29.46	-35.37
(U)B3LYP/6-31+G(d,p)	-25.90	-36.62	-41.08
(U)B3LYP-D3/6-31+G(d,p)	-24.40	-35.20	-39.95
(U)B2PLYP/cc-pVTZ//(U)B3LYP-D3/6-31+G(d,p)	-29.23	-40.03	-44.77
(U)B2PLYP/cc-pVQZ//(U)B3LYP-D3/6-31+G(d,p)	-32.51	-43.31	-48.06
ROB2PLYP/cc-pVTZ//(U)B3LYP-D3/6-31+G(d,p)	-31.80	-42.60	-47.35
ROB2PLYP/cc-pVQZ//(U)B3LYP-D3/6-31+G(d,p)	-35.33	-46.13	-50.88
DLPNO-CCSD(T)/cc-pVTZ//(U)B3LYP-D3/6-31+G(d,p)	-3.47	-14.27	-19.02
DLPNO-CCSD(T)/cc-pVQZ//(U)B3LYP-D3/6-31+G(d,p)	-7.81	-18.61	-23.36
DLPNO-CCSD(T)/CBS//(U)B3LYP-D3/6-31+G(d,p)	-10.14	-20.94	-25.68
G3B3-D3//(U)B3LYP-D3/6-31+G(d,p)	-17.42	-27.69	-32.49
G3B3-D3//(U)B3LYP-D3/6-31G(d)	-17.47	-27.62	-33.58
exp. (ATcT)^a		-28.4	

^a Data from ATcT, version 1.122p, **2020**: BDE(O-H,**20H**) = +468.89±0.56 kJ/mol, and BDE(O-H,**1H**) = +497.32±0.26 kJ/mol.

Table S2.4.20b. Energy values for all systems shown in Figure 2.4.20.

system	E _{tot} (U)B3LYP/ 6-31G(d)	H ₂₉₈ (U)B3LYP/ 6-31G(d)	G ₂₉₈ (U)B3LYP/ 6-31G(d)	E _{tot} (U)B3LYP-D3/ 6-31G(d)	H ₂₉₈ (U)B3LYP-D3/ 6-31G(d)	G ₂₉₈ (U)B3LYP-D3/ 6-31G(d)	E _{tot} G3B3-D3 ^(a)	H ₂₉₈ G3B3-D3 ^(a)
1H								
HOH	-76.4089533	-76.3840103	-76.4054563	-76.4089616	-76.3840216	-76.4054676	-76.4089616	-76.3840216
6								
HCO2	-189.0776800	-189.0570660	-189.0864530	-189.0781279	-189.0575149	-189.0867509	-189.0781279	-189.0575149
1								
HO	-75.7234548	-75.7118458	-75.7320928	-75.7234554	-75.7118464	-75.7320934	-75.7234554	-75.7118464
6H								
HCO2Ha	-189.7554578	-189.7174248	-189.7456088	-189.7564772	-189.7184702	-189.7466522	-189.7564772	-189.7184702
HCO2Hb	-189.7471686	-189.7094546	-189.7377206	-189.7480022	-189.7103442	-189.7386152	-189.7480022	-189.7103442

^(a) Using structures and thermal corrections from gas phase (U)B3LYP-D3/6-31G(d) calculations.

Table S2.4.20b. Energy values for all systems shown in Figure 2.4.20.

system	E _{tot} (U)B3LYP/ 6-31G(d)	H ₂₉₈ (U)B3LYP/ 6-31G(d)	G ₂₉₈ (U)B3LYP/ 6-31G(d)	E _{tot} (U)B3LYP-D3/ 6-31G(d)	H ₂₉₈ (U)B3LYP-D3/ 6-31G(d)	G ₂₉₈ (U)B3LYP-D3/ 6-31G(d)
1H						
HOH	-76.4089533	-76.3840103	-76.4054563	-76.4089616	-76.3840216	-76.4054676
20						
aco_001 (C2v, 2A1)	-189.0776793	-189.058093 (imag = -137 cm)	-189.085761	-189.0781260	-189.058577 (imag=-165 cm)	-189.086246
HCO2 (Cs, 2A')	-189.0776800	-189.0570660	-189.0864530	-189.0781279	-189.0575149	-189.0867509
1						
HO	-75.7234548	-75.7118458	-75.7320928	-75.7234554	-75.7118464	-75.7320934
20H						
HCO2Ha (Cs)	-189.7554578	-189.7174248	-189.7456088	-189.7564772	-189.7184702	-189.7466522
HCO2Hb	-189.7471686	-189.7094546	-189.7377206	-189.7480022	-189.7103442	-189.7386152

Table S2.4.20c. Energy values for all systems shown in Figure 2.4.20.

system	E _{tot} (U)B3LYP/ 6-31+G(d,p)	H ₂₉₈ (U)B3LYP/ 6-31+G(d,p)	G ₂₉₈ (U)B3LYP/ 6-31+G(d,p)	E _{tot} (U)B3LYP-D3/ 6-31+G(d,p)	H ₂₉₈ (U)B3LYP-D3/ 6-31+G(d,p)	G ₂₉₈ (U)B3LYP-D3/ 6-31+G(d,p)
1H						
HOH	-76.4340477	-76.4089807	-76.4304097	-76.4340566	-76.4089926	-76.4304206
20						
HCO ₂ (C _{2v} , 2A ₁)	-189.0903268	-189.0698328	-189.0985538	-189.0907760	-189.0703340	-189.0991610
1						
HO	-75.7390146	-75.7272716	-75.7475126	-75.7390151	-75.7272721	-75.7475131
20H						
HCO ₂ Ha (Cs)	-189.7754950	-189.7375950	-189.7658030	-189.7765237	-189.7386467	-189.7668527
HCO ₂ Hb	-189.7679416	-189.7303366	-189.7586206	-189.7687813	-189.7312323	-189.7595213

Table S2.4.20d. Energy values for all systems shown in Figure 2.4.20.

system	E _{tot} (U)B2PLYP/ cc-pVTZ ^(a)	E _{tot} (U)B2PLYP/ cc-pVQZ ^(a)	E _{tot} ROB2PLYP/ cc-pVTZ ^(a)	E _{tot} ROB2PLYP/ cc-pVQZ ^(a)	E _{tot} G3B3-D3 ^(a)	H ₂₉₈ G3B3-D3 ^(a)
1H						
HOH	-76.4068145	-76.4221036	-76.4068145	-76.4221036	-76.4040880	-76.3798740
20						
HCO ₂ (C _{2v} , 2A ₁)	-189.0292999	-189.0580772	-189.0284838	-189.0573040	-189.0003540	-188.9805090
1						
aco_018sp1	-75.7137796	-75.7266444	-75.7119819	-75.7247971	-75.6929956	-75.7132366
20H						
HCO ₂ Ha (Cs)	-189.7112031	-189.7411536	-189.7112031	-189.7411536	-189.6934067	-189.6568397
HCO ₂ Hb	-189.7040618	-189.7343918	-189.7040618	-189.7343918	-189.6867002	-189.6504422

^(a) Using structures and thermal corrections from gas phase (U)B3LYP-D3/6-31+G(d,p) calculations.

Table S2.4.20e. Energy values for all systems shown in Figure 2.4.20.

system	E _{tot} DLPNO- CCSD(T)/ cc-pVTZ ^(a)	H ₂₉₈ DLPNO- CCSD(T)/ cc-pVTZ ^(a)	E _{tot} DLPNO- CCSD(T)/ cc-pVQZ ^(a)	H ₂₉₈ DLPNO- CCSD(T)/ cc-pVQZ ^(a)	E _{tot} DLPNO- CCSD(T)/ CBS ^(a)	H ₂₉₈ DLPNO- CCSD(T)/ CBS ^(a)
1H						
HOH	-76.3319273	-76.3068633	-76.3594799	-76.3344159	-76.3759529	-76.3508889
20						
HCO2	-188.8076281	-188.7871861	-188.8648682	-188.8444262	-188.8997778	-188.8793358
1						
HO	-75.6376446	-75.6259016	-75.6612830	-75.6495400	-75.6754790	-75.6637360
20H						
HCO2Ha	-189.5005886	-189.4627116	-189.5600910	-189.5222140	-189.5963911	-189.5585141
HCO2Hb	-189.4934756	-189.4559266	-189.5532738	-189.5157248	-189.5896459	-189.5520969

^(a) Using structures and thermal corrections from gas phase (U)B3LYP-D3/6-31+G(d,p) calculations.

Table S2.5.1. Wavefunction-states for G3B3-D3//UB3LYP-D3/6-31+G(d,p)

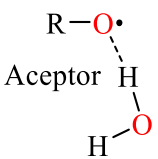
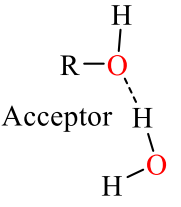
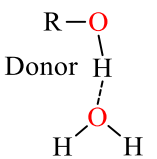
Filename	$\langle S^2 \rangle$ [a]	$\langle S^2 \rangle$ [b]	$\langle S^2 \rangle$ [c]	$\langle S^2 \rangle$ [d]	$\langle S^2 \rangle$ [e]	State [a]	State [b]	State [c]	State [d]	State [e]
BuO1	0.7537	0.7582	0.7582	0.7595	0.7595	2-A	2-A	2-A	2-A	2-A
BuO2	0.7537	0.7582	0.7582	0.7595	0.7595	2-A	2-A	2-A	2-A	2-A
BuO3	0.7538	0.7584	0.7584	0.7597	0.7597	2-A	2-A	2-A	2-A	2-A
BuO4	0.7537	0.7583	0.7583	0.7595	0.7595	2-A	2-A	2-A	2-A	2-A
BuO5	0.7537	0.7582	0.7582	0.7594	0.7594	2-A	2-A	2-A	2-A	2-A
CH3CH2O1	0.7537	0.7582	0.7582	0.7595	0.7595	2-A''	2-A''	2-A''	2-A''	2-A''
CH3O1	0.7535	0.7580	0.7580	0.7593	0.7593	2-A	2-A	2-A	2-A	2-A
CH3OO	0.7540	0.7602	0.7602	0.7629	0.7629	2-A	2-A	2-A	2-A	2-A
HCO2	0.7563	0.7669	0.7669	0.7678	0.7678	2-A1	2-A1	2-A1	2-A1	2-A1
HO	0.7524	0.7555	0.7555	0.7565	0.7565					
HOO	0.7538	0.7599	0.7599	0.7624	0.7624	2-A''	2-A''	2-A''	2-A''	2-A''
p-amino-PhO	0.7715	1.2899	1.2899	1.2695	1.2695	2-A'	2-A'	2-A'	2-A'	2-A'
PhCCH32O2_a	0.7542	1.2783	1.2783	1.2368	1.2792	2-A	2-A	2-A	2-A	2-A
PhCCH32O3	0.7536	1.2700	1.2700	1.2241	1.2241	2-A	2-A	2-A	2-A	2-A
PhCH2O2	0.7542	1.2797	1.2797	1.2322	1.2322	2-A''	2-A''	2-A''	2-A''	2-A''
PhCH2O3	0.7545	1.2865	1.2865	1.2448	1.2448	2-A'	2-A'	2-A'	2-A'	2-A'
PhCH2OO1	0.7542	1.2900	1.2900	1.2900	1.2900	2-A	2-A	2-A	2-A	2-A
PhCH2OO2	0.7542	0.7607	0.7633	0.7616	0.7640	2-A	2-A	2-A	2-A	2-A
PhO	0.7876	1.3859	1.3626	1.3843	1.3572	2-B1	2-B1	2-B1	2-B1	2-B1
p-methyl-PhO	0.7845	1.3749	1.3517	1.3725	1.3456	2-A	2-A	2-A	2-A	2-A
p-nitro-PhO	0.7911	1.4190	1.4062	1.4158	1.4008	2-B1	2-B1	2-B1	2-B1	2-B1
t-BuO2	0.7535	0.7581	0.7593	0.7587	0.7599	2-A'	2-A'	2-A'	2-A'	2-A'
t-BuOO	0.7542	0.7610	0.7634	0.7618	0.7642	2-A	2-A	2-A	2-A	2-A
TEMPO	0.7543	0.7675	0.7714	0.7688	0.7732	2-A'	2-A'	2-A'	2-A'	2-A'
3O2	2.0089	2.0351	2.0455	2.0370	2.0478	3-SGG	3-SGG	3-SGG	3-SGG	3-SGG
[a] UB3LYP-D3/6-31+G(d,p) [b] UHF/6-31G(d) [c] UHF/6-31+G(d) [d] UHF/6-31G(2df,p) [e] UHF/GTlarge										

Table S2.5.2. Wavefunction-states for G3B3-D3//UB3LYP-D3/6-31+G(d,p) (opt=stable)

Filename	$\langle S^2 \rangle$ ^[a]	$\langle S^2 \rangle$ ^[b]	$\langle S^2 \rangle$ ^[c]	$\langle S^2 \rangle$ ^[d]	$\langle S^2 \rangle$ ^[e]	State ^[a]	State ^[b]	State ^[c]	State ^[d]	State ^[e]
BuO1	0.7537	0.7582	0.7595	0.7589	0.7602	2-A	2-A	2-A	2-A	2-A
BuO2	0.7537	0.7582	0.7595	0.7589	0.7602	2-A	2-A	2-A	2-A	2-A
BuO3	0.7538	0.7584	0.7597	0.7591	0.7604	2-A	2-A	2-A	2-A	2-A
BuO4	0.7537	0.7583	0.7595	0.7589	0.7602	2-A	2-A	2-A	2-A	2-A
BuO5	0.7537	0.7582	0.7594	0.7588	0.7602	2-A	2-A	2-A	2-A	2-A
CH3CH2O1	0.7537	0.7582	0.7595	0.7588	0.7602	2-A''	2-A''	2-A''	2-A''	2-A''
CH3O1	0.7535	0.7580	0.7593	0.7587	0.7600	2-A	2-A	2-A	2-A	2-A
CH3OO	0.7540	0.7602	0.7629	0.7610	0.7636	2-A	2-A	2-A	2-A	2-A
HCO2	0.7563	0.7669	0.7678	0.7673	0.7686	2-A1	2-A1	2-A1	2-A1	2-A1
HO	0.7524	0.7555	0.7565	0.7559	0.7568					
HOO	0.7538	0.7599	0.7624	0.7606	0.7629	2-A''	2-A''	2-A''	2-A''	2-A''
p-amino-PhO	0.7715	1.2899	1.2695	1.2884	1.2884	2-A'	2-A'	2-A'	2-A'	2-A'
PhCCH32O2_a	0.7542	1.2783	1.2368	1.2792	1.2308	2-A	2-A	2-A	2-A	2-A
PhCCH32O3	0.7536	1.2700	1.2241	1.2702	1.2168	2-A	2-A	2-A	2-A	2-A
PhCH2O2	0.7542	1.2797	1.2322	1.2797	1.2239	2-A''	2-A''	2-A''	2-A''	2-A''
PhCH2O3	0.7545	1.2865	1.2448	1.2881	1.2389	2-A'	2-A'	2-A'	2-A'	2-A'
PhCH2OO1	0.7542	1.2900	1.2479	1.2908	1.2416	2-A	2-A	2-A	2-A	2-A
PhCH2OO2	0.7542	1.2889	1.2466	1.2898	1.2401	2-A	2-A	2-A	2-A	2-A
PhO	0.7876	1.3859	1.3626	1.3843	1.3572	2-B1	2-B1	2-B1	2-B1	2-B1
p-methyl-PhO	0.7845	1.3749	1.3517	1.3725	1.3456	2-A	2-A	2-A	2-A	2-A
p-nitro-PhO	0.7911	1.9011	1.8755	1.8944	1.8732	2-B1	2-B1	2-B1	2-B1	2-B1
t-BuO2	0.7535	0.7581	0.7593	0.7587	0.7599	2-A'	2-A'	2-A'	2-A'	2-A'
t-BuOO	0.7542	0.7610	0.7634	0.7618	0.7642	2-A	2-A	2-A	2-A	2-A
TEMPO	0.7543	0.7675	0.7714	0.7688	0.7732	2-A'	2-A'	2-A'	2-A'	2-A'
3O2	2.0089	2.0351	2.0455	2.0370	2.0478	3-SGG	3-SGG	3-SGG	3-SGG	3-SGG
[a] UB3LYP-D3/6-31+G(d,p) [b] UHF/6-31G(d) [c] UHF/6-31+G(d) [d] UHF/6-31G(2df,p) [e] UHF/GTlarge										

3. One explicit water

Table S3.1.1. RSE-A and RSE-D values (kJ mol⁻¹) calculated for selected O-centered radicals

 Acceptor		RSE(RO•)					
		 Acceptor			 Donor		
		Alcohol			Alcohol		
Radical		DFT ^[a]	CBS ^[b]	G3B3-D3 ^[c]	DFT ^[a]	CBS ^[b]	G3B3-D3 ^[c]
HO•	(1)	6.1	4.1		6.1	4.1	
HC(O)O•	(20)	-39.4	-10.3	-23.9	-9.0	16.4	3.1
CH ₃ O•	(6)	-60.6	-53.7	-51.6	-63.4	-55.3	-55.7
CH ₃ CH ₂ O•	(9)	-60.1	-51.5	-50.2	-65.7	-55.1	-56.1
<i>n</i> -Bu-O•	(11)	-62.7	-53.1	-52.2	-68.5	-57.1	-57.5
<i>t</i> -Bu-O•	(7)	-55.1	-44.3	-44.6	-62.9	-49.5	-52.7
PhCH ₂ O•	(8)	-56.6	-45.2	-45.0	-56.5	-43.6	-44.8
PhC(CH ₃) ₂ O•	(10)	-55.1	-41.5	-44.3	-53.5	-38.8	-40.1
PhO•	(2)	-144.0	-132.5	-130.4	-133.4	-124.0	-118.9
<i>p</i> -nitro-PhO•	(12)	-125.3	-115.3	-114.8	-104.7	-98.1	-95.6
<i>p</i> -methyl-PhO•	(14)	-153.1	-140.0	-138.5	-143.8	-132.7	-128.3
<i>p</i> -amino-PhO•	(18)	-183.2	-163.9	-165.7	-176.3	-158.2	-160.9
HOO•	(13)	-142.9	-137.1	-137.6	-142.9	-137.1	-137.6
CH ₃ OO•	(15)	-143.5	-136.0	-137.3	-132.3	-124.9	-126.1
<i>t</i> -Bu-OO•	(17)	-149.6	-139.5	-144.5	-137.1	-127.8	-131.8
PhCH ₂ OO•	(16)	-137.5	-126.8	-129.3	-127.5	-116.3	-118.7
TEMPO•	(5)	-215.5	-203.4	-208.8	-198.6	-189.8	-191.4
•OO•	(19)				-236.4	-258.2	-257.6

[a] (U)B3LYP-D3/6-31+G(d,p) level of theory
 [b] DLPNO-CCSD(T)/CBS using (U)B3LYP-D3/6-31+G(d,p) optimized geometries
 [c] Using (U)B3LYP-D3/6-31G(d) optimized geometries

Table S3.1.2. The calculated for selected O-centered radicals ΔRSE ($\Delta\Delta H_{c1}$) values (kJ mol^{-1})

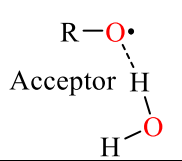
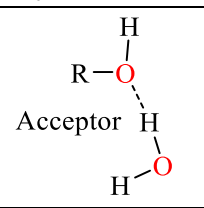
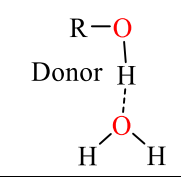
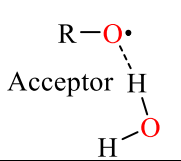
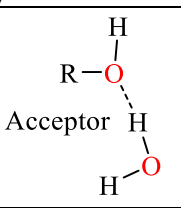
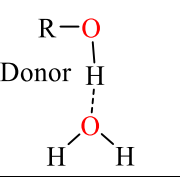
$\Delta RSE = \Delta\Delta H_{c1}$								
								
	Radical		Alcohol			Alcohol		
			DFT ^[a]	CBS ^[b]	G3B3-D3 ^[c]	DFT ^[a]	CBS ^[b]	G3B3-D3 ^[c]
	HO•	(1)	6.1	4.1		6.1	4.1	
	HC(O)O•	(20)	-4.2	10.7	3.7	26.2	37.3	30.7
Alkoxy	CH ₃ O•	(6)	4.7	3.0	4.1	2.0	1.4	0.1
Alkoxy	CH ₃ CH ₂ O•	(9)	6.5	4.3	4.6	0.9	0.7	-1.3
Alkoxy	<i>n</i> -Bu-O•	(11)	4.1	2.6	3.1	-1.6	-1.4	-2.2
Alkoxy	<i>t</i> -Bu-O•	(7)	2.5	2.5	3.1	-5.2	-2.7	-5.0
Alkoxy	PhCH ₂ O•	(8)	8.5	7.0	10.5	8.5	8.6	10.7
Alkoxy	PhC(CH ₃) ₂ O•	(10)	3.0	3.6	3.4	4.7	6.2	7.7
Aroma	PhO•	(2)	-11.1	-9.0	-8.8	-0.5	-0.5	2.7
Aroma	<i>p</i> -nitro-PhO•	(12)	-10.8	-9.2	-8.8	9.8	8.1	10.4
Aroma	<i>p</i> -methyl-PhO•	(14)	-11.8	-9.5	-9.2	-2.5	-2.3	1.1
Aroma	<i>p</i> -amino-PhO•	(18)	-14.4	-11.6	-11.9	-7.5	-5.9	-7.1
LP att.	HOO•	(13)	-8.5	-7.5	-8.0	-8.5	-7.5	-8.0
LP att.	CH ₃ OO•	(15)	-1.7	-1.2	-1.4	9.5	9.8	9.7
LP att.	<i>t</i> -Bu-OO•	(17)	-1.1	-0.8	-3.0	11.4	10.9	9.7
LP att.	PhCH ₂ OO•	(16)	1.5	1.1	2.2	11.5	11.7	12.9
LP att.	TEMPO•	(5)	-7.5	-8.0	-10.4	9.4	5.6	7.0
LP att.	•OO•	(19)				38.2	31.9	31.6
[a] (U)B3LYP-D3/6-31+G(d,p) level of theory								
[b] DLPNO-CCSD(T)/CBS using (U)B3LYP-D3/6-31+G(d,p) optimized geometries								
[c] Using (U)B3LYP-D3/6-31G(d) optimized geometries								
$\Delta RSE = \Delta\Delta H_{c1} =$ $\Delta H_{c1}(\text{RO}\cdot \dots \text{H}_2\text{O})$ minus $\Delta H_{c1}(\text{ROH} \dots \text{H}_2\text{O})$		$\Delta\Delta H_{c1} < 0$ Negative (Stabilization)	$\Delta\Delta H_{c1} \approx 0$ Neutral (Almost No Change)	$\Delta\Delta H_{c1} > 0$ Positive (Destabilization)				

Table S3.2.1. $\Delta H_{c1}(\text{Molecule} + \text{H}_2\text{O})$ values (kJ mol^{-1}) calculated for selected O-centered radicals

$\Delta H_{c1}(\text{Molecule} + \text{H}_2\text{O})$											
											
		Radical			Alcohol			Alcohol			
			DFT ^[a]	CBS ^[b]	G3B3-D3 ^[c]	DFT ^[a]	CBS ^[b]	G3B3-D3 ^[c]	DFT ^[a]	CBS ^[b]	G3B3-D3 ^[c]
	HO•	(1)	-14.6	-9.9		-20.7	-14.1	-7.5	-20.7	-14.1	-7.5
	HC(O)O•	(20)	-17.8	1.1	-2.9	-13.6	-9.5	-6.6	-44.1	-36.2	-33.6
Alkoxy	CH ₃ O•	(6)	-18.6	-13.5	-11.1	-23.3	-16.5	-15.2	-20.6	-14.9	-11.2
Alkoxy	CH ₃ CH ₂ O•	(9)	-19.5	-14.0	-12.2	-26.0	-18.3	-16.8	-20.4	-14.7	-11.0
Alkoxy	<i>n</i> -Bu-O•	(11)	-22.7	-16.5	-14.9	-26.8	-19.0	-18.0	-21.0	-15.0	-12.6
Alkoxy	<i>t</i> -Bu-O•	(7)	-25.6	-18.1	-16.1	-28.1	-20.5	-19.2	-20.4	-15.3	-11.2
Alkoxy	PhCH ₂ O•	(8)	-21.1	-14.5	-10.2	-29.6	-21.5	-20.7	-29.7	-23.1	-20.9
Alkoxy	PhC(CH ₃) ₂ O•	(10)	-25.7	-17.4	-16.3	-28.7	-21.0	-19.8	-30.4	-23.6	-24.0
Aroma	PhO•	(2)	-29.5	-22.6	-20.5	-18.4	-13.6	-11.7	-29.0	-22.1	-23.1
Aroma	<i>p</i> -nitro-PhO•	(12)	-27.2	-20.9	-18.8	-16.4	-11.7	-10.0	-37.0	-29.0	-29.2
Aroma	<i>p</i> -methyl-PhO•	(14)	-30.6	-23.6	-21.5	-18.9	-14.1	-12.4	-28.1	-21.3	-22.6
Aroma	<i>p</i> -amino-PhO•	(18)	-34.5	-26.5	-25.2	-20.1	-14.9	-13.2	-26.9	-20.6	-18.1
LP att.	HOO•	(13)	-38.6	-30.9	-28.6	-30.1	-23.4	-20.6	-30.1	-23.4	-20.6
LP att.	CH ₃ OO•	(15)	-19.9	-14.1	-11.9	-18.2	-12.9	-10.4	-29.4	-23.9	-21.5
LP att.	<i>t</i> -Bu-OO•	(17)	-20.4	-14.3	-14.8	-19.3	-13.5	-11.8	-31.8	-25.2	-24.5
LP att.	PhCH ₂ OO•	(16)	-25.8	-17.7	-16.5	-27.3	-18.8	-18.7	-37.3	-29.4	-29.3
LP att.	TEMPO•	(5)	-29.9	-23.7	-24.7	-22.4	-15.7	-14.2	-39.4	-29.3	-31.7
LP att.	•OO•	(19)	-0.4	1.0	3.0				-38.6	-30.9	-28.6
<p>[a] (U)B3LYP-D3/6-31+G(d,p) level of theory [b] DLPNO-CCSD(T)/CBS using (U)B3LYP-D3/6-31+G(d,p) optimized geometries [c] Using (U)B3LYP-D3/6-31G(d) optimized geometries</p>											
$\Delta RSE = \Delta \Delta H_{c1} =$ $\Delta H_{c1}(\text{RO}\bullet \dots \text{H}_2\text{O})$ minus $\Delta H_{c1}(\text{ROH} \dots \text{H}_2\text{O})$		$\Delta \Delta H_{c1} < 0$ Negative (Stabilization)			$\Delta \Delta H_{c1} \approx 0$ Neutral (Almost No Change)			$\Delta \Delta H_{c1} > 0$ Positive (Destabilization)			

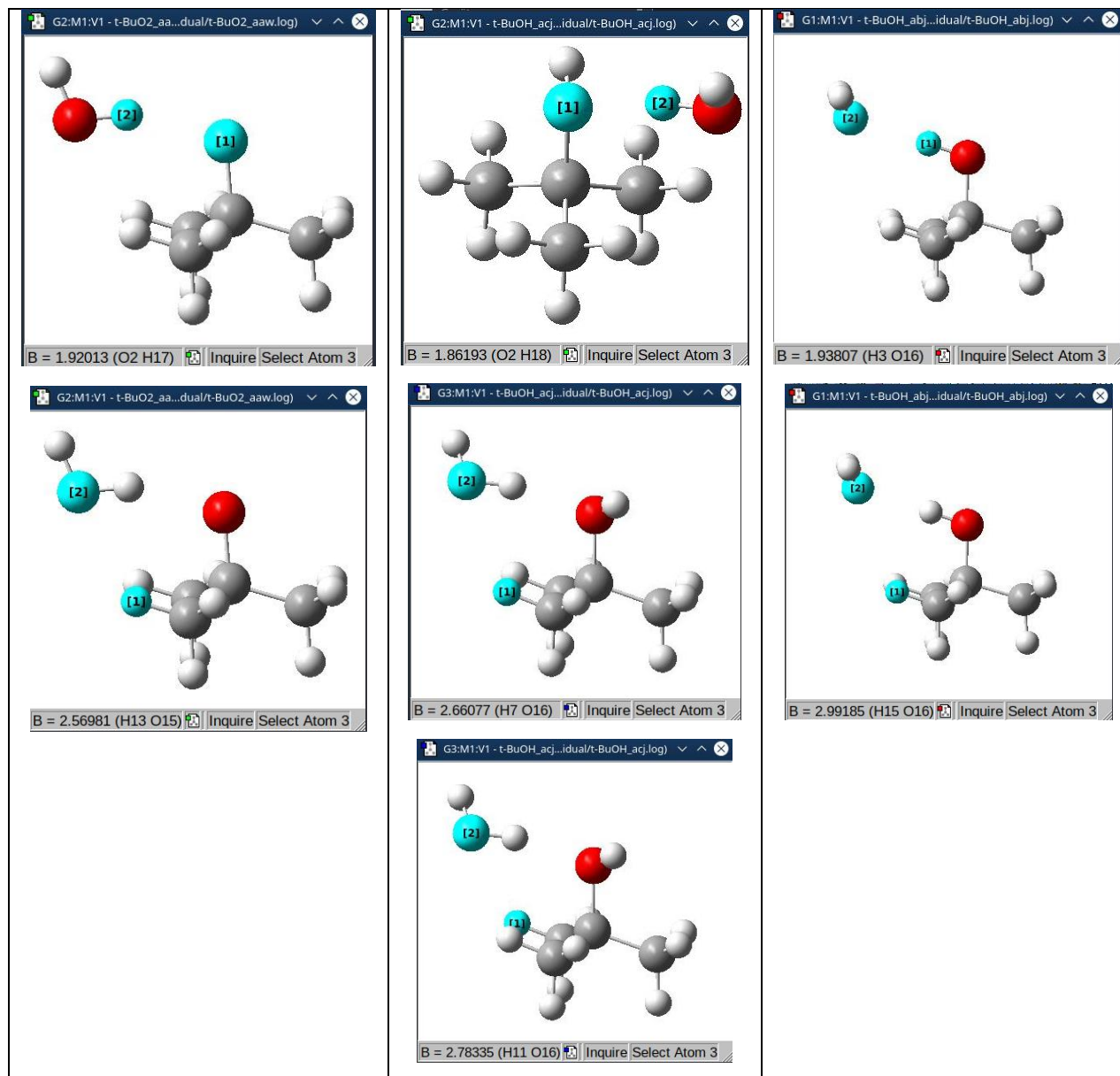
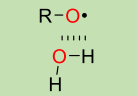
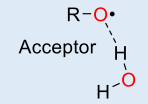
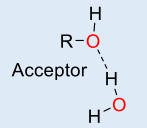
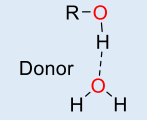
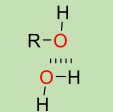
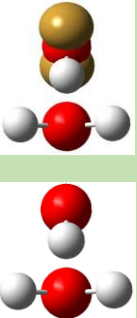
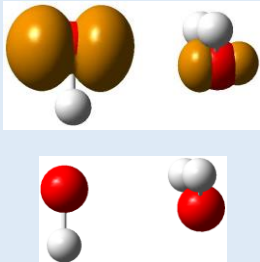
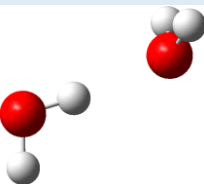
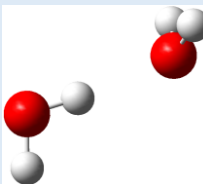
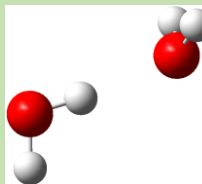
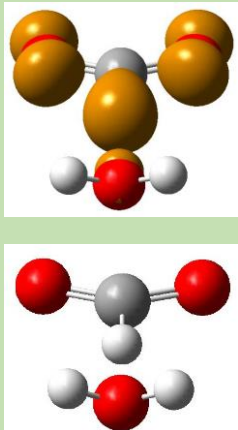
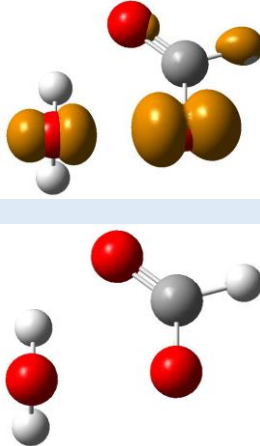
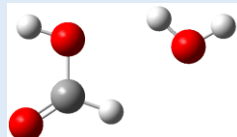
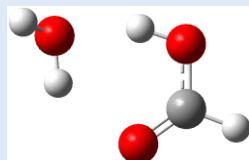
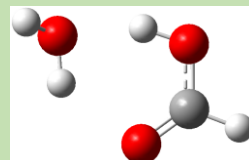
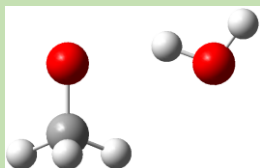
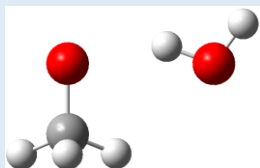
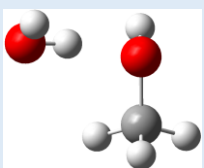
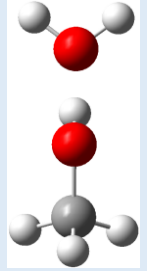
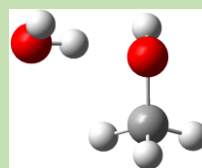
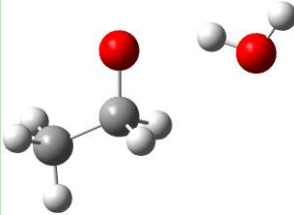
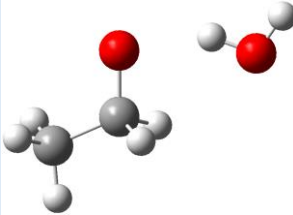
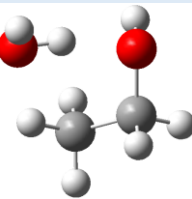
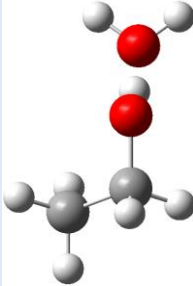
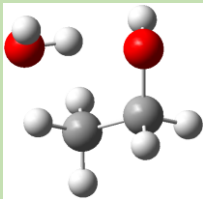
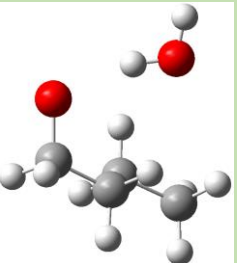
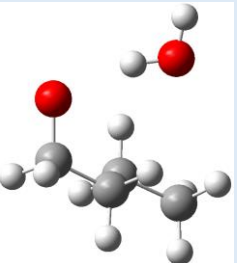
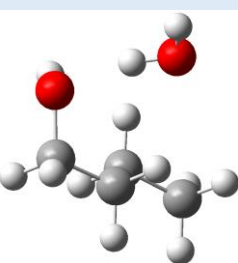
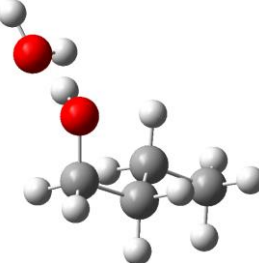
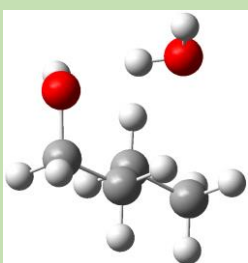
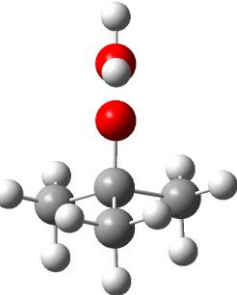
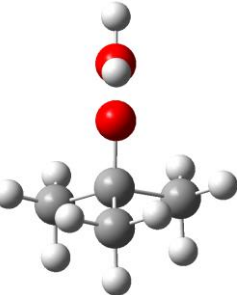
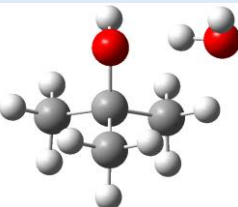
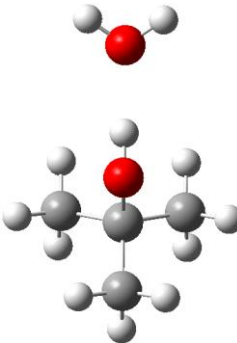
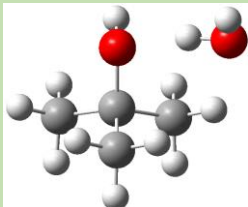
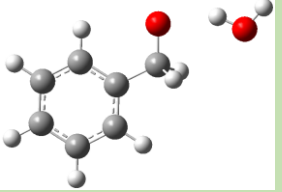
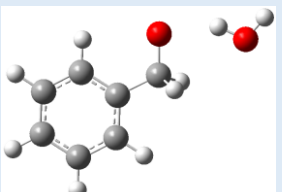
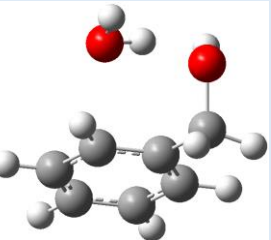
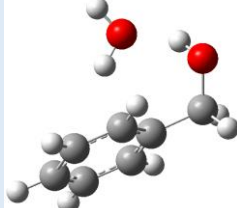
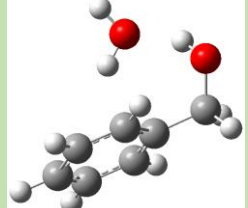
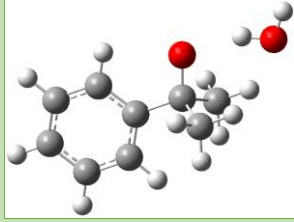
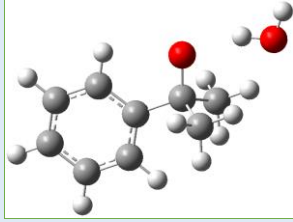
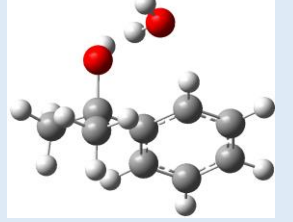
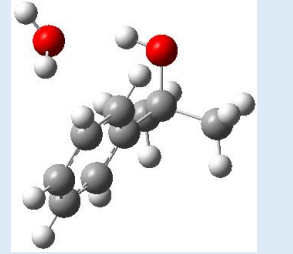
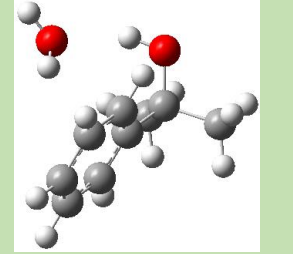
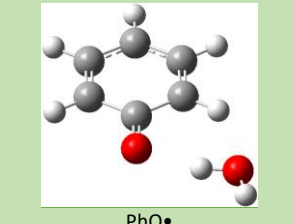
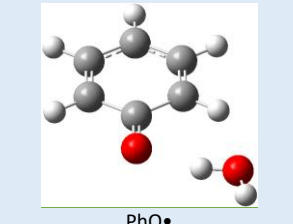
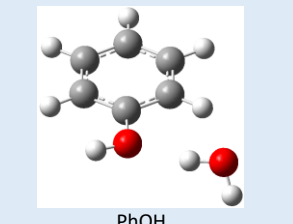
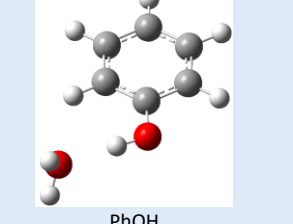
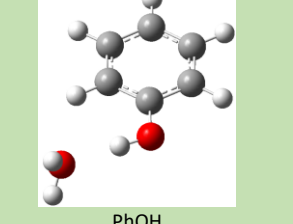
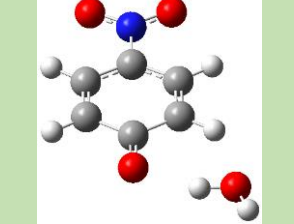
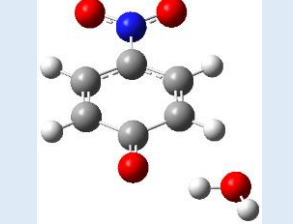
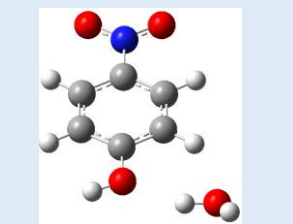
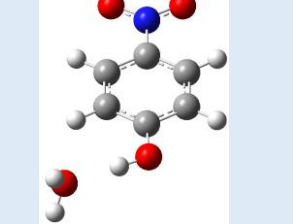
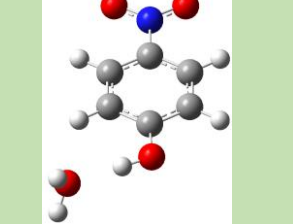
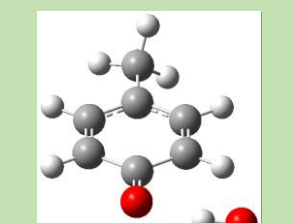
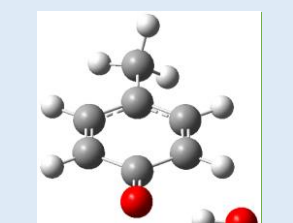
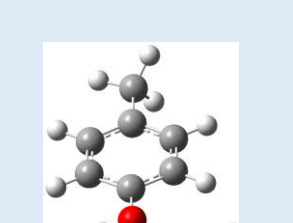
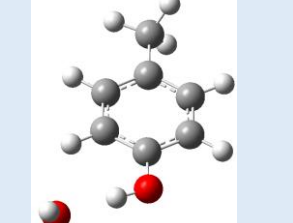
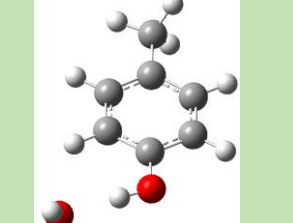
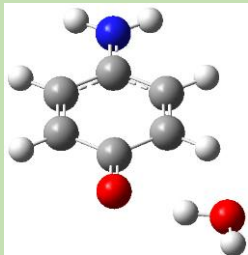
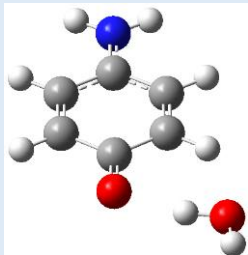
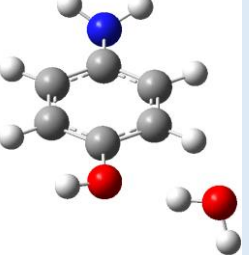
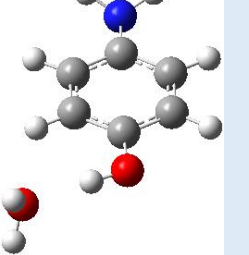
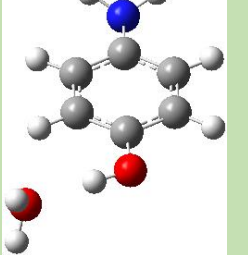
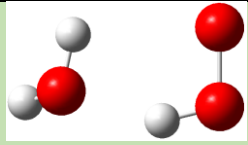
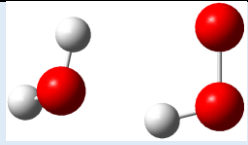
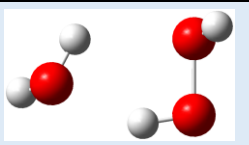
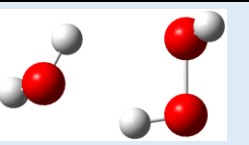
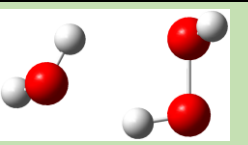
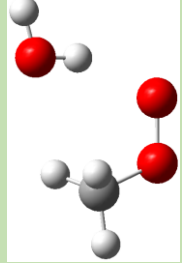
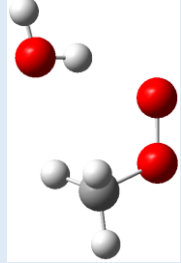
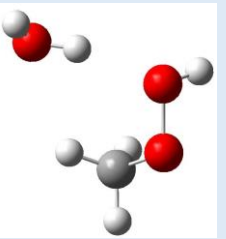
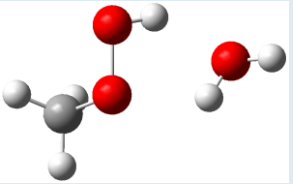
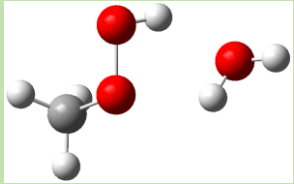
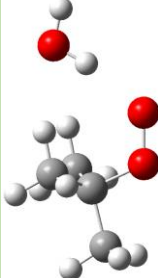
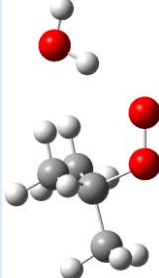
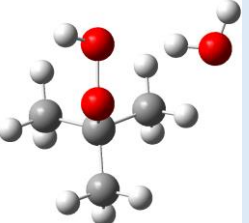
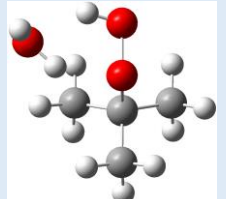
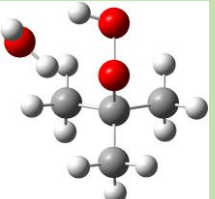


Figure S3.2.1. Calculated distances in selected t-BuOH...H₂O and t-BuO•...H₂O complexes. (U)B3LYP-D3/6-31+G(d,p) level of theory

 <p>Best by H^{gas}</p>	 <p>Selected</p>	 <p>Selected</p>	 <p>Selected</p>	 <p>Best by H^{gas}</p>	<p>Acceptor/Donor</p>
 <p>HO• (1)</p>	 <p>HO• (1)</p>	 <p>H₂O (1H)</p>	 <p>H₂O (1H)</p>	 <p>H₂O (1H)</p>	<p>Acceptor=Donor</p>
 <p>HC(O)O• (20)</p>	 <p>HC(O)O• (20)</p>	 <p>HC(O)OH (20H)</p>	 <p>HC(O)OH (20H)</p>	 <p>HC(O)OH (20H)</p>	<p>Donor</p>
 <p>CH₃O• (8)</p>	 <p>CH₃O• (8)</p>	 <p>CH₃OH (8H)</p>	 <p>CH₃OH</p>	 <p>CH₃OH (8H)</p>	<p>Acceptor</p>

 CH ₃ CH ₂ O• (9)	 CH ₃ CH ₂ O• (9)	 CH ₃ CH ₂ OH (9H)	(8H)  CH ₃ CH ₂ OH (9H)	 CH ₃ CH ₂ OH (9H)	Acceptor
 CH ₃ (CH ₂) ₃ O• (11)	 CH ₃ (CH ₂) ₃ O• (11)	 CH ₃ (CH ₂) ₃ OH (11H)	 CH ₃ (CH ₂) ₃ OH (11H)	 CH ₃ (CH ₂) ₃ OH (11H)	Acceptor
 t-Bu-O• (6)	 t-Bu-O• (6)	 t-Bu-OH (6H)	 t-Bu-OH (6H)	 t-Bu-OH (6H)	Acceptor
 PhCH ₂ O• (7)	 PhCH ₂ O•	 PhCH ₂ OH	 PhCH ₂ OH	 PhCH ₂ OH	Donor

	(7)	PhCH ₂ OH (7H)	(7H)	(7H)	
 <p>PhC(CH₃)₂O• (10)</p>	 <p>PhC(CH₃)₂O• (10)</p>	 <p>PhC(CH₃)₂OH (10H)</p>	 <p>PhC(CH₃)₂OH (10H)</p>	 <p>PhC(CH₃)₂OH (10H)</p>	Donor
 <p>PhO• (2)</p>	 <p>PhO• (2)</p>	 <p>PhOH (2H)</p>	 <p>PhOH (2H)</p>	 <p>PhOH (2H)</p>	Donor
 <p>p-nitro-PhO• (12)</p>	 <p>p-nitro-PhO• (12)</p>	 <p>p-nitro-PhOH (12H)</p>	 <p>p-nitro-PhOH (12H)</p>	 <p>p-nitro-PhOH (12H)</p>	Donor
 <p>p-methyl-PhO• (14)</p>	 <p>p-methyl-PhO• (14)</p>	 <p>p-methyl-PhOH (14H)</p>	 <p>p-methyl-PhOH (14H)</p>	 <p>p-methyl-PhOH (14H)</p>	Donor

 <p>p-amino-PhO• (18)</p>	 <p>p-amino-PhO• (18)</p>	 <p>p-amino-PhOH (18H)</p>	 <p>p-amino-PhOH (18H)</p>	 <p>p-amino-PhOH (18H)</p>	Donor
 <p>HOO• (13 or 19H)</p>	 <p>HOO• (13 or 19H)</p>	 <p>HOOH (13H)</p>	 <p>HOOH (13H)</p>	 <p>HOOH (13H)</p>	Acceptor=Donor
 <p>CH₃OO• (15)</p>	 <p>CH₃OO• (15)</p>	 <p>CH₃OOH (15H)</p>	 <p>CH₃OOH (15H)</p>	 <p>CH₃OOH (15H)</p>	Donor
 <p>t-Bu-OO• (17)</p>	 <p>t-Bu-OO• (17)</p>	 <p>t-Bu-OOH (17H)</p>	 <p>t-Bu-OOH (17H)</p>	 <p>t-Bu-OOH (17H)</p>	Donor

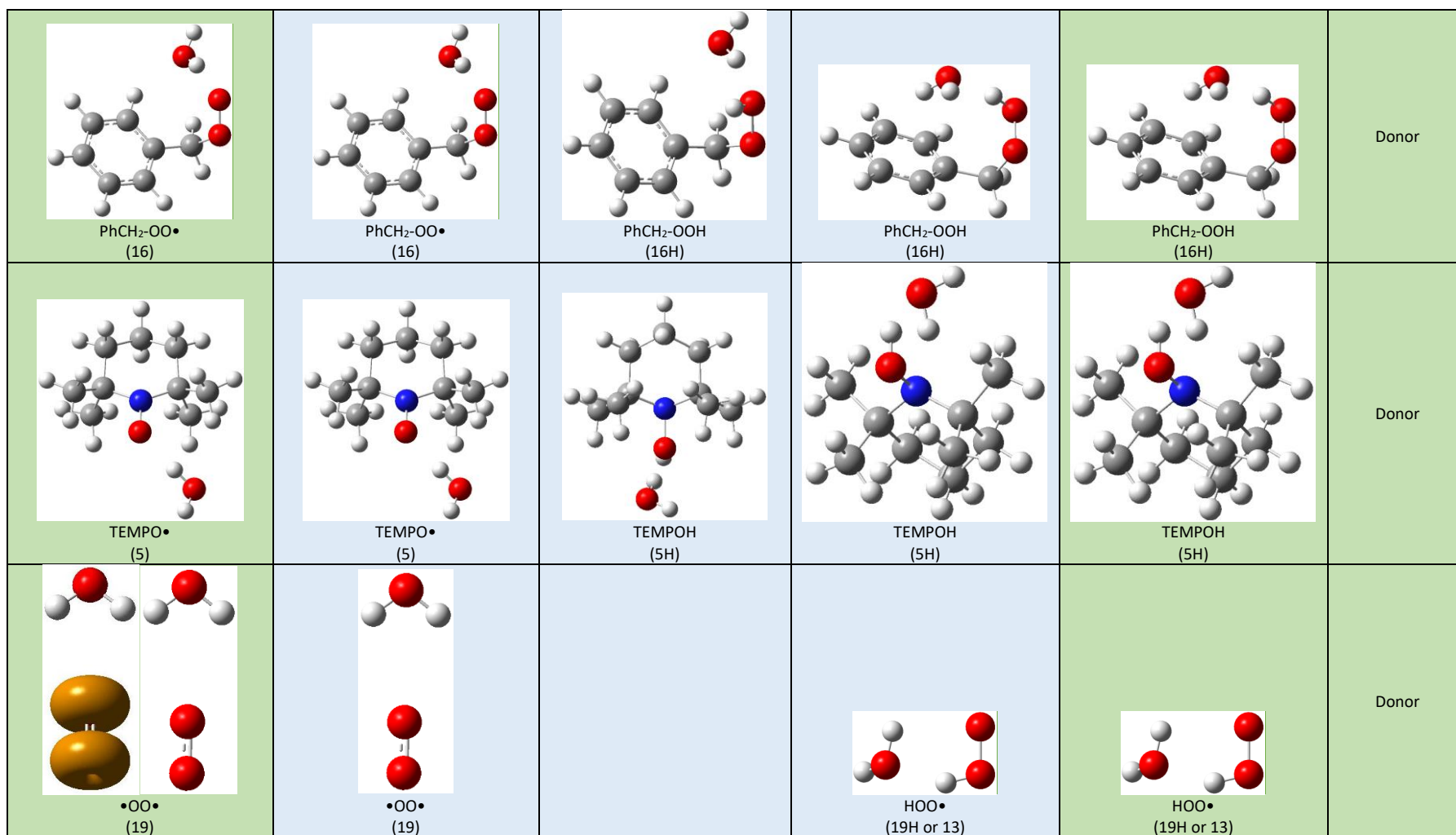
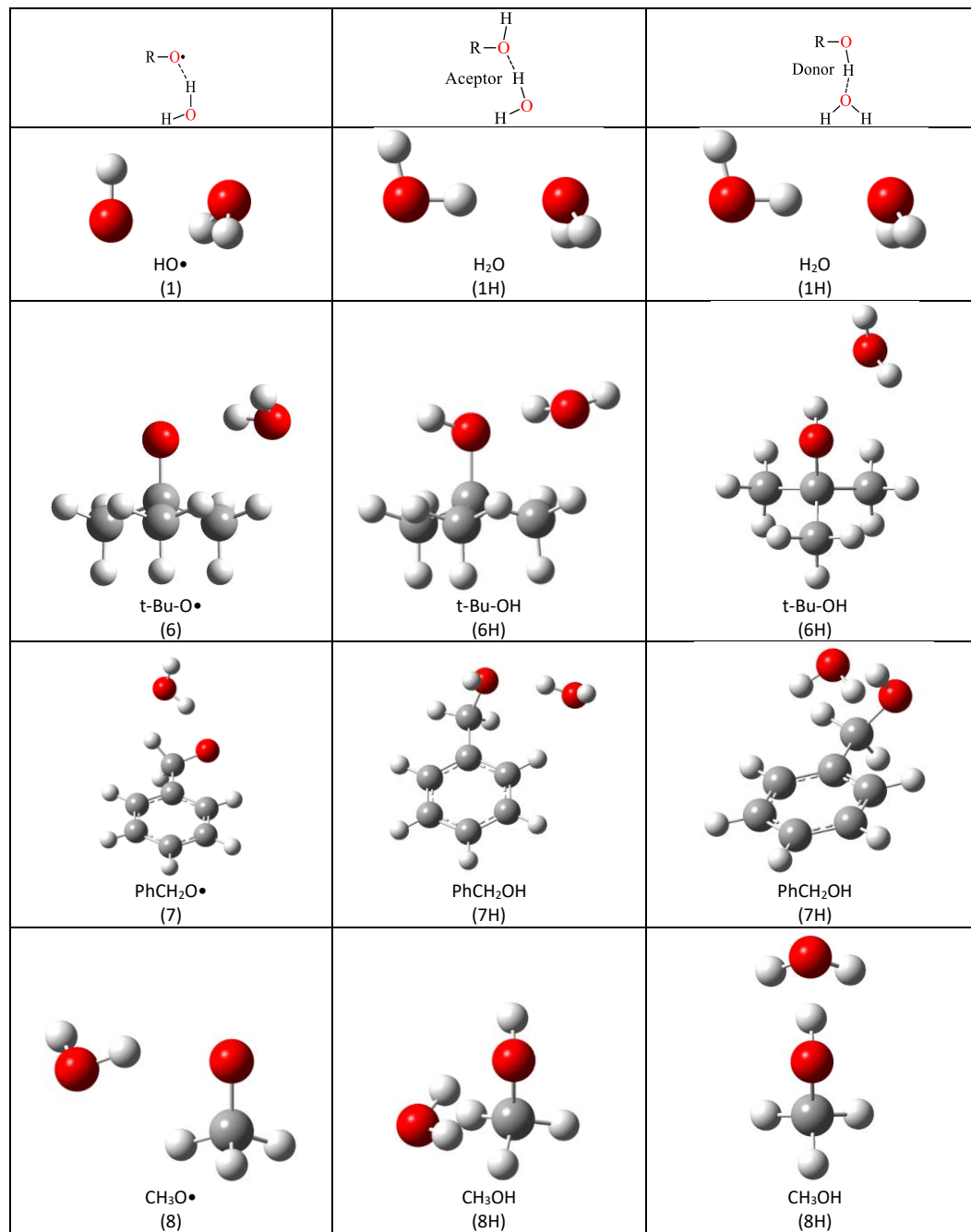
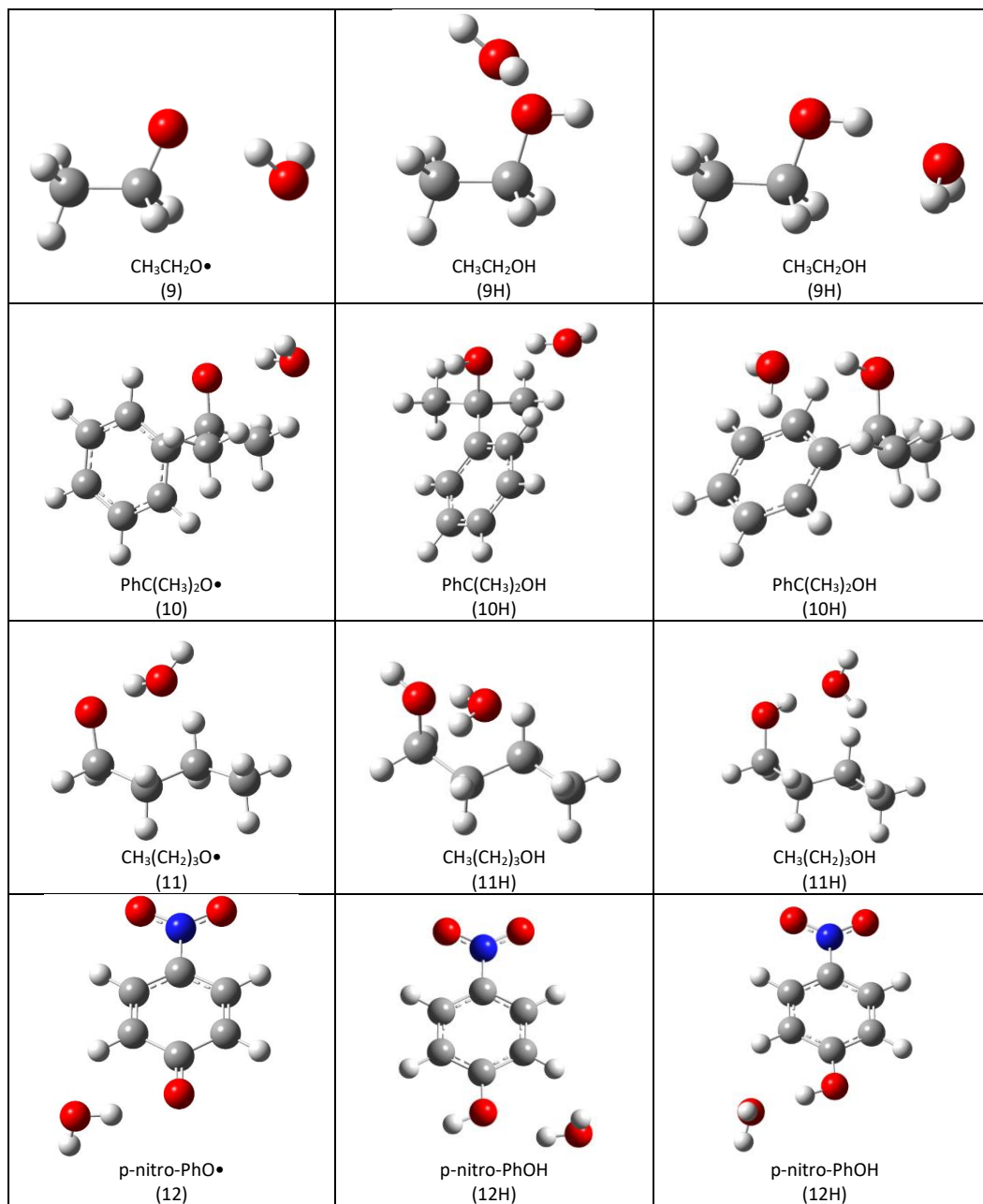
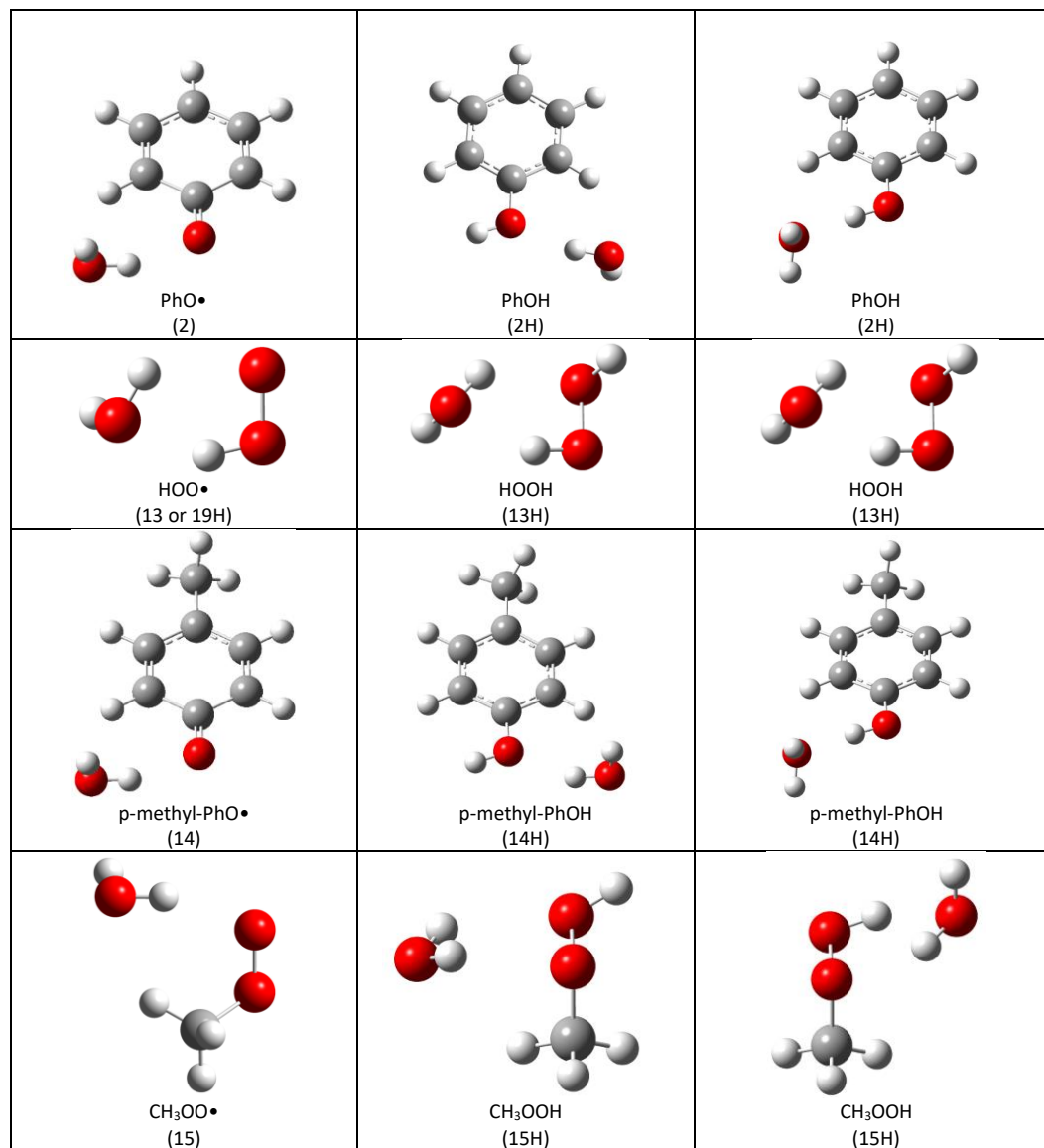


Figure S3.3.1. The best by H^{gas} (green) and artificially selected structures (blue). Spin density (orange, isovalue = 0.01 a.u.)
(U)B3LYP-D3/6-31+G(d,p)







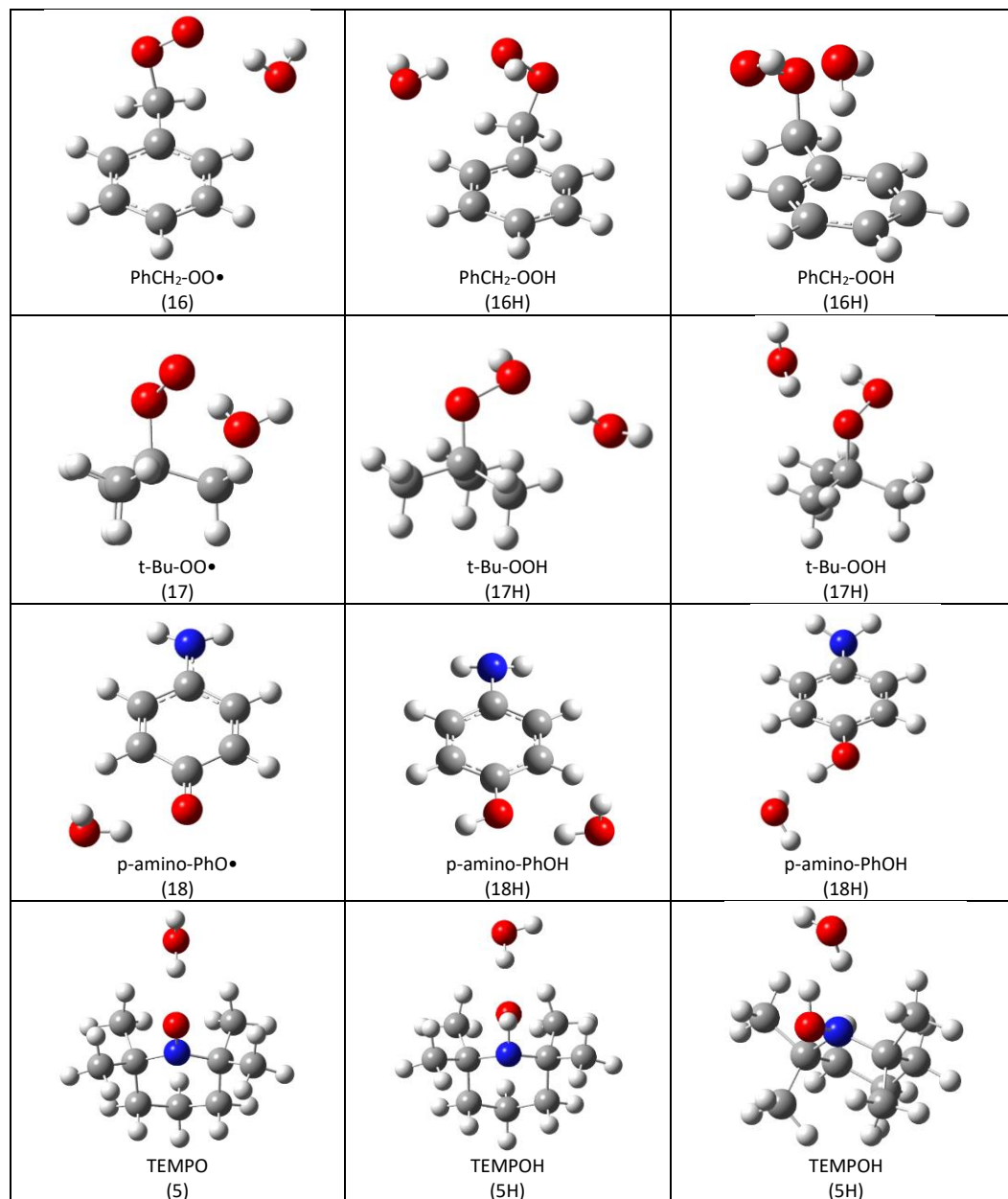




Figure S3.3.2. The best by H_{298} structures. (U)B3LYP-D3/6-31G(d)

Table S3.4.1. Calculated energies. Best selected conformers. (kJ mol⁻¹)

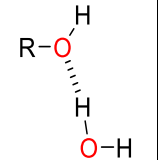
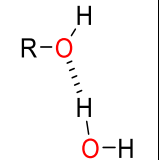
	(U)B3LYP-D3/6-31G(d)			(U)B3LYP-D3/6-31+G(d,p)		
	E _{tot}	H ₂₉₈	G ₂₉₈	E _{tot}	H ₂₉₈	G ₂₉₈
HOH (1Ha)				9.1	6.1	-0.9
HCO ₂ H	-46.1	-47.1	-46.5	-37.9	-39.4	-31.8
CH ₃ OH	-51.8	-56.1	-55.6	-55.4	-60.6	-64.2
CH ₃ CH ₂ OH	-49.1	-52.8	-57.5	-54.8	-60.1	-67.6
BuOH	-55.4	-59.1	-58.4	-57.9	-62.7	-67.5
t-BuOH	-47.5	-49.9	-65.5	-53.6	-55.1	-59.4
PhCH ₂ OH	-44.3	-49.0	-55.3	-53.5	-56.6	-64.9
PhC(CH ₃) ₂ OH	-48.4	-49.0	-53.6	-53.8	-55.1	-60.4
PhOH	-137.3	-136.5	-137.6	-144.6	-144.0	-144.8
p-nitro-PhOH	-118.4	-118.5	-121.4	-125.0	-125.3	-128.0
p-methyl-PhOH	-145.3	-144.3	-144.8	-154.0	-153.1	-153.0
p-amino-PhOH	-176.3	-173.9	-173.7	-185.2	-183.2	-185.5
HOOH	-144.3	-142.1	-143.6	-144.9	-142.9	-144.4
CH ₃ OOH	-141.1	-137.9	-140.5	-146.5	-143.5	-146.1
t-BuOOH	-144.9	-142.2	-148.0	-152.4	-149.6	-152.5
PhCH ₂ OOH	-133.2	-130.5	-135.0	-139.9	-137.5	-140.8
TEMPOH	-209.2	-205.3	-210.5	-219.6	-215.5	-215.8
HOO•						

Table S3.4.2. Calculated energies. Best selected conformers.

	DLPNO-CCSD(T)/cc-pVTZ// (U)B3LYP-D3/6-31+G(d,p)			DLPNO-CCSD(T)/cc-pVQZ// (U)B3LYP-D3/6-31+G(d,p)			DLPNO-CCSD(T)/CBS// (U)B3LYP-D3/6-31+G(d,p)		
	E _{tot}	H ₂₉₈	G ₂₉₈	E _{tot}	H ₂₉₈	G ₂₉₈	E _{tot}	H ₂₉₈	G ₂₉₈
HOH	8.1	5.0	-1.9	7.4	4.4	-2.6	7.2	4.1	-2.8
HCO ₂ H	-7.6	-9.1	-1.5	-8.4	-9.8	-2.3	-8.8	-10.3	-2.7
CH ₃ OH	-44.7	-49.9	-53.5	-47.1	-52.4	-55.9	-48.4	-53.7	-57.2
CH ₃ CH ₂ OH	-41.5	-46.5	-53.6	-44.1	-49.8	-56.9	-45.7	-51.5	-58.5
BuOH	-44.0	-48.7	-51.9	-46.8	-51.6	-55.9	-48.3	-53.1	-57.6
t-BuOH	-38.4	-39.9	-44.1	-41.4	-42.9	-47.1	-42.8	-44.3	-48.5
PhCH ₂ OH	-36.2	-39.8	-48.0	-38.9	-43.4	-50.7	-40.2	-45.2	-52.2
PhC(CH ₃) ₂ OH	-35.5	-37.3	-42.2	-38.3	-40.2	-45.3	-39.6	-41.5	-46.7
PhOH	-125.0	-124.4	-125.1	-130.3	-129.7	-130.4	-133.1	-132.5	-133.3
p-nitro-PhOH	-109.3	-109.6	-112.3	-113.1	-113.4	-116.2	-115.1	-115.3	-118.1
p-methyl-PhOH	-131.7	-130.9	-130.7	-137.7	-136.8	-136.7	-140.9	-140.0	-139.9
p-amino-PhOH	-155.6	-153.6	-156.0	-162.3	-160.3	-162.7	-165.9	-163.9	-166.3
HOOH	-134.2	-132.2	-133.8	-336.6	-334.6	-336.1	-139.1	-137.1	-138.6
CH ₃ OOH	-132.6	-129.6	-133.6	-136.9	-133.9	-138.2	-139.0	-136.0	-140.2
t-BuOOH	-136.8	-133.9	-135.5	-140.8	-137.7	-141.1	-142.6	-139.5	-143.4

PhCH ₂ OOH	-123.7	-121.2	-123.7	-127.6	-125.1	-128.8	-129.3	-126.8	-131.0
TEMPOH	-196.2	-192.2	-193.0	-203.4	-199.4	-199.8	-207.4	-203.4	-203.6
HOO•									

Table S3.4.3. Calculated energies. Best selected conformers.

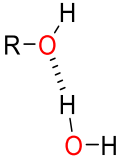
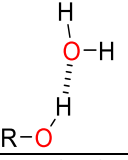
	G3B3-D3		
	E _{tot}	H ₂₉₈	G ₂₉₈
HOH			
HCO ₂ H	-17.0	-23.9	-23.3
CH ₃ OH	-47.6	-51.6	-54.0
CH ₃ CH ₂ OH	-45.9	-50.2	-56.2
BuOH	-48.5	-52.2	-55.8
t-BuOH	-43.6	-44.6	-50.2
PhCH ₂ OH	-39.6	-45.0	-52.0
PhC(CH ₃) ₂ OH	-43.1	-44.3	-49.4
PhOH	-131.1	-130.4	-131.4
p-nitro-PhOH	-114.6	-114.8	-117.6
p-methyl-PhOH	-139.5	-138.5	-139.0
p-amino-PhOH	-168.0	-165.7	-165.5
HOOH	-139.6	-137.6	-139.0
CH ₃ OOH	-139.5	-137.3	-148.6
t-BuOOH	-147.0	-144.5	-153.8
PhCH ₂ OOH	-131.9	-129.3	-138.4
TEMPOH	-211.9	-208.8	-213.7
HOO•			

Table S3.4.4. Calculated energies. Best selected conformers. (kJ mol⁻¹)

	(U)B3LYP-D3/6-31G(d)			(U)B3LYP-D3/6-31+G(d,p)		
	E _{tot}	H ₂₉₈	G ₂₉₈	E _{tot}	H ₂₉₈	G ₂₉₈
HOH (1Ha)	-0.7	-2.4	-2.3	9.1	6.1	-0.9
HCO ₂ H	-1.9	-4.9	-13.5	-6.0	-9.0	-11.4
CH ₃ OH	-52.7	-56.9	-53.6	-58.5	-63.4	-63.6
CH ₃ CH ₂ OH	-53.8	-57.5	-57.6	-60.9	-65.7	-67.2
BuOH	-59.0	-62.4	-59.5	-64.5	-68.5	-67.3
t-BuOH	-57.7	-59.4	-68.6	-62.1	-62.9	-60.3
PhCH ₂ OH	-37.8	-42.5	-50.6	-54.1	-56.5	-64.0
PhC(CH ₃) ₂ OH	-42.9	-43.3	-46.4	-52.8	-53.5	-57.0
PhOH	-125.9	-125.4	-122.6	-133.2	-133.4	-134.8
p-nitro-PhOH	-95.2	-95.9	-98.4	-103.0	-104.7	-110.2
p-methyl-PhOH	-134.8	-134.2	-131.3	-143.8	-143.8	-145.1
p-amino-PhOH	-167.4	-165.6	-166.5	-177.4	-176.3	-180.1

HOOH	-144.3	-142.1	-143.6	-144.9	-142.9	-144.4
CH ₃ OOH	-122.7	-121.2	-128.0	-134.5	-132.3	-138.8
t-BuOOH	-127.4	-126.1	-135.8	-139.1	-137.1	-147.5
PhCH ₂ OOH	-113.8	-112.3	-121.4	-129.3	-127.5	-134.0
TEMPOH	-185.6	-183.6	-194.3	-200.7	-198.6	-208.6
HOO•	-223.5	-221.8	-243.9	-239.0	-236.4	-247.3

Table S3.4.5. Calculated energies. Best selected conformers.

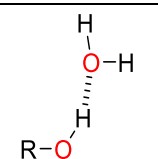
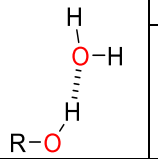
	DLPNO-CCSD(T)/cc-pVTZ// (U)B3LYP-D3/6-31+G(d,p)			DLPNO-CCSD(T)/cc-pVQZ// (U)B3LYP-D3/6-31+G(d,p)			DLPNO-CCSD(T)/CBS// (U)B3LYP-D3/6-31+G(d,p)		
	E _{tot}	H ₂₉₈	G ₂₉₈	E _{tot}	H ₂₉₈	G ₂₉₈	E _{tot}	H ₂₉₈	G ₂₉₈
HOH	8.1	5.0	-1.9	7.4	4.4	-2.6	7.2	4.1	-2.8
HCO ₂ H	23.6	20.7	18.3	20.6	17.7	15.3	19.3	16.4	14.0
CH ₃ OH	-45.0	-49.8	-50.0	-48.6	-53.4	-53.6	-50.4	-55.3	-55.5
CH ₃ CH ₂ OH	-44.2	-48.7	-50.5	-47.9	-53.1	-54.4	-49.9	-55.1	-56.3
BuOH	-46.9	-51.0	-49.1	-51.1	-55.2	-54.0	-52.9	-57.1	-56.3
t-BuOH	-43.3	-44.2	-41.5	-46.9	-47.7	-45.1	-48.6	-49.5	-46.9
PhCH ₂ OH	-34.0	-36.9	-44.5	-37.6	-41.4	-49.0	-39.2	-43.6	-51.1
PhC(CH ₃) ₂ OH	-31.8	-33.0	-36.5	-35.7	-37.1	-40.4	-37.5	-38.8	-42.2
PhOH	-112.9	-113.1	-114.5	-120.1	-120.3	-121.7	-123.8	-124.0	-125.4
p-nitro-PhOH	-88.1	-89.8	-95.4	-93.8	-95.5	-101.0	-96.4	-98.1	-103.6
p-methyl-PhOH	-120.8	-120.8	-122.1	-128.6	-128.7	-130.0	-132.7	-132.7	-134.0
p-amino-PhOH	-146.6	-145.6	-149.4	-155.0	-153.9	-157.7	-159.3	-158.2	-162.0
HOOH	-134.2	-132.2	-133.8	-336.6	-334.6	-336.1	-139.1	-137.1	-138.6
CH ₃ OOH	-119.2	-117.0	-124.4	-124.7	-122.5	-130.3	-127.1	-124.9	-132.6
t-BuOOH	-122.8	-120.8	-129.7	-127.7	-125.7	-136.5	-129.8	-127.8	-139.2
PhCH ₂ OOH	-110.3	-108.5	-115.3	-115.8	-114.0	-123.1	-118.1	-116.3	-126.0
TEMPOH	-179.1	-177.1	-187.6	-187.6	-185.5	-195.6	-191.9	-189.8	-199.9
HOO•	-250.6	-248.1	-259.9	-257.7	-255.1	-265.4	-260.8	-258.2	-268.3

Table S3.4.6. Calculated energies. Best selected conformers.

	G3B3-D3		
	E _{tot}	H ₂₉₈	G ₂₉₈
HOH			
HCO ₂ H	11.9	3.1	-5.5
CH ₃ OH	-52.5	-55.7	-51.5
CH ₃ CH ₂ OH	-52.9	-56.1	-54.5
BuOH	-54.1	-57.5	-58.6
t-BuOH	-52.3	-52.7	-51.8
PhCH ₂ OH	-39.4	-44.8	-48.1
PhC(CH ₃) ₂ OH	-39.5	-40.1	-43.9

PhOH	-119.7	-118.9	-116.0
p-nitro-PhOH	-94.9	-95.6	-98.0
p-methyl-PhOH	-129.1	-128.3	-125.1
p-amino-PhOH	-162.6	-160.9	-161.7
HOOH	-139.6	-137.6	-139.0
CH ₃ OOH	-126.9	-126.1	-143.1
t-BuOOH	-133.0	-131.8	-145.0
PhCH ₂ OOH	-120.1	-118.7	-132.4
TEMPOH	-193.2	-191.4	-202.2
HOO•	-259.4	-257.6	-279.7

Table S3.4.7. Calculated energies. Best selected conformers.

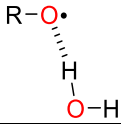
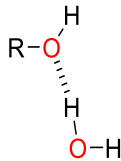
	(U)B3LYP-D3/6-31G(d)		
	E _{tot}	H ₂₉₈	G ₂₉₈
HO• (1a_3)	-152.1465975	-152.1075655	-152.1389925
HCO ₂ •	-265.5075068	-265.4557999	-265.4920149
CH ₃ O•	-191.4729895	-191.4043425	-191.4402005
CH ₃ CH ₂ O•	-230.7961992	-230.6973862	-230.7366822
BuO•	-309.4324787	-309.2734457	-309.3178948
t-BuO•	-309.4416337	-309.2835411	-309.3314371
PhCH ₂ O•	-422.5383244	-422.3837184	-422.4321589
PhC(CH ₃) ₂ O•	-501.1833401	-500.9683192	-501.0211692
PhO•	-383.2606529	-383.1346519	-383.1779329
p-nitro-PhO•	-587.7600871	-587.6292461	-587.6797481
p-methyl-PhO•	-422.5839767	-422.4284437	-422.4767157
p-amino-PhO•	-438.6281654	-438.4835124	-438.5297314
HOO•	-227.3321060	-227.2858670	-227.3187590
CH ₃ OO•	-266.6397411	-266.5640601	-266.6028541
t-BuOO•	-384.6083278	-384.4440058	-384.4920048
PhCH ₂ OO•	-497.7058911	-497.5440801	-497.5940221
TEMPO•	-560.1794735	-559.8743795	-559.9308634
³ O ₂	-226.7317449	-226.6981709	-226.7382699

Table S3.4.8. Calculated energies. Best selected conformers.

	(U)B3LYP-D3/6-31G(d)		
	E _{tot}	H ₂₉₈	G ₂₉₈
HOH (1Ha)	-152.8318213	-152.7788433	-152.8114843
HCO ₂ H	-266.1754636	-266.1100416	-266.1476686
CH ₃ OH	-192.1387684	-192.0551334	-192.0924013
CH ₃ CH ₂ OH	-231.4630119	-231.3494369	-231.3881581
BuOH	-310.0968831	-309.9230971	-309.9690111

t-BuOH	-310.1090345	-309.9367035	-309.9798735
PhCH ₂ OH	-423.2069474	-423.0372224	-423.0844624
PhC(CH ₃) ₂ OH	-501.8504166	-501.6218206	-501.6741180
PhOH	-383.8938673	-383.7548543	-383.7989143
p-nitro-PhOH	-588.4005120	-588.2562720	-588.3068910
p-methyl-PhOH	-423.2141255	-423.0456714	-423.0949435
p-amino-PhOH	-439.2465281	-439.0894531	-439.1369321
HOOH	-227.9626681	-227.9039341	-227.9374491
CH ₃ OOH	-267.2715186	-267.1837066	-267.2227126
t-BuOOH	-385.2386526	-385.0620236	-385.1090206
PhCH ₂ OOH	-498.3406620	-498.1665520	-498.2159740
TEMPOH	-560.7853105	-560.4683745	-560.5240795
HOO•			

Table S3.4.9. Calculated energies. Best selected conformers.

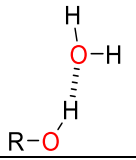
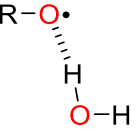
	(U)B3LYP-D3/6-31G(d)		
	E _{tot}	H ₂₉₈	G ₂₉₈
HOH (1Ha)	-152.8318213	-152.7788433	-152.8114843
HCO ₂ H	-266.1922978	-266.1261058	-266.1602548
CH ₃ OH	-192.1384134	-192.0548484	-192.0931620
CH ₃ CH ₂ OH	-231.4612036	-231.3476606	-231.3881106
BuOH	-310.0955283	-309.9218353	-309.9686020
t-BuOH	-310.1051749	-309.9330899	-309.9786929
PhCH ₂ OH	-423.2094341	-423.0397021	-423.0862631
PhC(CH ₃) ₂ OH	-501.8525141	-501.6240046	-501.6768566
PhOH	-383.8982015	-383.7590775	-383.8046154
p-nitro-PhOH	-588.4093503	-588.2648783	-588.3156543
p-methyl-PhOH	-423.2181494	-423.0495224	-423.1000770
p-amino-PhOH	-439.2498947	-439.0926247	-439.1396891
HOOH	-227.9626681	-227.9039341	-227.9374491
CH ₃ OOH	-267.2785038	-267.1900838	-267.2274928
t-BuOOH	-385.2453165	-385.0681415	-385.1136735
PhCH ₂ OOH	-498.3480630	-498.1734860	-498.2211500
TEMPOH	-560.7942974	-560.4766384	-560.5302304
HOO•	-227.3321060	-227.2858670	-227.3187590

Table S3.4.10. Calculated energies. Best selected conformers.

	G3B3-D3		
	E _{tot}	H ₂₉₈	G ₂₉₈
HO• (1a_3)	-152.1122504	-152.0744734	-152.1060594
HCO ₂ •	-265.4091505	-265.3614085	-265.3978575
CH ₃ O•	-191.4122958	-191.3460168	-191.3821224

CH ₃ CH ₂ O•	-230.7164502	-230.6213478	-230.6617478
BuO•	-309.3162287	-309.1631007	-309.2106530
t-BuO•	-309.3281339	-309.1752019	-309.2198349
PhCH ₂ O•	-422.3746434	-422.2258224	-422.2751354
PhC(CH ₃) ₂ O•	-500.9870737	-500.7799257	-500.8335177
PhO•	-383.1128539	-382.9912699	-383.0350319
p-nitro-PhO•	-587.5330314	-587.4066334	-587.4577874
p-methyl-PhO•	-422.4189092	-422.2688612	-422.3177302
p-amino-PhO•	-438.4648656	-438.3252636	-438.3720786
HOO•	-227.2617016	-227.2169926	-227.2500566
CH ₃ OO•	-266.5462115	-266.4733965	-266.5163485
t-BuOO•	-384.4652363	-384.3067463	-384.3567383
PhCH ₂ OO•	-497.5109813	-497.3548593	-497.4072126
TEMPO•	-559.9664068	-559.6724408	-559.7299918
³ O ₂	-226.6607931	-226.6282241	-226.6685121

Table S3.4.11. Calculated energies. Best selected conformers.

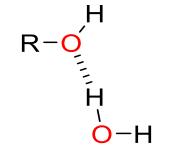
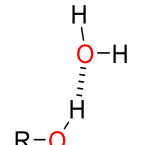
	G3B3-D3		
	E _{tot}	H ₂₉₈	G ₂₉₈
HOH (1Ha)	-152.8139511	-152.7627571	-152.7955861
HCO ₂ H	-266.1023908	-266.0391758	-266.0770668
CH ₃ OH	-192.0938537	-192.0132317	-192.0496247
CH ₃ CH ₂ OH	-231.3986662	-231.2891112	-231.3284264
BuOH	-309.9974505	-309.8301055	-309.8775015
t-BuOH	-310.0112257	-309.8450937	-309.8888177
PhCH ₂ OH	-423.0592487	-422.8955737	-422.9434137
PhC(CH ₃) ₂ OH	-501.6703425	-501.4499335	-501.5027995
PhOH	-383.7626171	-383.6285041	-383.6730841
p-nitro-PhOH	-588.1890769	-588.0497839	-588.1010879
p-methyl-PhOH	-423.0654797	-422.9029887	-422.9528898
p-amino-PhOH	-439.1005950	-438.9490270	-438.9971440
HOOH	-227.9082240	-227.8514780	-227.8852070
CH ₃ OOH	-267.1927726	-267.1080006	-267.1478421
t-BuOOH	-385.1089389	-384.9385929	-384.9862339
PhCH ₂ OOH	-498.1604493	-497.9924913	-498.0425873
TEMPOH	-560.5853835	-560.2797865	-560.3366685
HOO•			

Table S3.4.12. Calculated energies. Best selected conformers.

	G3B3-D3		
	E _{tot}	H ₂₉₈	G ₂₉₈

HOH (1Ha)	-152.8139511	-152.7627571	-152.7955861
HCO ₂ H	-266.1133819	-266.0494709	-266.0838399
CH ₃ OH	-192.0920172	-192.0116942	-192.0505752
CH ₃ CH ₂ OH	-231.3960055	-231.2868775	-231.3290775
BuOH	-309.9953308	-309.8280738	-309.8764100
t-BuOH	-310.0079289	-309.8420229	-309.8881909
PhCH ₂ OH	-423.0593217	-422.8956457	-422.9449025
PhC(CH ₃) ₂ OH	-501.6717311	-501.4515381	-501.5048779
PhOH	-383.7669725	-383.6328535	-383.6789295
p-nitro-PhOH	-588.1966054	-588.0571004	-588.1085504
p-methyl-PhOH	-423.0694455	-422.9068925	-422.9581645
p-amino-PhOH	-439.1026238	-438.9508818	-438.9985636
HOOH	-227.9082240	-227.8514780	-227.8852070
CH ₃ OOH	-267.1975684	-267.1122364	-267.1499494
t-BuOOH	-385.1142760	-384.9434300	-384.9895810
PhCH ₂ OOH	-498.1649393	-497.9965503	-498.0448713
TEMPOH	-560.5925399	-560.2864389	-560.3410489
HOO•	-227.2617016	-227.2169926	-227.2500566

Table S3.4.13. Calculated energies. Best selected conformers.

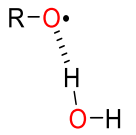
	(U)B3LYP-D3/6-31+G(d,p)		
	E _{tot}	H ₂₉₈	G ₂₉₈
HO• (1a_2)	-152.1803707	-152.1418317	-152.1758067
HCO ₂ •	-265.5374856	-265.4861126	-265.5207356
CH ₃ O•	-191.5078593	-191.4397733	-191.4769883
CH ₃ CH ₂ O•	-230.8339204	-230.7361309	-230.7774889
BuO•	-309.4755335	-309.3177405	-309.3652302
t-BuO•	-309.4854393	-309.3279283	-309.3728993
PhCH ₂ O•	-422.5878221	-422.4329678	-422.4828748
PhC(CH ₃) ₂ O•	-501.2368645	-501.0229939	-501.0766059
PhO•	-383.3042402	-383.1787062	-383.2233942
p-nitro-PhO•	-587.8111909	-587.6809379	-587.7327549
p-methyl-PhO•	-422.6308106	-422.4760046	-422.5258676
p-amino-PhO•	-438.6815915	-438.5375305	-438.5864275
HOO•	-227.3673314	-227.3213374	-227.3552984
CH ₃ OO•	-266.6761922	-266.6008622	-266.6406838
t-BuOO•	-384.6542691	-384.4909071	-384.5403479
PhCH ₂ OO•	-497.7556124	-497.5943754	-497.6452677
TEMPO•	-560.2400591	-559.9369001	-559.9939151
³ O ₂	-226.7633108	-226.7296668	-226.7692103

Table S3.4.14. Calculated energies. Best selected conformers.

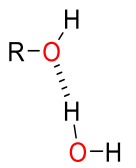
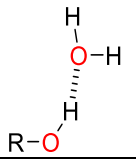
Conformer 	(U)B3LYP-D3/6-31+G(d,p)		
	E _{tot}	H ₂₉₈	G ₂₉₈
HOH (1Ha)	-152.8788957	-152.8258677	-152.8583797
HCO ₂ H	-266.2180769	-266.1528269	-266.1915219
CH ₃ OH	-192.1818168	-192.0983958	-192.1354398
CH ₃ CH ₂ OH	-231.5081012	-231.3949692	-231.4346502
BuOH	-310.1485136	-309.9755826	-310.0224252
t-BuOH	-310.1600504	-309.9886454	-310.0331904
PhCH ₂ OH	-423.2624712	-423.0931452	-423.1410682
PhC(CH ₃) ₂ OH	-501.9114064	-501.6837214	-501.7365260
PhOH	-383.9441927	-383.8055687	-383.8511607
p-nitro-PhOH	-588.4586379	-588.3149519	-588.3669089
p-methyl-PhOH	-423.2672077	-423.0994177	-423.1505107
p-amino-PhOH	-439.3061128	-439.1494888	-439.1986658
HOOH	-228.0071774	-227.9486274	-227.9831884
CH ₃ OOH	-267.3154339	-267.2279209	-267.2679500
t-BuOOH	-385.2912534	-385.1156534	-385.1651574
PhCH ₂ OOH	-498.3973609	-498.2237399	-498.2745490
TEMPOH	-560.8514646	-560.5365226	-560.5946146
HOO•			

Table S3.4.15. Calculated energies. Best selected conformers.

Conformer 	(U)B3LYP-D3/6-31+G(d,p)		
	E _{tot}	H ₂₉₈	G ₂₉₈
HOH (1Ha)	-152.8788957	-152.8258677	-152.8583797
HCO ₂ H	-266.2302275	-266.1644195	-266.1993165
CH ₃ OH	-192.1806009	-192.0973579	-192.1356679
CH ₃ CH ₂ OH	-231.5057597	-231.3928417	-231.4348052
BuOH	-310.1460146	-309.9733856	-310.0225041
t-BuOH	-310.1568402	-309.9856822	-310.0328412
PhCH ₂ OH	-423.2622649	-423.0931739	-423.1413889
PhC(CH ₃) ₂ OH	-501.9117965	-501.6843555	-501.7378077
PhOH	-383.9485501	-383.8096111	-383.8549621
p-nitro-PhOH	-588.4669965	-588.3227945	-588.3736785
p-methyl-PhOH	-423.2710744	-423.1029364	-423.1534904
p-amino-PhOH	-439.3090547	-439.1520897	-439.2007237
HOOH	-228.0071774	-227.9486274	-227.9831884
CH ₃ OOH	-267.3199916	-267.2321836	-267.2707406
t-BuOOH	-385.2963238	-385.1204028	-385.1670718

PhCH ₂ OOH	-498.4013947	-498.2275437	-498.2771307
TEMPOH	-560.8586666	-560.5429816	-560.5973646
HOO•	-227.3673314	-227.3213374	-227.3579179

Table S3.4.16. Calculated energies. Best selected conformers.

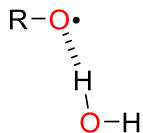
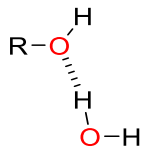
	DLPNO-CCSD(T)/cc-pVTZ// (U)B3LYP-D3/6-31+G(d,p)			DLPNO-CCSD(T)/cc-pVQZ// (U)B3LYP-D3/6-31+G(d,p)			DLPNO-CCSD(T)/CBS// (U)B3LYP-D3/6-31+G(d,p)		
	E _{tot}	H ₂₉₈	G ₂₉₈	E _{tot}	H ₂₉₈	G ₂₉₈	E _{tot}	H ₂₉₈	G ₂₉₈
HO• (1a ₂)	-151.9757359	-151.9371969	-151.9711719	-152.0264294	-151.9878904	-152.0218654	-152.0569529	-152.0184139	-152.0523889
HCO ₂ •	-265.1474739	-265.0961009	-265.1307239	-265.2305141	-265.1791411	-265.2137641	-265.2811729	-265.2297999	-265.2644229
CH ₃ O•	-191.2148530	-191.1467670	-191.1839820	-191.2769642	-191.2088782	-191.2460932	-191.3147506	-191.2466646	-191.2838796
CH ₃ CH ₂ O•	-230.4591874	-230.3612794	-230.4026374	-230.5325112	-230.4348874	-230.4762454	-230.5774931	-230.4799053	-230.5212633
BuO•	-308.9394218	-308.7817518	-308.8291523	-309.0357341	-308.8780641	-308.9257413	-309.0951137	-308.9374437	-308.9852008
t-BuO•	-308.9498819	-308.7923709	-308.8373419	-309.0461061	-308.8885951	-308.9335661	-309.1054728	-308.9479618	-308.9929328
PhCH ₂ O•	-421.8296737	-421.6750180	-421.7249250	-421.9555656	-421.8012743	-421.8511813	-422.0333897	-421.8792789	-421.9291859
PhC(CH ₃) ₂ O•	-500.3191994	-500.1055304	-500.1591424	-500.4677291	-500.2540601	-500.3076721	-500.5598151	-500.3461461	-500.3997581
PhO•	-382.6267884	-382.5012544	-382.5459424	-382.7421138	-382.6165798	-382.6612678	-382.8132218	-382.6876878	-382.7323758
p-nitro-PhO•	-586.8501417	-586.7198887	-586.7717057	-587.0281254	-586.8978724	-586.9496894	-587.1375825	-587.0073295	-587.0591465
p-methyl-PhO•	-421.8716077	-421.7168017	-421.7666647	-421.9986961	-421.8438901	-421.8937531	-422.0771823	-421.9223763	-421.9722393
p-amino-PhO•	-437.9107155	-437.7666545	-437.8155515	-438.0446693	-437.9006083	-437.9495053	-438.1271767	-437.9831157	-438.0320127
HOO•	-227.0600436	-227.0140496	-227.0480106	-227.1332118	-227.0872178	-227.1211788	-227.1778250	-227.1318310	-227.1657920
CH ₃ OO•	-266.2831135	-266.2077835	-266.2479864	-266.3682003	-266.2928703	-266.3331999	-266.4201260	-266.3447960	-266.3850969
t-BuOO•	-384.0197322	-383.8563702	-383.9053298	-384.1388190	-383.9754570	-384.0250708	-384.2122905	-384.0489285	-384.0987611
PhCH ₂ OO•	-496.8987114	-496.7374744	-496.7884838	-497.0473471	-496.8861101	-496.9379697	-497.1391863	-496.9779493	-497.0300677
TEMPO•	-559.2216329	-558.9184739	-558.9756730	-559.3914796	-559.0883206	-559.1453635	-559.4970514	-559.1938924	-559.2509074
•OO•	-226.4612261	-226.4275761	-226.4670925	-226.5331585	-226.4995085	-226.5386392	-226.5766791	-226.5430291	-226.5821441

Table S3.4.17. Calculated energies. Best selected conformers.

	DLPNO-CCSD(T)/cc-pVTZ// (U)B3LYP-D3/6-31+G(d,p)			DLPNO-CCSD(T)/cc-pVQZ// (U)B3LYP-D3/6-31+G(d,p)			DLPNO-CCSD(T)/CBS// (U)B3LYP-D3/6-31+G(d,p)		
	E _{tot}	H ₂₉₈	G ₂₉₈	E _{tot}	H ₂₉₈	G ₂₉₈	E _{tot}	H ₂₉₈	G ₂₉₈
HOH (1Ha)	-152.6731057	-152.6200777	-152.6525897	-152.7274519	-152.6744239	-152.7069359	-152.7601617	-152.7071337	-152.7396457
HCO ₂ H	-265.8388504	-265.7736004	-265.8122954	-265.9255200	-265.8602700	-265.8989650	-265.9782849	-265.9130349	-265.9517299
CH ₃ OH	-191.8921279	-191.8087069	-191.8457509	-191.9572352	-191.8738142	-191.9108582	-191.9967983	-191.9133773	-191.9504213
CH ₃ CH ₂ OH	-231.1376808	-231.0245488	-231.0643876	-231.2139118	-231.1007798	-231.1406241	-231.2605770	-231.1474483	-231.1873123
BuOH	-309.6169486	-309.4441796	-309.4915421	-309.7161024	-309.5432970	-309.5905041	-309.7772099	-309.6043845	-309.6515895
t-BuOH	-309.6295403	-309.4581353	-309.5026803	-309.7285509	-309.5571459	-309.6016909	-309.7896487	-309.6182437	-309.6627887
PhCH ₂ OH	-422.5101644	-422.3408384	-422.3887764	-422.6389398	-422.4696138	-422.5179505	-422.7185359	-422.5492099	-422.5976598
PhC(CH ₃) ₂ OH	-500.9999606	-500.7722756	-500.8252048	-501.1513211	-500.9236361	-500.9764792	-501.2451950	-501.0175100	-501.0703016
PhOH	-383.2734668	-383.1348428	-383.1804348	-383.3906950	-383.2520710	-383.2976630	-383.4629917	-383.3243677	-383.3699597
p-nitro-PhOH	-587.5028109	-587.3591249	-587.4110819	-587.6832398	-587.5395538	-587.5915108	-587.7942345	-587.6505485	-587.7025055
p-methyl-PhOH	-422.5157144	-422.3479244	-422.3990174	-422.6444568	-422.4766668	-422.5277598	-422.7239998	-422.5562098	-422.6073028
p-amino-PhOH	-438.5457292	-438.3891052	-438.4382822	-438.6810510	-438.5244270	-438.5736040	-438.7644517	-438.6078277	-438.6570047
HOOH	-227.7032047	-227.6446547	-227.6792157	-227.7790261	-227.7204761	-227.7550371	-227.8253138	-227.7667638	-227.8013248

CH ₃ OOH	-266.9268820	-266.8393690	-266.8792684	-267.0142527	-266.9267397	-266.9666147	-267.0676725	-266.9801595	-267.0200345
t-BuOOH	-384.6619246	-384.4863490	-384.5358530	-384.7833855	-384.6078955	-384.6573995	-384.8584530	-384.6829630	-384.7324670
PhCH ₂ OOH	-497.5458882	-497.3722672	-497.4235143	-497.6969494	-497.5233284	-497.5749588	-497.7904095	-497.6167885	-497.6685184
TEMPOH	-559.8411803	-559.5262383	-559.5843303	-560.0121869	-559.6972449	-559.7553369	-560.1185319	-559.8035899	-559.8616819
HOO•									

Table S3.4.18. Calculated energies. Best selected conformers.

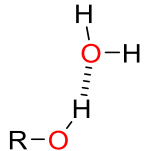
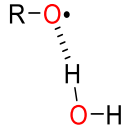
	DLPNO-CCSD(T)/cc-pVTZ// (U)B3LYP-D3/6-31+G(d,p)			DLPNO-CCSD(T)/cc-pVQZ// (U)B3LYP-D3/6-31+G(d,p)			DLPNO-CCSD(T)/CBS// (U)B3LYP-D3/6-31+G(d,p)		
	E _{tot}	H ₂₉₈	G ₂₉₈	E _{tot}	H ₂₉₈	G ₂₉₈	E _{tot}	H ₂₉₈	G ₂₉₈
HOH (1Ha)	-152.6731057	-152.6200777	-152.6525897	-152.7274519	-152.6744239	-152.7069359	-152.7601617	-152.7071337	-152.7396457
HCO ₂ H	-265.8507511	-265.7849431	-265.8198401	-265.9365719	-265.8707639	-265.9056609	-265.9890000	-265.9231920	-265.9580890
CH ₃ OH	-191.8920076	-191.8087646	-191.8470746	-191.9566571	-191.8734141	-191.9117241	-191.9960152	-191.9127722	-191.9510822
CH ₃ CH ₂ OH	-231.1366266	-231.0237086	-231.0655436	-231.2124469	-231.0995289	-231.1416047	-231.2589655	-231.1460845	-231.1881745
BuOH	-309.6158437	-309.4432827	-309.4926077	-309.7144797	-309.5419187	-309.5912437	-309.7754340	-309.6028510	-309.6520849
t-BuOH	-309.6276702	-309.4565122	-309.5036712	-309.7264474	-309.5552894	-309.6024484	-309.7874221	-309.6162641	-309.6634231
PhCH ₂ OH	-422.5110218	-422.3419388	-422.3901208	-422.6394570	-422.4703660	-422.5185810	-422.7189205	-422.5498295	-422.5980445
PhC(CH ₃) ₂ OH	-501.0013758	-500.7739086	-500.8273988	-501.1523178	-500.9248224	-500.9783408	-501.2460177	-501.0185053	-501.0720407
PhOH	-383.2780761	-383.1391371	-383.1844881	-383.3945793	-383.2556403	-383.3009913	-383.4665405	-383.3276015	-383.3729525
p-nitro-PhOH	-587.5108550	-587.3666530	-587.4175370	-587.6905927	-587.5463907	-587.5972747	-587.8013309	-587.6571289	-587.7080129
p-methyl-PhOH	-422.5198750	-422.3517370	-422.4022910	-422.6478996	-422.4797616	-422.5303156	-422.7271083	-422.5589703	-422.6095243
p-amino-PhOH	-438.5491428	-438.3921778	-438.4408118	-438.6838460	-438.5268810	-438.5755150	-438.7669651	-438.6100001	-438.6586341
HOOH	-227.7032047	-227.6446547	-227.6792157	-227.7032047	-227.6446547	-227.6792157	-227.8253138	-227.7667638	-227.8013248
CH ₃ OOH	-266.9319970	-266.8441890	-266.8827460	-267.0189016	-266.9310936	-266.9696506	-267.0721768	-266.9843688	-267.0229258
t-BuOOH	-384.6672604	-384.4913394	-384.5380653	-384.7883871	-384.6124661	-384.6591351	-384.8633289	-384.6874079	-384.7340769
PhCH ₂ OOH	-497.5509804	-497.3771294	-497.4267164	-497.7014254	-497.5275744	-497.5771614	-497.7946625	-497.6208115	-497.6703985
TEMPOH	-559.8476818	-559.5319968	-559.5863798	-560.0182386	-559.7025536	-559.7569366	-560.1244299	-559.8087449	-559.8631279
HOO•	-227.0600436	-227.0140496	-227.0502649	-227.1332118	-227.0872178	-227.1236033	-227.1778249	-227.1318309	-227.1682823

Table S3.4.19. Calculated energies. Individual selected conformers.

№		(U)B3LYP-D3/6-31G(d)		
		E _{tot}	H ₂₉₈	G ₂₉₈
MIN	HO• (1a_3)	-152.1465975	-152.1075655	-152.1389925
1	HO_aab (1a_3)	-152.1465975	-152.1075655	-152.1389925
MIN	CH3O•	-191.4729895	-191.4043425	-191.4402005
1	CH3O1_acd	-191.4729895	-191.4043425	-191.4402005
2	CH3O1_aad	-191.4726359	-191.4039309	-191.4398819
MIN	CH3CH2O•	-230.7961992	-230.6973862	-230.7366822
1	CH3CH2O1_abd	-230.7961992	-230.6973862	-230.7364582
2	CH3CH2O1_abo	-230.7957842	-230.6971192	-230.7366822
3	CH3CH2O1_abx	-230.7951939	-230.6967789	-230.7363199
4	CH3CH2O1_abj	-230.7960285	-230.6964685	-230.7353175
5	CH3CH2O1_aav	-230.7948403	-230.6963913	-230.7365003

6	CH3CH2O1_abz	-230.7956448	-230.6960388	-230.7348728
MIN	BuO•	-309.4324787	-309.2734457	-309.3178948
1	BuO3_abc	-309.4324787	-309.2734457	-309.3176227
2	BuO2_aaa	-309.4314038	-309.2725758	-309.3178948
3	BuO3_aad	-309.4307874	-309.2717324	-309.3166044
4	BuO3_adf	-309.4310282	-309.2713832	-309.3155722
5	BuO4_adt	-309.4297304	-309.2709574	-309.3171954
6	BuO4_abg	-309.4305514	-309.2707834	-309.3157184
7	BuO3_aah	-309.4303135	-309.2706785	-309.3154845
8	BuO1_abl	-309.4294657	-309.2706147	-309.3174397
9	BuO4_ack	-309.4291498	-309.2704148	-309.3164408
10	BuO2_adh	-309.4298526	-309.2704086	-309.3165736
11	BuO2_aao	-309.4288749	-309.2704039	-309.3172439
12	BuO2_aac	-309.4289461	-309.2703831	-309.3168691
13	BuO4_adn	-309.4300321	-309.2703131	-309.3155341
14	BuO1_aat	-309.4301479	-309.2703019	-309.3162299
15	BuO2_adn	-309.4299518	-309.2702808	-309.3152538
16	BuO1_aax	-309.4288820	-309.2701110	-309.3169130
17	BuO2_abr	-309.4296972	-309.2700472	-309.3152192
18	BuO2_aaj	-309.4285452	-309.2700252	-309.3176912
19	BuO2_acg	-309.4286188	-309.2699878	-309.3166928
20	BuO5_aak	-309.4297069	-309.2698559	-309.3156319
21	BuO1_abq	-309.4297182	-309.2698532	-309.3158842
22	BuO4_aau	-309.4294783	-309.2697263	-309.3156173
23	BuO4_ace	-309.4283425	-309.2696075	-309.3160225
24	BuO5_add	-309.4293999	-309.2695969	-309.3156099
25	BuO1_aae	-309.4281213	-309.2695903	-309.3164563
26	BuO5_aah	-309.4292766	-309.2694316	-309.3151796
27	BuO4_aaq	-309.4290836	-309.2693626	-309.3149876
28	BuO5_acq	-309.4281446	-309.2692146	-309.3154356
29	BuO1_adh	-309.4278105	-309.2692075	-309.3161375
30	BuO5_aay	-309.4276476	-309.2690156	-309.3158126
31	BuO5_ads	-309.4287568	-309.2689258	-309.3149878
32	BuO5_abg	-309.4276559	-309.2689149	-309.3154499
33	BuO5_acf	-309.4272073	-309.2687793	-309.3158073
34	BuO5_ach	-309.4274988	-309.2687378	-309.3152528
MIN	tBuO•	-309.4416337	-309.2835411	-309.3314371
1	t-BuO2_aai	-309.4415251	-309.2835411	-309.3314371
2	t-BuO2_aag	-309.4416337	-309.2830397	-309.3271307
MIN	PhCH2O•	-422.5383244	-422.3837184	-422.4321589
1	PhCH2O2_aaj	-422.5383244	-422.3837184	-422.4318154
2	PhCH2O2_aam	-422.5376979	-422.3834369	-422.4321589
3	PhCH2O2_aax	-422.5374325	-422.3829815	-422.4309065
MIN	PhC(CH3)2O•	-501.1833401	-500.9683192	-501.0211692
1	PhCCH32O2_a_aau	-501.1830592	-500.9683192	-501.0211692
2	PhCCH32O2_a_abn	-501.1831008	-500.9683038	-501.0210088
3	PhCCH32O3_acd	-501.1828874	-500.9680544	-501.0199874
4	PhCCH32O2_a_adc	-501.1833401	-500.9680141	-501.0194181
5	PhCCH32O2_a_aab	-501.1827266	-500.9673916	-501.0190046

6	PhCCH32O2_a_aam	-501.1823342	-500.9670852	-501.0188872
7	PhCCH32O3_aal	-501.1808938	-500.9661008	-501.0186888
8	PhCCH32O3_abm	-501.1805091	-500.9657701	-501.0187921
9	PhCCH32O3_abl	-501.1798823	-500.9651223	-501.0191623
MIN	PhO•	-383.2606529	-383.1346519	-383.1779329
1	PhO_aam	-383.2606529	-383.1346519	-383.1779329
MIN	p-nitro-PhO•	-587.7600871	-587.6292461	-587.6797481
1	p-nitro-PhO_aac	-587.7600871	-587.6292461	-587.6797481
MIN	p-methyl-PhO•	-422.5839767	-422.4284437	-422.4767157
1	p-methyl-PhO_aah	-422.5839767	-422.4284437	-422.4767157
MIN	p-amino-PhO•	-438.6281654	-438.4835124	-438.5297314
1	p-amino-PhO_aav	-438.6281654	-438.4835124	-438.5297314
MIN	HOO•	-227.3321060	-227.2858670	-227.3187590
1	HOO_aaa	-227.3321060	-227.2858670	-227.3187590
2	HOO_aaj	-227.3165603	-227.2713033	-227.3087103
MIN	CH3OO•	-266.6397411	-266.5640601	-266.6028541
1	CH3OO_aaa	-266.6397411	-266.5640601	-266.6028541
2	CH3OO_aar	-266.6389780	-266.5633640	-266.6022530
3	CH3OO_act	-266.6353934	-266.5599714	-266.6013634
4	CH3OO_aaq	-266.6351932	-266.5598102	-266.6024582
MIN	t-BuOO•	-384.6083278	-384.4440058	-384.4920048
1	t-BuOO_aal	-384.6083158	-384.4440058	-384.4920048
2	t-BuOO_aaq	-384.6083278	-384.4439958	-384.4917268
3	t-BuOO_acz	-384.6068333	-384.4426103	-384.4901113
4	t-BuOO_aay	-384.6041102	-384.4401302	-384.4902332
MIN	PhCH2OO•	-497.7058911	-497.5440801	-497.5940221
1	PhCH2OO1_aae	-497.7058911	-497.5440801	-497.5940221
2	PhCH2OO2_aar	-497.7056301	-497.5438571	-497.5939821
3	PhCH2OO2_abo	-497.7033394	-497.5414894	-497.5909224
4	PhCH2OO1_adc	-497.7024489	-497.5408689	-497.5928219
5	PhCH2OO2_aak	-497.7017007	-497.5401147	-497.5912827
6	PhCH2OO1_acd	-497.7014028	-497.5399038	-497.5914908
7	PhCH2OO1_aai	-497.7012662	-497.5398532	-497.5924442
8	PhCH2OO2_abq	-497.7010461	-497.5396831	-497.5908091
9	PhCH2OO2_abb	-497.7007409	-497.5394549	-497.5917019
10	PhCH2OO2_ace	-497.6989783	-497.5375523	-497.5911033
11	PhCH2OO1_aaw	-497.6984610	-497.5370760	-497.5911030
MIN	TEMPO•	-560.1794735	-559.8743795	-559.9308634
1	TEMPO_ack	-560.1794735	-559.8743795	-559.9306925
2	TEMPO_aag	-560.1792257	-559.8742747	-559.9308347
3	TEMPO_aai	-560.1791714	-559.8742064	-559.9308634
4	TEMPO_aad	-560.1792210	-559.8742040	-559.9307350
5	TEMPO_abk	-560.1779003	-559.8728653	-559.9295243
6	TEMPO_aam	-560.1775945	-559.8726775	-559.9285995
7	TEMPO_abp	-560.1775258	-559.8723938	-559.9283878
MIN	•OO•	-226.7317449	-226.6981709	-226.7382699
1	3O2_aab	-226.7317449	-226.6981709	-226.7382699
MIN	HCO2•	-265.5075068	-265.4557999	-265.4920149
1	HCO2_aac	-265.5051349	-265.4557999	-265.4920149

2	HCO2_aaw	-265.5075068	-265.4556378	-265.4896828
---	----------	--------------	--------------	--------------

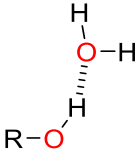
Table S3.4.20. Calculated energies. Individual selected conformers.

Ne		(U)B3LYP-D3/6-31G(d)		
		E _{tot}	H ₂₉₈	G ₂₉₈
MIN	HOH (1Ha)	-152.8318213	-152.7788433	-152.8114843
1	HOH_aaa (1Ha)	-152.8318213	-152.7788433	-152.8114843
2	HOH_aaq	-152.8305406	-152.7776816	-152.8104666
MIN	CH3OH	-192.1387684	-192.0551334	-192.0924013
1	CH3OH_aaa	-192.1387684	-192.0551334	-192.0910744
2	CH3OH_aac	-192.1384146	-192.0548476	-192.0909886
3	CH3OH_aad	-192.1383573	-192.0547343	-192.0924013
MIN	CH3CH2OH	-231.4630119	-231.3494369	-231.3881581
1	CH3CH2OH1_aam	-231.4630119	-231.3494369	-231.3880259
2	CH3CH2OH2_abq	-231.4625321	-231.3489141	-231.3875051
3	CH3CH2OH1_aaa	-231.4622623	-231.3487053	-231.3871753
4	CH3CH2OH2_aaw	-231.4611122	-231.3476282	-231.3864442
5	CH3CH2OH1_aae	-231.4609752	-231.3474862	-231.3870562
6	CH3CH2OH1_acl	-231.4607995	-231.3472355	-231.3863665
7	CH3CH2OH1_aaf	-231.4604591	-231.3469341	-231.3881581
MIN	BuOH	-310.0968831	-309.9230971	-309.9690111
1	BuOH4d_aaa	-310.0968831	-309.9230971	-309.9690111
2	BuOH5c_acz	-310.0967116	-309.9229606	-309.9678696
3	BuOH3a_abw	-310.0965797	-309.9229407	-309.9681797
4	BuOH5c_adg	-310.0966849	-309.9228719	-309.9678799
5	BuOH5c_adh	-310.0966360	-309.9228390	-309.9673950
6	BuOH2b_aaw	-310.0965356	-309.9226466	-309.9673536
7	BuOH1a_abc	-310.0961281	-309.9225111	-309.9682071
8	BuOH3a_ada	-310.0960100	-309.9223510	-309.9672660
9	BuOH8b_aam	-310.0959364	-309.9222194	-309.9680644
10	BuOH14b_abm	-310.0960351	-309.9221751	-309.9668281
11	BuOH6b_aae	-310.0958568	-309.9221058	-309.9679808
12	BuOH3a_adj	-310.0956663	-309.9220503	-309.9668363
13	BuOH4d_acp	-310.0957650	-309.9220490	-309.9689930
14	BuOH1a_abz	-310.0957415	-309.9219515	-309.9665165
15	BuOH1a_ace	-310.0955317	-309.9219407	-309.9674897
16	BuOH6b_abo	-310.0957716	-309.9219116	-309.9666556
17	BuOH1a_aax	-310.0952522	-309.9217712	-309.9676002
18	BuOH3a_abm	-310.0951620	-309.9216310	-309.9682810
19	BuOH7b_aaa	-310.0953738	-309.9216098	-309.9672118
20	BuOH12c_adf	-310.0954299	-309.9216079	-309.9661469
21	BuOH8b_aao	-310.0952782	-309.9215762	-309.9673102
22	BuOH13c_abc	-310.0952867	-309.9215307	-309.9655907
23	BuOH2b_acm	-310.0952752	-309.9214872	-309.9672432
24	BuOH13c_aau	-310.0951959	-309.9213909	-309.9661009

25	BuOH1a_aad	-310.0948227	-309.9212337	-309.9671917
26	BuOH6b_aax	-310.0950194	-309.9211644	-309.9670024
27	BuOH11d_aak	-310.0948501	-309.9211211	-309.9670161
28	BuOH2b_abj	-310.0948069	-309.9210439	-309.9658819
29	BuOH3a_aah	-310.0944585	-309.9208475	-309.9671985
30	BuOH12c_abw	-310.0947876	-309.9208166	-309.9646186
31	BuOH6b_acr	-310.0946884	-309.9207834	-309.9662114
32	BuOH13c_aaa	-310.0943369	-309.9207829	-309.9664129
33	BuOH12c_aba	-310.0943047	-309.9205947	-309.9652267
34	BuOH3a_adm	-310.0940853	-309.9205793	-309.9683463
35	BuOH10d_aar	-310.0943452	-309.9205762	-309.9664272
36	BuOH10d_abi	-310.0944154	-309.9205564	-309.9660494
37	BuOH4d_aaq	-310.0939763	-309.9204653	-309.9676033
38	BuOH11d_aab	-310.0941816	-309.9204596	-309.9662436
39	BuOH4d_adc	-310.0940501	-309.9204111	-309.9675541
40	BuOH7b_aao	-310.0939229	-309.9203359	-309.9662969
41	BuOH2b_adp	-310.0940372	-309.9203222	-309.9655042
42	BuOH2b_abz	-310.0939254	-309.9202234	-309.9665014
43	BuOH8b_aal	-310.0940025	-309.9201935	-309.9659715
44	BuOH8b_aba	-310.0938485	-309.9201545	-309.9665155
45	BuOH5c_ado	-310.0939418	-309.9201488	-309.9665508
46	BuOH14b_adf	-310.0939106	-309.9201186	-309.9648676
47	BuOH14b_aag	-310.0938211	-309.9200301	-309.9650621
48	BuOH13c_aaz	-310.0934367	-309.9197327	-309.9658037
49	BuOH12c_abm	-310.0933458	-309.9195268	-309.9647658
50	BuOH14b_abi	-310.0933243	-309.9195263	-309.9643193
51	BuOH6b_aai	-310.0932690	-309.9195260	-309.9661070
52	BuOH10d_abd	-310.0929629	-309.9193449	-309.9652989
53	BuOH10d_acf	-310.0929783	-309.9192863	-309.9652873
54	BuOH10d_aab	-310.0929138	-309.9191308	-309.9656488
55	BuOH11d_ada	-310.0927448	-309.9189908	-309.9652498
56	BuOH12c_aas	-310.0922050	-309.9185270	-309.9633760
57	BuOH14b_aar	-310.0919647	-309.9183337	-309.9646067
MIN	tBuOH	-310.1090345	-309.9367035	-309.9798735
1	t-BuOH_ads	-310.1090345	-309.9367035	-309.9798735
2	t-BuOH_aar	-310.1078698	-309.9356678	-309.9790388
3	t-BuOH_abx	-310.1051120	-309.9330050	-309.9777460
MIN	PhCH2OH	-423.2069474	-423.0372224	-423.0844624
1	PhCH2OH2_aam	-423.2069474	-423.0372224	-423.0844624
2	PhCH2OH2_aae	-423.2065049	-423.0368399	-423.0840489
3	PhCH2OH1_aae	-423.2041475	-423.0344465	-423.0816815
4	PhCH2OH2_abc	-423.2037433	-423.0341233	-423.0823083
5	PhCH2OH1_adg	-423.2020263	-423.0324783	-423.0799413
MIN	PhC(CH3)2OH	-501.8504166	-501.6218206	-501.6741180
1	PhCCH32OH1_abp	-501.8504166	-501.6218206	-501.6733246
2	PhCCH32OH2_acf	-501.8503006	-501.6216656	-501.6739946
3	PhCCH32OH1_acl	-501.8502890	-501.6216540	-501.6741180
4	PhCCH32OH2_aaf	-501.8498454	-501.6213054	-501.6728384
5	PhCCH32OH3_aae	-501.8496603	-501.6211693	-501.6722743

6	PhCCH32OH1_abq	-501.8495829	-501.6209449	-501.6721109
7	PhCCH32OH2_aan	-501.8493368	-501.6207588	-501.6729698
8	PhCCH32OH1_aao	-501.8471231	-501.6185781	-501.6701991
9	PhCCH32OH1_acb	-501.8463524	-501.6177974	-501.6694924
10	PhCCH32OH3_ads	-501.8458870	-501.6176830	-501.6702970
11	PhCCH32OH3_adt	-501.8459161	-501.6174741	-501.6705451
12	PhCCH32OH3_abt	-501.8457134	-501.6172074	-501.6691584
13	PhCCH32OH1_abv	-501.8452340	-501.6168110	-501.6686940
MIN	PhOH	-383.8938673	-383.7548543	-383.7989143
1	PhOH_aae	-383.8938673	-383.7548543	-383.7989143
MIN	p-nitro-PhOH	-588.4005120	-588.2562720	-588.3068910
1	p-nitro-PhOH_aai	-588.4005120	-588.2562720	-588.3068910
MIN	p-methyl-PhOH	-423.2141255	-423.0456714	-423.0949435
1	p-methyl-PhOH_aca	-423.2141255	-423.0456705	-423.0949435
2	p-methyl-PhOH_aad	-423.2141244	-423.0456714	-423.0948264
MIN	p-amino-PhOH	-439.2465281	-439.0894531	-439.1369321
1	p-amino-PhOH_ach	-439.2465281	-439.0894531	-439.1369321
MIN	HOOH	-227.9626681	-227.9039341	-227.9374491
1	HOOH_aab	-227.9626681	-227.9039341	-227.9374491
MIN	CH3OOH	-267.2715186	-267.1837066	-267.2227126
1	CH3OOH_aam	-267.2715186	-267.1837066	-267.2227126
2	CH3OOH_abj	-267.2711899	-267.1831489	-267.2224869
3	CH3OOH_adl	-267.2700475	-267.1824045	-267.2226915
MIN	t-BuOOH	-385.2386526	-385.0620236	-385.1090206
1	t-BuOOH_acm	-385.2386526	-385.0620236	-385.1090206
MIN	PhCH2OOH	-498.3406620	-498.1665520	-498.2159740
1	PhCH2OOH2_aan	-498.3406620	-498.1665520	-498.2159740
2	PhCH2OOH2_abr	-498.3393105	-498.1653365	-498.2147635
3	PhCH2OOH3_aah	-498.3379918	-498.1640528	-498.2137558
4	PhCH2OOH3_aae	-498.3370756	-498.1631916	-498.2129366
5	PhCH2OOH3_abg	-498.3363383	-498.1625513	-498.2127703
MIN	TEMPOH	-560.7853105	-560.4683745	-560.5240795
1	TEMPOH_aah	-560.7853105	-560.4683745	-560.5240795
2	TEMPOH_aag	-560.7846894	-560.4676444	-560.5232194
3	TEMPOH_adl	-560.7847137	-560.4676117	-560.5234447
4	TEMPOHa_add	-560.7801677	-560.4634627	-560.5198577
5	TEMPOHa_aaw	-560.7799902	-560.4633512	-560.5208452
MIN	HCO2H	-266.1754636	-266.1100416	-266.1476686
1	HCO2Ha_aab	-266.1754636	-266.1100416	-266.1476686

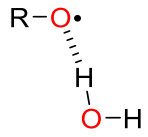
Table S3.4.21. Calculated energies. Individual selected conformers.

№		(U)B3LYP-D3/6-31G(d)		
		E _{tot}	H ₂₉₈	G ₂₉₈
MIN	HOH (1Ha)	-152.8318213	-152.7788433	-152.8114843
1	HOH_aaa (1Ha)	-152.8318213	-152.7788433	-152.8114843
2	HOH_aaq	-152.8305406	-152.7776816	-152.8104666
MIN	CH3OH	-192.1384134	-192.0548484	-192.0931620
1	CH3OH_aai	-192.1384134	-192.0548484	-192.0920964
2	CH3OH_aby	-192.1377860	-192.0545340	-192.0931620
3	CH3OH_aab	-192.1378897	-192.0544807	-192.0921067
MIN	CH3CH2OH	-231.4612036	-231.3476606	-231.3881106
1	CH3CH2OH1_aan	-231.4612036	-231.3476606	-231.3873066
2	CH3CH2OH1_abb	-231.4606979	-231.3473929	-231.3870459
3	CH3CH2OH1_aai	-231.4605585	-231.3470535	-231.3877855
4	CH3CH2OH2_aan	-231.4594236	-231.3462596	-231.3881106
5	CH3CH2OH2_aar	-231.4594427	-231.3461337	-231.3872397
MIN	BuOH	-310.0955283	-309.9218353	-309.9686020
1	BuOH13c_acf	-310.0955283	-309.9218353	-309.9669573
2	BuOH1a_ads	-310.0952738	-309.9218108	-309.9674188
3	BuOH3a_aar	-310.0952961	-309.9217911	-309.9675591
4	BuOH13c_abh	-310.0953543	-309.9217363	-309.9663703
5	BuOH1a_adh	-310.0952400	-309.9217130	-309.9674150
6	BuOH6b_abc	-310.0953852	-309.9217122	-309.9665272
7	BuOH2b_adi	-310.0951269	-309.9214209	-309.9667329
8	BuOH5c_adn	-310.0948707	-309.9212147	-309.9670877
9	BuOH5c_abp	-310.0945647	-309.9209097	-309.9670367
10	BuOH3a_abi	-310.0940940	-309.9205250	-309.9686020
11	BuOH14b_aaj	-310.0941628	-309.9204918	-309.9648298
12	BuOH14b_abp	-310.0941465	-309.9204375	-309.9654035
13	BuOH8b_abi	-310.0940798	-309.9204178	-309.9672238
14	BuOH5c_aca	-310.0935844	-309.9198324	-309.9678294
15	BuOH1a_abi	-310.0931485	-309.9197155	-309.9671155
16	BuOH11d_aar	-310.0927707	-309.9192237	-309.9658797
17	BuOH11d_aap	-310.0929504	-309.9191924	-309.9658754
18	BuOH11d_acr	-310.0925534	-309.9190854	-309.9659164
19	BuOH11d_aaw	-310.0925191	-309.9189731	-309.9658771
20	BuOH7b_abs	-310.0921135	-309.9188655	-309.9676445
21	BuOH7b_adg	-310.0921195	-309.9188495	-309.9675395
22	BuOH2b_acw	-310.0925423	-309.9187953	-309.9666783
23	BuOH7b_aag	-310.0921390	-309.9187820	-309.9669940
24	BuOH7b_aat	-310.0921218	-309.9186848	-309.9664438
25	BuOH11d_adr	-310.0922229	-309.9185459	-309.9666099
26	BuOH12c_acg	-310.0918508	-309.9183448	-309.9662348
27	BuOH12c_aco	-310.0916695	-309.9182725	-309.9661345
28	BuOH12c_aay	-310.0917452	-309.9181772	-309.9660602

29	BuOH10d_acv	-310.0911148	-309.9177628	-309.9660938
30	BuOH10d_aae	-310.0911928	-309.9176398	-309.9651628
MIN	tBuOH	-310.1051749	-309.9330899	-309.9786929
1	t-BuOH_aap	-310.1051749	-309.9330899	-309.9786929
2	t-BuOH_aaa	-310.1048403	-309.9329803	-309.9780773
MIN	PhCH2OH	-423.2094341	-423.0397021	-423.0862631
1	PhCH2OH2_abd	-423.2094341	-423.0397021	-423.0862631
2	PhCH2OH1_abq	-423.2009243	-423.0318553	-423.0829833
3	PhCH2OH1_aar	-423.2007198	-423.0316838	-423.0825738
MIN	PhC(CH3)2OH	-501.8525141	-501.6240046	-501.6768566
1	PhCCH32OH1_adc	-501.8523846	-501.6240046	-501.6768566
2	PhCCH32OH1_aci	-501.8525141	-501.6239331	-501.6753841
3	PhCCH32OH2_adc	-501.8522595	-501.6238885	-501.6762005
4	PhCCH32OH3_aah	-501.8462174	-501.6180484	-501.6727324
5	PhCCH32OH3_acq	-501.8461026	-501.6179936	-501.6712196
MIN	PhOH	-383.8982015	-383.7590775	-383.8046154
1	PhOH_abt	-383.8982015	-383.7590775	-383.8031395
2	PhOH_act	-383.8980774	-383.7590534	-383.8046154
3	PhOH_abu	-383.8980447	-383.7588847	-383.8028247
MIN	p-nitro-PhOH	-588.4093503	-588.2648783	-588.3156543
1	p-nitro-PhOH_aae	-588.4093503	-588.2648783	-588.3156543
2	p-nitro-PhOH_aab	-588.4087967	-588.2643327	-588.3147547
MIN	p-methyl-PhOH	-423.2181494	-423.0495224	-423.1000770
1	p-methyl-PhOH_aay	-423.2179630	-423.0494390	-423.1000770
2	p-methyl-PhOH_abt	-423.2181494	-423.0495224	-423.0987424
3	p-methyl-PhOH_adp	-423.2180410	-423.0494110	-423.0983930
MIN	p-amino-PhOH	-439.2498947	-439.0926247	-439.1396891
1	p-amino-PhOH_aab	-439.2498947	-439.0926247	-439.1393327
2	p-amino-PhOH_aau	-439.2494673	-439.0922173	-439.1390053
3	p-amino-PhOH_aaa	-439.2493861	-439.0921631	-439.1396891
MIN	HOOH	-227.9626681	-227.9039341	-227.9374491
1	HOOH_aab	-227.9626681	-227.9039341	-227.9374491
MIN	CH3OOH	-267.2785038	-267.1900838	-267.2274928
1	CH3OOH_aaq	-267.2785038	-267.1900838	-267.2274928
2	CH3OOH_aaf	-267.2774429	-267.1891539	-267.2267939
MIN	t-BuOOH	-385.2453165	-385.0681415	-385.1136735
1	t-BuOOH_acs	-385.2453165	-385.0681415	-385.1136735
2	t-BuOOH_acv	-385.2444670	-385.0674050	-385.1130930
MIN	PhCH2OOH	-498.3480630	-498.1734860	-498.2211500
1	PhCH2OOH2_aai	-498.3480630	-498.1734860	-498.2211500
2	PhCH2OOH1_abr	-498.3423271	-498.1678301	-498.2166751
3	PhCH2OOH2_aav	-498.3406827	-498.1665397	-498.2160427
4	PhCH2OOH3_aan	-498.3405167	-498.1663507	-498.2165387
5	PhCH2OOH1_adh	-498.3403045	-498.1661105	-498.2168415
6	PhCH2OOH3_abv	-498.3395469	-498.1655039	-498.2159699
7	PhCH2OOH3_abh	-498.3377985	-498.1639675	-498.2134945
MIN	TEMPOH	-560.7942974	-560.4766384	-560.5302304
1	TEMPOH_ach	-560.7942974	-560.4766384	-560.5302304
2	TEMPOHa_abr	-560.7793399	-560.4628629	-560.5198469

MIN	HOO•	-227.3321060	-227.2858670	-227.3187590
1	HOO_aaa	-227.3321060	-227.2858670	-227.3187590
MIN	HCO2H	-266.1922978	-266.1261058	-266.1602548
1	HCO2Ha_aan	-266.1922978	-266.1261058	-266.1602548
2	HCO2Hb_aad	-266.1769062	-266.1114562	-266.1495672
3	HCO2Hb_aab	-266.1763272	-266.1109152	-266.1486852

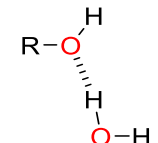
Table S3.4.22. Calculated energies. Individual selected conformers.

No		G3B3-D3			UB3LYP-D3/ 6-31G(d)	UHF/ 6-31G(d)	UHF/ 6-31+G(d)	UHF/ 6-31G(2df,p)	UHF/ GTLarge	DE(HLC)
		E _{tot}	H ₂₉₈	G ₂₉₈	<S ² >	<S ² >	<S ² >	<S ² >	<S ² >	
MIN	HO• (1a_3)	-152.1122504	-152.0744734	-152.1060594						
1	HO_aab (1a_3)	-152.1122504	-152.0744734	-152.1060594	0.7529	0.7563	0.7578	0.7568	0.7582	-0.0505530
MIN	CH3O•	-191.4122958	-191.3460168	-191.3821224						
1	CH3O1_acd	-191.4122958	-191.3460168	-191.3821058	0.7532	0.7586	0.7596	0.7592	0.7604	-0.0708330
2	CH3O1_aad	-191.4122744	-191.3459404	-191.3821224	0.7531	0.7586	0.7596	0.7592	0.7604	-0.0708330
MIN	CH3CH2O•	-230.7164502	-230.6213478	-230.6617478						
1	CH3CH2O1_abd	-230.7160225	-230.6206955	-230.6600895	0.7532	0.7587	0.7597	0.7593	0.7604	-0.0911130
2	CH3CH2O1_abo	-230.7162643	-230.6210753	-230.6609643	0.7533	0.7588	0.7597	0.7593	0.7605	-0.0911130
3	CH3CH2O1_abx	-230.7163008	-230.6213478	-230.6612198	0.7533	0.7588	0.7598	0.7593	0.7606	-0.0911130
4	CH3CH2O1_abj	-230.7162759	-230.6202319	-230.6594029	0.7532	0.7590	0.7599	0.7595	0.7605	-0.0911130
5	CH3CH2O1_aav	-230.7162948	-230.6213098	-230.6617478	0.7533	0.7587	0.7598	0.7593	0.7605	-0.0911130
6	CH3CH2O1_abz	-230.7164502	-230.6203632	-230.6595192	0.7532	0.7590	0.7599	0.7595	0.7606	-0.0911130
MIN	BuO•	-309.3162287	-309.1631007	-309.2106530						
1	BuO3_abc	-309.3158039	-309.1624859	-309.2071679	0.7534	0.7590	0.7600	0.7596	0.7607	-0.1316730
2	BuO2_aaa	-309.3162287	-309.1631007	-309.2089317	0.7533	0.7588	0.7598	0.7594	0.7605	-0.1316730
3	BuO3_aad	-309.3150032	-309.1616632	-309.2070412	0.7534	0.7589	0.7598	0.7595	0.7606	-0.1316730
4	BuO3_adf	-309.3143120	-309.1604060	-309.2051000	0.7536	0.7598	0.7608	0.7604	0.7614	-0.1316730
5	BuO4_adt	-309.3148993	-309.1618233	-309.2085753	0.7533	0.7589	0.7598	0.7594	0.7606	-0.1316730
6	BuO4_abg	-309.3146182	-309.1605962	-309.2060352	0.7535	0.7596	0.7605	0.7601	0.7611	-0.1316730
7	BuO3_aah	-309.3147301	-309.1608341	-309.2061451	0.7536	0.7600	0.7610	0.7606	0.7616	-0.1316730
8	BuO1_abl	-309.3147576	-309.1616056	-309.2089456	0.7533	0.7587	0.7597	0.7593	0.7604	-0.1316730
9	BuO4_ack	-309.3137433	-309.1607013	-309.2072433	0.7532	0.7586	0.7596	0.7593	0.7604	-0.1316730
10	BuO2_adh	-309.3149657	-309.1612467	-309.2079237	0.7535	0.7596	0.7605	0.7602	0.7611	-0.1316730
11	BuO2_aao	-309.3153087	-309.1625177	-309.2098767	0.7533	0.7588	0.7598	0.7594	0.7606	-0.1316730
12	BuO2_aac	-309.3152405	-309.1623625	-309.2093655	0.7533	0.7588	0.7598	0.7594	0.7606	-0.1316730
13	BuO4_adn	-309.3145069	-309.1605299	-309.2062569	0.7535	0.7597	0.7607	0.7603	0.7613	-0.1316730
14	BuO1_aat	-309.3154765	-309.1613745	-309.2078115	0.7534	0.7595	0.7605	0.7600	0.7600	-0.1316730
15	BuO2_adn	-309.3146797	-309.1607457	-309.2062277	0.7534	0.7596	0.7605	0.7601	0.7611	-0.1316730
16	BuO1_aax	-309.3148631	-309.1617871	-309.2091041	0.7533	0.7588	0.7598	0.7594	0.7605	-0.1316730
17	BuO2_abr	-309.3150760	-309.1611620	-309.2068430	0.7535	0.7597	0.7606	0.7602	0.7613	-0.1316730
18	BuO2_aaj	-309.3153070	-309.1624700	-309.2106530	0.7533	0.7588	0.7598	0.7594	0.7606	-0.1316730
19	BuO2_acg	-309.3151996	-309.1622576	-309.2094776	0.7533	0.7588	0.7597	0.7594	0.7605	-0.1316730
20	BuO5_aak	-309.3149005	-309.1607955	-309.2070785	0.7534	0.7595	0.7605	0.7600	0.7611	-0.1316730
21	BuO1_abq	-309.3156923	-309.1615723	-309.2081123	0.7534	0.7595	0.7605	0.7601	0.7611	-0.1316730

22	BuO4_aau	-309.3145502	-309.1605412	-309.2069382	0.7535	0.7598	0.7607	0.7604	0.7614	-0.1316730
23	BuO4_ace	-309.3145432	-309.1615042	-309.2084322	0.7533	0.7589	0.7598	0.7594	0.7606	-0.1316730
24	BuO5_add	-309.3151250	-309.1610660	-309.2075860	0.7534	0.7595	0.7605	0.7600	0.7611	-0.1316730
25	BuO1_aae	-309.3147382	-309.1618892	-309.2092732	0.7533	0.7588	0.7598	0.7594	0.7606	-0.1316730
26	BuO5_aah	-309.3143885	-309.1602895	-309.2065445	0.7534	0.7596	0.7606	0.7601	0.7612	-0.1316730
27	BuO4_aaq	-309.3146548	-309.1606748	-309.2068068	0.7535	0.7599	0.7608	0.7605	0.7615	-0.1316730
28	BuO5_acq	-309.3132668	-309.1600418	-309.2067738	0.7533	0.7587	0.7597	0.7594	0.7605	-0.1316730
29	BuO1_adh	-309.3147270	-309.1618100	-309.2092570	0.7533	0.7588	0.7598	0.7594	0.7606	-0.1316730
30	BuO5_aay	-309.3133391	-309.1603931	-309.2077091	0.7533	0.7587	0.7597	0.7593	0.7605	-0.1316730
31	BuO5_ads	-309.3145651	-309.1604781	-309.2070481	0.7534	0.7596	0.7606	0.7602	0.7612	-0.1316730
32	BuO5_abg	-309.3133543	-309.1603063	-309.2073573	0.7533	0.7588	0.7598	0.7594	0.7606	-0.1316730
33	BuO5_acf	-309.3138129	-309.1610589	-309.2086089	0.7533	0.7588	0.7598	0.7594	0.7606	-0.1316730
34	BuO5_ach	-309.3140010	-309.1609370	-309.2079640	0.7533	0.7587	0.7598	0.7593	0.7606	-0.1316730
MIN	tBuO•	-309.3281339	-309.1752019	-309.2198349						
1	t-BuO2_aai	-309.3218621	-309.1694901	-309.2179541	0.7529	0.7581	0.7593	0.7588	0.7599	-0.1316730
2	t-BuO2_aag	-309.3281339	-309.1752019	-309.2198349	0.7532	0.7588	0.7596	0.7593	0.7602	-0.1316730
MIN	PhCH2O•	-422.3746434	-422.2258224	-422.2751354						
1	PhCH2O2_aaj	-422.3743574	-422.2252084	-422.2738934	0.7536	1.2737	1.2267	1.2738	1.2189	-0.1654730
2	PhCH2O2_aam	-422.3746434	-422.2258224	-422.2751354	0.7538	1.2715	1.2241	1.2713	1.2159	-0.1654730
3	PhCH2O2_aax	-422.3739053	-422.2248993	-422.2734183	0.7536	1.2622	1.2195	1.2617	1.2109	-0.1654730
MIN	PhC(CH3)2O•	-500.9870737	-500.7799257	-500.8335177						
1	PhCCH32O2_a_aau	-500.9869537	-500.7798597	-500.8335177	0.7534	1.2613	1.2152	1.2612	1.2077	-0.2060330
2	PhCCH32O2_a_abn	-500.9870737	-500.7799257	-500.8334387	0.7534	1.2613	1.2152	1.2613	1.2080	-0.2060330
3	#N/A	#N/A	#N/A	#N/A	#N/A	#N/A	#N/A	#N/A	#N/A	#N/A
4	PhCCH32O2_a_adc	-500.9864027	-500.7787577	-500.8309587	0.7545	1.2770	1.2369	1.2781	1.2315	-0.2060330
5	PhCCH32O2_a_aab	-500.9856322	-500.7779782	-500.8303882	0.7548	1.2799	1.2407	1.2814	1.2357	-0.2060330
6	PhCCH32O2_a_aam	-500.9855545	-500.7779795	-500.8305825	0.7545	1.2729	1.2365	1.2745	1.2315	-0.2060330
7	PhCCH32O3_aal	-500.9857074	-500.7785614	-500.8319594	0.7534	1.2752	1.2304	1.2745	1.2228	-0.2060330
8	PhCCH32O3_abm	-500.9852833	-500.7781893	-500.8320213	0.7534	1.2670	1.2250	1.2662	1.2172	-0.2060330
9	PhCCH32O3_abl	-500.9849894	-500.7778724	-500.8327244	0.7533	1.2606	1.2156	1.2606	1.2082	-0.2060330
MIN	PhO•	-383.1128539	-382.9912699	-383.0350319						
1	PhO_aam	-383.1128539	-382.9912699	-383.0350319	0.7867	1.3558	1.3328	1.3545	1.3282	-0.1451930
MIN	p-nitro-PhO•	-587.5330314	-587.4066334	-587.4577874						
1	p-nitro-PhO_aac	-587.5330314	-587.4066334	-587.4577874	0.7900	1.3971	1.3839	1.3938	1.3789	-0.1992730
1	p-methyl-PhO_aah	-422.4189092	-422.2688612	-422.3177302	0.7832	1.3413	1.3180	1.3392	1.3127	-0.1654730
1	p-amino-PhO_aav	-438.4648656	-438.3252636	-438.3720786	0.7692	1.2447	1.2242	1.2438	1.2204	-0.1654730
1	HOO_aaa	-227.2617016	-227.2169926	-227.2500566	0.7529	0.7609	0.7637	0.7616	0.7644	-0.0708330
2	HOO_aaj	-227.2526175	-227.2088055	-227.2464315	0.7528	0.7604	0.7624	0.7610	0.7631	-0.0708330
1	CH3OO_aaa	-266.5461916	-266.4731016	-266.5121866	0.7530	0.7611	0.7638	0.7619	0.7645	-0.0911130
2	CH3OO_aar	-266.5455184	-266.4724904	-266.5116724	0.7530	0.7611	0.7638	0.7619	0.7645	-0.0911130
3	CH3OO_act	-266.5456695	-266.4728155	-266.5145105	0.7529	0.7607	0.7631	0.7615	0.7639	-0.0911130
4	CH3OO_aaq	-266.5462115	-266.4733965	-266.5163485	0.7530	0.7610	0.7634	0.7617	0.7642	-0.0911130
1	t-BuOO_aal	-384.4652363	-384.3067463	-384.3553613	0.7533	0.7619	0.7644	0.7626	0.7651	-0.1519530
2	t-BuOO_aaq	-384.4645089	-384.3059989	-384.3543429	0.7533	0.7618	0.7643	0.7626	0.7651	-0.1519530
3	t-BuOO_acz	-384.4637146	-384.3053036	-384.3534226	0.7533	0.7609	0.7631	0.7618	0.7639	-0.1519530
4	t-BuOO_aay	-384.4641943	-384.3060103	-384.3567383	0.7533	0.7615	0.7636	0.7622	0.7644	-0.1519530
1	PhCH2OO1_aae	-497.5109813	-497.3548593	-497.4054463	0.7532	1.2778	1.2361	1.2795	1.2301	-0.1857530
2	PhCH2OO2_aar	-497.5105440	-497.3544580	-497.4052280	0.7532	1.2779	1.2360	1.2792	1.2297	-0.1857530
3	PhCH2OO2_abo	-497.5077386	-497.3515796	-497.4016566	0.7534	1.2660	1.2257	1.2660	1.2187	-0.1857530

4	PhCH2OO1_adc	-497.5086430	-497.3527380	-497.4053420	0.7532	1.2811	1.2395	1.2819	1.2332	-0.1857530
5	PhCH2OO2_aak	-497.5071879	-497.3512769	-497.4030949	0.7534	1.2670	1.2227	1.2681	1.2161	-0.1857530
6	PhCH2OO1_acd	-497.5068066	-497.3509766	-497.4032166	0.7535	1.2689	1.2243	1.2700	1.2178	-0.1857530
7	PhCH2OO1_aai	-497.5080754	-497.3523194	-497.4055734	0.7532	1.2750	1.2319	1.2765	1.2261	-0.1857530
8	PhCH2OO2_abq	-497.5092722	-497.3535652	-497.4053512	0.7534	1.2700	1.2337	1.2713	1.2265	-0.1857530
9	PhCH2OO2_abb	-497.5092124	-497.3535754	-497.4064864	0.7534	1.2668	1.2303	1.2681	1.2229	-0.1857530
10	PhCH2OO2_ace	-497.5081321	-497.3523651	-497.4065761	0.7532	1.2781	1.2363	1.2793	1.2300	-0.1857530
11	PhCH2OO1_aaw	-497.5082536	-497.3525256	-497.4072126	0.7531	1.2782	1.2364	1.2794	1.2305	-0.1857530
1	TEMPO_ack	-559.9656607	-559.6716237	-559.7289527	0.7538	0.7692	0.7727	0.7705	0.7744	-0.2465930
2	TEMPO_aag	-559.9661668	-559.6722648	-559.7298428	0.7539	0.7695	0.7726	0.7710	0.7743	-0.2465930
3	TEMPO_aai	-559.9655184	-559.6716034	-559.7292784	0.7538	0.7691	0.7727	0.7704	0.7743	-0.2465930
4	TEMPO_aad	-559.9664068	-559.6724408	-559.7299918	0.7541	0.7707	0.7724	0.7721	0.7743	-0.2465930
5	TEMPO_abk	-559.9629954	-559.6690144	-559.7266904	0.7538	0.7693	0.7724	0.7707	0.7741	-0.2465930
6	TEMPO_aam	-559.9624144	-559.6685414	-559.7254854	0.7541	0.7697	0.7717	0.7712	0.7736	-0.2465930
7	TEMPO_abp	-559.9627372	-559.6686572	-559.7256742	0.7539	0.7681	0.7712	0.7697	0.7730	-0.2465930
1	3O2_aab	-226.6607931	-226.6282241	-226.6685121	2.0067	2.0354	2.0447	2.0374	2.0470	-0.0673060
1	HCO2_aac	-265.4091505	-265.3614085	-265.3978575	0.7548	0.7673	0.7685	0.7678	0.7693	-0.0843530
2	HCO2_aaw	-265.4084015	-265.3582555	-265.3925055	0.7552	0.7621	0.7634	0.7624	0.7637	-0.0843530

Table S3.4.23. Calculated energies. Individual selected conformers.

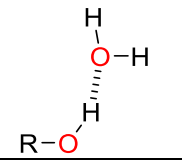
No		G3B3-D3			DE(HLC)
		E _{tot}	H ₂₉₈	G ₂₉₈	
MIN	HOH (1Ha)	-152.8139511	-152.7627571	-152.7955861	
1	HOH_aaa (1Ha)	-152.8139511	-152.7627571	-152.7955861	-0.0540800
2	HOH_aaq	-152.8134637	-152.7623797	-152.7953567	-0.0540800
MIN	CH3OH	-192.0938537	-192.0132317	-192.0496247	
1	CH3OH_aaa	-192.0934020	-192.0127180	-192.0489070	-0.0743600
2	CH3OH_aac	-192.0938537	-192.0132317	-192.0496247	-0.0743600
3	CH3OH_aad	-192.0923554	-192.0116804	-192.0495974	-0.0743600
MIN	CH3CH2OH	-231.3986662	-231.2891112	-231.3284264	
1	CH3CH2OH1_aam	-231.3983824	-231.2888674	-231.3277954	-0.0946400
2	CH3CH2OH2_abq	-231.3986662	-231.2891112	-231.3280392	-0.0946400
3	CH3CH2OH1_aaa	-231.3976547	-231.2881557	-231.3269647	-0.0946400
4	CH3CH2OH2_aaw	-231.3974991	-231.2880701	-231.3272271	-0.0946400
5	CH3CH2OH1_aae	-231.3975441	-231.2881091	-231.3280211	-0.0946400
6	CH3CH2OH1_acl	-231.3950751	-231.2855651	-231.3250401	-0.0946400
7	CH3CH2OH1_aaf	-231.3963314	-231.2868594	-231.3284264	-0.0946400
MIN	BuOH	-309.9974505	-309.8301055	-309.8775015	
1	BuOH4d_aaa	-309.9974477	-309.8299467	-309.8763877	-0.1352000
2	BuOH5c_acz	-309.9968824	-309.8294134	-309.8748494	-0.1352000
3	BuOH3a_abw	-309.9965503	-309.8291883	-309.8749553	-0.1352000
4	BuOH5c_adg	-309.9964762	-309.8289492	-309.8744822	-0.1352000
5	BuOH5c_adh	-309.9960664	-309.8285554	-309.8736374	-0.1352000
6	BuOH2b_aaw	-309.9964467	-309.8288517	-309.8740797	-0.1352000
7	BuOH1a_abc	-309.9974505	-309.8301055	-309.8763335	-0.1352000

8	BuOH3a_ada	-309.9970122	-309.8296292	-309.8750742	-0.1352000
9	BuOH8b_aam	-309.9968276	-309.8293906	-309.8757636	-0.1352000
10	BuOH14b_abm	-309.9946381	-309.8270701	-309.8722441	-0.1352000
11	BuOH6b_aae	-309.9964508	-309.8289828	-309.8753838	-0.1352000
12	BuOH3a_adj	-309.9961744	-309.8288314	-309.8741494	-0.1352000
13	BuOH4d_acp	-309.9960312	-309.8285962	-309.8760672	-0.1352000
14	BuOH1a_abz	-309.9966523	-309.8291493	-309.8742383	-0.1352000
15	BuOH1a_ace	-309.9967955	-309.8294785	-309.8755565	-0.1352000
16	BuOH6b_abo	-309.9946750	-309.8271040	-309.8723730	-0.1352000
17	BuOH1a_aax	-309.9972834	-309.8300654	-309.8764304	-0.1352000
18	BuOH3a_abm	-309.9960721	-309.8288101	-309.8759941	-0.1352000
19	BuOH7b_aaa	-309.9970394	-309.8295584	-309.8756884	-0.1352000
20	BuOH12c_adf	-309.9953929	-309.8278589	-309.8729219	-0.1352000
21	BuOH8b_aao	-309.9962148	-309.8287908	-309.8750538	-0.1352000
22	BuOH13c_abc	-309.9941976	-309.8267236	-309.8713116	-0.1352000
23	BuOH2b_acm	-309.9967208	-309.8292178	-309.8754998	-0.1352000
24	BuOH13c_aau	-309.9953702	-309.8278502	-309.8730872	-0.1352000
25	BuOH1a_aad	-309.9962363	-309.8289193	-309.8754083	-0.1352000
26	BuOH6b_aax	-309.9950519	-309.8274859	-309.8738479	-0.1352000
27	BuOH11d_aak	-309.9955359	-309.8280879	-309.8745099	-0.1352000
28	BuOH2b_abj	-309.9959646	-309.8284856	-309.8738496	-0.1352000
29	BuOH3a_aah	-309.9959427	-309.8286077	-309.8754867	-0.1352000
30	BuOH12c_abw	-309.9945697	-309.8268957	-309.8712187	-0.1352000
31	BuOH6b_acr	-309.9949945	-309.8273785	-309.8733335	-0.1352000
32	BuOH13c_aaa	-309.9935693	-309.8262863	-309.8724463	-0.1352000
33	BuOH12c_aba	-309.9947252	-309.8272952	-309.8724552	-0.1352000
34	BuOH3a_adm	-309.9964395	-309.8292005	-309.8775015	-0.1352000
35	BuOH10d_aar	-309.9959358	-309.8284498	-309.8748278	-0.1352000
36	BuOH10d_abi	-309.9960411	-309.8284701	-309.8744891	-0.1352000
37	BuOH4d_aaq	-309.9963561	-309.8291121	-309.8767831	-0.1352000
38	BuOH11d_aab	-309.9950290	-309.8275870	-309.8738990	-0.1352000
39	BuOH4d_adc	-309.9959938	-309.8286308	-309.8763028	-0.1352000
40	BuOH7b_aao	-309.9957847	-309.8284687	-309.8749617	-0.1352000
41	BuOH2b_adp	-309.9940505	-309.8266165	-309.8723255	-0.1352000
42	BuOH2b_abz	-309.9959013	-309.8284793	-309.8752853	-0.1352000
43	BuOH8b_aal	-309.9937432	-309.8262152	-309.8725232	-0.1352000
44	BuOH8b_aba	-309.9959631	-309.8285471	-309.8754381	-0.1352000
45	BuOH5c_ado	-309.9954624	-309.8279554	-309.8748814	-0.1352000
46	BuOH14b_adf	-309.9927999	-309.8252949	-309.8705679	-0.1352000
47	BuOH14b_aag	-309.9935167	-309.8260107	-309.8715687	-0.1352000
48	BuOH13c_aaz	-309.9937654	-309.8263434	-309.8729394	-0.1352000
49	BuOH12c_abm	-309.9936116	-309.8260796	-309.8718446	-0.1352000
50	BuOH14b_abi	-309.9923221	-309.8248111	-309.8701281	-0.1352000
51	BuOH6b_aai	-309.9955914	-309.8281284	-309.8752384	-0.1352000
52	BuOH10d_abd	-309.9947228	-309.8273788	-309.8738628	-0.1352000
53	BuOH10d_acf	-309.9947051	-309.8272911	-309.8738221	-0.1352000
54	BuOH10d_aab	-309.9947835	-309.8272835	-309.8743295	-0.1352000
55	BuOH11d_ada	-309.9924236	-309.8249476	-309.8717386	-0.1352000
56	BuOH12c_aas	-309.9926909	-309.8252909	-309.8706689	-0.1352000

57	BuOH14b_aar	-309.9938144	-309.8264584	-309.8732604	-0.1352000
MIN	tBuOH	-310.0112257	-309.8450937	-309.8888177	
1	t-BuOH_ads	-310.0112257	-309.8450937	-309.8888177	-0.1352000
2	t-BuOH_aar	-310.0102642	-309.8442532	-309.8881812	-0.1352000
3	t-BuOH_abx	-310.0073518	-309.8414258	-309.8867308	-0.1352000
MIN	PhCH2OH	-423.0592487	-422.8955737	-422.9434137	
1	PhCH2OH2_aam	-423.0592487	-422.8955737	-422.9434137	-0.1690000
2	PhCH2OH2_aae	-423.0585729	-422.8949549	-422.9427639	-0.1690000
3	PhCH2OH1_aae	-423.0569630	-422.8933140	-422.9411450	-0.1690000
4	PhCH2OH2_abc	-423.0569375	-422.8933615	-422.9421475	-0.1690000
5	PhCH2OH1_adg	-423.0546034	-422.8910974	-422.9391614	-0.1690000
MIN	PhC(CH3)2OH	-501.6703425	-501.4499335	-501.5027995	
1	PhCCH32OH1_abp	-501.6703425	-501.4499335	-501.5022595	-0.2095600
2	PhCCH32OH2_acf	-501.6700204	-501.4495774	-501.5027254	-0.2095600
3	PhCCH32OH1_acl	-501.6699595	-501.4495165	-501.5027995	-0.2095600
4	PhCCH32OH2_aaf	-501.6700307	-501.4496747	-501.5020307	-0.2095600
5	PhCCH32OH3_aae	-501.6694276	-501.4491186	-501.5010466	-0.2095600
6	PhCCH32OH1_abq	-501.6690618	-501.4486148	-501.5006008	-0.2095600
7	PhCCH32OH2_aan	-501.6693224	-501.4489324	-501.5019644	-0.2095600
8	PhCCH32OH1_aao	-501.6680803	-501.4477193	-501.5001633	-0.2095600
9	PhCCH32OH1_acb	-500.9808353	-500.7604663	-500.8129823	-0.2095600
10	PhCCH32OH3_ads	-501.6675441	-501.4475061	-501.5009481	-0.2095600
11	PhCCH32OH3_adt	-501.6672284	-501.4469604	-501.5008604	-0.2095600
12	PhCCH32OH3_abt	-501.6661968	-501.4458748	-501.4986478	-0.2095600
13	PhCCH32OH1_abv	-500.9799139	-500.7596689	-500.8123769	-0.2095600
MIN	PhOH	-383.7626171	-383.6285041	-383.6730841	
1	PhOH_aae	-383.7626171	-383.6285041	-383.6730841	-0.1487200
MIN	p-nitro-PhOH	-588.1890769	-588.0497839	-588.1010879	
1	p-nitro-PhOH_aai	-588.1890769	-588.0497839	-588.1010879	-0.2028000
MIN	p-methyl-PhOH	-423.0654797	-422.9029887	-422.9528898	
1	p-methyl-PhOH_aca	-423.0654728	-422.9029788	-422.9528898	-0.1690000
2	p-methyl-PhOH_aad	-423.0654797	-422.9029887	-422.9527807	-0.1690000
MIN	p-amino-PhOH	-439.1005950	-438.9490270	-438.9971440	
1	p-amino-PhOH_ach	-439.1005950	-438.9490270	-438.9971440	-0.1690000
MIN	HOOH	-227.9082240	-227.8514780	-227.8852070	
1	HOOH_aab	-227.9082240	-227.8514780	-227.8852070	-0.0743600
MIN	CH3OOH	-267.1927726	-267.1080006	-267.1478421	
1	CH3OOH_aam	-267.1927726	-267.1080006	-267.1473346	-0.0946400
2	CH3OOH_abj	-267.1925004	-267.1075094	-267.1471744	-0.0946400
3	CH3OOH_adl	-267.1918371	-267.1072191	-267.1478421	-0.0946400
MIN	t-BuOOH	-385.1089389	-384.9385929	-384.9862339	
1	t-BuOOH_acm	-385.1089389	-384.9385929	-384.9862339	-0.1554800
MIN	PhCH2OOH	-498.1604493	-497.9924913	-498.0425873	
1	PhCH2OOH2_aan	-498.1604493	-497.9924913	-498.0425873	-0.1892800
2	PhCH2OOH2_abr	-498.1583463	-497.9905153	-498.0406203	-0.1892800
3	PhCH2OOH3_aah	-498.1578201	-497.9900211	-498.0404041	-0.1892800
4	PhCH2OOH3_aae	-498.1566962	-497.9889442	-498.0393752	-0.1892800
5	PhCH2OOH3_abg	-498.1575673	-497.9899103	-498.0408133	-0.1892800
MIN	TEMPOH	-560.5853835	-560.2797865	-560.3366685	

1	TEMPOH_aah	-560.5850558	-560.2796128	-560.3363728	-0.2501200
2	TEMPOH_aag	-560.5847324	-560.2791874	-560.3358144	-0.2501200
3	TEMPOH_adl	-560.5853835	-560.2797865	-560.3366685	-0.2501200
4	TEMPOHa_add	-560.5808500	-560.2756330	-560.3330780	-0.2501200
5	TEMPOHa_aaw	-560.5802631	-560.2751081	-560.3336531	-0.2501200
MIN	HCO2H	-266.1023908	-266.0391758	-266.0770668	
1	HCO2Ha_aab	-266.1023908	-266.0391758	-266.0770668	-0.0878800

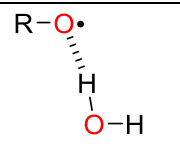
Table S3.4.24. Calculated energies. Individual selected conformers.

No		G3B3-D3			DE(HLC)
		E _{tot}	H ₂₉₈	G ₂₉₈	
MIN	HOH	-152.8139511	-152.7627571	-152.7955861	
1	HOH_aaa	-152.8139511	-152.7627571	-152.7955861	-0.0540800
2	HOH_aaq	-152.8134637	-152.7623797	-152.7953567	-0.0540800
MIN	CH3OH	-192.0920172	-192.0116942	-192.0505752	
1	CH3OH_aai	-192.0917888	-192.0111698	-192.0486688	-0.0743600
2	CH3OH_aby	-192.0920172	-192.0116942	-192.0505752	-0.0743600
3	CH3OH_aab	-192.0909951	-192.0105231	-192.0484021	-0.0743600
MIN	CH3CH2OH	-231.3960055	-231.2868775	-231.3290775	
1	CH3CH2OH1_aan	-231.3959147	-231.2864257	-231.3264157	-0.0946400
2	CH3CH2OH1_abb	-231.3957584	-231.2864954	-231.3264944	-0.0946400
3	CH3CH2OH1_aai	-231.3958153	-231.2863623	-231.3274383	-0.0946400
4	CH3CH2OH2_aan	-231.3960055	-231.2868775	-231.3290775	-0.0946400
5	CH3CH2OH2_aar	-231.3948867	-231.2856197	-231.3270717	-0.0946400
MIN	BuOH	-309.9953308	-309.8280738	-309.8764100	
1	BuOH13c_acf	-309.9940603	-309.8266503	-309.8722963	-0.1352000
2	BuOH1a_ads	-309.9951931	-309.8279971	-309.8741371	-0.1352000
3	BuOH3a_aar	-309.9940836	-309.8268466	-309.8731466	-0.1352000
4	BuOH13c_abh	-309.9927020	-309.8253630	-309.8705220	-0.1352000
5	BuOH1a_adh	-309.9953308	-309.8280738	-309.8743078	-0.1352000
6	BuOH6b_abc	-309.9949594	-309.8275654	-309.8729074	-0.1352000
7	BuOH2b_adi	-309.9949229	-309.8274959	-309.8733369	-0.1352000
8	BuOH5c_adn	-309.9941650	-309.8267870	-309.8731880	-0.1352000
9	BuOH5c_abp	-309.9939119	-309.8265339	-309.8731899	-0.1352000
10	BuOH3a_abi	-309.9944584	-309.8271614	-309.8757674	-0.1352000
11	BuOH14b_aaj	-309.9922457	-309.8248537	-309.8697187	-0.1352000
12	BuOH14b_abp	-309.993592	-309.8261302	-309.8716242	-0.1352000
13	BuOH8b_abi	-309.9943967	-309.8270077	-309.8743467	-0.1352000
14	BuOH5c_aca	-309.9940346	-309.8265636	-309.8750906	-0.1352000
15	BuOH1a_abi	-309.9934383	-309.8262693	-309.8742023	-0.1352000
16	BuOH11d_aar	-309.9929427	-309.8256637	-309.8728527	-0.1352000
17	BuOH11d_aap	-309.9932018	-309.8257218	-309.8729358	-0.1352000
18	BuOH11d_acr	-309.9929502	-309.8257462	-309.8731122	-0.1352000
19	BuOH11d_aaw	-309.9927643	-309.8254873	-309.8729233	-0.1352000

20	BuOH7b_abs	-309.9940910	-309.8270960	-309.8764100	-0.1352000
21	BuOH7b_adg	-309.9940178	-309.8270018	-309.8762288	-0.1352000
22	BuOH2b_acw	-309.9938170	-309.8263510	-309.8747630	-0.1352000
23	BuOH7b_aag	-309.9935854	-309.8264864	-309.8752344	-0.1352000
24	BuOH7b_aat	-309.9929290	-309.8257540	-309.8740480	-0.1352000
25	BuOH11d_adr	-309.9929170	-309.8255150	-309.8741110	-0.1352000
26	BuOH12c_acg	-309.9920393	-309.8248023	-309.8732233	-0.1352000
27	BuOH12c_aco	-309.9912925	-309.8241585	-309.8725525	-0.1352000
28	BuOH12c_aay	-309.9921730	-309.8248770	-309.8732910	-0.1352000
29	BuOH10d_acv	-309.9930156	-309.8259236	-309.8747886	-0.1352000
30	BuOH10d_aae	-309.9918373	-309.8245523	-309.8726083	-0.1352000
MIN	tBuOH	-310.0079289	-309.8420229	-309.8881909	
1	t-BuOH_aap	-310.0079289	-309.8420229	-309.8881909	-0.1352000
2	t-BuOH_aaa	-310.0075385	-309.8418445	-309.8875105	-0.1352000
MIN	PhCH2OH	-423.0593217	-422.8956457	-422.9449025	
1	PhCH2OH2_abd	-423.0593217	-422.8956457	-422.9428007	-0.1690000
2	PhCH2OH1_abq	-423.0562185	-422.8931625	-422.9449025	-0.1690000
3	PhCH2OH1_aar	-423.0544135	-422.8913875	-422.9428905	-0.1690000
MIN	PhC(CH3)2OH	-501.6717311	-501.4515381	-501.5048779	
1	PhCCH32OH1_adc	-501.6714059	-501.4512049	-501.5048779	-0.2095600
2	PhCCH32OH1_aci	-501.6711315	-501.4507405	-501.5030095	-0.2095600
3	PhCCH32OH2_adc	-501.6717311	-501.4515381	-501.5046721	-0.2095600
4	PhCCH32OH3_aah	-501.6681223	-501.4481133	-501.5036293	-0.2095600
5	PhCCH32OH3_acq	-501.6667593	-501.4468073	-501.5008663	-0.2095600
MIN	PhOH	-383.7669725	-383.6328535	-383.6789295	
1	PhOH_abt	-383.7652314	-383.6310204	-383.6755944	-0.1487200
2	PhOH_act	-383.7669725	-383.6328535	-383.6789295	-0.1487200
3	PhOH_abu	-383.7655713	-383.6313283	-383.6757773	-0.1487200
MIN	p-nitro-PhOH	-588.1966054	-588.0571004	-588.1085504	
1	p-nitro-PhOH_aae	-588.1966054	-588.0571004	-588.1085504	-0.2028000
2	p-nitro-PhOH_aab	-588.1948240	-588.0553260	-588.1064230	-0.2028000
MIN	p-methyl-PhOH	-423.0694455	-422.9068925	-422.9581645	
1	p-methyl-PhOH_aay	-423.0694455	-422.9068925	-422.9581645	-0.1690000
2	p-methyl-PhOH_abt	-423.0677270	-422.9050790	-422.9549250	-0.1690000
3	p-methyl-PhOH_adp	-423.0679566	-422.9053066	-422.9549156	-0.1690000
MIN	p-amino-PhOH	-439.1026238	-438.9508818	-438.9985636	
1	p-amino-PhOH_aab	-439.1026238	-438.9508818	-438.9982138	-0.1690000
2	p-amino-PhOH_aau	-439.1023231	-438.9505991	-438.9980121	-0.1690000
3	p-amino-PhOH_aaa	-439.1021106	-438.9504096	-438.9985636	-0.1690000
MIN	HOOH	-227.9082240	-227.8514780	-227.8852070	
1	HOOH_aab	-227.9082240	-227.8514780	-227.8852070	-0.0743600
MIN	CH3OOH	-267.1975684	-267.1122364	-267.1499494	
1	CH3OOH_aaq	-267.1975684	-267.1122364	-267.1499494	-0.0946400
2	CH3OOH_aaf	-267.1966106	-267.1114016	-267.1493486	-0.0946400
MIN	t-BuOOH	-385.1142760	-384.9434300	-384.9895810	
1	t-BuOOH_acs	-385.1142760	-384.9434300	-384.9895810	-0.1554800
2	t-BuOOH_acv	-385.1128137	-384.9420727	-384.9883837	-0.1554800
MIN	PhCH2OOH	-498.1649393	-497.9965503	-498.0448713	
1	PhCH2OOH2_aai	-498.1649393	-497.9965503	-498.0448713	-0.1892800

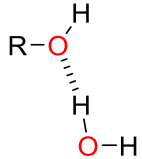
2	PhCH2OOH1_abr	-498.1617306	-497.9934146	-498.0429206	-0.1892800
3	PhCH2OOH2_aav	-498.1588279	-497.9908399	-498.0410159	-0.1892800
4	PhCH2OOH3_aan	-498.1601433	-497.9921423	-498.0429943	-0.1892800
5	PhCH2OOH1_adh	-498.1600304	-497.9919994	-498.0433974	-0.1892800
6	PhCH2OOH3_abv	-498.1592267	-497.9913407	-498.0424737	-0.1892800
7	PhCH2OOH3_abh	-498.1570598	-497.9893658	-498.0395718	-0.1892800
MIN	TEMPOH	-560.5925399	-560.2864389	-560.3410489	
1	TEMPOH_ach	-560.5925399	-560.2864389	-560.3410489	-0.2501200
2	TEMPOHa_abr	-560.5791991	-560.2741911	-560.3322351	-0.2501200
MIN	HOO•	-227.2617016	-227.2169926	-227.2500566	
1	HOO_aaa	-227.2617016	-227.2169926	-227.2500566	-0.0708330
MIN	HCO2H	-266.1133819	-266.0494709	-266.0838399	
1	HCO2Ha_aan	-266.1133819	-266.0494709	-266.0838399	-0.0878800
2	HCO2Hb_aad	-266.1043132	-266.0410792	-266.0794462	-0.0878800
3	HCO2Hb_aab	-266.1029124	-266.0397124	-266.0777404	-0.0878800

Table S3.4.25. Calculated energies. Individual selected conformers.

№		(U)B3LYP-D3/6-31+G(d,p)		
		E _{tot}	H ₂₉₈	G ₂₉₈
MIN	HO• (1a_2)	-152.1803707	-152.1418317	-152.1758067
1	HO_aab (1a_2)	-152.1803707	-152.1418317	-152.1758067
MIN	CH3O•	-191.5078593	-191.4397733	-191.4769883
1	CH3O1_aab	-191.5078593	-191.4397733	-191.4769883
MIN	CH3CH2O•	-230.8339204	-230.7361309	-230.7774889
1	CH3CH2O1_aah	-230.8337179	-230.7361309	-230.7774889
2	CH3CH2O1_aac	-230.8339204	-230.7359744	-230.7762974
3	CH3CH2O1_acm	-230.8333250	-230.7345190	-230.7743110
MIN	BuO•	-309.4755335	-309.3177405	-309.3652302
1	BuO2_acz	-309.4754105	-309.3177405	-309.3639755
2	BuO3_adb	-309.4755335	-309.3176655	-309.3628325
3	BuO2_aal	-309.4741572	-309.3168312	-309.3652302
4	BuO1_abu	-309.4741098	-309.3163738	-309.3638068
5	BuO4_abu	-309.4739092	-309.3162202	-309.3626342
6	BuO3_aay	-309.4739490	-309.3161860	-309.3638530
7	BuO4_aap	-309.4733220	-309.3158440	-309.3641620
8	BuO1_aab	-309.4745544	-309.3157644	-309.3624794
9	BuO4_act	-309.4732997	-309.3156577	-309.3625107
10	BuO4_acc	-309.4741205	-309.3155425	-309.3616005
11	BuO3_aao	-309.4738983	-309.3155243	-309.3615113
12	BuO5_aak	-309.4740568	-309.3153208	-309.3617828
13	BuO2_acl	-309.4738593	-309.3153103	-309.3621633
14	BuO5_abp	-309.4729077	-309.3152577	-309.3630507
15	BuO4_aar	-309.4734705	-309.3148995	-309.3614435
16	BuO5_abt	-309.4735974	-309.3148274	-309.3617224
MIN	tBuO•	-309.4854393	-309.3279283	-309.3728993
1	t-BuO2_aaw	-309.4854393	-309.3279283	-309.3728993

MIN	PhCH2O•	-422.5878221	-422.4329678	-422.4828748
1	PhCH2O2_aah	-422.5865078	-422.4329678	-422.4828748
2	PhCH2O3_aaj	-422.5878221	-422.4322011	-422.4796251
3	PhCH2O2_acc	-422.5859053	-422.4320943	-422.4823983
4	PhCH2O2_aaw	-422.5853425	-422.4316515	-422.4809345
MIN	PhC(CH3)2O•	-501.2368645	-501.0229939	-501.0766059
1	PhCCH32O2_a_aau	-501.2366629	-501.0229939	-501.0766059
2	PhCCH32O2_a_aam	-501.2368645	-501.0225675	-501.0748935
3	PhCCH32O3_acx	-501.2354193	-501.0216423	-501.0749403
4	PhCCH32O2_a_abh	-501.2345706	-501.0208196	-501.0748476
5	PhCCH32O3_abq	-501.2344181	-501.0207631	-501.0754011
6	PhCCH32O2_a_ads	-501.2343904	-501.0203694	-501.0735924
MIN	PhO•	-383.3042402	-383.1787062	-383.2233942
1	PhO_ace	-383.3042402	-383.1787062	-383.2233942
MIN	p-nitro-PhO•	-587.8111909	-587.6809379	-587.7327549
1	p-nitro-PhO_aac	-587.8111909	-587.6809379	-587.7327549
MIN	p-methyl-PhO•	-422.6308106	-422.4760046	-422.5258676
1	p-methyl-PhO_aak	-422.6308106	-422.4760046	-422.5258676
MIN	p-amino-PhO•	-438.6815915	-438.5375305	-438.5864275
1	p-amino-PhO_abh	-438.6815915	-438.5375305	-438.5864275
MIN	HOO•	-227.3673314	-227.3213374	-227.3579179
1	HOO_aae	-227.3673314	-227.3213374	-227.3552984
2	HOO_aag	-227.3561194	-227.3107414	-227.3487464
3	HOO_adq	-227.3663789	-227.3205959	-227.3579179
MIN	CH3OO•	-266.6761922	-266.6008622	-266.6406838
1	CH3OO_adp	-266.6761922	-266.6008622	-266.6405222
2	CH3OO_aay	-266.6737808	-266.5985968	-266.6406838
3	CH3OO_aal	-266.6737601	-266.5985661	-266.6405381
MIN	t-BuOO•	-384.6542691	-384.4909071	-384.5403479
1	t-BuOO_acq	-384.6542691	-384.4909071	-384.5385191
2	t-BuOO_aao	-384.6526906	-384.4894716	-384.5399576
3	t-BuOO_aad	-384.6525289	-384.4893629	-384.5403479
MIN	PhCH2OO•	-497.7556124	-497.5943754	-497.6452677
1	PhCH2OO2_adm	-497.7556124	-497.5943754	-497.6445764
2	PhCH2OO1_aae	-497.7536627	-497.5926197	-497.6449277
3	PhCH2OO2_adu	-497.7524067	-497.5916327	-497.6445787
4	PhCH2OO1_aaw	-497.7514360	-497.5905110	-497.6448980
5	PhCH2OO2_acs	-497.7512817	-497.5903167	-497.6446577
6	PhCH2OO1_aap	-497.7510737	-497.5901957	-497.6452677
MIN	TEMPO•	-560.2400591	-559.9369001	-559.9939151
1	TEMPO_ace	-560.2400591	-559.9369001	-559.9939151
2	TEMPO_aab	-560.2396722	-559.9365182	-559.9933102
3	TEMPO_acg	-560.2394436	-559.9363246	-559.9936096
MIN	•OO•	-226.7633108	-226.7296668	-226.7692103
1	3O2_aai	-226.7633108	-226.7296668	-226.7691958
2	3O2_aaa	-226.7632984	-226.7296484	-226.7687634
3	3O2_aam	-226.7632623	-226.7296103	-226.7692103
MIN	HCO2•	-265.5374856	-265.4861126	-265.5207356
1	HCO2_acr	-265.5374856	-265.4861126	-265.5207356

Table S3.4.26. Calculated energies. Individual selected conformers.

No	Conformer 	(U)B3LYP-D3/6-31+G(d,p)		
		E _{tot}	H ₂₉₈	G ₂₉₈
MIN	HOH (1Ha)	-152.8788957	-152.8258677	-152.8583797
1	HOH_aaa (1Ha)	-152.8788957	-152.8258677	-152.8583797
MIN	CH3OH	-192.1818168	-192.0983958	-192.1354398
1	CH3OH_aap	-192.1818168	-192.0983958	-192.1354398
MIN	CH3CH2OH	-231.5081012	-231.3949692	-231.4346502
1	CH3CH2OH1_adi	-231.5081012	-231.3949692	-231.4341282
2	CH3CH2OH2_abj	-231.5077721	-231.3946761	-231.4345261
3	CH3CH2OH1_aaf	-231.5071262	-231.3940902	-231.4346502
MIN	BuOH	-310.1485136	-309.9755826	-310.0224252
1	BuOH4d_aae	-310.1485136	-309.9755826	-310.0222126
2	BuOH3a_ada	-310.1481396	-309.9754066	-310.0219756
3	BuOH5c_aap	-310.1482212	-309.9752952	-310.0207392
4	BuOH8b_aas	-310.1481201	-309.9752291	-310.0217871
5	BuOH1a_abs	-310.1479892	-309.9752202	-310.0224252
6	BuOH7b_aam	-310.1476566	-309.9747616	-310.0216716
7	BuOH6b_aax	-310.1475060	-309.9745080	-310.0207460
8	BuOH1a_adi	-310.1471886	-309.9744106	-310.0211246
9	BuOH4d_aag	-310.1471581	-309.9743051	-310.0217251
10	BuOH2b_ada	-310.1471786	-309.9742896	-310.0213696
11	BuOH8b_abv	-310.1470356	-309.9742156	-310.0222346
12	BuOH3a_adl	-310.1467172	-309.9741702	-310.0219982
13	BuOH2b_ade	-310.1471109	-309.9741439	-310.0199449
14	BuOH9b_abb	-310.1471429	-309.9741099	-310.0203599
15	BuOH11d_aab	-310.1468974	-309.9739604	-310.0204954
16	BuOH5c_abn	-310.1464907	-309.9736617	-310.0216247
17	BuOH10d_acr	-310.1465335	-309.9735705	-310.0204905
18	BuOH14b_aah	-310.1463391	-309.9734341	-310.0187601
19	BuOH6b_aaf	-310.1463049	-309.9734119	-310.0210329
20	BuOH12c_acs	-310.1462615	-309.9733625	-310.0195335
21	BuOH13c_aau	-310.1460611	-309.9732861	-310.0194741
22	BuOH9b_abv	-310.1460831	-309.9731471	-310.0208251
23	BuOH11d_aai	-310.1459275	-309.9730015	-310.0206455
24	BuOH13c_abd	-310.1452507	-309.9725727	-310.0210757
25	BuOH12c_abd	-310.1451852	-309.9722512	-310.0178382
26	BuOH14b_aaa	-310.1448359	-309.9719919	-310.0192569
MIN	tBuOH	-310.1600504	-309.9886454	-310.0331904
1	t-BuOH_acj	-310.1600504	-309.9886454	-310.0331904
MIN	PhCH2OH	-423.2624712	-423.0931452	-423.1410682
1	PhCH2OH2_aae	-423.2624712	-423.0931452	-423.1406522
2	PhCH2OH2_aaa	-423.2598772	-423.0907282	-423.1410682

3	PhCH2OH1_aad	-423.2595190	-423.0903240	-423.1384540
4	PhCH2OH1_adk	-423.2593230	-423.0902280	-423.1390810
5	PhCH2OH2_aca	-423.2333044	-423.0734624	-423.1277024
MIN	PhC(CH3)2OH	-501.9114064	-501.6837214	-501.7365260
1	PhCCH32OH1_abo	-501.9114064	-501.6837214	-501.7364754
2	PhCCH32OH1_abf	-501.9109790	-501.6832760	-501.7365260
3	PhCCH32OH3_abn	-501.9099818	-501.6824948	-501.7353678
4	PhCCH32OH1_ack	-501.9095178	-501.6820088	-501.7351898
5	PhCCH32OH1_aal	-501.9082154	-501.6805144	-501.7329314
6	PhCCH32OH1_adj	-501.9077085	-501.6801595	-501.7334465
7	PhCCH32OH3_abt	-501.9077358	-501.6800828	-501.7328938
MIN	PhOH	-383.9441927	-383.8055687	-383.8511607
1	PhOH_aab	-383.9441927	-383.8055687	-383.8511607
MIN	p-nitro-PhOH	-588.4586379	-588.3149519	-588.3669089
1	p-nitro-PhOH_aak	-588.4586379	-588.3149519	-588.3669089
MIN	p-methyl-PhOH	-423.2672077	-423.0994177	-423.1505107
1	p-methyl-PhOH_aac	-423.2672077	-423.0994177	-423.1505107
MIN	p-amino-PhOH	-439.3061128	-439.1494888	-439.1986658
1	p-amino-PhOH_adq	-439.3061128	-439.1494888	-439.1986658
2	p-amino-PhOH_adf	-439.3060507	-439.1494237	-439.1985517
MIN	HOOH	-228.0071774	-227.9486274	-227.9831884
1	HOOH_aam	-228.0071774	-227.9486274	-227.9831884
2	HOOH_acd	-228.0016627	-227.9434277	-227.9808447
3	HOOH_acf	-228.0063729	-227.9479129	-227.9827669
4	HOOH_acn	-228.0016418	-227.9434228	-227.9810958
MIN	CH3OOH	-267.3160354	-267.2285244	-267.2694834
1	CH3OOH_aax	-267.3160354	-267.2285244	-267.2694834
2	CH3OOH_acq	-267.3154339	-267.2279209	-267.2677959
3	CH3OOH_aau	-267.3152490	-267.2276890	-267.2679500
MIN	t-BuOOH	-385.2912534	-385.1156534	-385.1651574
1	t-BuOOH_aby	-385.2911434	-385.1156534	-385.1651574
2	t-BuOOH_adj	-385.2912534	-385.1156264	-385.1639684
MIN	PhCH2OOH	-498.3973609	-498.2237399	-498.2745490
1	PhCH2OOH2_aag	-498.3973609	-498.2237399	-498.2736039
2	PhCH2OOH3_abi	-498.3953730	-498.2220250	-498.2732340
3	PhCH2OOH2_aai	-498.3937600	-498.2204550	-498.2745490
4	PhCH2OOH3_aae	-498.3930040	-498.2197630	-498.2711130
5	PhCH2OOH1_acj	-498.3923173	-498.2190423	-498.2719703
MIN	TEMPOH	-560.8529015	-560.5378095	-560.5946146
1	TEMPOHa_abx	-560.8529015	-560.5378095	-560.5935355
2	TEMPOH_aab	-560.8514646	-560.5365226	-560.5946146
3	TEMPOH_aba	-560.8514390	-560.5362450	-560.5941360
4	TEMPOHa_ade	-560.8470410	-560.5323580	-560.5911660
1	HCO2Ha_aaa	-266.2180769	-266.1528269	-266.1915219
2	HCO2Hb_aap	-266.2118439	-266.1467599	-266.1854919

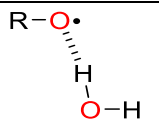
Table S3.4.27. Calculated energies. Individual selected conformers.

No	(U)B3LYP-D3/6-31+G(d,p)
----	-------------------------

		E _{tot}	H ₂₉₈	G ₂₉₈
MIN	HOH (1Ha)	-152.8788957	-152.8258677	-152.8583797
1	HOH_aaa (1Ha)	-152.8788957	-152.8258677	-152.8583797
MIN	CH ₃ OH	-192.1806009	-192.0973579	-192.1356679
1	CH ₃ OH_aad	-192.1806009	-192.0973579	-192.1356679
MIN	CH ₃ CH ₂ OH	-231.5057597	-231.3928417	-231.4348052
1	CH ₃ CH ₂ OH1_adc	-231.5057597	-231.3928417	-231.4345447
2	CH ₃ CH ₂ OH2_aac	-231.5055962	-231.3927152	-231.4348052
MIN	BuOH	-310.1460146	-309.9733856	-310.0225041
1	BuOH4d_aam	-310.1460146	-309.9733856	-310.0204646
2	BuOH4d_aan	-310.1458135	-309.9732155	-310.0199015
3	BuOH3a_abg	-310.1457401	-309.9731791	-310.0225041
4	BuOH1a_abw	-310.1456670	-309.9730840	-310.0211910
5	BuOH4d_aaj	-310.1457031	-309.9730681	-310.0211031
6	BuOH6b_aaj	-310.1457266	-309.9729256	-310.0192076
7	BuOH6b_aco	-310.1454734	-309.9727474	-310.0187914
8	BuOH7b_aac	-310.1452882	-309.9726582	-310.0218062
9	BuOH5c_aai	-310.1451066	-309.9723796	-310.0209866
10	BuOH2b_aad	-310.1449048	-309.9721828	-310.0211958
11	BuOH13c_aay	-310.1447026	-309.9719996	-310.0182506
12	BuOH9b_abm	-310.1445683	-309.9717783	-310.0202143
13	BuOH11d_aag	-310.1443988	-309.9716568	-310.0205268
14	BuOH10d_ace	-310.1441468	-309.9714628	-310.0200078
15	BuOH14b_abp	-310.1438578	-309.9711038	-310.0167318
16	BuOH12c_aay	-310.1436168	-309.9710228	-310.0197468
17	BuOH14b_aad	-310.1426844	-309.9700614	-310.0179524
MIN	tBuOH	-310.1568402	-309.9856822	-310.0328412
1	t-BuOH_abj	-310.1568402	-309.9856822	-310.0328412
MIN	PhCH ₂ OH	-423.2622649	-423.0931739	-423.1413889
1	PhCH ₂ OH2_abt	-423.2622649	-423.0931739	-423.1413889
2	PhCH ₂ OH2_acy	-423.2619349	-423.0928519	-423.1409129
3	PhCH ₂ OH1_aaw	-423.2576000	-423.0887560	-423.1403290
MIN	PhC(CH ₃) ₂ OH	-501.9117965	-501.6843555	-501.7378077
1	PhCCH ₃ OH2_abp	-501.9117965	-501.6843555	-501.7377925
2	PhCCH ₃ OH1_adt	-501.9117847	-501.6842417	-501.7378077
3	PhCCH ₃ OH2_act	-501.9113477	-501.6839507	-501.7373657
4	PhCCH ₃ OH3_aah	-501.9080685	-501.6807175	-501.7363955
MIN	PhOH	-383.9485501	-383.8096111	-383.8549621
1	PhOH_abf	-383.9485501	-383.8096111	-383.8549621
MIN	p-nitro-PhOH	-588.4669965	-588.3227945	-588.3736785
1	p-nitro-PhOH_aab	-588.4669965	-588.3227945	-588.3736785
MIN	p-methyl-PhOH	-423.2710744	-423.1029364	-423.1534904
1	p-methyl-PhOH_aax	-423.2710744	-423.1029364	-423.1534904
MIN	p-amino-PhOH	-439.3090547	-439.1520897	-439.2007237

1	p-amino-PhOH_abd	-439.3090547	-439.1520897	-439.2007237
2	p-amino-PhOH_aab	-439.2698179	-439.1116649	-439.1539019
MIN	HOOH	-228.0071774	-227.9486274	-227.9831884
1	HOOH_aam	-228.0071774	-227.9486274	-227.9831884
2	HOOH_acf	-228.0063729	-227.9479129	-227.9827669
MIN	CH3OOH	-267.3199916	-267.2321836	-267.2707406
1	CH3OOH_aac	-267.3199916	-267.2321836	-267.2707406
2	CH3OOH_aci	-267.3190828	-267.2313568	-267.2704078
MIN	t-BuOOH	-385.2963238	-385.1204028	-385.1670718
1	t-BuOOH_aav	-385.2963238	-385.1204028	-385.1670718
2	t-BuOOH_ace	-385.2949870	-385.1192420	-385.1665140
MIN	PhCH2OOH	-498.4013947	-498.2275437	-498.2771307
1	PhCH2OOH2_acb	-498.4013947	-498.2275437	-498.2771307
2	PhCH2OOH2_aak	-498.4008168	-498.2270908	-498.2768988
3	PhCH2OOH1_acd	-498.3978303	-498.2242093	-498.2754443
4	PhCH2OOH1_aar	-498.3963760	-498.2228730	-498.2742700
5	PhCH2OOH3_adj	-498.3960192	-498.2226332	-498.2740592
6	PhCH2OOH3_acq	-498.3960151	-498.2224901	-498.2737491
7	PhCH2OOH3_aad	-498.3951751	-498.2218671	-498.2736591
MIN	TEMPOH	-560.8586666	-560.5429816	-560.5973646
1	TEMPOH_aaq	-560.8586666	-560.5429816	-560.5973646
2	TEMPOHa_abd	-560.8450804	-560.5304954	-560.5889814
MIN	HOO•	-227.3673314	-227.3213374	-227.3579179
1	HOO_aae	-227.3673314	-227.3213374	-227.3552984
2	HOO_adq	-227.3663789	-227.3205959	-227.3579179
MIN	HCO2H	-266.2302275	-266.1644195	-266.1993165
1	HCO2Ha_acd	-266.2302275	-266.1644195	-266.1993165
2	HCO2Hb_aab	-266.2192902	-266.1538732	-266.1920022

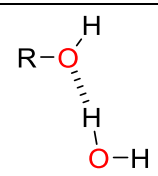
Table S3.4.28. Calculated energies. Individual selected conformers.

№		DLPNO-CCSD(T)/cc-pVTZ// (U)B3LYP-D3/6-31+G(d,p)				DLPNO-CCSD(T)/cc-pVQZ// (U)B3LYP-D3/6-31+G(d,p)				DLPNO-CCSD(T)/CBS// (U)B3LYP-D3/6-31+G(d,p)		
		E _{tot}	H ₂₉₈	G ₂₉₈	<S ² >	E _{tot}	H ₂₉₈	G ₂₉₈	<S ² >	E _{tot}	H ₂₉₈	G ₂₉₈
MIN	HO• (1a_2)	-151.9757359	-151.9371969	-151.9711719		-152.0264294	-151.9878904	-152.0218654		-152.0569529	-152.0184139	-152.0523889
2	HO_aab (1a_2)	-151.9757359	-151.9371969	-151.9711719	0.7565	-152.0264294	-151.9878904	-152.0218654	0.7570	-152.0569529	-152.0184139	-152.0523889
MIN	CH3O•	-191.2148530	-191.1467670	-191.1839820		-191.2769642	-191.2088782	-191.2460932		-191.3147506	-191.2466646	-191.2838796
1	CH3O1_aab	-191.2148530	-191.1467670	-191.1839820	0.7599	-191.2769642	-191.2088782	-191.2460932	0.7603	-191.3147506	-191.2466646	-191.2838796
MIN	CH3CH2O•	-230.4591874	-230.3612794	-230.4026374		-230.5325112	-230.4348874	-230.4762454		-230.5774931	-230.4799053	-230.5212633
1	CH3CH2O1_aah	-230.4588664	-230.3612794	-230.4026374	0.7602	-230.5324744	-230.4348874	-230.4762454	0.7606	-230.5774923	-230.4799053	-230.5212633
2	CH3CH2O1_aac	-230.4590022	-230.3610562	-230.4013792	0.7601	-230.5325085	-230.4345625	-230.4748855	0.7605	-230.5774931	-230.4795471	-230.5198701
3	CH3CH2O1_acm	-230.4591874	-230.3603814	-230.4001734	0.7601	-230.5325112	-230.4337052	-230.4734972	0.7605	-230.5774105	-230.4786045	-230.5183965
MIN	BuO•	-308.9394218	-308.7817518	-308.8291523		-309.0357341	-308.8780641	-308.9257413		-309.0951137	-308.9374437	-308.9852008
1	BuO2_acz	-308.9394218	-308.7817518	-308.8279868	0.7602	-309.0357341	-308.8780641	-308.9242991	0.7606	-309.0951137	-308.9374437	-308.9836787
2	BuO3_adb	-308.9388118	-308.7809438	-308.8261108	0.7604	-309.0349102	-308.8770422	-308.9222092	0.7608	-309.0941984	-308.9363304	-308.9814974
3	BuO2_aal	-308.9380793	-308.7807533	-308.8291523	0.7602	-309.0346683	-308.8773423	-308.9257413	0.7606	-309.0941278	-308.9368018	-308.9852008
4	BuO1_abu	-308.9377818	-308.7800458	-308.8274788	0.7601	-309.0343653	-308.8766293	-308.9240623	0.7606	-309.0938198	-308.9360838	-308.9835168
5	BuO4_abu	-308.9378445	-308.7801555	-308.8265695	0.7602	-309.0342211	-308.8765321	-308.9229461	0.7606	-309.0936213	-308.9359323	-308.9823463

6	BuO3_aay	-308.9377405	-308.7799775	-308.8276445	0.7602	-309.0340177	-308.8762547	-308.9239217	0.7607	-309.0933587	-308.9355957	-308.9832627
7	BuO4_aap	-308.9372957	-308.7798177	-308.8281357	0.7602	-309.0338128	-308.8763348	-308.9246528	0.7607	-309.0932341	-308.9357561	-308.9840741
8	BuO1_aab	-308.9383738	-308.7795838	-308.8262988	0.7607	-309.0348528	-308.8760628	-308.9227778	0.7611	-309.0942795	-308.9354895	-308.9822045
9	BuO4_act	-308.9377411	-308.7800991	-308.8269521	0.7600	-309.0338535	-308.8762115	-308.9230645	0.7604	-309.0931232	-308.9354812	-308.9823342
10	BuO4_acc	-308.9376950	-308.7791170	-308.8251750	0.7610	-309.0339740	-308.8753960	-308.9214540	0.7614	-309.0933256	-308.9347476	-308.9808056
11	BuO3_aao	-308.9375812	-308.7792072	-308.8251942	0.7612	-309.0336444	-308.8752704	-308.9212574	0.7616	-309.0929108	-308.9345368	-308.9805238
12	BuO5_aak	-308.9377092	-308.7789732	-308.8254352	0.7607	-309.0340793	-308.8753433	-308.9218053	0.7611	-309.0934402	-308.9347042	-308.9811662
13	BuO2_acl	-308.9377993	-308.7792503	-308.8261033	0.7609	-309.0341591	-308.8756101	-308.9224631	0.7613	-309.0935102	-308.9349612	-308.9818142
14	BuO5_abp	-308.9366561	-308.7790061	-308.8267991	0.7601	-309.0333646	-308.8757146	-308.9235076	0.7606	-309.0928679	-308.9352179	-308.9830109
15	BuO4_aar	-308.9373283	-308.7787573	-308.8253013	0.7611	-309.0336385	-308.8750675	-308.9216115	0.7615	-309.0929806	-308.9344096	-308.9809536
16	BuO5_abt	-308.9372698	-308.7784998	-308.8253948	0.7608	-309.0337355	-308.8749655	-308.9218605	0.7613	-309.0931544	-308.9343844	-308.9812794
MIN	tBuO•	-308.9498819	-308.7923709	-308.8373419		-309.0461061	-308.8885951	-308.9335661		-309.1054728	-308.9479618	-308.9929328
1	t-BuO2_aaw	-308.9498819	-308.7923709	-308.8373419	0.7599	-309.0461061	-308.8885951	-308.9335661	0.7603	-309.1054728	-308.9479618	-308.9929328
MIN	PhCH2O•	-421.8296737	-421.6750180	-421.7249250		-421.9555656	-421.8012743	-421.8511813		-422.0333897	-421.8792789	-421.9291859
1	PhCH2O2_aah	-421.8285580	-421.6750180	-421.7249250	0.7610	-421.9548143	-421.8012743	-421.8511813	0.7614	-422.0328189	-421.8792789	-421.9291859
2	PhCH2O3_aaj	-421.8296737	-421.6740527	-421.7214767	1.2549	-421.9555656	-421.7999446	-421.8473686	1.2540	-422.0333897	-421.8777687	-421.9251927
3	PhCH2O2_acc	-421.8281661	-421.6743551	-421.7246591	1.2191	-421.9545012	-421.8006902	-421.8509942	1.2176	-422.0325387	-421.8787277	-421.9290317
4	PhCH2O2_aaw	-421.8280694	-421.6743784	-421.7236614	0.8511	-421.9539295	-421.8002385	-421.8495215	0.8260	-422.0317128	-421.8780218	-421.9273048
MIN	PhC(CH3)2O•	-500.3191994	-500.1055304	-500.1591424		-500.4677291	-500.2540601	-500.3076721		-500.5598151	-500.3461461	-500.3997581
1	PhCCH32O2_a_aau	-500.3191994	-500.1055304	-500.1591424	0.7604	-500.4677291	-500.2540601	-500.3076721	0.7608	-500.5598151	-500.3461461	-500.3997581
2	PhCCH32O2_a_aam	-500.3181451	-500.1038481	-500.1561741	1.2577	-500.4667754	-500.2524784	-500.3048044	1.2569	-500.5589355	-500.3446385	-500.3969645
3	PhCCH32O3_acx	-500.3186717	-500.1048947	-500.1581927	0.7665	-500.4666561	-500.2528791	-500.3061771	0.7623	-500.5585025	-500.3447255	-500.3980235
4	PhCCH32O2_a_abh	-500.3177741	-500.1040231	-500.1580511	1.2442	-500.4663933	-500.2526423	-500.3066703	0.7743	-500.5583435	-500.3445925	-500.3986205
5	PhCCH32O3_abq	-500.3168987	-500.1032437	-500.1578817	0.8156	-500.4658018	-500.2521468	-500.3067848	0.8168	-500.5580671	-500.3444121	-500.3990501
6	PhCCH32O2_a_ads	-500.3168405	-500.1028195	-500.1560425	0.7600	-500.4651526	-500.2511316	-500.3043546	0.8443	-500.5572774	-500.3432564	-500.3964794
MIN	PhO•	-382.6267884	-382.5012544	-382.5459424		-382.7421138	-382.6165798	-382.6612678		-382.8132218	-382.6876878	-382.7323758
1	PhO_ace	-382.6267884	-382.5012544	-382.5459424	1.3416	-382.7421138	-382.6165798	-382.6612678	1.3406	-382.8132218	-382.6876878	-382.7323758
MIN	p-nitro-PhO•	-586.8501417	-586.7198887	-586.7717057		-587.0281254	-586.8978724	-586.9496894		-587.1375825	-587.0073295	-587.0591465
1	p-nitro-PhO_aac	-586.8501417	-586.7198887	-586.7717057	1.3882	-587.0281254	-586.8978724	-586.9496894	1.3894	-587.1375825	-587.0073295	-587.0591465
MIN	p-methyl-PhO•	-421.8716077	-421.7168017	-421.7666647		-421.9986961	-421.8438901	-421.8937531		-422.0771823	-421.9223763	-421.9722393
1	p-methyl-PhO_aak	-421.8716077	-421.7168017	-421.7666647	1.3265	-421.9986961	-421.8438901	-421.8937531	1.3253	-422.0771823	-421.9223763	-421.9722393
MIN	p-amino-PhO•	-437.9107155	-437.7666545	-437.8155515		-438.0446693	-437.9006083	-437.9495053		-438.1271767	-437.9831157	-438.0320127
1	p-amino-PhO_abh	-437.9107155	-437.7666545	-437.8155515	1.2226	-438.0446693	-437.9006083	-437.9495053	1.2233	-438.1271767	-437.9831157	-438.0320127
MIN	HOO•	-227.0600436	-227.0140496	-227.0480106		-227.1332118	-227.0872178	-227.1211788		-227.1778250	-227.1318310	-227.1657920
1	HOO_aae	-227.0600436	-227.0140496	-227.0480106	0.7628	-227.1332118	-227.0872178	-227.1211788	0.7641	-227.1778250	-227.1318310	-227.1657920
2	HOO_aaf	-227.0493808	-227.0040058	-227.0420348	0.7624	-227.1232718	-227.0778968	-227.1159258	0.7634	-227.1680248	-227.1226498	-227.1606788
3	HOO_aag	-227.0494936	-227.0041156	-227.0421206	0.7623	-227.1233088	-227.0779308	-227.1159358	0.7632	-227.1680422	-227.1226642	-227.1606692
MIN	CH3OO•	-266.2831135	-266.2077835	-266.2479864		-266.3682003	-266.2928703	-266.3331999		-266.4201260	-266.3447960	-266.3850969
1	CH3OO_adp	-266.2831135	-266.2077835	-266.2474435	0.7634	-266.3682003	-266.2928703	-266.3325303	0.7644	-266.4201260	-266.3447960	-266.3844560
2	CH3OO_aay	-266.2810775	-266.2058935	-266.2479805	0.7632	-266.3662969	-266.2911129	-266.3331999	0.7642	-266.4181939	-266.3430099	-266.3850969
3	CH3OO_aal	-266.2812084	-266.2060144	-266.2479864	0.7631	-266.3663192	-266.2911252	-266.3330972	0.7640	-266.4181815	-266.3429875	-266.3849595
MIN	t-BuOO•	-384.0197322	-383.8563702	-383.9053298		-384.1388190	-383.9754570	-384.0250708		-384.2122905	-384.0489285	-384.0987611
1	t-BuOO_acq	-384.0197322	-383.8563702	-383.9053298	0.7642	-384.1388190	-383.9754570	-384.0230690	0.7651	-384.2122905	-384.0489285	-384.0965405
2	t-BuOO_aao	-384.0178004	-383.8545814	-383.9050674	0.7638	-384.1374195	-383.9742005	-384.0246865	0.7647	-384.2110869	-384.0478679	-384.0983539
3	t-BuOO_aad	-384.0175108	-383.8543448	-383.9053298	0.7641	-384.1372518	-383.9740858	-384.0250708	0.7649	-384.2109421	-384.0477761	-384.0987611
MIN	PhCH2OO•	-496.8987114	-496.7374744	-496.7884838		-497.0473471	-496.8861101	-496.9379697		-497.1391863	-496.9779493	-497.0300677
1	PhCH2OO2_adm	-496.8987114	-496.7374744	-496.7876754	0.7642	-497.0473471	-496.8861101	-496.9363111	0.7649	-497.1391863	-496.9779493	-497.0281503
2	PhCH2OO1_aae	-496.8964677	-496.7354247	-496.7877327	0.7640	-497.0457966	-496.8847536	-496.9370616	0.7649	-497.1379076	-496.9768646	-497.0291726
3	PhCH2OO2_adu	-496.8959457	-496.7351717	-496.7881177	0.7748	-497.0449558	-496.8841818	-496.9371278	0.7700	-497.1369690	-496.9761950	-497.0291410

4	PhCH2OO1_aaw	-496.8948460	-496.7339210	-496.7883080	0.7635	-497.0441426	-496.8832176	-496.9376046	0.7672	-497.1361891	-496.9752641	-497.0296511
5	PhCH2OO2_acs	-496.8948434	-496.7338784	-496.7882194	0.7727	-497.0441005	-496.8831355	-496.9374765	0.7736	-497.1361448	-496.9751798	-497.0295208
6	PhCH2OO1_aap	-496.8942898	-496.7334118	-496.7884838	0.7638	-497.0437757	-496.8828977	-496.9379697	0.7653	-497.1358737	-496.9749957	-497.0300677
MIN	TEMPO•	-559.2216329	-558.9184739	-558.9756730		-559.3914796	-559.0883206	-559.1453635		-559.4970514	-559.1938924	-559.2509074
1	TEMPO_ace	-559.2216329	-558.9184739	-558.9754889	0.7733	-559.3914796	-559.0883206	-559.1453356	0.7744	-559.4970514	-559.1938924	-559.2509074
2	TEMPO_aab	-559.2213938	-558.9182398	-558.9750318	0.7734	-559.3911281	-559.0879741	-559.1447661	0.7744	-559.4966593	-559.1935053	-559.2502973
3	TEMPO_acg	-559.2215070	-558.9183880	-558.9756730	0.7737	-559.3911975	-559.0880785	-559.1453635	0.7743	-559.4967180	-559.1935990	-559.2508840
MIN	•OO•	-226.4612261	-226.4275761	-226.4670925		-226.5331585	-226.4995085	-226.5386392		-226.5766791	-226.5430291	-226.5821441
1	3O2_aai	-226.4610732	-226.4274292	-226.4669582	2.0432	-226.5326790	-226.4990350	-226.5385640	2.0472	-226.5760125	-226.5423685	-226.5818975
2	3O2_aaa	-226.4612261	-226.4275761	-226.4666911	2.0434	-226.5331585	-226.4995085	-226.5386235	2.0470	-226.5766791	-226.5430291	-226.5821441
3	3O2_aam	-226.4611445	-226.4274925	-226.4670925	2.0433	-226.5326912	-226.4990392	-226.5386392	2.0473	-226.5759895	-226.5423375	-226.5819375
MIN	HCO2•	-265.1474740	-265.0961010	-265.1307240		-265.2305141	-265.1791411	-265.2137641		-265.2811729	-265.2297999	-265.2644229
1	HCO2_acr	-265.1474740	-265.0961010	-265.1307240	0.7628	-265.2305141	-265.1791411	-265.2137641	0.7633	-265.2811729	-265.2297999	-265.2644229

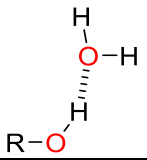
Table S3.4.29. Calculated energies. Individual selected conformers.

№		DLPNO-CCSD(T)/cc-pVTZ// (U)B3LYP-D3/6-31+G(d,p)			DLPNO-CCSD(T)/cc-pVQZ// (U)B3LYP-D3/6-31+G(d,p)			DLPNO-CCSD(T)/CBS// (U)B3LYP-D3/6-31+G(d,p)		
		E _{tot}	H ₂₉₈	G ₂₉₈	E _{tot}	H ₂₉₈	G ₂₉₈	E _{tot}	H ₂₉₈	G ₂₉₈
MIN	HOH (1Ha)	-152.6731057	-152.6200777	-152.6525897	-152.7274519	-152.6744239	-152.7069359	-152.7601617	-152.7071337	-152.7396457
1	HOH_aaa (1Ha)	-152.6731057	-152.6200777	-152.6525897	-152.7274519	-152.6744239	-152.7069359	-152.7601617	-152.7071337	-152.7396457
MIN	CH3OH	-191.8921279	-191.8087069	-191.8457509	-191.9572352	-191.8738142	-191.9108582	-191.9967983	-191.9133773	-191.9504213
1	CH3OH_aap	-191.8921279	-191.8087069	-191.8457509	-191.9572352	-191.8738142	-191.9108582	-191.9967983	-191.9133773	-191.9504213
MIN	CH3CH2OH	-231.1376808	-231.0245488	-231.0643876	-231.2139118	-231.1007798	-231.1406241	-231.2605770	-231.1474483	-231.1873123
1	CH3CH2OH1_adi	-231.1376808	-231.0245488	-231.0637078	-231.2139118	-231.1007798	-231.1399388	-231.2605770	-231.1474450	-231.1866040
2	CH3CH2OH2_abj	-231.1376336	-231.0245376	-231.0643876	-231.2138701	-231.1007741	-231.1406241	-231.2605443	-231.1474483	-231.1872983
3	CH3CH2OH1_aaf	-231.1365169	-231.0234809	-231.0640409	-231.2130355	-231.0999995	-231.1405595	-231.2597883	-231.1467523	-231.1873123
MIN	BuOH	-309.6169486	-309.4441796	-309.4915421	-309.7161024	-309.5432970	-309.5905041	-309.7772099	-309.6043845	-309.6515895
1	BuOH4d_aae	-309.6169073	-309.4439763	-309.4906063	-309.7161024	-309.5431714	-309.5898014	-309.7772099	-309.6042789	-309.6509089
2	BuOH3a_ada	-309.6163497	-309.4436167	-309.4901857	-309.7157081	-309.5429751	-309.5895441	-309.7768852	-309.6041522	-309.6507212
3	BuOH5c_aap	-309.6167760	-309.4438500	-309.4892940	-309.7158193	-309.5428933	-309.5883373	-309.7768883	-309.6039623	-309.6494063
4	BuOH8b_aas	-309.6166517	-309.4437607	-309.4903187	-309.7159934	-309.5431024	-309.5896604	-309.7771556	-309.6042646	-309.6508226
5	BuOH1a_abs	-309.6169486	-309.4441796	-309.4913846	-309.7160660	-309.5432970	-309.5905020	-309.7771535	-309.6043845	-309.6515895
6	BuOH7b_aam	-309.6164326	-309.4435376	-309.4904476	-309.7157487	-309.5428537	-309.5897637	-309.7769086	-309.6040136	-309.6509236
7	BuOH6b_aax	-309.6159141	-309.4429161	-309.4891541	-309.7151058	-309.5421078	-309.5883458	-309.7762209	-309.6032229	-309.6494609
8	BuOH1a_adi	-309.6165653	-309.4437873	-309.4905013	-309.7155468	-309.5427688	-309.5894828	-309.7765518	-309.6037738	-309.6504878
9	BuOH4d_aag	-309.6153808	-309.4425278	-309.4899478	-309.7149782	-309.5421252	-309.5895452	-309.7762241	-309.6033711	-309.6507911
10	BuOH2b_ada	-309.6162778	-309.4433888	-309.4904688	-309.7153077	-309.5424187	-309.5894987	-309.7763513	-309.6034623	-309.6505423
11	BuOH8b_abv	-309.6152798	-309.4424598	-309.4904788	-309.7149118	-309.5420918	-309.5901108	-309.7761601	-309.6033401	-309.6513591
12	BuOH3a_adl	-309.6162611	-309.4437141	-309.4915421	-309.7152231	-309.5426761	-309.5905041	-309.7762153	-309.6036683	-309.6514963
13	BuOH2b_ade	-309.6165611	-309.4435941	-309.4893951	-309.7152765	-309.5423095	-309.5881105	-309.7761979	-309.6032309	-309.6490319
14	BuOH9b_abb	-309.6157015	-309.4426685	-309.4889185	-309.7149894	-309.5419564	-309.5882064	-309.7761205	-309.6030875	-309.6493375
15	BuOH11d_aab	-309.6153788	-309.4424418	-309.4889768	-309.7147112	-309.5417742	-309.5883092	-309.7758698	-309.6029328	-309.6494678
16	BuOH5c_abn	-309.6150479	-309.4422189	-309.4901819	-309.7144029	-309.5415739	-309.5895369	-309.7755447	-309.6027157	-309.6506787
17	BuOH10d_acr	-309.6153105	-309.4423475	-309.4892675	-309.7146087	-309.5416457	-309.5885657	-309.7757589	-309.6027959	-309.6497159
18	BuOH14b_aah	-309.6149870	-309.4420820	-309.4874080	-309.7137451	-309.5408401	-309.5861661	-309.7746838	-309.6017788	-309.6471048
19	BuOH6b_aaf	-309.6145137	-309.4416207	-309.4892417	-309.7141063	-309.5412133	-309.5888343	-309.7753556	-309.6024626	-309.6500836

20	BuOH12c_acs	-309.6155352	-309.4426362	-309.4888072	-309.7140954	-309.5411964	-309.5873674	-309.7749487	-309.6020497	-309.6482207
21	BuOH13c_aau	-309.6149118	-309.4421368	-309.4883248	-309.7137957	-309.5410207	-309.5872087	-309.7747997	-309.6020247	-309.6482127
22	BuOH9b_abv	-309.6143694	-309.4414334	-309.4891114	-309.7139691	-309.5410331	-309.5887111	-309.7752023	-309.6022663	-309.6499443
23	BuOH11d_aai	-309.6141896	-309.4412636	-309.4889076	-309.7137683	-309.5408423	-309.5884863	-309.7749947	-309.6020687	-309.6497127
24	BuOH13c_abd	-309.6136807	-309.4410027	-309.4895057	-309.7128293	-309.5405153	-309.5886543	-309.7738946	-309.6012166	-309.6497196
25	BuOH12c_abd	-309.6150363	-309.4421023	-309.4876893	-309.7134880	-309.5405540	-309.5861410	-309.7742884	-309.6013544	-309.6469414
26	BuOH14b_aaa	-309.6130309	-309.4401869	-309.4874519	-309.7125220	-309.5396780	-309.5869430	-309.7737171	-309.6008731	-309.6481381
MIN	tBuOH	-309.6295403	-309.4581353	-309.5026803	-309.7285509	-309.5571459	-309.6016909	-309.7896487	-309.6182437	-309.6627887
1	t-BuOH_acj	-309.6295403	-309.4581353	-309.5026803	-309.7285509	-309.5571459	-309.6016909	-309.7896487	-309.6182437	-309.6627887
MIN	PhCH2OH	-422.5101644	-422.3408384	-422.3887764	-422.6389398	-422.4696138	-422.5179505	-422.7185359	-422.5492099	-422.5976598
1	PhCH2OH2_aae	-422.5101644	-422.3408384	-422.3883454	-422.6389398	-422.4696138	-422.5171208	-422.7185359	-422.5492099	-422.5967169
2	PhCH2OH2_aaa	-422.5075854	-422.3384364	-422.3887764	-422.6367595	-422.4676105	-422.5179505	-422.7164688	-422.5473198	-422.5976598
3	PhCH2OH1_aad	-422.5077548	-422.3385598	-422.3866898	-422.6364834	-422.4672884	-422.5154184	-422.7160349	-422.5468399	-422.5949699
4	PhCH2OH1_adk	-422.5074274	-422.3383324	-422.3871854	-422.6362011	-422.4671061	-422.5159591	-422.7157604	-422.5466654	-422.5955184
5	PhCH2OH2_aca	-422.4773756	-422.3175336	-422.3717736	-422.6054117	-422.4455697	-422.4998097	-422.6843839	-422.5245419	-422.5787819
MIN	PhC(CH3)2OH	-500.9999606	-500.7722756	-500.8252048	-501.1513211	-500.9236361	-500.9764792	-501.2451950	-501.0175100	-501.0703016
1	PhCCH32OH1_abo	-500.9999606	-500.7722756	-500.8250296	-501.1513211	-500.9236361	-500.9763901	-501.2451950	-501.0175100	-501.0702640
2	PhCCH32OH1_abf	-500.9996578	-500.7719548	-500.8252048	-501.1509322	-500.9232292	-500.9764792	-501.2447546	-501.0170516	-501.0703016
3	PhCCH32OH3_abn	-500.9992887	-500.7718017	-500.8246747	-501.1501108	-500.9226238	-500.9754968	-501.2437311	-501.0162441	-501.0691171
4	PhCCH32OH1_ack	-500.9990503	-500.7715413	-500.8247223	-501.1499794	-500.9224704	-500.9756514	-501.2436539	-501.0161449	-501.0693259
5	PhCCH32OH1_aal	-500.9971921	-500.7694911	-500.8219081	-501.1483079	-500.9206069	-500.9730239	-501.2420490	-501.0143480	-501.0667650
6	PhCCH32OH1_adj	-500.9965721	-500.7690231	-500.8223101	-501.1482709	-500.9207219	-500.9740089	-501.2422747	-501.0147257	-501.0680127
7	PhCCH32OH3_abt	-500.9970403	-500.7693873	-500.8221983	-501.1483495	-500.9206965	-500.9735075	-501.2421655	-501.0145125	-501.0673235
MIN	PhOH	-383.2734668	-383.1348428	-383.1804348	-383.3906950	-383.2520710	-383.2976630	-383.4629917	-383.3243677	-383.3699597
1	PhOH_aab	-383.2734668	-383.1348428	-383.1804348	-383.3906950	-383.2520710	-383.2976630	-383.4629917	-383.3243677	-383.3699597
MIN	p-nitro-PhOH	-587.5028109	-587.3591249	-587.4110819	-587.6832398	-587.5395538	-587.5915108	-587.7942345	-587.6505485	-587.7025055
1	p-nitro-PhOH_aak	-587.5028109	-587.3591249	-587.4110819	-587.6832398	-587.5395538	-587.5915108	-587.7942345	-587.6505485	-587.7025055
MIN	p-methyl-PhOH	-422.5157144	-422.3479244	-422.3990174	-422.6444568	-422.4766668	-422.5277598	-422.7239998	-422.5562098	-422.6073028
1	p-methyl-PhOH_aac	-422.5157144	-422.3479244	-422.3990174	-422.6444568	-422.4766668	-422.5277598	-422.7239998	-422.5562098	-422.6073028
MIN	p-amino-PhOH	-438.5457292	-438.3891052	-438.4382822	-438.6810510	-438.5244270	-438.5736040	-438.7644517	-438.6078277	-438.6570047
1	p-amino-PhOH_adq	-438.5457292	-438.3891052	-438.4382822	-438.6810510	-438.5244270	-438.5736040	-438.7644517	-438.6078277	-438.6570047
2	p-amino-PhOH_adf	-438.5456081	-438.3889811	-438.4381091	-438.6809538	-438.5243268	-438.5734548	-438.7643647	-438.6077377	-438.6568657
MIN	HOOH	-227.7032047	-227.6446547	-227.6792157	-227.7032047	-227.6446547	-227.6792157	-227.8253138	-227.7667638	-227.8013248
1	HOOH_aam	-227.7032047	-227.6446547	-227.6792157	-227.7032047	-227.6446547	-227.6792157	-227.8253138	-227.7667638	-227.8013248
2	HOOH_acd	-227.6975987	-227.6393637	-227.6767807	-227.6975987	-227.6393637	-227.6767807	-227.8203229	-227.7620879	-227.7995049
3	HOOH_acf	-227.7023510	-227.6438910	-227.6787450	-227.7023510	-227.6438910	-227.6787450	-227.8245253	-227.7660653	-227.8009193
4	HOOH_acn	-227.6975095	-227.6392905	-227.6769635	-227.6975095	-227.6392905	-227.6769635	-227.8199653	-227.7617463	-227.7994193
MIN	CH3OOH	-266.9275901	-266.8400791	-266.8810381	-267.0148989	-266.9273879	-266.9683469	-267.0682908	-266.9807798	-267.0217388
1	CH3OOH_aax	-266.9275901	-266.8400791	-266.8810381	-267.0148989	-266.9273879	-266.9683469	-267.0682908	-266.9807798	-267.0217388
2	CH3OOH_acq	-266.9268820	-266.8393690	-266.8792440	-267.0142527	-266.9267397	-266.9666147	-267.0676725	-266.9801595	-267.0200345
3	CH3OOH_aau	-266.9265674	-266.8390074	-266.8792684	-267.0138973	-266.9263373	-266.9665983	-267.0673198	-266.9797598	-267.0200208
MIN	t-BuOOH	-384.6619246	-384.4863490	-384.5358530	-384.7833855	-384.6078955	-384.6573995	-384.8584530	-384.6829630	-384.7324670
1	t-BuOOH_aby	-384.6618390	-384.4863490	-384.5358530	-384.7833855	-384.6078955	-384.6573995	-384.8584530	-384.6829630	-384.7324670
2	t-BuOOH_adj	-384.6619246	-384.4862976	-384.5346396	-384.7833018	-384.6076748	-384.6560168	-384.8582964	-384.6826694	-384.7310114
MIN	PhCH2OOH	-497.5458882	-497.3722672	-497.4235143	-497.6969494	-497.5233284	-497.5749588	-497.7904095	-497.6167885	-497.6685184
1	PhCH2OOH2_aag	-497.5458882	-497.3722672	-497.4221312	-497.6969494	-497.5233284	-497.5731924	-497.7904095	-497.6167885	-497.6666525
2	PhCH2OOH3_abi	-497.5436716	-497.3703236	-497.4215326	-497.6949695	-497.5216215	-497.5728305	-497.7885235	-497.6151755	-497.6663845
3	PhCH2OOH2_aai	-497.5427253	-497.3694203	-497.4235143	-497.6941698	-497.5208648	-497.5749588	-497.7877294	-497.6144244	-497.6685184
4	PhCH2OOH3_aae	-497.5427805	-497.3695395	-497.4208895	-497.6931651	-497.5199241	-497.5712741	-497.7863272	-497.6130862	-497.6644362

5	PhCH2OOH1_acj	-497.5412760	-497.3680010	-497.4209290	-497.6928750	-497.5196000	-497.5725280	-497.7864931	-497.6132181	-497.6661461
MIN	TEMPOH	-559.8417605	-559.5266685	-559.5843303	-560.0121869	-559.6972449	-559.7553369	-560.1185319	-559.8035899	-559.8616819
1	TEMPOHa_abx	-559.8417605	-559.5266685	-559.5823945	-560.0121830	-559.6970910	-559.7528170	-560.1182613	-559.8031693	-559.8588953
2	TEMPOH_aab	-559.8411803	-559.5262383	-559.5843303	-560.0121869	-559.6972449	-559.7553369	-560.1185319	-559.8035899	-559.8616819
3	TEMPOH_aba	-559.8407255	-559.5255315	-559.5834225	-560.0119223	-559.6967283	-559.7546193	-560.1183517	-559.8031577	-559.8610487
4	TEMPOHa_ade	-559.8358576	-559.5211746	-559.5799826	-560.0075814	-559.6928984	-559.7517064	-560.1142119	-559.7995289	-559.8583369
MIN	HCO2H	-265.8388504	-265.7736004	-265.8122954	-265.9255200	-265.8602700	-265.8989650	-265.9782849	-265.9130349	-265.9517299
1	HCO2Ha_aaa	-265.8388504	-265.7736004	-265.8122954	-265.9255200	-265.8602700	-265.8989650	-265.9782849	-265.9130349	-265.9517299
2	HCO2Hb_aap	-265.8332961	-265.7682121	-265.8069441	-265.9198546	-265.8547706	-265.8935026	-265.9724850	-265.9074010	-265.9461330

Table S3.4.30. Calculated energies. Individual selected conformers.

No		DLPNO-CCSD(T)/cc-pVTZ// (U)B3LYP-D3/6-31+G(d,p)			DLPNO-CCSD(T)/cc-pVQZ// (U)B3LYP-D3/6-31+G(d,p)			DLPNO-CCSD(T)/CBS// (U)B3LYP-D3/6-31+G(d,p)		
		E _{tot}	H ₂₉₈	G ₂₉₈	E _{tot}	H ₂₉₈	G ₂₉₈	E _{tot}	H ₂₉₈	G ₂₉₈
MIN	HOH (1Ha)	-152.6731057	-152.6200777	-152.6525897	-152.7274519	-152.6744239	-152.7069359	-152.7601617	-152.7071337	-152.7396457
1	HOH_aaa (1Ha)	-152.6731057	-152.6200777	-152.6525897	-152.7274519	-152.6744239	-152.7069359	-152.7601617	-152.7071337	-152.7396457
MIN	CH3OH	-191.8920076	-191.8087646	-191.8470746	-191.9566571	-191.8734141	-191.9117241	-191.9960152	-191.9127722	-191.9510822
1	CH3OH_aad	-191.8920076	-191.8087646	-191.8470746	-191.9566571	-191.8734141	-191.9117241	-191.9960152	-191.9127722	-191.9510822
MIN	CH3CH2OH	-231.1366266	-231.0237086	-231.0655436	-231.2124469	-231.0995289	-231.1416047	-231.2589655	-231.1460845	-231.1881745
1	CH3CH2OH1_adc	-231.1366266	-231.0237086	-231.0655436	-231.2124469	-231.0995289	-231.1416047	-231.2589655	-231.1460845	-231.1881745
2	CH3CH2OH2_aac	-231.1363346	-231.0234536	-231.0655436	-231.2123957	-231.0995147	-231.1416047	-231.2589655	-231.1460845	-231.1881745
MIN	BuOH	-309.6158437	-309.4432827	-309.4926077	-309.7144797	-309.5419187	-309.5912437	-309.7754340	-309.6028510	-309.6520849
1	BuOH4d_aam	-309.6156970	-309.4430680	-309.4901470	-309.7144751	-309.5418461	-309.5889251	-309.7753901	-309.6027611	-309.6498401
2	BuOH4d_aan	-309.6154851	-309.4428871	-309.4895731	-309.7142748	-309.5416768	-309.5883628	-309.7751998	-309.6026018	-309.6492878
3	BuOH3a_abg	-309.6158437	-309.4432827	-309.4926077	-309.7144797	-309.5419187	-309.5912437	-309.7753209	-309.6027599	-309.6520849
4	BuOH1a_abw	-309.6155279	-309.4429449	-309.4910519	-309.7144592	-309.5418762	-309.5899832	-309.7754340	-309.6028510	-309.6509580
5	BuOH4d_aaj	-309.6153393	-309.4427043	-309.4907393	-309.7141723	-309.5415373	-309.5895723	-309.7751136	-309.6024786	-309.6505136
6	BuOH6b_aaj	-309.6153949	-309.4425939	-309.4888759	-309.7140911	-309.5412901	-309.5875721	-309.7749985	-309.6021975	-309.6484795
7	BuOH6b_aco	-309.6150789	-309.4423529	-309.4883969	-309.7138919	-309.5411659	-309.5872099	-309.7748499	-309.6021239	-309.6481679
8	BuOH7b_aac	-309.6149361	-309.4423061	-309.4914541	-309.7140608	-309.5414308	-309.5905788	-309.7751086	-309.6024786	-309.6516266
9	BuOH5c_aai	-309.6153161	-309.4425891	-309.4911961	-309.7138882	-309.5411612	-309.5897682	-309.7747014	-309.6019744	-309.6505814
10	BuOH2b_aad	-309.6149407	-309.4422187	-309.4912317	-309.7138309	-309.5411089	-309.5901219	-309.7747883	-309.6020663	-309.6510793
11	BuOH13c_aay	-309.6145750	-309.4418720	-309.4881230	-309.7129382	-309.5402352	-309.5864862	-309.7736984	-309.6009954	-309.6472464
12	BuOH9b_abm	-309.6143628	-309.4415728	-309.4900088	-309.7132438	-309.5404538	-309.5888898	-309.7741758	-309.6013858	-309.6498218
13	BuOH11d_aag	-309.6141664	-309.4414244	-309.4902944	-309.7130418	-309.5402998	-309.5891698	-309.7739730	-309.6012310	-309.6501010
14	BuOH10d_ace	-309.6138649	-309.4411809	-309.4897259	-309.7129556	-309.5402716	-309.5888166	-309.7739870	-309.6013030	-309.6498480
15	BuOH14b_abp	-309.6138453	-309.4410913	-309.4867193	-309.7123095	-309.5395555	-309.5851835	-309.7731185	-309.6003645	-309.6459925
16	BuOH12c_aay	-309.6135309	-309.4409369	-309.4896609	-309.7122183	-309.5396243	-309.5883483	-309.7731017	-309.6005077	-309.6492317
17	BuOH14b_aad	-309.6124393	-309.4398163	-309.4877073	-309.7110791	-309.5384561	-309.5863471	-309.7719546	-309.5993316	-309.6472226
MIN	tBuOH	-309.6276702	-309.4565122	-309.5036712	-309.7264474	-309.5552894	-309.6024484	-309.7874221	-309.6162641	-309.6634231
1	t-BuOH_abj	-309.6276702	-309.4565122	-309.5036712	-309.7264474	-309.5552894	-309.6024484	-309.7874221	-309.6162641	-309.6634231
MIN	PhCH2OH	-422.5110218	-422.3419388	-422.3901208	-422.6394570	-422.4703660	-422.5185810	-422.7189205	-422.5498295	-422.5980445
1	PhCH2OH2_abt	-422.5109968	-422.3419058	-422.3901208	-422.6394570	-422.4703660	-422.5185810	-422.7189205	-422.5498295	-422.5980445
2	PhCH2OH2_acy	-422.5110218	-422.3419388	-422.3899998	-422.6393019	-422.4702189	-422.5182799	-422.7186828	-422.5495998	-422.5976608
3	PhCH2OH1_aaw	-422.5069197	-422.3380757	-422.3896487	-422.6356443	-422.4668003	-422.5183733	-422.7151969	-422.5463529	-422.5979259
MIN	PhC(CH3)2OH	-501.0013758	-500.7739086	-500.8273988	-501.1523178	-500.9248224	-500.9783408	-501.2460177	-501.0185053	-501.0720407

1	PhCCH32OH2_abp	-501.0013496	-500.7739086	-500.8273456	-501.1522634	-500.9248224	-500.9782594	-501.2459463	-501.0185053	-501.0719423
2	PhCCH32OH1_adt	-501.0013758	-500.7738328	-500.8273988	-501.1523178	-500.9247748	-500.9783408	-501.2460177	-501.0184747	-501.0720407
3	PhCCH32OH2_act	-501.0011222	-500.7737252	-500.8271402	-501.1519694	-500.9245724	-500.9779874	-501.2456235	-501.0182265	-501.0716415
4	PhCCH32OH3_aah	-500.9981375	-500.7707865	-500.8264645	-501.1493162	-500.9219652	-500.9776432	-501.2431005	-501.0157495	-501.0714275
MIN	PhOH	-383.2780761	-383.1391371	-383.1844881	-383.3945793	-383.2556403	-383.3009913	-383.4665405	-383.3276015	-383.3729525
1	PhOH_abf	-383.2780761	-383.1391371	-383.1844881	-383.3945793	-383.2556403	-383.3009913	-383.4665405	-383.3276015	-383.3729525
MIN	p-nitro-PhOH	-587.5108550	-587.3666530	-587.4175370	-587.6905927	-587.5463907	-587.5972747	-587.8013309	-587.6571289	-587.7080129
1	p-nitro-PhOH_aab	-587.5108550	-587.3666530	-587.4175370	-587.6905927	-587.5463907	-587.5972747	-587.8013309	-587.6571289	-587.7080129
MIN	p-methyl-PhOH	-422.5198750	-422.3517370	-422.4022910	-422.6478996	-422.4797616	-422.5303156	-422.7271083	-422.5589703	-422.6095243
1	p-methyl-PhOH_aax	-422.5198750	-422.3517370	-422.4022910	-422.6478996	-422.4797616	-422.5303156	-422.7271083	-422.5589703	-422.6095243
MIN	p-amino-PhOH	-438.5491428	-438.3921778	-438.4408118	-438.6838460	-438.5268810	-438.5755150	-438.7669651	-438.6100001	-438.6586341
1	p-amino-PhOH_abd	-438.5491428	-438.3921778	-438.4408118	-438.6838460	-438.5268810	-438.5755150	-438.7669651	-438.6100001	-438.6586341
2	p-amino-PhOH_aab	-438.5135662	-438.3554132	-438.3976502	-438.6475855	-438.4894325	-438.5316695	-438.7303592	-438.5722062	-438.6144432
MIN	HOOH	-227.7032047	-227.6446547	-227.6792157	-227.7032047	-227.6446547	-227.6792157	-227.8253138	-227.7667638	-227.8013248
1	HOOH_aam	-227.7032047	-227.6446547	-227.6792157	-227.7032047	-227.6446547	-227.6792157	-227.8253138	-227.7667638	-227.8013248
2	HOOH_acf	-227.7023510	-227.6438910	-227.6787450	-227.7023510	-227.6438910	-227.6787450	-227.8245253	-227.7660653	-227.8009193
MIN	CH3OOH	-266.9319970	-266.8441890	-266.8827460	-267.0189016	-266.9310936	-266.9696506	-267.0721768	-266.9843688	-267.0229258
1	CH3OOH_aac	-266.9319970	-266.8441890	-266.8827460	-267.0189016	-266.9310936	-266.9696506	-267.0721768	-266.9843688	-267.0229258
2	CH3OOH_aci	-266.9312443	-266.8435183	-266.8825693	-267.0181192	-266.9303932	-266.9694442	-267.0713804	-266.9836544	-267.0227054
MIN	t-BuOOH	-384.6672604	-384.4913394	-384.5380653	-384.7883871	-384.6124661	-384.6591351	-384.8633289	-384.6874079	-384.7340769
1	t-BuOOH_aav	-384.6672604	-384.4913394	-384.5380653	-384.7883871	-384.6124661	-384.6591351	-384.8633289	-384.6874079	-384.7340769
2	t-BuOOH_ace	-384.6665383	-384.4907933	-384.5380653	-384.7874946	-384.6117496	-384.6590216	-384.8623524	-384.6866074	-384.7338794
MIN	PhCH2OOH	-497.5509804	-497.3771294	-497.4267164	-497.7014254	-497.5275744	-497.5771614	-497.7946625	-497.6208115	-497.6703985
1	PhCH2OOH2_acb	-497.5509804	-497.3771294	-497.4267164	-497.7014254	-497.5275744	-497.5771614	-497.7946625	-497.6208115	-497.6703985
2	PhCH2OOH2_aak	-497.5504243	-497.3766983	-497.4265063	-497.7009235	-497.5271975	-497.5770055	-497.7941818	-497.6204558	-497.6702638
3	PhCH2OOH1_acd	-497.5473720	-497.3737510	-497.4249860	-497.6983979	-497.5247769	-497.5760119	-497.7918273	-497.6182063	-497.6694413
4	PhCH2OOH1_aar	-497.5461549	-497.3726519	-497.4240489	-497.6972670	-497.5237640	-497.5751610	-497.7907384	-497.6172354	-497.6686324
5	PhCH2OOH3_adj	-497.5459113	-497.3725253	-497.4239513	-497.6968023	-497.5234163	-497.5748423	-497.7901857	-497.6167997	-497.6682257
6	PhCH2OOH3_acq	-497.5456741	-497.3721491	-497.4234081	-497.6967199	-497.5231949	-497.5744539	-497.7901605	-497.6166355	-497.6678945
7	PhCH2OOH3_aad	-497.5453207	-497.3720127	-497.4238047	-497.6961215	-497.5228135	-497.5746055	-497.7894608	-497.6161528	-497.6679448
MIN	TEMPOH	-559.8476818	-559.5319968	-559.5863798	-560.0182386	-559.7025536	-559.7569366	-560.1244299	-559.8087449	-559.8631279
1	TEMPOH_aaq	-559.8476818	-559.5319968	-559.5863798	-560.0182386	-559.7025536	-559.7569366	-560.1244299	-559.8087449	-559.8631279
2	TEMPOHa_abd	-559.8359444	-559.5213594	-559.5798454	-560.0066661	-559.6920811	-559.7505671	-560.1128891	-559.7983041	-559.8567901
MIN	HOO•	-227.0600436	-227.0140496	-227.0502649	-227.1332118	-227.0872178	-227.1236033	-227.1778249	-227.1318309	-227.1682823
1	HOO_aae	-227.0600436	-227.0140496	-227.0502649	-227.1332118	-227.0872178	-227.1236033	-227.1778249	-227.1318309	-227.1657919
2	HOO_adq	-227.0587259	-227.0129429	-227.0502649	-227.1320643	-227.0862813	-227.1236033	-227.1767433	-227.1309603	-227.1682823
MIN	HCO2H	-265.8507511	-265.7849431	-265.8198401	-265.9365719	-265.8707639	-265.9056609	-265.9890000	-265.9231920	-265.9580890
1	HCO2Ha_acd	-265.8507511	-265.7849431	-265.8198401	-265.9365719	-265.8707639	-265.9056609	-265.9890000	-265.9231920	-265.9580890
2	HCO2Hb_aab	-265.8403897	-265.7749727	-265.8131017	-265.9266726	-265.8612556	-265.8993846	-265.9791870	-265.9137700	-265.9518990

3. The Redox Properties of Modified DNA Bases:

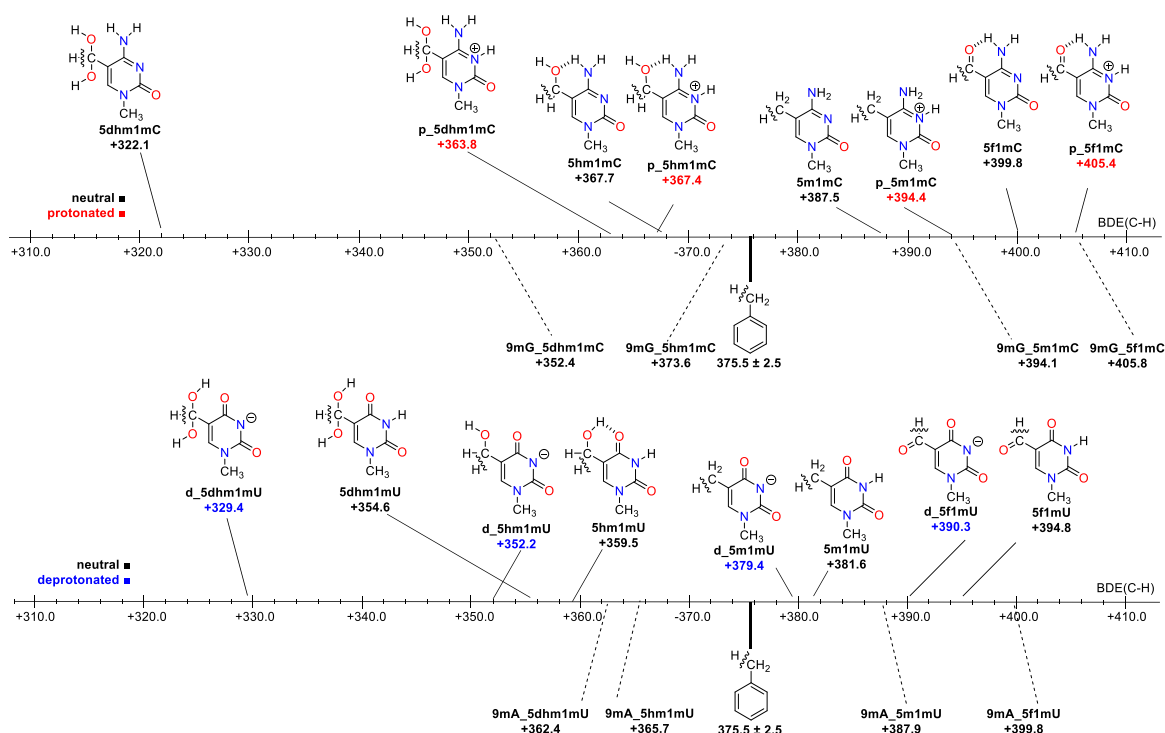
C-H Bond Dissociation Energies

Vasily Korotenko, Hendrik Zipse

Submitted manuscript.

Author contributions: The project was conceived by V.K. and H.Z. The computational study was performed by V.K. The manuscript was written by V.K and H.Z. The supplementary information was prepared by V.K.

The properties of the oxidation products of 5mC and 5mU in their protonated, neutral and deprotonated forms were studied. Radical stabilization energies (RSE) have been calculated at the SMD(H₂O)/(U)B3LYP-D3 and SMD(H₂O)/DLPNO-CCSD(T) levels of theory. In the derivatives of uracil and cytosine, among the substituents at the 5th position, the following trend in BDE values is observed: 5dhm- < 5hm- < 5m- < 5f- (where 5dhm is dihydroxymethyl, 5hm — hydroxymethyl, 5m — methyl, 5f — formyl). It has been established that the charge distribution will strongly affect the reactivity of both closed- and open-shell systems. Protonation increases the calculated BDE(C-H) values in cytosine derivatives, while deprotonation decreases them in uracil derivatives. Addition of one explicit water does not change the results notably. Attaching a complementary base increases the calculated BDE(C-H) value and does not change the observed trend.



The Redox Properties of Modified DNA Bases: C-H Bond Dissociation Energies

V. Korotenko, H. Zipse*

Dept. Chemistry, LMU Munich, Butenandtstr. 5-13, D-81377 Munich, Germany

Oxidation, thermodynamic stability, radical stabilization energy, radicals, isodesmic equations, DFT, DLPNO-CCSD(T), nucleic base

The properties of the oxidation products of 5mC and 5mU in their protonated, neutral and deprotonated forms were studied. Radical stabilization energies (RSE) have been calculated at the SMD(H₂O)/(U)B3LYP-D3 and SMD(H₂O)/DLPNO-CCSD(T) levels of theory. In the derivatives of uracil and cytosine, among the substituents at the 5th position, the following trend in BDE values is observed: 5dhm- < 5hm- < 5m- < 5f- (where 5dhm is dihydroxymethyl, 5hm — hydroxymethyl, 5m — methyl, 5f — formyl). It has been established that the charge distribution will strongly affect the reactivity of both closed- and open-shell systems. Protonation increases the calculated BDE(C-H) values in cytosine derivatives, while deprotonation decreases them in uracil derivatives. Addition of one explicit water does not change the results notably. Attaching a complementary base increases the calculated BDE(C-H) value and does not change the observed trend.

Introduction

Epigenetic control of gene expression involves the methylation and demethylation of cytosine (C).¹ Therefore, the fundamental steps of the oxidation process of 5-methyl-cytosine are important to understand the reaction pathways under physiological conditions. Starting from 5-methylcytosine (5mC), the latter process is currently assumed to proceed in a stepwise manner with 5-hydroxymethylcytosine (5hmC), 5-formylcytosine (5fC), 5-carboxycytosine (5caC) as discrete intermediates (Fig. 1).² While their formation in epigenetic regulation is controlled by 2-oxoglutarate dependent ten-eleven-translocation (TET) oxidases, unregulated formation of these intermediates is also observed in chemical oxidation reactions of 5mC. In aqueous solution all these cytosine derivatives are prone to undergo solvolytic deamination to the respective thymine (T, 5mU, 6) or uracil (U) derivatives (Figure 1).

It has been observed experimentally that 5-methyl-2'-deoxycytidine (5mdC) can be sequentially oxidized by air to 5-hydroxymethyl-2'-deoxycytidine (5hmdC), 5-formyl-2'-deoxycytidine (5fdC), 5-carboxy-2'-deoxycytidine (5hmdC) at 60.0°C and pH 7.4.³ In other work, authors⁴ report about the use of a biomimetic iron(IV)-oxo complex, reminiscent of the activity of TET enzymes. These studies show that 5hmC is preferentially turned over compared with 5mC and 5fC and this is in line with the calculated bond dissociation enthalpies.⁵ However, it has been noted that 5fC may partially exist in a hydrated form in aqueous solution. In our recent theoretical and experimental study,⁶ it has been found that in water solution there is > 0.5% of 5fC in hydrated form (5dhmC) and of about 2% of 5fU (5dhmU). BDE values for the hydrated forms of 5fC and 5fU are not yet available in the literature.

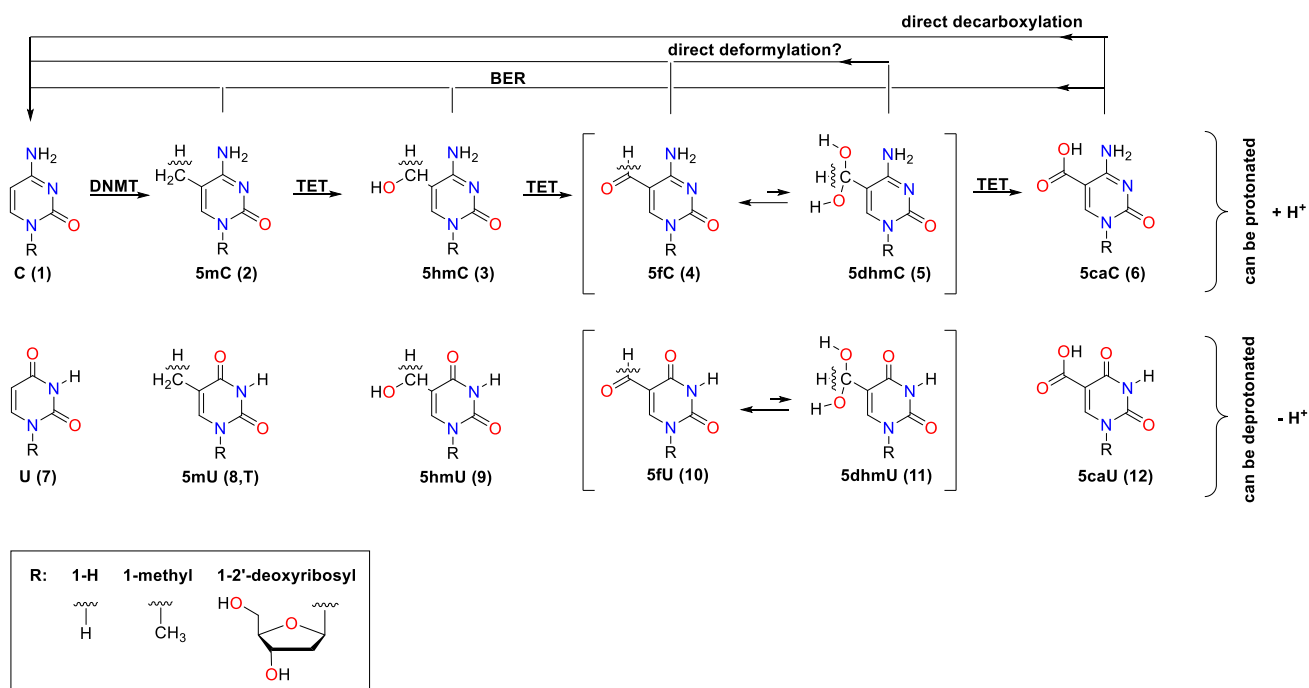


Figure 1. Cytosine derivatives formed during epigenetic gene regulation together with their deamination products. The wavy line indicates the C-H bonds for which the homolytic dissociation enthalpies (BDE) were calculated. DNMT - DNA methyltransferases, TET - ten-eleven translocation enzymes, BER - base excision repair.

It is well known from experimental data that cytosine derivatives 1-6 can be protonated^{7,8} in aqueous solution, while uracil derivatives 7-12 can be deprotonated.⁷⁻¹⁰ The protonated cytosine molecule might contribute significantly to the stabilization of the triplex C-G-C⁺ structure.^{11,12} Key parameters determining the ease of oxidation of these nucleotide bases are the respective homolytic C-H bond dissociation enthalpies (BDE). These are currently not available from experimental measurements, and we therefore report here the results of quantum chemical studies using a hierarchy of theoretical methods and employing the benzylic C-H bond enthalpy in toluene (Ph-CH₃) as a reference. The latter has been determined experimentally in the gas phase as $\text{BDE}_{\text{exp}}^{\text{gas}}(\text{PhCH}_2\text{-H}) = +375.5 \pm 2.5 \text{ kJ mol}^{-1}$.^{13,14} The protonation and deprotonation processes can affect BDE values by creating a positive or a negative charge on the nucleotide base and make its oxidation either more endergonic or more exergonic.

Computational details

BDE values were calculated relative to the reference compound using the isodesmic hydrogen transfer reaction in the solution phase (Figure 2) and equations 1-4, which allows more accurate determination of the stability of C-centered radicals and BDE values.¹⁵ A «gas» symbol (^{gas}) denotes a standard state of 1 atm in the gas phase and «solution» (^{sol}) denotes 1 mol l⁻¹ in the solution phase. Unlike the hydrogen abstraction reaction (HAR), the isodesmic hydrogen transfer reaction (HTR) involves products and substrates that are similar in stability and structure. To use this strategy, in addition to the calculated values of the formation enthalpy of reactants and products, the experimental value of $\text{BDE}_{\text{exp}}^{\text{gas}}(\text{PhCH}_2\text{-H}) = +375.5 \pm 2.5 \text{ kJ mol}^{-1}$ is required.^{13,14}

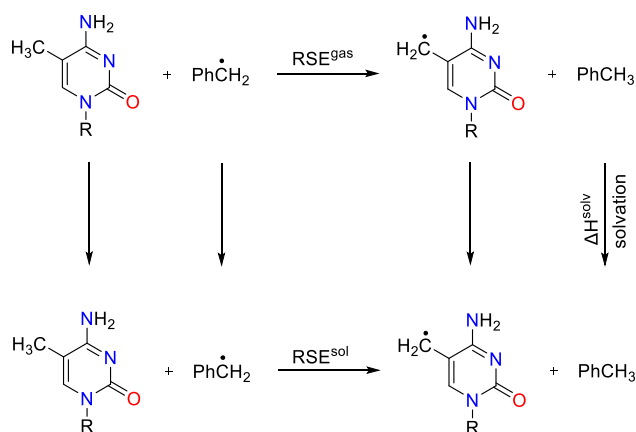


Figure 2. Thermodynamic cycle used in the calculation of BDE(C-H) in solution phase.

$$RSE^{\text{gas}} = H^{\text{gas}}(\text{R}\cdot) + H^{\text{gas}}(\text{PhCH}_3) - H^{\text{gas}}(\text{R-H}) - H^{\text{gas}}(\text{PhCH}_2\cdot) \quad (1)$$

$$RSE^{\text{sol}} = H^{\text{sol}}(\text{R}\cdot) + H^{\text{sol}}(\text{PhCH}_3) - H^{\text{sol}}(\text{R-H}) - H^{\text{sol}}(\text{PhCH}_2\cdot) \quad (2)$$

$$\Delta RSE^{\text{solv}} = RSE^{\text{sol}} - RSE^{\text{gas}} \quad (3)$$

$$BDE^{\text{sol}}(\text{C-H}) = BDE_{\text{exp}}^{\text{gas}}(\text{PhCH}_2\text{-H}) + RSE^{\text{gas}} + \Delta RSE^{\text{solv}} \quad (4)$$

In this work, all geometries were optimized at the SMD(H₂O)/B3LYP-D3/6-31+G(d,p) level of theory with the SMD implicit solvent model¹⁶ using Gaussian09, Revision D.01. The D3 version of Grimme's dispersion was added to the method of optimization to account for dispersion interactions.^{18,19} Since the relative tautomeric stability of the studied molecules is not trivial and can change due to solvation effects, we tested all possible tautomers. Tautomers also varied across base pairs, allowing for the possibility of intermolecular proton transfer. Using the expression $C_n^k = \frac{n!}{(n-k)! \cdot k!}$, one can estimate the number of possible tautomers of an asymmetric molecule having *n* lone pairs and *k* acidic protons ($k \leq n$). The initial geometries of tautomers were created manually and then fully optimized.

To identify the conformations of diol molecules and their radicals, a relaxed potential energy surface scan on two dihedral angles H-O-C-C (two hydroxyl groups) was performed. The conformations with the lowest energies on the potential energy surface were then fully optimized. For each studied nucleobase, all the stable tautomers and conformers were considered when calculating the Boltzmann-weighted enthalpies of formation in the solution phase H^{sol} . The individuality of the found conformers/tautomers was confirmed using an energy criterion of $\Delta E_{\text{tot}} > 10^{-7}$ a.u. and comparing geometries by distances between each atom and the centroid point.^{20,21} Thermochemical corrections to H^{sol} were calculated with GoodVibes using the quasi-harmonic approximation.²² Frequency calculations have been carried out to verify that the optimized structures are true minima.

Single point energies were calculated for the optimized geometries at the DLPNO-CCSD(T) level of theory.²³⁻²⁵ Two-point (cc-pVTZ and cc-pVQZ) extrapolation was employed at the DLPNO-CCSD(T) level to estimate a result obtained using a complete (infinitely large) basis set.^{24,26} Standard state solvation enthalpies ΔH^{solv} were computed as the difference between the solution phase enthalpy H^{sol} of the solution phase optimized molecule (SMD(H₂O)/(U)B3LYP-D3/6-31+G(d,p)), and the gas phase single point enthalpy H^{gas} ((U)B3LYP-D3/6-31+G(d,p)//SMD(H₂O)/(U)B3LYP-D3/6-31+G(d,p)):

$$\Delta H^{\text{solv}} = H^{\text{sol}} - H^{\text{gas}} \quad (5)$$

The solution phase enthalpies H^{sol} at the DLPNO-CCSD(T) level of theory are computed by combining the gas phase enthalpies with the solvation enthalpies ΔH^{solv} :

$$H^{\text{sol}} = E_{\text{tot}}^{\text{DLPNO-CCSD(T)}} + \text{ZPE}^{\text{SMD/(U)B3LYP-D3}} + \Delta H_{0\text{K} \rightarrow 298\text{K}}^{\text{SMD/(U)B3LYP-D3}} + \Delta H_{0\text{K} \rightarrow 298\text{K}}^{1\text{atm} \rightarrow 1\text{M}} + \Delta H^{\text{solv}} \quad (6)$$

$\Delta H_{0\text{K} \rightarrow 298\text{K}}^{1\text{atm} \rightarrow 1\text{M}} = +7.91 \text{ kJ mol}^{-1}$ is the enthalpy difference for converting from the standard state concentration of 1 atm to the standard state concentration of 1 mol l⁻¹.

The SMD implicit solvation model augmented with one explicit water molecule was also used to calculate BDE values. The optimized water-complexed geometries have been located by a stochastic search procedure. This procedure generates geometries with random arrangement water molecules around the respective structure.²⁷⁻²⁹ 100 random structures with one explicit water were generated for all species from Figure 1 and their C-centered radicals and then fully optimized. This procedure was made only for the most stable conformers/tautomers that contribute to the Boltzmann average E_{tot} values more than 2%. All the calculated BDE values in this work are Boltzmann averaged values.

Results and discussion

Calculated BDE(C-H) values

The calculated BDE and RSE values are presented in Table 1 and in Figure 3. The presence or absence of the 1-methyl group does not cause a large difference in the calculated BDEs. According to DLPNO-CCSD(T) results, the C-H bond in 5m1mC with calculated BDE = +387.5 kJ mol⁻¹ is slightly stronger (RSE = +12.0) than in toluene (exp. +375.5 ± 2.5 kJ mol⁻¹). Protonation of 5m1mC makes C-H bond in p_5m1mC stronger, BDE = +394.4 kJ mol⁻¹ (RSE = +18.9). In the following, the RSE values are given in kJ mol⁻¹ in parentheses.

In 5hm1mC, the calculated BDE(C-H) = +367.7 kJ mol⁻¹ is -7.8 kJ mol⁻¹ smaller than in toluene. It is interesting to note that the best tautomer of r_5hm1mC is having a formyl group (Table S11) due to the migration of the proton H⁺ from the hydroxy group to the N3 atom. This radical tautomer is structurally similar to the protonated 5f1mC molecule. Protonation of 5hm1mC almost does not change BDE(C-H) = +367.4 kJ mol⁻¹ value notably for p_5hm1mC.

It is more difficult to abstract a H atom from the 5-formyl group: in 5f1mC BDE(C-H) = +399.8 kJ mol⁻¹ (+24.3), and protonation of 5f1mC makes the H abstraction in p_5f1mC even more endothermic with BDE(C-H) = +405.4 kJ mol⁻¹ (+29.9).

Surprisingly, 5dhm1mC is having a very weak C-H bond with BDE = +322.1 kJ mol⁻¹ (-53.4). The most stable tautomer of r_5dhm1mC is having a carboxy group (See SI) because of migration of a H⁺ from the -C(OH)₂• group to the N3 atom. Protonation of 5dhm1mC has a very large effect on the BDE value, which gives +363.8 kJ mol⁻¹ (-11.7) in p_5dhm1mC. The protonated radical pr_5dhm1mC is also (like the neutral r_5dhm1mC radical) having a carboxy group, but in this case a proton H⁺ moves from the hydroxy (diol) to the amino group. Thus, we can make the general conclusion, that protonation of cytosine derivatives increases their BDE(C-H) values.

The C-H bond in 5m1mU has almost the same BDE = +381.6 kJ mol⁻¹ (+6.1) as in toluene. Deprotonation of 5m1mU slightly weakens C-H bond bringing BDE in d_5m1mU to + 379.4 kJ mol⁻¹ (+3.9). The C-H bond strength in 5hm1mU is weaker than in toluene with BDE = + 359.5 kJ mol⁻¹ (-16.0). Deprotonation of 5hm1mU has a large effect on BDE, which is equal to + 352.2 kJ mol⁻¹ (-23.3) in d_5hm1mU, the most stable tautomer of dr_5hm1mU is having a formyl group (Table S11) because of moving a H⁺ from the hydroxy group to the N3 atom. It is more difficult to remove a H atom from the 5-formyl group, the BDE value in 5f1mU being +394.8 kJ mol⁻¹ (+19.3), while deprotonation of 5f1mU only slightly decreases BDE in d_5f1mU to +390.3 kJ mol⁻¹ (+14.8).

In 5dhm1mU, the C-H bond turns out to be as strong as in 5hm1mU, but slightly weaker and corresponds to BDE = +354.6 kJ mol⁻¹ (-20.9). Deprotonation of 5dhm1mU dramatically weakens C-H bond bringing its BDE value to +329.4 kJ mol⁻¹ (-46.1) in d_5dhm1mU, herein dr_5dhm1mU radical is having a carboxy group because of moving of H⁺ from hydroxy group to amino group. (Table S11) Thus, deprotonation decreases BDEs(C-H) in uracil derivatives

Table 1. The calculated Boltzmann avg. BDE(C-H) values in kJ mol⁻¹ at 298.15 K are presented for 5-substituted N-1-methyl-cytosine (1mC) and 5-substituted N-1-methyl-uracil (1mU) molecules.

5-sub.	q	BDE (5-sub.-1mC)						BDE (5-sub.-1mC)					
		-		+ H ₂ O		+ 9mG		-		+ H ₂ O		+ 9mA	
		DFT	CBS	DFT	CBS	DFT	CBS	DFT	CBS	DFT	CBS	DFT	CBS
m-	-1							371.4	379.4	372.7	380.3		
	0	380.5	387.5	380.8	384.7	380.7	394.1	376.7	381.6	378.6	382.3	377.0	387.9
	+1	389.0	394.4	387.2	393.7								
hm-	-1							324.6	352.2	325.9	350.9		
	0	355.0	367.7	354.8	363.8	357.7	373.6	347.2	359.5	348.1	358.2	348.1	365.7
	+1	357.4	367.4	356.4	369.6								
f-	-1							386.4	390.3	387.4	390.6		
	0	397.7	399.8	406.2	407.6	396.8	405.8	392.5	394.8	393.1	395.7	391.2	399.8
	+1	404.3	405.4	403.7	403.4								
dhm-	-1							305.0	329.4	310.5	335.1		
	0	304.6	322.1	306.1	323.9	332.2	352.4	341.2	354.6	332.5	349.4	339.5	362.4
	+1	358.4	363.8	348.1	358.1								

RSE – calculated ΔBDE value relative to toluene
 BDE – the sum of the RSE value and exp. BDE(C-H) value of +375.5 kJ mol⁻¹(toluene)
 DFT – SMD(H₂O)/(U)B3LYP-D3/6-31+G(d,p)
 CBS – SMD(H₂O)/DLPNO-CCSD(T)/CBS//SMD(H₂O)/(U)B3LYP-D3/6-31+G(d,p)

Effect of one explicit water on the calculated BDE(C-H) values

Introduction of one explicit water molecule in case of neutral 5f1mC increases the calculated BDE(C-H) value by +7.8 kJ mol⁻¹ (CBS; Table 1). Another case, in which a notable explicit-water-effect can be observed, is the protonated diol p_5dhm1mC with ΔBDE(C-H) = -5.7 kJ mol⁻¹. Also, a positive effect of +5.7 kJ mol⁻¹ can be seen for the deprotonated d_5dhm1mU diol molecule, while for its neutral 5dhm1mU form this effect is apposite with ΔBDE(C-H) = -5.1 kJ mol⁻¹. For the other molecules in Table 1 one explicit water molecule has almost no effect on the calculated BDE values.

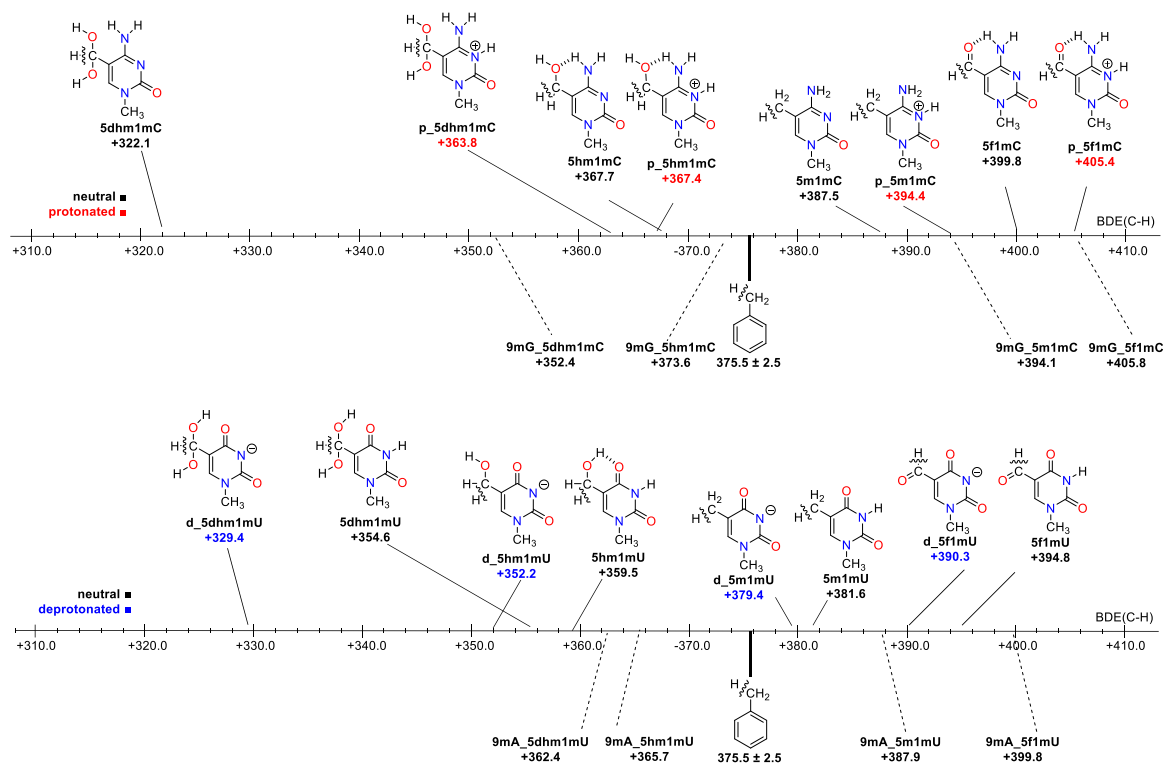


Figure 3. The Boltzmann averaged BDE(C-H) values in kJ mol^{-1} at 298.15 K without explicit water calculated at the SMD(H₂O)/DLPNO-CCSD(T)/CBS//SMD(H₂O)/(U)B3LYP-D3/6-31+G(d,p) level of theory.

Effect of base pairing

In the general case, the presence of a complementary base (guanine) increases the BDE(C-H) values in modified cytosines, which may play a role in protecting methylated/modified DNA from spontaneous oxidation. It is important to note that the relative position of the modified nucleobases on the BDE scale is maintained even when a complementary base is attached. The effect of adding of a complementary base $\Delta\text{BDE}_{\text{sol}}(+ \text{c. base})$ is equal to the difference in complexation enthalpies between radical-base pair and neutral base-base pair:

$$\Delta\text{BDE}_{\text{sol}}(+ \text{c. base}) = \text{BDE}^{\text{sol}}(\text{base} + \text{c. base}) - \text{BDE}^{\text{sol}}(\text{base}) = \Delta\text{H}_{\text{complex.}}^{\text{sol}}(\text{radical} + \text{c. base}) - \Delta\text{H}_{\text{complex.}}^{\text{sol}}(\text{base} + \text{c. base}) \quad (7)$$

$$\Delta\text{H}_{\text{complex.}}^{\text{sol}}(\text{base} + \text{c. base}) = \text{H}^{\text{sol}}(\text{base} + \text{c. base}) - \text{H}^{\text{sol}}(\text{base}) - \text{H}^{\text{sol}}(\text{c. base}) \quad (8)$$

$$\Delta\text{H}_{\text{complex.}}^{\text{sol}}(\text{radical} + \text{c. base}) = \text{H}^{\text{sol}}(\text{radical} + \text{c. base}) - \text{H}^{\text{sol}}(\text{radical}) - \text{H}^{\text{sol}}(\text{c. base}) \quad (9)$$

Hydrogen bond interactions with a complementary pair cause³⁰ inter- and intramolecular redistribution of charges: 1) in pairs G-C type guanine G is negatively charged, modified cytosine C is positively charged, while in A-U type pairs adenine A is positively charged, modified uracil U is negatively charged; 2) atomic charges in the corresponding radical on the spin-carrying atoms become more positive, which reduces the radical stability. (See NBO and Mulliken charges in SI) This effect is about +5-8 kJ mol^{-1} (CBS).

The 9mG...5dhm1mC complex should be considered separately, where the presence of a complementary base (9mG) blocks the resulting 5r_5dhm1mC radical from transferring an acidic proton from the spin-carrying $-C(OH)_2\bullet$ group to the 3N atom, which additionally increases the BDE(C-H) value by $+28 \text{ kJ mol}^{-1}$ (CBS).

These effects indicate that G-C type base pairs need to be detached from each other for a less energetically expensive oxidation. This is consistent with the structure of the TET2-DNA complex³¹, in which cytosine does not come into contact with guanine.

Conclusions

In the C and U derivatives, among the substituents in the 5th position, the following trend in BDE values is observed $5dhm- < 5hm- < 5m- < 5f-$ (where 5dhm is dihydroxymethyl, 5hm — hydroxymethyl, 5m — methyl, 5f — formyl). The presence or absence of the 1-methyl group has almost no effect on the calculated $BDE_{sol}(C-H)$ values. The charge effect is clearly visible: protonation increases $BDE_{sol}(C-H)$ in cytosine derivatives, while deprotonation decreases $BDE_{sol}(C-H)$ in uracil derivatives. In general, one explicit water molecule does not cause a large difference in the calculated BDE values. The presence of a complementary base increases the $BDE_{sol}(C-H)$ values in all studied modified nucleobases by $+6-8 \text{ kJ mol}^{-1}$. The relative position of the modified nucleobases on the $BDE_{sol}(C-H)$ scale is maintained even when a complementary base is attached. Consequently, base pairs (G-C) need to be detached from each other for a more facile C-H bond activation step.

Supporting Information Description

Supplementally information is attached as a separate document.

Acknowledgment

Thanks to SFB1309 for financial support.

References

- [1] E. Gibney, C. Nolan, *Heredity* **2010**, *105*, 4.
- [2] K. D. Rasmussen, K. Helin, *Genes Dev.* **2016**, *30*, 733.
- [3] S. Schiesser, T. Pfaffeneder, K. Sadeghian, B. Hackner, B. Steigenberger, A. S. Schröder, J. Steinbacher, G. Kashiwazaki, G. Höfner, K. T. Wanner, C. Ochsenfeld, T. Carell, *J. Am. Chem. Soc.* **2013**, *135*, 14593.
- [4] N. S. Jonasson, L. J. Daumann, *Chem. Eur. J.* **2019**, *25*, 12091.
- [5] L. Hu, J. Lu, J. Cheng, Q. Rao, Z. Li, H. Hou, Z. Lou, L. Zhang, W. Li, W. Gong, *Nature* **2015**, *527*, 118.
- [6] F. L. Zott, V. Korotenko, H. Zipse, *ChemBioChem* **2022**, *23*, e202100651.
- [7] S. Ganguly, K. K. Kundu, *Can. J. Chem.* **1994**, *72*, 1120.
- [8] J.-Y. Salpin, S. Guillaumont, J. Tortajada, L. Mac Aleese, J. Lemaire, P. Maitre, *ChemPhysChem* **2007**, *8*, 2235.
- [9] A. K. Chandra, M. T. Nguyen, T. Zeegers-Huyskens, *J. Phys. Chem. A* **1998**, *102*, 6010.
- [10] A. Semmeq, M. Badawi, A. Hasnaoui, S. Ouaskit, A. Monari, *Eur. J. Chem.* **2020**, *26*, 11340-11344.
- [11] C. Colominas, F. J. Luque, M. Orozco, *J. Am. Chem. Soc.* **1996**, *118*, 6811.
- [12] G. R. Pack, L. Wong, G. Lamm, *Int. J. Quantum Chem* **1998**, *70*, 1177.
- [13] Y.-R. Luo. Comprehensive handbook of chemical bond energies; CRC press, **2007**.

- [14] S. J. Blanksby, G. B. Ellison, *Acc. Chem. Res.* **2003**, *36*, 255.
- [15] E. G. Bakalbassis, A. T. Lithoxoidou, A. P. Vafiadis, *J. Phys. Chem. A* **2003**, *107*, 8594.
- [16] C. J. Cramer, D. G. Truhlar, *Chemical Reviews* **1999**, *99*, 2161.
- [17] Gaussian 09, Revision A.02, M. J. Frisch, G. W. Trucks, H. B. Schlegel, G. E. Scuseria, M. A. Robb, J. R. Cheeseman, G. Scalmani, V. Barone, G. A. Petersson, H. Nakatsuji, X. Li, M. Caricato, A. Marenich, J. Bloino, B. G. Janesko, R. Gomperts, B. Mennucci, et. al. *Gaussian, Inc., Wallingford CT*, **2016**.
- [18] S. Grimme, J. Antony, S. Ehrlich, H. Krieg, *J. Chem. Phys.* **2010**, *132*, 154104.
- [19] A. V. Marenich, C. J. Cramer, D. G. Truhlar, *J. Phys. Chem. B* **2009**, *113*, 6378.
- [20] V. Korotenko, <https://github.com/vnkorotenko/ess>.
- [21] V. Korotenko, <https://github.com/vnkorotenko/ccs>.
- [22] G. Luchini, J. V. Alegre-Requena, I. Funes-Ardoiz, R. S. Paton, *F1000Research* **2020**, *9*, 291.
- [23] A. Altun, F. Neese, G. Bistoni, *J. Chem. Theory Comput.* **2018**, *15*, 215.
- [24] F. Neese, E. F. Valeev, *J. Chem. Theory Comput.* **2011**, *7*, 33.
- [25] M. Saitow, U. Becker, C. Riplinger, E. F. Valeev, F. Neese, *J. Chem. Phys.* **2017**, *146*, 164105.
- [26] A. Altun, F. Neese, G. Bistoni, *Beilstein J. Org. Chem.* **2018**, *14*, 919.
- [27] M. Saunders, *J. Comput. Chem.* **2004**, *25*, 621.
- [28] D. Šakić, V. Vrček, *J. Phys. Chem. A* **2012**, *116*, 1298.
- [29] D. Šakić, <https://kick.science/KICK.html>.
- [30] C. Fonseca Guerra, F. M. Bickelhaupt, J. G. Snijders, E. J. Baerends, *Chem. Eur. J.* **1999**, *5*, 3581.
- [31] L. Hu, Z. Li, J. Cheng, Q. Rao, W. Gong, M. Liu, Y. G. Shi, J. Zhu, P. Wang, Y. Xu, *Cell* **2013**, *155*, 1545.

4.2

Supplementary Information

The Redox Properties of Cytosine derivatives:
CH Bond Dissociation Energies

1. General Results

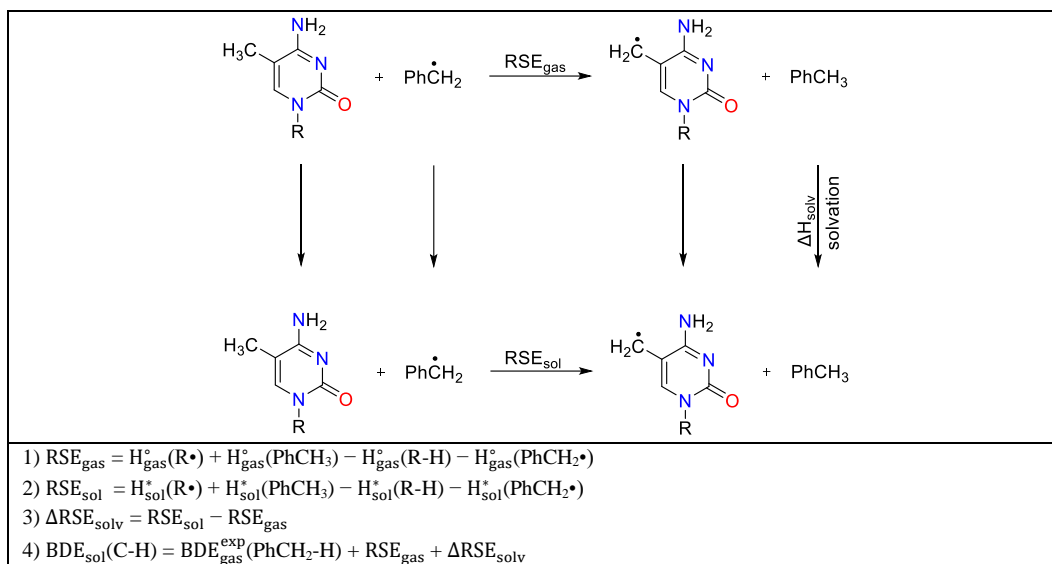


Figure 1.1.1. Thermodynamic cycle used in the calculation of BDE.

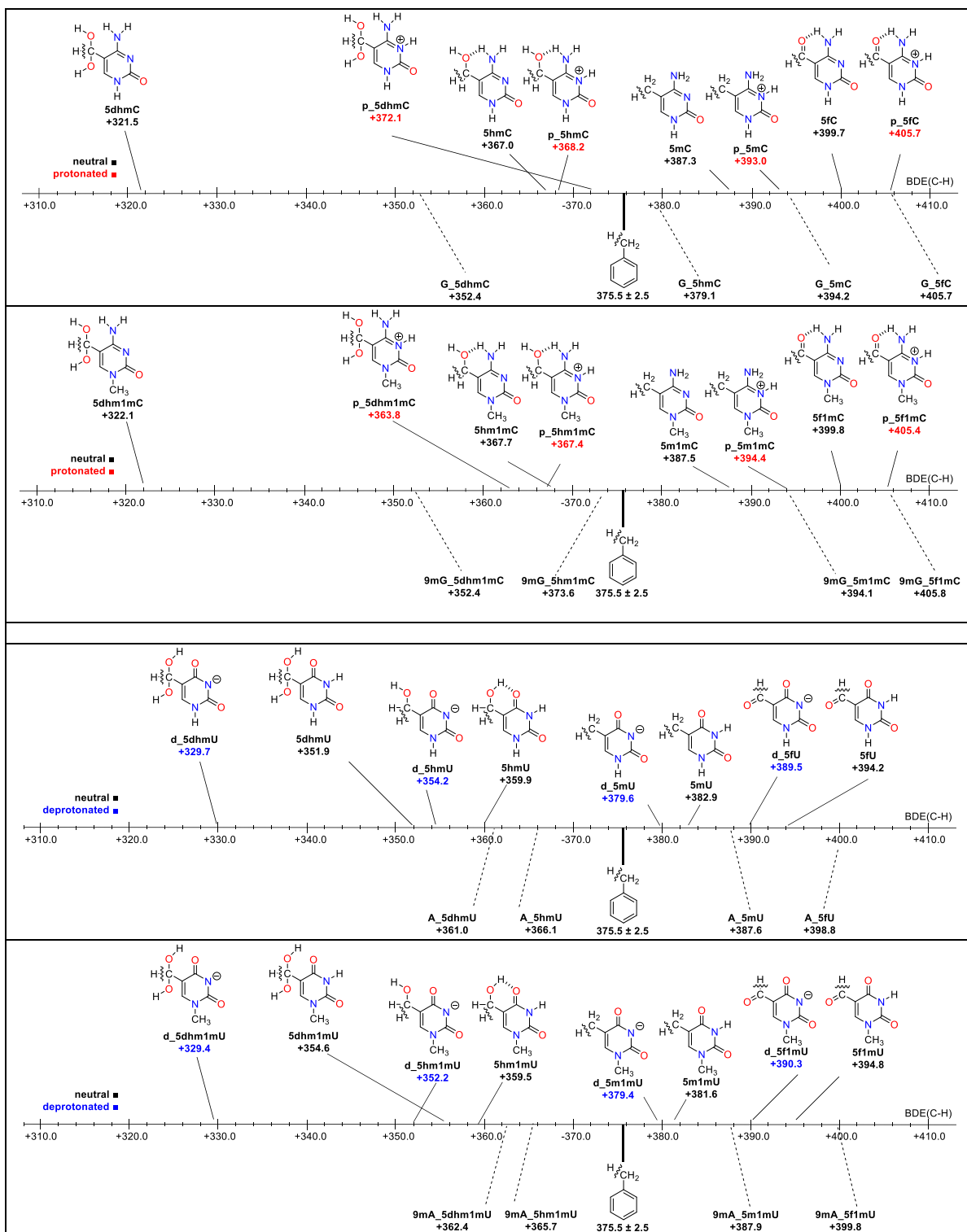


Figure 1.2.1. The Boltzmann averaged BDE(C-H) values in kJ mol⁻¹ at 298.15 K without explicit water calculated at the SMD(H₂O)/DLPNO-CCSD(T)/CBS//SMD(H₂O)/(U)B3LYP-D3/6-31+G(d,p) level of theory.

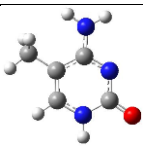
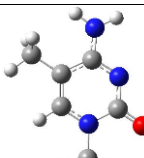
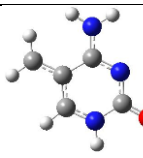
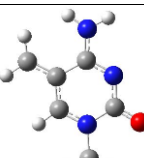
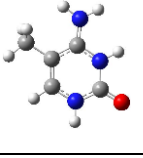
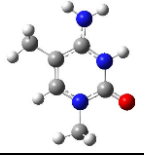

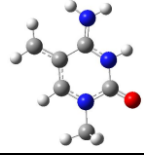

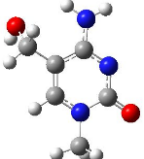

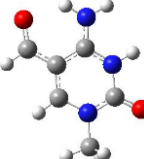
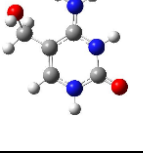
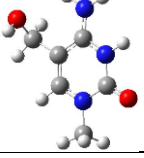
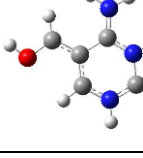

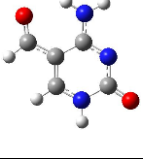
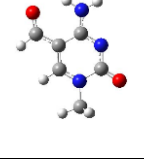
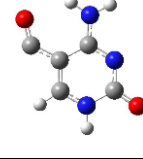
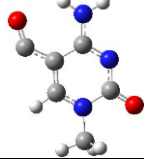
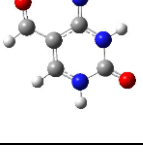
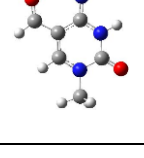
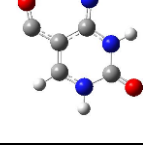
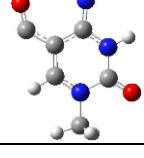
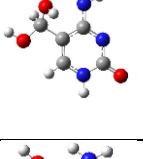
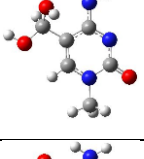
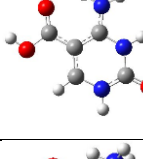
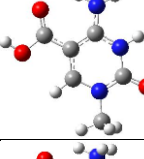
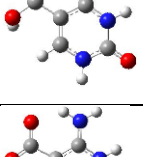
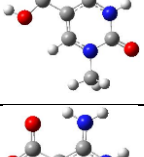
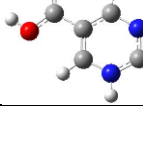
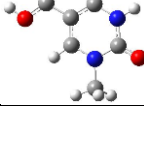
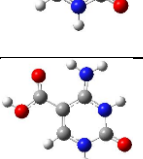
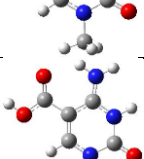
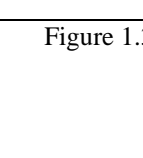
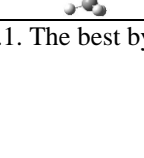
5-Sub.	q	-H	-CH ₃		-H	-CH ₃	-H	-CH ₃	-H	-CH ₃
		Molecule	Molecule		Radical	Radical	BDE DFT		BDE CBS	
m-	-1									
	0						381.2	380.5	387.3	387.5
	1						388.3	389.0	393.0	394.4
hm-	-1									
	0						355.6	355.0	367.0	367.7
	1						358.6	357.4	368.2	367.4
f-	-1									
	0						398.1	397.7	399.7	399.8
	1						405.0	404.3	405.7	405.4
dhm-	-1									
	0						304.2	304.6	321.5	322.1
	1						353.9	358.4	372.1	363.8
ca-	0									
										

Figure 1.3.1. The best by DFT-H* calculated C-structures and their BDE(C-H).

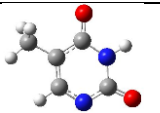
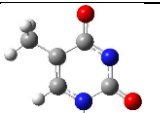
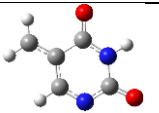
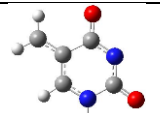
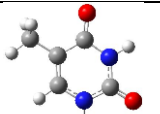

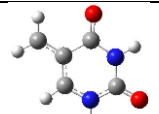


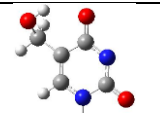
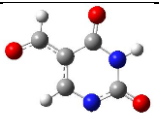
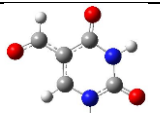
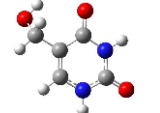

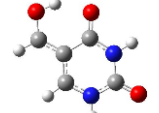
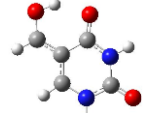

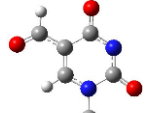



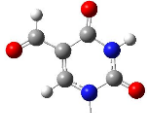
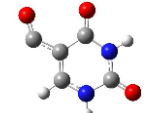





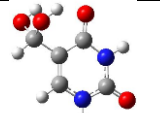
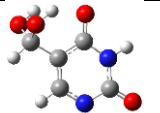



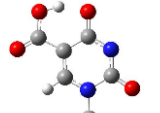
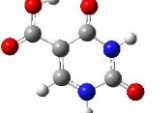

5-Sub.	q	-H	-CH ₃		-H	-CH ₃	-H	-CH ₃	-H	-CH ₃
							BDE		BDE	
		Molecule	Molecule		Radical	Radical	DFT		CBS	
m-	-1						370.6	371.4	379.6	379.4
	0						378.1	376.7	382.9	381.6
	1									
hm-	-1						333.2	324.6	354.2	352.2
	0						346.7	347.2	359.9	359.5
	1									
f-	-1						388.4	386.4	389.5	390.3
	0						392.4	392.5	394.2	394.8
	1									
dhm-	-1						306.3	305.0	329.7	329.4
	0						336.8	341.2	351.9	354.6
	1									
	-1									
ca-	0									

Figure 1.3.2. The best by DFT-H* calculated U-structures and their BDE(C-H).

Table 1.4.1. Structures (best by DFT-H*) and the calculated BDE values. Mulliken charges (above) and spin densities (below).

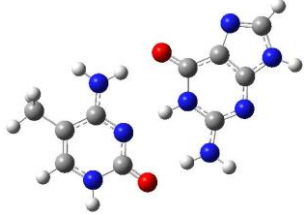
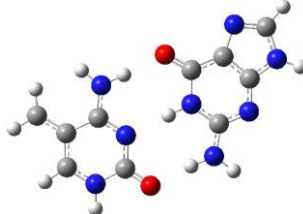
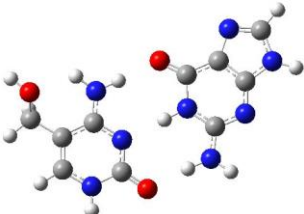
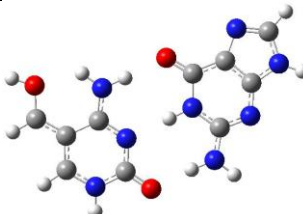
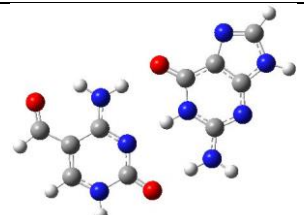
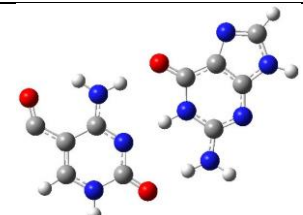
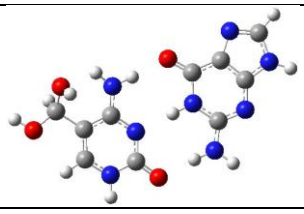
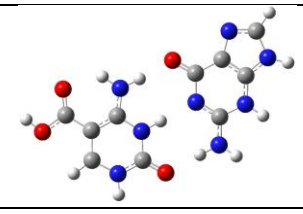
5-Sub.	Substrate	Product	BDE	BDE
	Best str.	Best str.	DFT	CBS
m			381.7	394.2
	G_5mC1	G_r5mC1		
	0.0395 -0.0395 0.0000 0.0000	0.0330 -0.0330 0.9999 0.0001		
hm			361.0	379.1
	G_5hmC1	G_r5hmC1		
	0.0347 -0.0347 0.0000 0.0000	0.0284 -0.0284 0.9997 0.0003		
f			397.9	405.7
	G_5fC1	G_r5fC1		
	0.0241 -0.0241 0.0000 0.0000	0.0213 -0.0213 0.9988 0.0012		
dhm			333.4	352.4
	G_5dhmC1	G_r5dhmC1liss		
	0.0312 -0.0312 0.0000 0.0000	-0.0823 0.0823 1.0025 -0.0025		

Table 1.4.2. Structures (best by DFT-H*) and the calculated BDE values. Mulliken charges (above) and spin densities (below).

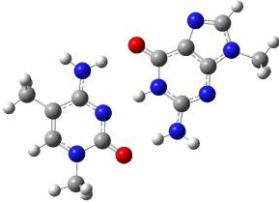
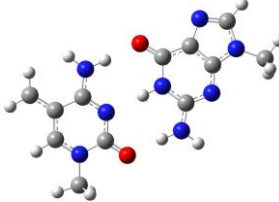
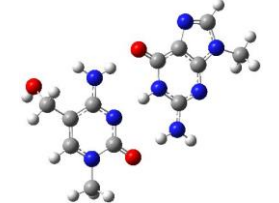
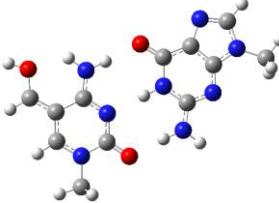
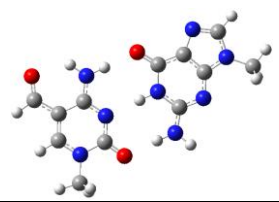
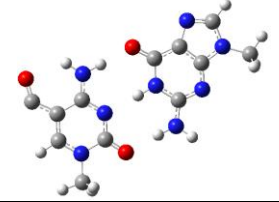
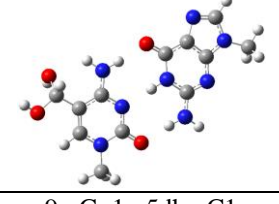
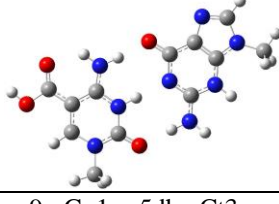
5-Sub.	Substrate	Product	BDE	BDE
	Best str.	Best str.	DFT	CBS
m			380.7	394.1
	9mG_1m5mC	9mG_1mr5mC		
	0.0251 -0.0251 0.0000 0.0000	0.0211 -0.0211 0.9998 0.0002		
hm			357.7	373.6
	9mG_1m5hmCh	9mG_1mr5hmC1		
	0.0267 -0.0267 0.0000 0.0000	0.0173 -0.0173 0.9998 0.0002		
f			396.8	405.8
	9mG_1m5fC	9mG_1mr5fC		
	0.0165 -0.0165 0.0000 0.0000	0.0147 -0.0147 0.9976 0.0024		
dhm			332.2	352.4
	9mG_1m5dhmC1	9mG_1mr5dhmCt3ss		
	0.0213 -0.0213 0.0000 0.0000	-0.0951 0.0951 0.9985 0.0015		

Table 1.4.3. Structures (best by DFT-H*). Mulliken charges (left column) and spin densities (right column).

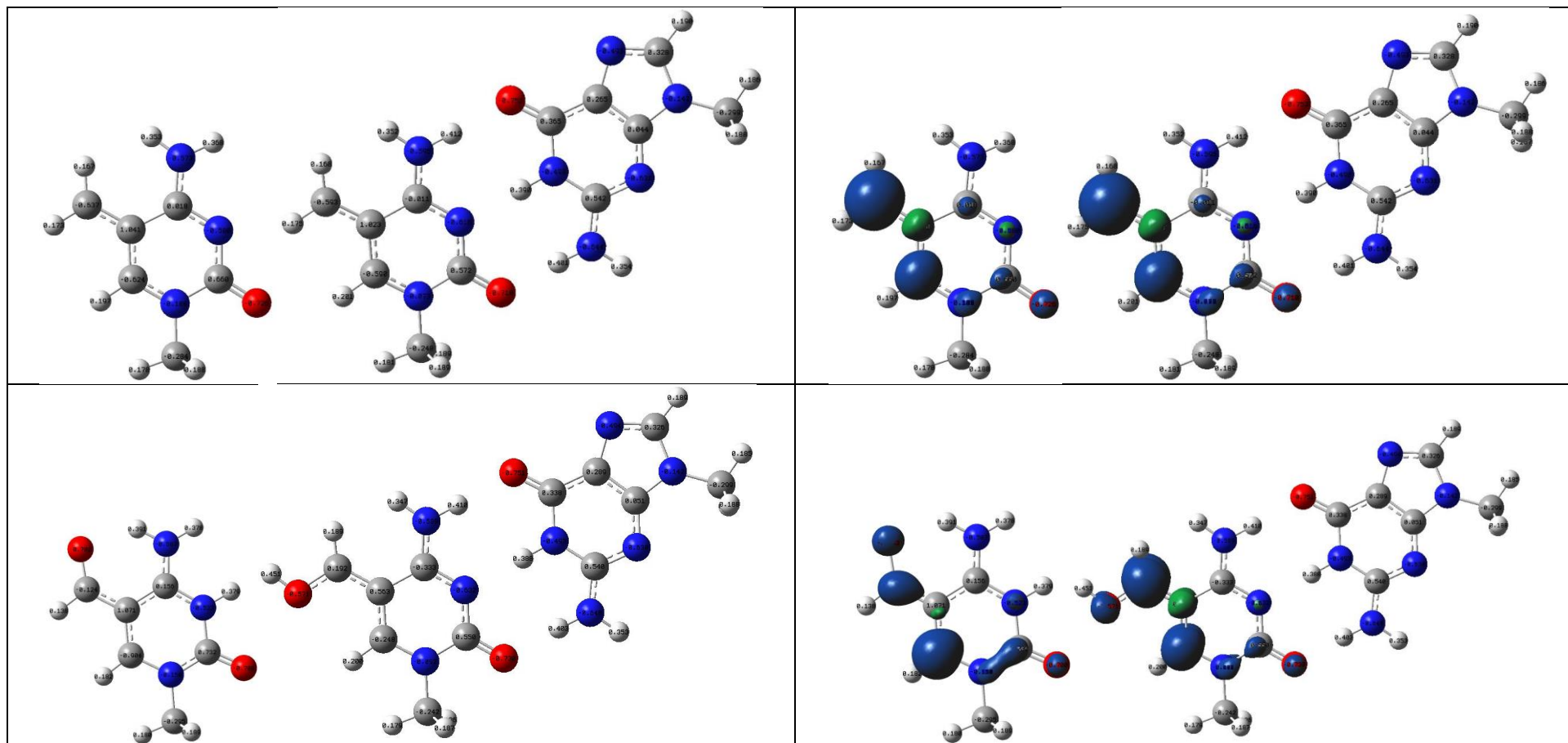


Table 1.4.3. Structures (best by DFT-H*). Mulliken charges (left column) and spin densities (right column).

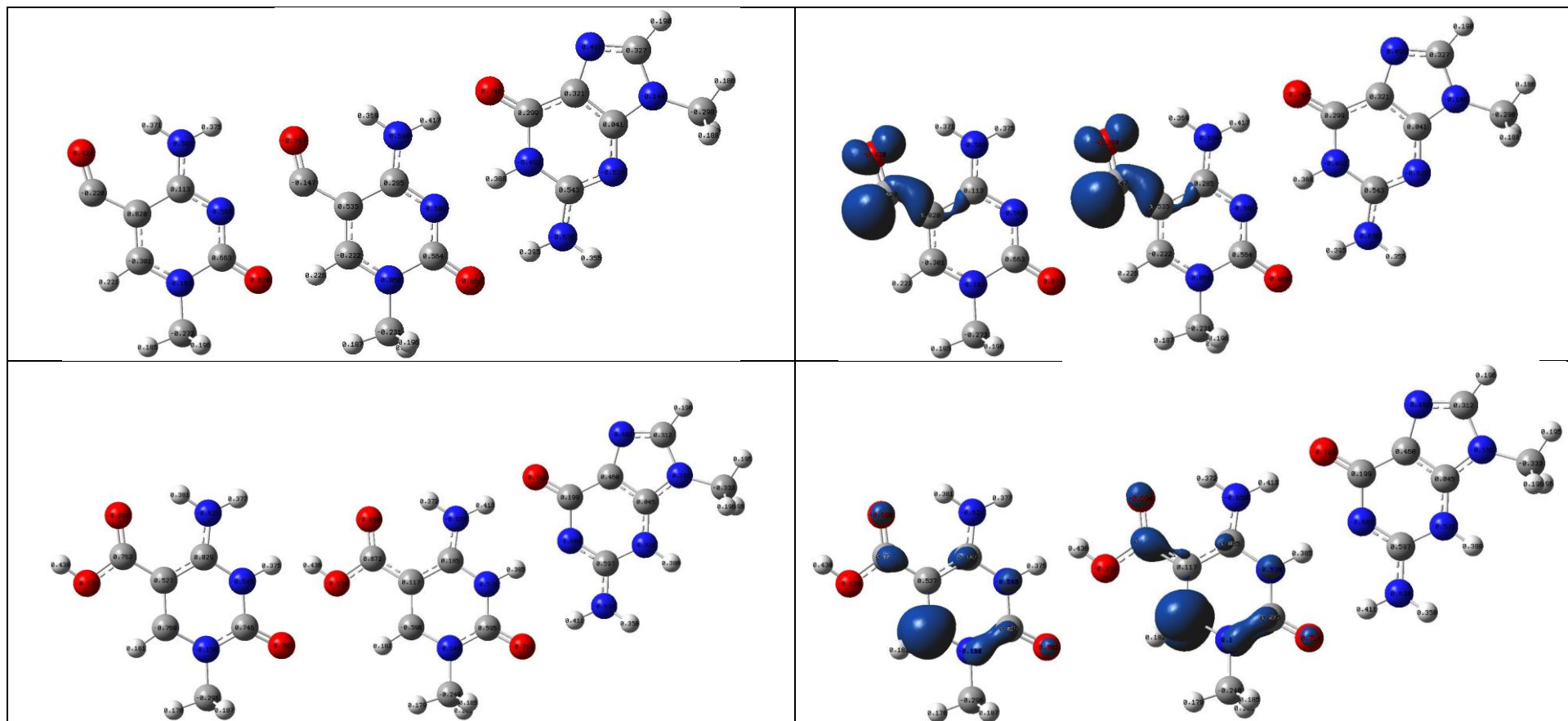


Table 1.4.4. Structures (best by DFT-H*). NBO charges (left column) and spin densities (right column).

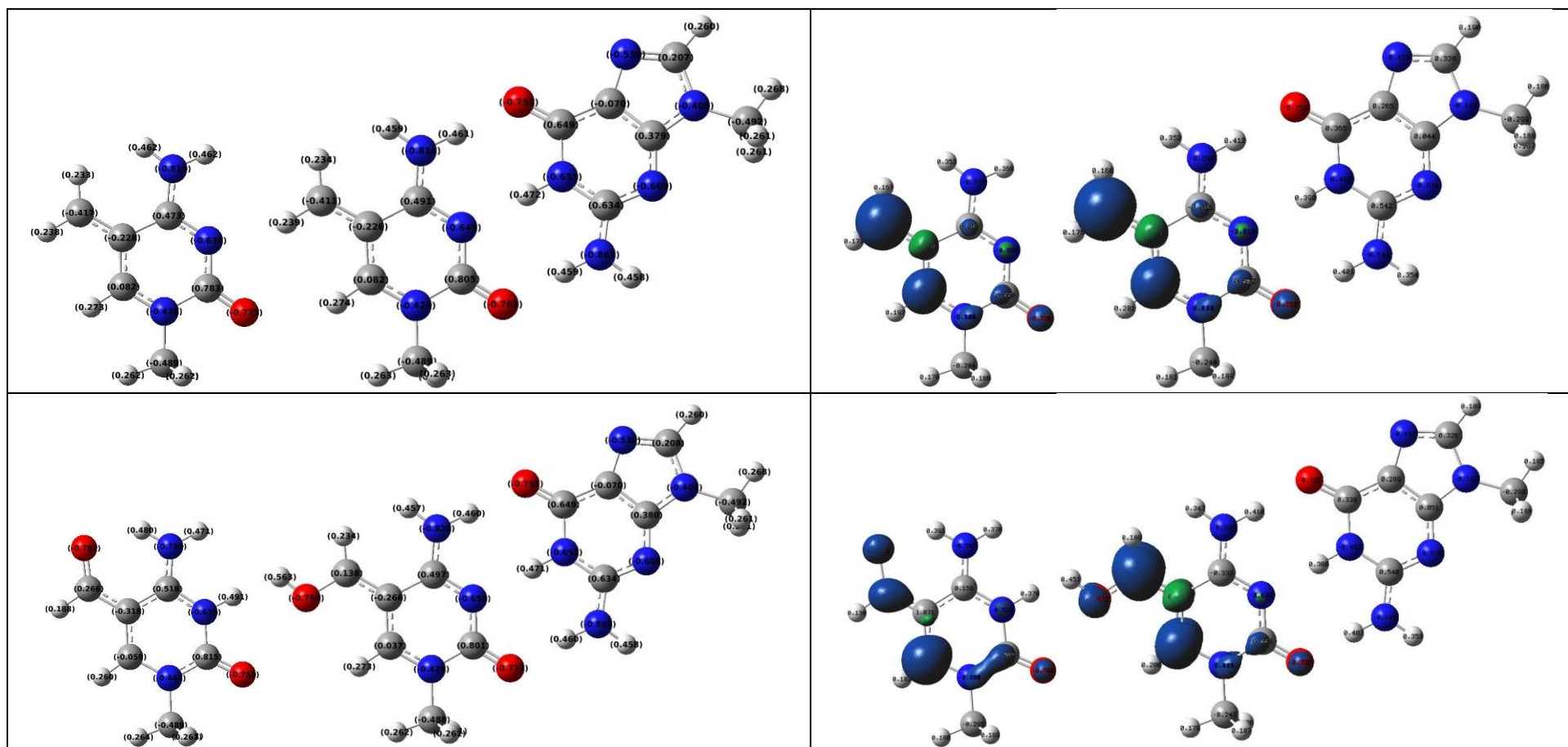
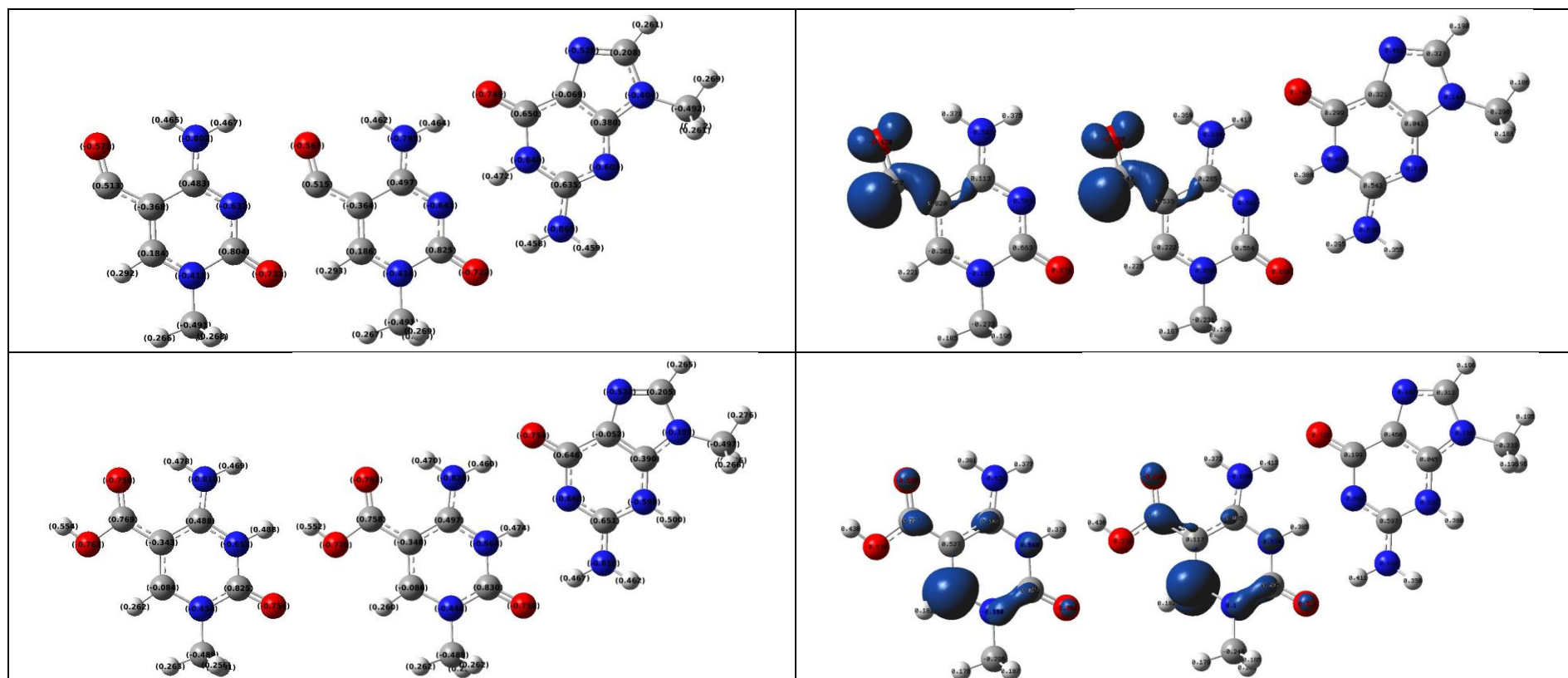


Table 1.4.4. Structures (best by DFT-H*). NBO charges (left column) and spin densities (right column).



LINK
 /scr7/vasily/DNA/1mC/
 /scr7/vasily/DNA/1mU/
 /scr7/vasily/DNA/9mG_1mC/
 /scr7/vasily/DNA/9mA_1mU/

Table 1.5.1. Structures (best by DFT-H*) and the calculated BDE values. Mulliken charges (above) and spin densities (below).

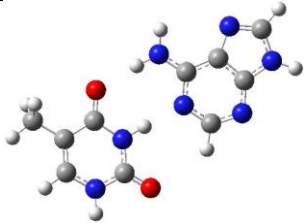
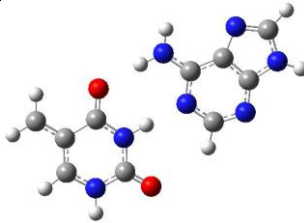
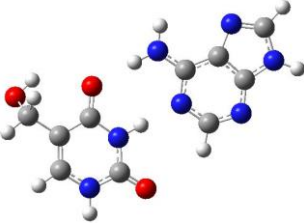
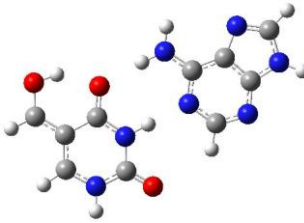
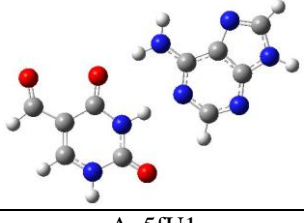
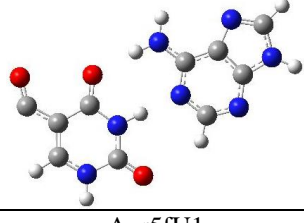
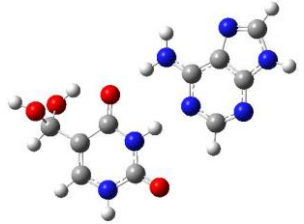
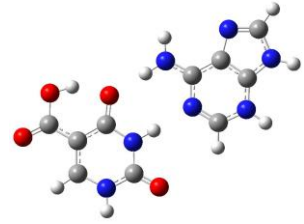
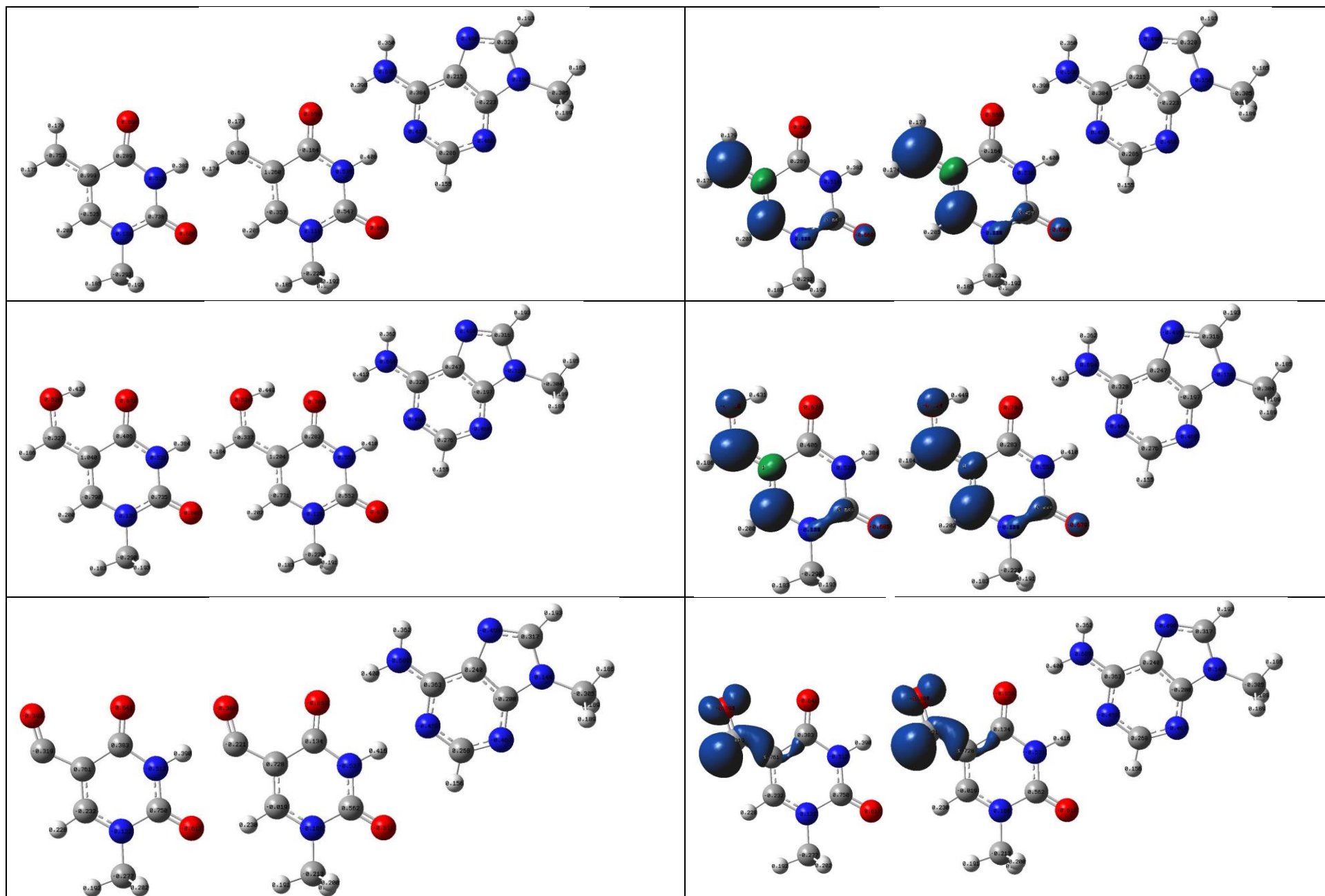
5-Sub.	Substrate	Product	BDE	
	Best str.	Best str.	DFT	CBS
m			377.5	387.6
	A_T1	A_r5mU1		
hm			349.0	366.1
	A_5hmU1	A_r5hmU21		
f			391.8	398.8
	A_5fU1	A_r5fU1		
dhm			339.7	361.0
	A_5dhmU1	A_r5dhmU1s7		

Table 1.5.2. Structures (best by DFT-H*) and the calculated BDE values. Mulliken charges (above) and spin densities (below).

5-Sub.	Substrate	Product	BDE	
	Best str.	Best str.	DFT	CBS
m			377.0	387.9
	9mA_1mT	9mA_1mr5mU		
	-0.0775 0.0775 0.0000 0.0000	-0.0783 0.0783 0.9997 0.0003		
hm			348.1	365.7
	9mA_1m5hmU	9mA_1mr5hmU1		
	-0.0788 0.0788 0.0000 0.0000	-0.0762 0.0762 0.9995 0.0005		
f			391.2	399.8
	9mA_1m5fU1	9mA_1mr5fU		
	-0.0859 0.0859 0.0000 0.0000	-0.0859 0.0859 0.9980 0.0020		
dhm			339.5	362.4
	9mA_1m5dhmU1	9mA_1mr5dhmU_3iss		
	-0.0884 0.0885 0.0000 0.0000			

Table 1.5.3. Structures (best by DFT-H*). Mulliken charges (left column) and spin densities (right column).



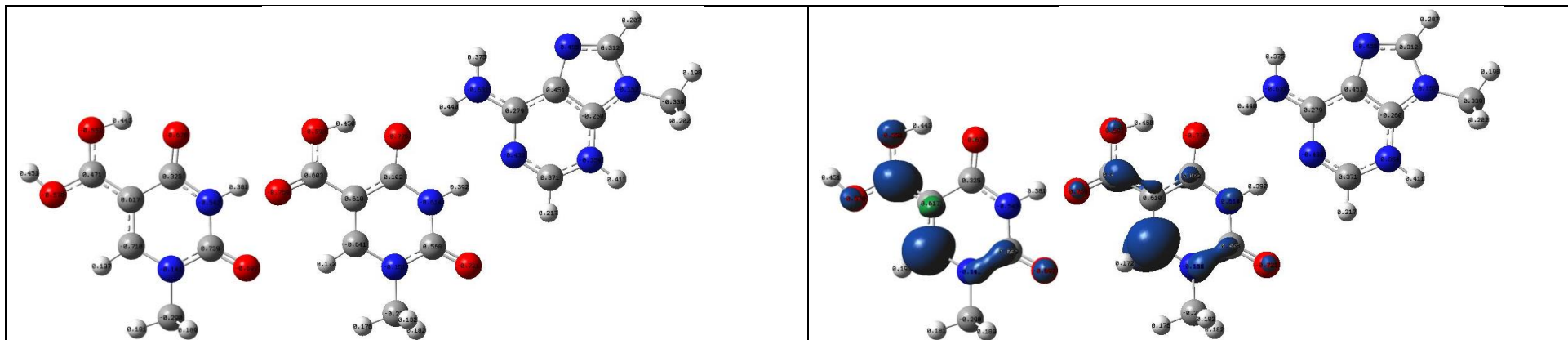
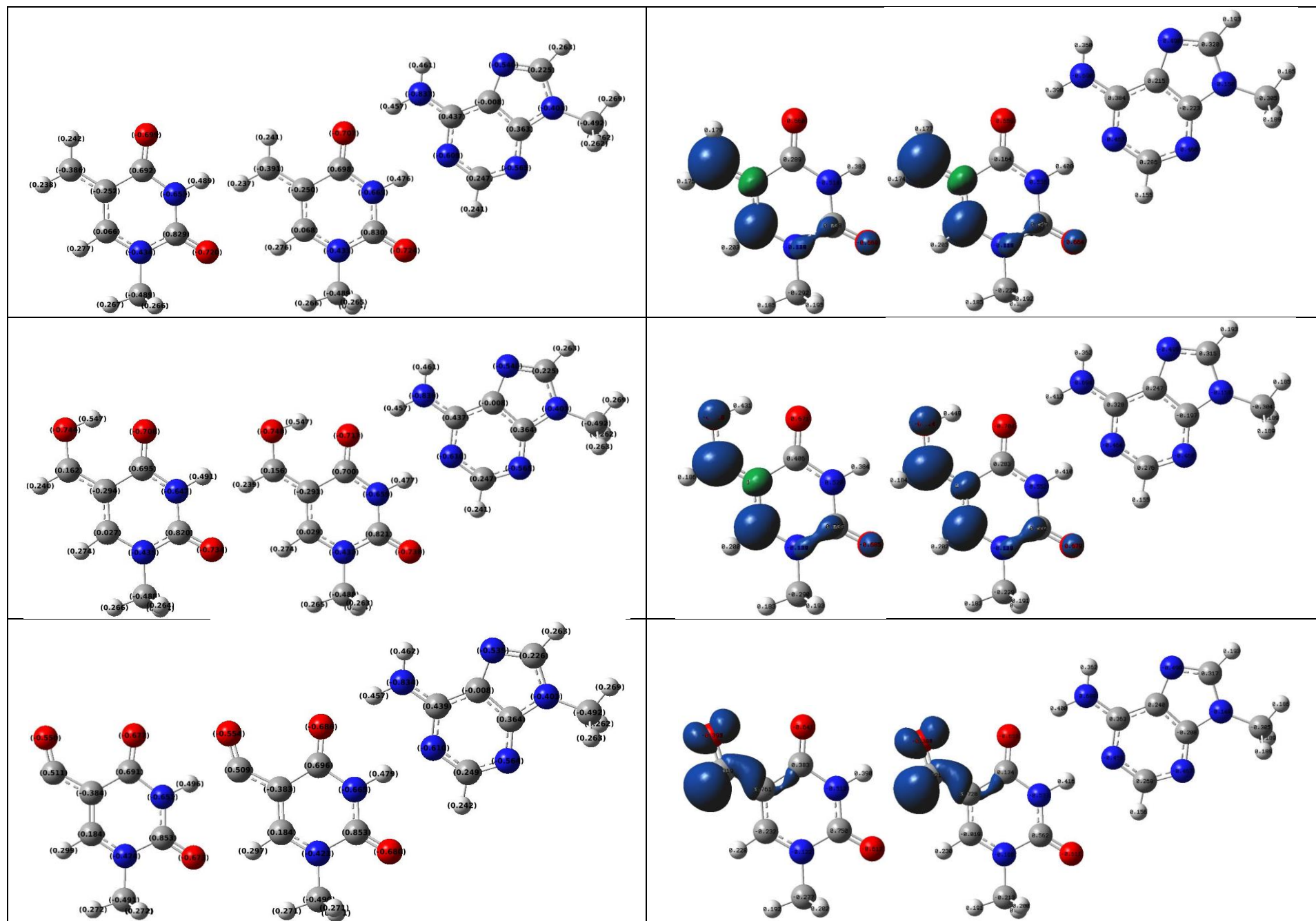
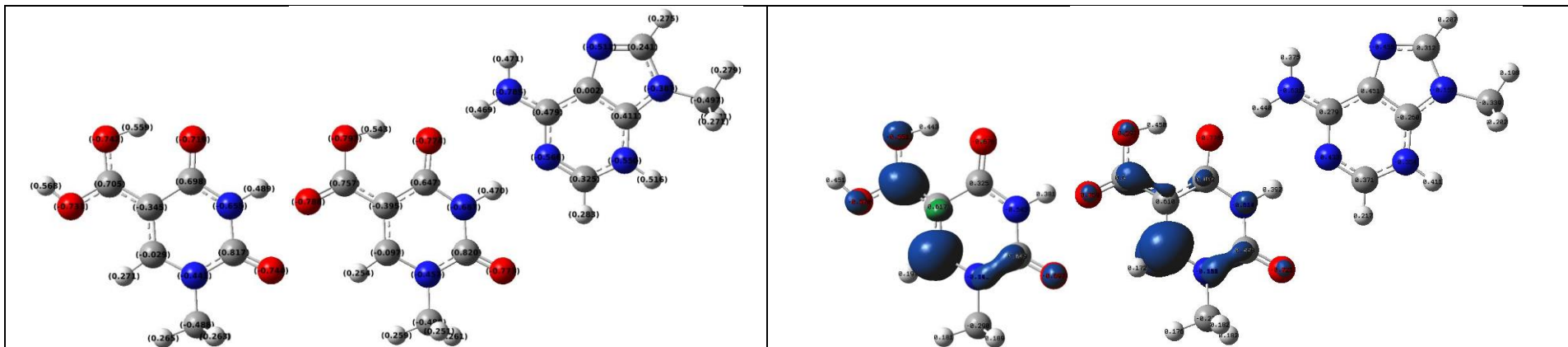


Table 1.5.4. Structures (best by DFT-H*). NBO charges (left column) and spin densities (right column).





LINK
 /scr7/vasily/DNA/1mC/
 /scr7/vasily/DNA/1mU/
 /scr7/vasily/DNA/9mG_1mC/
 /scr7/vasily/DNA/9mA_1mU/

2. Detailed results

Table 2.1.1. The Boltzmann averaged RSE and BDE values calculated at the (U)B3LYP-D3 and DLPNO-CCSD(T) level of theory for the systems **WITHOUT** the addition of explicit water. (Quasi-Harmonic Approximation) (kJ/mol)

Molecule	Net Charge	Multipl	RSE/BDE	SMD/(U)B3LYP-D3/6-31+G(d,p)		DLPNO-CCSD(T)/BASIS// SMD/(U)B3LYP-D3/6-31+G(d,p)						
					Single Point Wihout SMD		cc-pVTZ	cc-pVQZ	CBS	cc-pVTZ	cc-pVQZ	CBS
				solution	gas	solution	gas	gas	gas	solution	solution	solution
				ΔH_{298}	ΔH_{298}	$\Delta \Delta H_{SOLV}$ = ΔRSE_{SOLV}	ΔH_{298}	ΔH_{298}	ΔH_{298}	ΔH_{298} + ΔRSE_{SOLV}	ΔH_{298} + ΔRSE_{SOLV}	ΔH_{298} + ΔRSE_{SOLV}
5mC	0	1	RSE	5.7	0.8	4.9	10.8	10.8	10.8	11.0	11.5	11.8
			BDE	381.2	376.3		386.3	386.3	386.3	386.5	387.0	387.3
p_5mC	1	1	RSE	12.8	13.4	-0.6	17.4	17.8	17.9	16.8	17.3	17.5
			BDE	388.3	388.9		392.9	393.3	393.4	392.3	392.8	393.0
5hmC	0	1	RSE	-19.9	-42.0	22.1	11.7	9.9	8.8	-7.0	-8.3	-8.5
			BDE	355.6	333.5		387.2	385.4	384.3	368.5	367.2	367.0
p_5hmC	1	1	RSE	-16.9	-37.5	20.6	-3.2	-2.4	-1.9	-6.8	-7.4	-7.3
			BDE	358.6	338.0		372.3	373.1	373.6	368.7	368.1	368.2
5fC	0	1	RSE	22.6	12.0	10.6	21.6	22.4	23.0	22.1	23.4	24.2
			BDE	398.1	387.5		397.1	397.9	398.5	397.6	398.9	399.7
p_5fC	1	1	RSE	29.5	25.2	4.3	25.2	26.1	26.8	28.4	29.4	30.2
			BDE	405.0	400.7		400.7	401.6	402.3	403.9	404.9	405.7
5dhmC	0	1	RSE	-71.3	-108.5	37.2	-44.4	-46.7	-48.0	-53.5	-53.4	-54.0
			BDE	304.2	267.0		331.1	328.8	327.5	322.0	322.1	321.5
p_5dhmC	1	1	RSE	-21.6	-30.7	9.2	-7.0	-7.1	-6.8	-17.9	-3.6	-3.4
			BDE	353.9	344.8		368.5	368.4	368.7	357.6	371.9	372.1

Table 2.1.2. The Boltzmann averaged RSE and BDE values calculated at the (U)B3LYP-D3 and DLPNO-CCSD(T) level of theory for the systems **WITHOUT** the addition of explicit water. (Quasi-Harmonic Approximation) (kJ/mol)

Molecule	Net Charge	Multipl	RSE/BDE	SMD/(U)B3LYP-D3/6-31+G(d,p)		DLPNO-CCSD(T)/BASIS// SMD/(U)B3LYP-D3/6-31+G(d,p)						
					Single Point Wihout SMD		cc-pVTZ	cc-pVQZ	CBS	cc-pVTZ	cc-pVQZ	CBS
				solution	gas	solvation	gas	gas	gas	solution	solution	solution
				ΔH_{298}	ΔH_{298}	$\Delta \Delta H_{SOLV}$ = ΔRSE_{SOLV}	ΔH_{298}	ΔH_{298}	ΔH_{298}	ΔH_{298} + ΔRSE_{SOLV}	ΔH_{298} + ΔRSE_{SOLV}	ΔH_{298} + ΔRSE_{SOLV}
1m5mC	0	1	RSE	5.0	-3.4	8.4	11.0	11.6	12.0	11.0	11.6	12.0
			BDE	380.5	372.1		386.5	387.1	387.5	386.5	387.1	387.5
p_1m5mC	1	1	RSE	13.5	12.9	0.7	18.8	19.0	19.2	18.4	18.7	18.9
			BDE	389.0	388.4		394.3	394.5	394.7	393.9	394.2	394.4
1m5hmC	0	1	RSE	-20.5	-46.1	25.6	0.1	0.1	-0.2	-6.7	-6.9	-7.8
			BDE	355.0	329.4		375.6	375.6	375.3	368.8	368.6	367.7
p_1m5hmC	1	1	RSE	-18.1	-37.6	19.6	-4.8	-3.4	-3.5	-7.9	-12.3	-8.1
			BDE	357.4	337.9		370.7	372.1	372.0	367.6	363.2	367.4
1m5fC	0	1	RSE	22.2	8.3	13.9	22.0	23.4	24.3	22.1	23.4	24.3
			BDE	397.7	383.8		397.5	398.9	399.8	397.6	398.9	399.8
p_1m5fC	1	1	RSE	28.8	24.3	4.5	25.2	26.4	27.5	28.0	28.5	29.9
			BDE	404.3	399.8		400.7	401.9	403.0	403.5	404.0	405.4
1m5dhmC	0	1	RSE	-70.9	-104.8	33.9	-53.7	-55.1	-55.9	-51.3	-52.4	-53.4
			BDE	304.6	270.7		321.8	320.4	319.6	324.2	323.1	322.1
p_1m5dhmC	1	1	RSE	-17.1	-25.8	8.7	-3.4	-2.4	-3.1	-12.9	-12.2	-11.7
			BDE	358.4	349.7		372.1	373.1	372.4	362.6	363.3	363.8

Table 2.1.3. The Boltzmann averaged RSE and BDE values calculated at the (U)B3LYP-D3 and DLPNO-CCSD(T) level of theory for the systems **WITH** the addition of explicit water. (Quasi-Harmonic Approximation)
(kJ/mol)

Molecule	Net Charge	Multipl	RSE/BDE	SMD/(U)B3LYP-D3/6-31+G(d,p)		DLPNO-CCSD(T)/BASIS// SMD/(U)B3LYP-D3/6-31+G(d,p)						
					Single Point Wihout SMD		cc-pVTZ	cc-pVQZ	CBS	cc-pVTZ	cc-pVQZ	CBS
				solution	gas	solvation	gas	gas	gas	solution	solution	solution
				ΔH_{298}	ΔH_{298}	$\Delta \Delta H_{SOLV}$ = ΔRSE_{SOLV}	ΔH_{298}	ΔH_{298}	ΔH_{298}	ΔH_{298} + ΔRSE_{SOLV}	ΔH_{298} + ΔRSE_{SOLV}	ΔH_{298} + ΔRSE_{SOLV}
1m5mC	0	1	RSE	5.3	-5.4	10.7	20.5	14.4	5.9	1.7	12.4	9.2
			BDE	380.8	370.1		396.0	389.9	381.4	377.2	387.9	384.7
p_1m5mC	1	1	RSE	11.7	13.7	-1.9	16.7	17.1	17.3	17.5	17.9	18.2
			BDE	387.2	389.2		392.2	392.6	392.8	393.0	393.4	393.7
1m5hmC	0	1	RSE	-20.7	-43.9	23.2	-6.7	-3.4	-1.9	-12.9	-12.5	-11.7
			BDE	354.8	331.6		368.8	372.1	373.6	362.6	363.0	363.8
p_1m5hmC	1	1	RSE	-19.1	-29.0	9.9	-6.7	-5.9	-5.5	-5.9	-5.9	-5.9
			BDE	356.4	346.5		368.8	369.6	370.0	369.6	369.6	369.6
1m5fC	0	1	RSE	30.7	20.5	10.2	29.3	31.3	32.5	28.9	30.8	32.1
			BDE	406.2	396.0		404.8	406.8	408.0	404.4	406.3	407.6
p_1m5fC	1	1	RSE	28.2	21.9	6.2	27.7	29.0	29.9	25.2	26.8	27.9
			BDE	403.7	397.4		403.2	404.5	405.4	400.7	402.3	403.4
1m5dhmC	0	1	RSE	-69.4	-105.8	36.4	-59.5	-58.5	-58.1	-49.1	-52.1	-51.6
			BDE	306.1	269.7		316.0	317.0	317.4	326.4	323.4	323.9
p_1m5dhmC	1	1	RSE	-27.4	-28.5	1.1	-10.9	-10.8	-10.9	-15.3	-14.8	-17.4
			BDE	348.1	347.0		364.6	364.7	364.6	360.2	360.7	358.1

Table 2.1.4. The Boltzmann averaged Δ RSE and Δ BDE values calculated at the (U)B3LYP-D3 and DLPNO-CCSD(T) level of theory as difference in RSE and BDE values between systems **WITH** and **WITHOUT** the addition of explicit water. (Quasi-Harmonic Approximation) (kJ/mol)

Molecule	Net Charge	Multipl	Δ RSE/ Δ BDE	SMD/(U)B3LYP-D3/6-31+G(d,p)		DLPNO-CCSD(T)/BASIS// SMD/(U)B3LYP-D3/6-31+G(d,p)						
					Single Point Without SMD		cc-pVTZ	cc-pVQZ	CBS	cc-pVTZ	cc-pVQZ	CBS
				solution	gas	solvation	gas	gas	gas	solution	solution	solution
				$\Delta\Delta H_{298}$	$\Delta\Delta H_{298}$	$\Delta\Delta\Delta H_{SOLV}$ = $\Delta\Delta RSE_{SOLV}$	$\Delta\Delta H_{298}$	$\Delta\Delta H_{298}$	$\Delta\Delta H_{298}$	$\Delta\Delta H_{298}$ + $\Delta\Delta RSE_{SOLV}$	$\Delta\Delta H_{298}$ + $\Delta\Delta RSE_{SOLV}$	$\Delta\Delta H_{298}$ + $\Delta\Delta RSE_{SOLV}$
1m5mC	0	1	Δ RSE/ Δ BDE	0.4	-2.0	0.0	9.4	2.9	-6.1	-9.3	0.8	-2.8
p_1m5mC	1	1	Δ RSE/ Δ BDE	-1.8	0.8	0.0	-2.2	-2.0	-1.9	-0.8	-0.8	-0.7
1m5hmC	0	1	Δ RSE/ Δ BDE	-0.2	2.1	0.0	-6.8	-3.5	-1.8	-6.1	-5.7	-3.9
p_1m5hmC	1	1	Δ RSE/ Δ BDE	-1.0	8.6	0.0	-1.9	-2.6	-2.1	2.0	6.4	2.2
1m5fC	0	1	Δ RSE/ Δ BDE	8.5	12.2	0.0	7.2	7.9	8.2	6.9	7.4	7.8
p_1m5fC	1	1	Δ RSE/ Δ BDE	-0.6	-2.4	0.0	2.5	2.6	2.4	-2.8	-1.7	-2.0
1m5dhmC	0	1	Δ RSE/ Δ BDE	1.5	-1.0	0.0	-5.8	-3.4	-2.2	2.2	0.2	1.8
p_1m5dhmC	1	1	Δ RSE/ Δ BDE	-10.3	-2.8	0.0	-7.5	-8.5	-7.8	-2.4	-2.7	-5.7

Table 2.2.1. The Boltzmann averaged RSE and BDE values calculated at the (U)B3LYP-D3 and DLPNO-CCSD(T) level of theory for the systems **WITHOUT** the addition of explicit water. (Quasi-Harmonic Approximation) (kJ/mol)

Molecule	Net Charge	Multipl	RSE/BDE	SMD/(U)B3LYP-D3/6-31+G(d,p)		DLPNO-CCSD(T)/BASIS// SMD/(U)B3LYP-D3/6-31+G(d,p)						
					Single Point Wihout SMD		cc-pVTZ	cc-pVQZ	CBS	cc-pVTZ	cc-pVQZ	CBS
				solution	gas	solvation	gas	gas	gas	solution	solution	solution
				ΔH_{298}	ΔH_{298}	ΔRSE_{SOLV}	ΔH_{298}	ΔH_{298}	ΔH_{298}	ΔH_{298} + ΔRSE_{SOLV}	ΔH_{298} + ΔRSE_{SOLV}	ΔH_{298} + ΔRSE_{SOLV}
d_5mU	-1	1	RSE	-4.9	-20.5	15.6	-13.2	-12.6	-12.2	2.5	3.4	4.1
			BDE	370.6	355.0		362.3	362.9	363.3	378.0	378.9	379.6
5mU	0	1	RSE	2.6	-3.4	5.9	0.7	1.2	1.4	6.6	7.1	7.4
			BDE	378.1	372.1		376.2	376.7	376.9	382.1	382.6	382.9
d_5hmU	-1	1	RSE	-42.3	-45.6	3.4	-30.6	-28.4	-27.6	-22.8	-21.9	-21.3
			BDE	333.2	329.9		344.9	347.1	347.9	352.7	353.6	354.2
5hmU	0	1	RSE	-28.8	-48.7	19.9	-40.0	-37.8	-36.6	-18.6	-16.6	-15.6
			BDE	346.7	326.8		335.5	337.7	338.9	356.9	358.9	359.9
d_5fU	-1	1	RSE	12.9	7.9	5.0	5.7	6.7	7.5	12.2	13.3	14.0
			BDE	388.4	383.4		381.2	382.2	383.0	387.7	388.8	389.5
5fU	0	1	RSE	16.9	19.6	-2.8	15.9	17.3	18.5	16.7	17.9	18.7
			BDE	392.4	395.1		391.4	392.8	394.0	392.2	393.4	394.2
d_5dhmU	-1	1	RSE	-69.2	-99.2	30.0	-79.0	-77.1	-76.7	-47.6	-46.1	-45.8
			BDE	306.3	276.3		296.5	298.4	298.8	327.9	329.4	329.7
5dhmU	0	1	RSE	-38.7	-70.9	32.2	-57.0	-55.9	-55.4	-24.8	-23.9	-23.6
			BDE	336.8	304.6		318.5	319.6	320.1	350.7	351.6	351.9

Table 2.2.2. The Boltzmann averaged RSE and BDE values calculated at the (U)B3LYP-D3 and DLPNO-CCSD(T) level of theory for the systems **WITHOUT** the addition of explicit water. (Quasi-Harmonic Approximation) (kJ/mol)

Molecule	Net Charge	Multipl	RSE/BDE	SMD/(U)B3LYP-D3/6-31+G(d,p)		DLPNO-CCSD(T)/BASIS// SMD/(U)B3LYP-D3/6-31+G(d,p)						
					Single Point Without SMD		cc-pVTZ	cc-pVQZ	CBS	cc-pVTZ	cc-pVQZ	CBS
				solution	gas	solvation	gas	gas	gas	solution	solution	solution
				ΔH_{298}	ΔH_{298}	ΔRSE_{SOLV}	ΔH_{298}	ΔH_{298}	ΔH_{298}	ΔH_{298} + ΔRSE_{SOLV}	ΔH_{298} + ΔRSE_{SOLV}	ΔH_{298} + ΔRSE_{SOLV}
d_1m5mU	-1	1	RSE	-4.1	-19.3	15.2	-12.2	-11.7	-11.3	3.0	3.6	3.9
			BDE	371.4	356.2		363.3	363.8	364.2	378.5	379.1	379.4
1m5mU	0	1	RSE	1.2	-5.0	6.2	-0.7	-0.3	-0.1	5.5	5.9	6.1
			BDE	376.7	370.5		374.8	375.2	375.4	381.0	381.4	381.6
d_1m5hmU	-1	1	RSE	-50.9	-93.9	42.9	-67.1	-66.3	-66.3	-25.8	-23.8	-23.3
			BDE	324.6	281.6		308.4	309.2	309.2	349.7	351.7	352.2
1m5hmU	0	1	RSE	-28.3	-49.5	21.1	-40.8	-38.8	-37.8	-17.8	-16.5	-16.0
			BDE	347.2	326.0		334.7	336.7	337.7	357.7	359.0	359.5
d_1m5fU	-1	1	RSE	10.9	14.6	-3.6	12.9	14.3	15.6	12.5	13.9	14.8
			BDE	386.4	390.1		388.4	389.8	391.1	388.0	389.4	390.3
1m5fU	0	1	RSE	17.0	19.7	-2.7	16.6	18.0	19.3	17.0	18.3	19.3
			BDE	392.5	395.2		392.1	393.5	394.8	392.5	393.8	394.8
d_1m5dhmU	-1	1	RSE	-70.5	-104.7	34.2	-81.9	-81.1	-81.3	-46.5	-46.0	-46.1
			BDE	305.0	270.8		293.6	294.4	294.2	329.0	329.5	329.4
1m5dhmU	0	1	RSE	-34.3	-66.6	32.3	-57.7	-56.6	-56.0	-22.1	-21.2	-20.9
			BDE	341.2	308.9		317.8	318.9	319.5	353.4	354.3	354.6

Table 2.2.3. The Boltzmann averaged RSE and BDE values calculated at the (U)B3LYP-D3 and DLPNO-CCSD(T) level of theory for the systems **WITH** the addition of explicit water. (Quasi-Harmonic Approximation)
(kJ/mol)

Molecule	Net Charge	Multipl	RSE/BDE	SMD/(U)B3LYP-D3/6-31+G(d,p)		DLPNO-CCSD(T)/BASIS// SMD/(U)B3LYP-D3/6-31+G(d,p)						
					Single Point Wihtout SMD		cc-pVTZ	cc-pVQZ	CBS	cc-pVTZ	cc-pVQZ	CBS
				solution	gas	solvation	gas	gas	gas	solution	solution	solution
				ΔH_{298}	ΔH_{298}	ΔRSE_{SOLV}	ΔH_{298}	ΔH_{298}	ΔH_{298}	ΔH_{298} + ΔRSE_{SOLV}	ΔH_{298} + ΔRSE_{SOLV}	ΔH_{298} + ΔRSE_{SOLV}
d_1m5mU	-1	1	RSE	-2.8	-16.1	13.3	4.0	4.4	4.7	3.6	4.3	4.8
			BDE	372.7	359.4		379.5	379.9	380.2	379.1	379.8	380.3
1m5mU	0	1	RSE	3.1	-2.6	5.7	5.3	6.8	7.7	6.3	6.5	6.8
			BDE	378.6	372.9		380.8	382.3	383.2	381.8	382.0	382.3
d_1m5hmU	-1	1	RSE	-49.6	-87.0	37.4	-28.0	-26.1	-25.6	-25.1	-24.6	-24.6
			BDE	325.9	288.5		347.5	349.4	349.9	350.4	350.9	350.9
1m5hmU	0	1	RSE	-27.4	-34.2	6.8	-10.0	-8.9	-8.2	-19.1	-18.0	-17.3
			BDE	348.1	341.3		365.5	366.6	367.3	356.4	357.5	358.2
d_1m5fU	-1	1	RSE	11.9	18.0	-6.1	9.1	10.5	11.7	13.2	14.3	15.1
			BDE	387.4	393.5		384.6	386.0	387.2	388.7	389.8	390.6
1m5fU	0	1	RSE	17.6	22.2	-4.6	17.1	18.2	19.3	16.6	19.0	20.2
			BDE	393.1	397.7		392.6	393.7	394.8	392.1	394.5	395.7
d_1m5dhmU	-1	1	RSE	-65.0	-98.7	33.7	-41.1	-42.5	-43.4	-38.3	-39.6	-40.4
			BDE	310.5	276.8		334.4	333.0	332.1	337.2	335.9	335.1
1m5dhmU	0	1	RSE	-43.0	-68.1	25.2	-31.9	-31.1	-30.8	-27.5	-26.4	-26.1
			BDE	332.5	307.4		343.6	344.4	344.7	348.0	349.1	349.4

Table 2.2.4. The Boltzmann averaged Δ RSE and Δ BDE values calculated at the (U)B3LYP-D3 and DLPNO-CCSD(T) level of theory as difference in RSE and BDE values between systems **WITH** and **WITHOUT** the addition of explicit water. (Quasi-Harmonic Approximation) (kJ/mol)

Molecule	Net Charge	Multipl	Δ RSE/ Δ BDE	SMD/(U)B3LYP-D3/6-31+G(d,p)		DLPNO-CCSD(T)/BASIS// SMD/(U)B3LYP-D3/6-31+G(d,p)						
					Single Point Without SMD		cc-pVTZ	cc-pVQZ	CBS	cc-pVTZ	cc-pVQZ	CBS
				solution	gas	solvation	gas	gas	gas	solution	solution	solution
				$\Delta\Delta H_{298}$	$\Delta\Delta H_{298}$	$\Delta\Delta RSE_{SOLV}$	$\Delta\Delta H_{298}$	$\Delta\Delta H_{298}$	$\Delta\Delta H_{298}$	$\Delta\Delta H_{298}$ + $\Delta\Delta RSE_{SOLV}$	$\Delta\Delta H_{298}$ + $\Delta\Delta RSE_{SOLV}$	$\Delta\Delta H_{298}$ + $\Delta\Delta RSE_{SOLV}$
d_1m5mU	-1	1	Δ RSE/ Δ BDE	1.3	3.2	0.0	16.2	16.0	16.0	0.6	0.8	0.9
1m5mU	0	1	Δ RSE/ Δ BDE	1.9	2.4	0.0	6.1	7.1	7.8	0.8	0.6	0.7
d_1m5hmU	-1	1	Δ RSE/ Δ BDE	1.4	6.9	0.0	39.1	40.2	40.7	0.6	-0.7	-1.3
1m5hmU	0	1	Δ RSE/ Δ BDE	0.9	15.2	0.0	30.8	29.9	29.6	-1.3	-1.4	-1.3
d_1m5fU	-1	1	Δ RSE/ Δ BDE	0.9	3.4	0.0	-3.8	-3.8	-3.8	0.6	0.4	0.3
1m5fU	0	1	Δ RSE/ Δ BDE	0.5	2.5	0.0	0.5	0.2	0.0	-0.4	0.6	1.0
d_1m5dhmU	-1	1	Δ RSE/ Δ BDE	5.5	6.0	0.0	40.9	38.6	37.8	8.2	6.5	5.7
1m5dhmU	0	1	Δ RSE/ Δ BDE	-8.7	-1.6	0.0	25.8	25.5	25.2	-5.4	-5.2	-5.1

Table 2.3.1. Effect of base pairing on BDE values.

5-Sub.	q	BDE			Complexation		
		DFT			DFT		
		1mC	9mG_1mC	9mG effect	9mG_1mC	9mG_1mC 5-radical	Δ
m-	-1						
	0	380.5	380.7	0.2	-48.8	-48.6	0.2
	1	389.0					
hm-	-1						
	0	355.0	357.7	2.8	-49.1	-46.4	2.8
	1	357.4					
f-	-1						
	0	397.7	396.8	-0.9	-46.4	-47.3	-0.9
	1	404.3					
dhm-	-1						
	0	304.6	332.2	27.6	-50.2	-22.7	27.6
	1	358.4					

5-Sub.	q	BDE			Complexation		
		CBS			CBS		
		1mC	9mG_1mC	9mG effect	9mG_1mC	9mG_1mC 5-radical	Δ
m-	-1						
	0	387.5	394.1	6.6	-39.5	-32.9	6.6
	1	394.4					
hm-	-1						
	0	367.7	373.6	5.9	-40.5	-34.6	5.9
	1	367.4					
f-	-1						
	0	399.8	405.8	6.0	-39.1	-33.1	6.0
	1	405.4					
dhm-	-1						
	0	322.1	352.4	30.3	-39.3	-9.0	30.3 2.4+27.9
	1	363.8					

Table 2.3.2. Effect of base pairing on BDE values.

5-Sub.	q	BDE			Complexation		
		DFT			DFT		
		1mU	9mA_1mU	9mA effect	9mA_1mU	9mA_1mU 5-radical	Δ
m-	-1	371.4					
	0	376.7	377.0	0.3	-33.6	-33.3	0.3
	1						
hm-	-1	324.6					
	0	347.2	348.1	0.9	-36.4	-35.5	0.9
	1						
f-	-1	386.4					
	0	392.5	391.2	-1.4	-35.9	-37.2	-1.4
	1						
dhm-	-1	305.0					
	0	341.2	339.5	-1.7	-36.7	-38.4	-1.7
	1						

5-Sub.	q	BDE			Complexation		
		CBS			CBS		
		1mU	9mA_1mU	9mA effect	9mA_1mU	9mA_1mU 5-radical	Δ
m-	-1	379.4					
	0	381.6	387.9	6.3	-27.6	-21.3	6.3
	1						
hm-	-1	352.2					
	0	359.5	365.7	6.2	-28.7	-22.5	6.2
	1						
f-	-1	390.3					
	0	394.8	399.8	5.0	-29.4	-24.4	5.0
	1						
dhm-	-1	329.4					
	0	354.6	362.4	7.8	-30.8	-23.0	7.8
	1						

Table 2.4.1. Structures and Boltzmann averaged complexation enthalpies calculated by SMD(H₂O)/(U)B3LYP-D3/6-31+G(d,p). The best conformer/tautomer in terms of enthalpy is shown ($\Delta\Delta H_{sol}^* = 0.0$), for not the best structures, the relative enthalpy ($\Delta\Delta H_{sol}^* > 0.0$) is assigned below


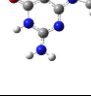
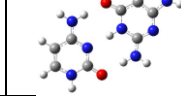
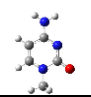
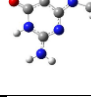
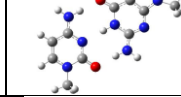
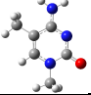
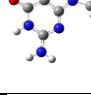
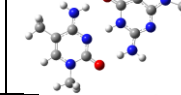
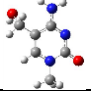
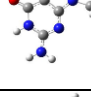
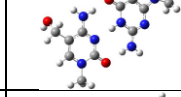
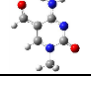
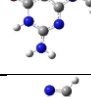
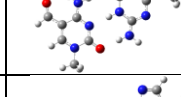
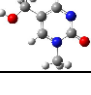
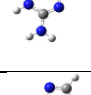
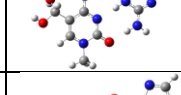
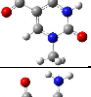
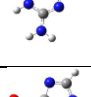
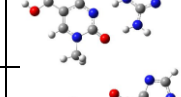
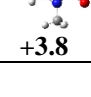
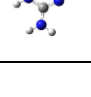
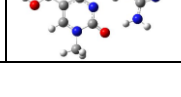
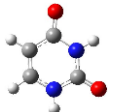
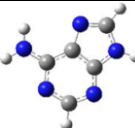
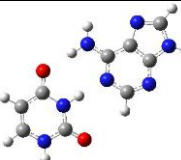
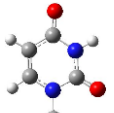
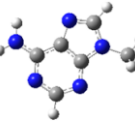
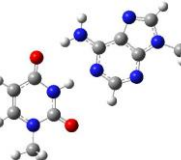
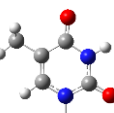
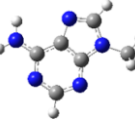

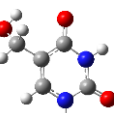
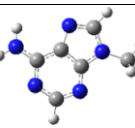
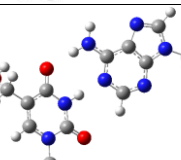
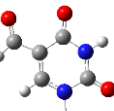
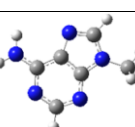

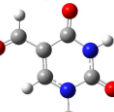
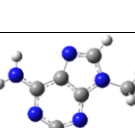

5-Sub.	Substrate		Product	Substrate		Product	Complexation DFT		Complexation CBS	
	File Name	File Name	File Name	Best str./ same str.	Best str.	Best str.	ΔH_{sol}^*	$\Delta\Delta H_{sol}^*$	ΔH_{sol}^*	$\Delta\Delta H_{sol}^*$
	C1	G	G_C1				-49.6	0.0	-40.4	0.0
	1mC	9mG	9mG_1mC				-49.4	0.0	-40.1	0.0
m	1m5mC	9mG	9mG_1m5mC				-48.8	0.0	-39.5	0.0
hm	1m5hmCh	9mG	9mG_1m5hmCh				-49.1	0.0	-40.5	0.0
f	1m5fCb	9mG	9mG_1m5fC				-46.4	0.0	-39.1	0.0
dhm	1m5dhmCha	9mG	9mG_1m5dhmC1				-50.2	0.0	-39.3	0.0
ca	1m5caC7_a	9mG	9mG_1m5caC1				-43.1	0.0	-39.5	0.0
	1m5caC3_b	9mG	9mG_1m5caC1	 +3.8			-46.9	-3.8		

Table 2.4.2. Structures and Boltzmann averaged complexation enthalpies calculated by SMD(H₂O)/(U)B3LYP-D3/6-31+G(d,p). The best conformer/tautomer in terms of enthalpy is shown ($\Delta\Delta H_{sol}^* = 0.0$), for not the best structures, the relative enthalpy ($\Delta\Delta H_{sol}^* > 0.0$) is assigned below

	Substrate		Product	Substrate		Product	Complexation DFT		Complexation CBS	
	File Name	File Name	File Name	Best str./ same str.	Best str.	ΔH_{sol}^*	ΔH_{sol}^*	$\Delta\Delta H_{sol}^*$	ΔH_{sol}^*	$\Delta\Delta H_{sol}^*$
m	5r_1m5mC	9mG	9mG_1mr5mC				-48.6	0.0	-32.9	0.0
hm	5r_1m5hmC1c	9mG	9mG_1mr5hmC1				-46.4	0.0	-34.6	0.0
f	5r_1m5fCb	9mG	9mG_1mr5fC				-47.3	0.0	-33.1	0.0
dhm	5r_1m5dhmCd9	9mG	9mG_1mr5dhmCt3ss	 NEUTRAL	 NEUTRAL	 NEUTRAL	-22.7	0.0	-9.0	0.0
	5r_1m5dhmCd9	9mG	9mG_1mr5dhmC	 NEUTRAL	 NEUTRAL	 NEUTRAL +34.8 +34.7	+12.1	+34.8		
	5r_1m5dhmCa1	9mG	9mG_1mr5dhmC	 +64.2 +62.6		 +34.8 +34.7	-52.1	+34.8 -64.2 = -29.4	-36.9	+34.7 -62.6 = -27.9

Table 2.5.1. Structures and complexation enthalpies calculated by SMD(H₂O)/(U)B3LYP-D3/6-31+G(d,p)

5-Sub.	Substrate		Product	Substrate		Product	Complexation DFT		Complexation CBS	
	File Name	File Name	File Name	Best str./same str.	Best str.	ΔH_{sol}^*	ΔH_{sol}^*	$\Delta\Delta H_{sol}^*$	ΔH_{sol}^*	$\Delta\Delta H_{sol}^*$
	U14	A	A_U1				-36.6	0.0	-29.6	0.0
	1mU3	9mA	9mA_1mU				-34.3	0.0	-61.3	0.0
m	1m5mU	9mA	9mA_1mT				-33.6	0.0	-27.6	0.0
hm	1m5hmU2	9mA	9mA_1m5hmU				-36.4	0.0	-28.7	0.0
f	1m5fU3_	9mA	9mA_1m5fU1				-35.9	0.0	-29.4	0.0
	1m5fU3_a	9mA	9mA_1m5fU1	 +0.5			-36.4	-0.5		


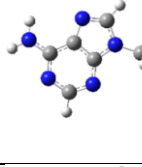

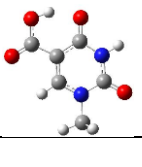
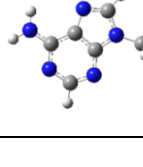
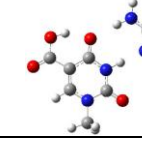
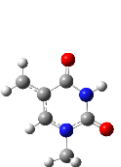
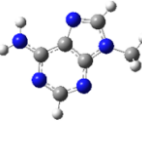


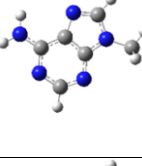
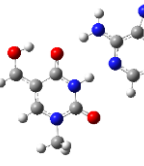
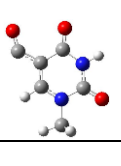
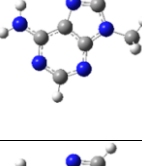
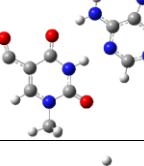
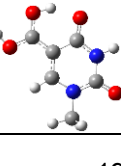
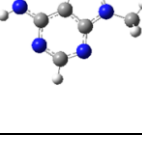
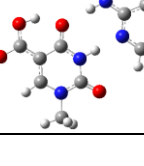
dhm	1m5dhmU_a_10	9mA	9mA_1m5dhmU1				-36.7	0.0	-30.8	0.0
ca	1m5caU35_a	9mA	9mA_1m5caU1				-36.7	0.0	-29.1	0.0

Table 2.5.2. Structures and complexation enthalpies calculated by SMD(H₂O)/(U)B3LYP-D3/6-31+G(d,p)

5-Sub.	Substrate		Product		Substrate		Product		Complexation DFT		Complexation CBS	
	File Name	File Name	File Name	Best str./same str.	ΔH_{sol}^*	$\Delta\Delta H_{sol}^*$	ΔH_{sol}^*	$\Delta\Delta H_{sol}^*$	ΔH_{sol}^*	$\Delta\Delta H_{sol}^*$	ΔH_{sol}^*	$\Delta\Delta H_{sol}^*$
m	5r_1m5mU	9mA	9mA_1mr5mU				-33.3	0.0	-21.3	0.0		
hm	5r_1m5hmU32_b	9mA	9mA_1mr5hmU1				-35.5	0.0	-22.5	0.0		
f	5r_1m5fU3_b	9mA	9mA_1mr5fU				-37.2	0.0	-24.4	0.0		
dhm	5r_1m5dhmU_32_b_a	9mA	9mA_1mr5dhmU_3iss				-38.4	0.0	-23.0	0.0		

3. Boltzmann Averaged Data

Table 3.1.1. The Boltzmann averaged **enthalpies** calculated at the (U)B3LYP-D3 and DLPNO-CCSD(T) level of theory for the systems **WITHOUT** the addition of explicit water. (**Quasi-Harmonic Approximation**)
(for 1 mol at 1 atm)

Molecule	Net Charge	Multipl	SMD/(U)B3LYP-D3/6-31+G(d,p)		DLPNO-CCSD(T)/BASIS// SMD/(U)B3LYP-D3/6-31+G(d,p)						
				Single Point Without SMD		cc-pVTZ	cc-pVQZ	CBS	cc-pVTZ	cc-pVQZ	CBS
			solution	gas	solvation	gas	gas	gas	solution	solution	solution
			H_{298}	H_{298}	ΔH_{SOLV} = ΔE_{SOLV}	H_{298}	H_{298}	H_{298}	H_{298} + ΔE_{SOLV}	H_{298} + ΔE_{SOLV}	H_{298} + ΔE_{SOLV}
CH3-Ph	0	1	-271.4636040	-271.4626275	-0.0009765	-270.9115772	-270.9889446	-271.0372150	-270.9125537	-270.9899211	-271.0381915
•CH2-Ph	0	2	-270.8246499	-270.8239369	-0.0007130	-270.2717247	-270.3478077	-270.3952238	-270.2724377	-270.3485207	-270.3959368

Table 3.2.1. The Boltzmann averaged **enthalpies** calculated at the (U)B3LYP-D3 and DLPNO-CCSD(T) level of theory for the systems **WITHOUT** the addition of explicit water. (**Quasi-Harmonic Approximation**)
(for 1 mol at 1 atm)

Molecule	Net Charge	Multipl	SMD/(U)B3LYP-D3/6-31+G(d,p)		DLPNO-CCSD(T)/BASIS// SMD/(U)B3LYP-D3/6-31+G(d,p)						
				Single Point Wihtout SMD		cc-pVTZ	cc-pVQZ	CBS	cc-pVTZ	cc-pVQZ	CBS
			solution	gas	solvation	gas	gas	gas	solution	solution	solution
			H ₂₉₈	H ₂₉₈	ΔH_{SOLV} = ΔE_{SOLV}	H ₂₉₈	H ₂₉₈	H ₂₉₈	H ₂₉₈ + ΔE_{SOLV}	H ₂₉₈ + ΔE_{SOLV}	H ₂₉₈ + ΔE_{SOLV}
C	0	1	-394.9002852	-394.8630216	-0.0372637	-394.1901311	-394.3090823	-394.3824296	-394.2229695	-394.3426726	-394.4163627
p_C	1	1	-395.3402582	-395.2277152	-0.1125430	-394.5569036	-394.6731181	-394.7449135	-394.6664686	-394.7827477	-394.8546113
5mC	0	1	-434.1948936	-434.1579944	-0.0368993	-433.4042339	-433.5347888	-433.6154152	-433.4368219	-433.5681545	-433.6491569
r_5mC	0	2	-433.5537729	-433.5190049	-0.0347681	-432.7621167	-432.8913965	-432.9711715	-432.7924973	-432.9223705	-433.0023986
p_5mC	1	1	-434.6358882	-434.5276891	-0.1081991	-433.7756603	-433.9036812	-433.9828680	-433.8809986	-434.0090800	-434.0883237
pr_5mC	1	2	-433.9920718	-433.8838962	-0.1081756	-433.1289290	-433.2555416	-433.3338079	-433.2344797	-433.3611077	-433.4394111
5hmC	0	1	-509.4145310	-509.3732999	-0.0412311	-508.5223747	-508.6772191	-508.7727253	-508.5592912	-508.7149302	-508.8108203
r_5hmC	0	2	-508.7831389	-508.7505939	-0.0325450	-507.8864902	-508.0407372	-508.1358034	-507.9218394	-508.0766903	-508.1717891
p_5hmC	1	1	-509.8541340	-509.7381814	-0.1159526	-508.8898892	-509.0421492	-509.1361814	-509.0028449	-509.1550559	-509.2491150
pr_5hmC	1	2	-509.2216057	-509.1137582	-0.1078474	-508.2590957	-508.4097608	-508.5027522	-508.3653216	-508.5164837	-508.6096518
5fC	0	1	-508.2303128	-508.1940904	-0.0362224	-507.3450550	-507.4973134	-507.5911362	-507.3773748	-507.5303044	-507.6244223
r_5fC	0	2	-507.5827454	-507.5508132	-0.0319322	-506.7010189	-506.8516567	-506.9444084	-506.7288353	-506.8800087	-506.9729640
p_5fC	1	1	-508.6646309	-508.5456219	-0.1190090	-507.6996487	-507.8490624	-507.9412490	-507.8176793	-507.9671595	-508.0594140
pr_5fC	1	2	-508.0144230	-507.8973217	-0.1171014	-507.0518565	-507.1996266	-507.2906860	-507.1667467	-507.3145491	-507.4056583
5dhmC	0	1	-584.6470168	-584.6006968	-0.0463199	-583.6539392	-583.8329866	-583.9434257	-583.6966148	-583.8764511	-583.9872316
r_5dhmC	0	2	-584.0352135	-584.0033428	-0.0318706	-583.0451685	-583.2238161	-583.3339080	-583.0768619	-583.2553883	-583.3655281
p_5dhmC	1	1	-585.0856230	-584.9676398	-0.1179832	-584.0234104	-584.1995284	-584.3083261	-584.1393633	-584.3154649	-584.4242682
pr_5dhmC	1	2	-584.4548875	-584.3406585	-0.1142290	-583.3897198	-583.5645822	-583.6723995	-583.5060589	-583.6754214	-583.7832898
d_5caC	-1	1	-583.0421912	-582.9277882	-0.1144029	-581.9670249	-582.1509334	-582.2635259	-582.0814923	-582.2653868	-582.3779745
5caC	0	1	-583.4839942	-583.4461629	-0.0378314	-582.5020037	-582.6786761	-582.7875733	-582.5348828	-582.7121301	-582.8213558
p_5caC	1	1	-583.9180477	-583.8023071	-0.1157405	-582.8605021	-583.0342190	-583.1414065	-582.9753375	-583.1490837	-583.2563229

Table 3.2.2. The Boltzmann averaged **enthalpies** calculated at the (U)B3LYP-D3 and DLPNO-CCSD(T) level of theory for the systems **WITHOUT** the addition of explicit water. (**Quasi-Harmonic Approximation**) (for 1 mol at 1 atm)

Molecule	Net Charge	Multipl	DLPNO-CCSD(T)/BASIS// SMD/(U)B3LYP-D3/6-31+G(d,p)								
			SMD/(U)B3LYP-D3/6-31+G(d,p)			cc-pVTZ	cc-pVQZ	CBS	cc-pVTZ	cc-pVQZ	CBS
			Single Point Without SMD			gas	gas	gas	solution	solution	solution
			solution H_{298}	gas H_{298}	solvation ΔH_{SOLV} = ΔE_{SOLV}	gas H_{298}	gas H_{298}	gas H_{298}	solution H_{298} + ΔE_{SOLV}	solution H_{298} + ΔE_{SOLV}	solution H_{298} + ΔE_{SOLV}
1mC	0	1	-434.1828809	-434.1483167	-0.0345642	-433.3905446	-433.5213513	-433.6020400	-433.4251088	-433.5559155	-433.6366042
p_1mC	1	1	-434.6242995	-434.5186796	-0.1056199	-433.7665914	-433.8941713	-433.9731067	-433.8691372	-433.9968475	-434.0758679
1m5mC	0	1	-473.4772959	-473.4425587	-0.0347372	-472.6041522	-472.7465964	-472.8346048	-472.6388893	-472.7813336	-472.8693420
r_1m5mC	0	2	-472.8364535	-472.8051645	-0.0312890	-471.9632832	-472.1042371	-472.1912405	-471.9945722	-472.1355261	-472.2225295
p_1m5mC	1	1	-473.9200379	-473.8181780	-0.1018599	-472.9851439	-473.1244898	-473.2107888	-473.0838835	-473.2233626	-473.3097423
pr_1m5mC	1	2	-473.2759310	-473.1745921	-0.1013389	-472.3383798	-472.4763556	-472.5617533	-472.4367674	-472.5748317	-472.6602941
1m5hmC	0	1	-548.6971223	-548.6575170	-0.0396054	-547.7218813	-547.8886965	-547.9915901	-547.7615266	-547.9286475	-548.0312196
r_1m5hmC	0	2	-548.0659799	-548.0363757	-0.0296042	-547.0917352	-547.2572641	-547.3593939	-547.1239755	-547.2898562	-547.3919294
p_1m5hmC	1	1	-549.1375754	-549.0283743	-0.1092011	-548.0988038	-548.2626612	-548.3635893	-548.2049976	-548.3599575	-548.4700231
pr_1m5hmC	1	2	-548.5055028	-548.4040235	-0.1014793	-547.4682357	-547.6302613	-547.7303740	-547.5678811	-547.7232318	-547.8308546
1m5fC	0	1	-547.5142059	-547.4808442	-0.0333618	-546.5472962	-546.7113818	-546.8125323	-546.5806589	-546.7447450	-546.8458955
r_1m5fC	0	2	-546.8667838	-546.8389978	-0.0277859	-545.9043619	-546.0666441	-546.1665986	-545.9321438	-546.0944334	-546.1943918
p_1m5fC	1	1	-547.9493050	-547.8388851	-0.1104199	-546.9105186	-547.0713535	-547.1707118	-547.0207721	-547.1816715	-547.2810553
pr_1m5fC	1	2	-547.2993792	-547.1909313	-0.1084479	-546.2627613	-546.4218568	-546.5199468	-546.3699912	-546.5294036	-546.6274083
1m5dhmC	0	1	-623.9295773	-623.8869992	-0.0425780	-622.8556760	-623.0464682	-623.1642105	-622.8988207	-623.0896872	-623.2074402
r_1m5dhmC	0	2	-623.3176379	-623.2882291	-0.0294087	-622.2491941	-622.4392134	-622.5564204	-622.2782433	-622.4682335	-622.5855381
p_1m5dhmC	1	1	-624.3695957	-624.2583499	-0.1112459	-623.2328294	-623.4206865	-623.5361777	-623.3419509	-623.5295365	-623.6454706
pr_1m5dhmC	1	2	-623.7371530	-623.6294700	-0.1076830	-622.5975675	-622.7837497	-622.8986641	-622.7067502	-622.8927674	-623.0076679
d_1m5caC	-1	1	-622.3248894	-622.2117856	-0.1131038	-621.1709784	-621.3658121	-621.4853136	-621.2840822	-621.4789159	-621.5984174
1m5caC	0	1	-622.7680558	-622.7321466	-0.0359092	-621.7033812	-621.8918541	-622.0080775	-621.7379119	-621.9264868	-622.0424962
p_1m5caC	1	1	-623.2027056	-623.0947087	-0.1079969	-622.0706377	-622.2557768	-622.3701232	-622.1784518	-622.3638313	-622.4780510

Table 3.2.3. The Boltzmann averaged **enthalpies** calculated at the (U)B3LYP-D3 and DLPNO-CCSD(T) level of theory for the systems **WITH** the addition of explicit water. (**Quasi-Harmonic Approximation**) (for 1 mol at 1 atm)

Molecule	Net Charge	Multipl	DLPNO-CCSD(T)/BASIS // SMD/(U)B3LYP-D3/6-31+G(d,p)								
			SMD/(U)B3LYP-D3/6-31+G(d,p)		SMD/(U)B3LYP-D3/6-31+G(d,p)						
			Single Point Wihtout SMD		cc-pVTZ	cc-pVQZ	CBS	cc-pVTZ	cc-pVQZ	CBS	
			solution H_{298}	gas H_{298}	solvation ΔH_{SOLV} = ΔE_{SOLV}	gas H_{298}	gas H_{298}	gas H_{298}	solution H_{298} + ΔE_{SOLV}	solution H_{298} + ΔE_{SOLV}	solution H_{298} + ΔE_{SOLV}
1m5mC	0	1	-549.9076660	-549.8669149	-0.0407511	-548.9244369	-549.0936364	-549.1979438	-548.9662454	-549.1355689	-549.2398756
r_1m5mC	0	2	-549.2666813	-549.2302670	-0.0364143	-548.2808642	-548.4510728	-548.5577822	-548.3254747	-548.4894550	-548.5941195
p_1m5mC	1	1	-550.3505541	-550.2550684	-0.0954857	-549.3160046	-549.4811336	-549.5833101	-549.4125569	-549.5778461	-549.6800806
pr_1m5mC	1	2	-549.7071269	-549.6111720	-0.0959549	-548.6690705	-548.8327643	-548.9340105	-548.7657620	-548.9296099	-549.0308979
1m5hmC	0	1	-625.1272570	-625.0831647	-0.0440923	-624.0418193	-624.2358525	-624.3552840	-624.0889121	-624.2822544	-624.4014369
r_1m5hmC	0	2	-624.4961903	-624.4612101	-0.0349802	-623.4133832	-623.6048535	-623.7228807	-623.4536939	-623.6456273	-623.7636258
p_1m5hmC	1	1	-625.5691043	-625.4671266	-0.1019777	-624.4316752	-624.6211194	-624.7381787	-624.5346008	-624.7244429	-624.8415118
pr_1m5hmC	1	2	-624.9374176	-624.8394839	-0.0979337	-623.7981516	-623.9860266	-624.1020722	-623.8967259	-624.0852762	-624.2014925
1m5fC	0	1	-623.9436718	-623.9046318	-0.0390400	-622.8661426	-623.0573583	-623.1749587	-622.9071879	-623.0981599	-623.2156144
r_1m5fC	0	2	-623.2930148	-623.2581321	-0.0348827	-622.2190376	-622.4082071	-622.5244705	-622.2560625	-622.4450125	-622.5611380
p_1m5fC	1	1	-624.3813547	-624.2789275	-0.1024272	-623.2471137	-623.4337169	-623.5489590	-623.3499009	-623.5367215	-623.6520588
pr_1m5fC	1	2	-623.7316709	-623.6318829	-0.0997881	-622.5990868	-622.7839151	-622.8979599	-622.7001758	-622.8851139	-622.9991651
1m5dhmC	0	1	-700.3599577	-700.3127200	-0.0472378	-699.1758447	-699.3940082	-699.5283679	-699.2274677	-699.4440190	-699.5776351
r_1m5dhmC	0	2	-699.7474408	-699.7143130	-0.0331278	-698.5725055	-698.7889948	-698.9223577	-698.6060472	-698.8224703	-698.9550341
p_1m5dhmC	1	1	-700.8005960	-700.6941548	-0.1064412	-699.5635963	-699.7771410	-699.9090081	-699.6715418	-699.8851161	-700.0157566
pr_1m5dhmC	1	2	-700.1720863	-700.0663363	-0.1057500	-698.9283144	-699.1405597	-699.2715892	-699.0372466	-699.2493592	-699.3801233
d_1m5caC	-1	1	-698.7562066	-698.6478637	-0.1083428	-697.5033405	-697.5033405	-697.8599491	-697.6125406	-697.6125406	-697.9692036
1m5caC	0	1	-699.1990162	-699.1557079	-0.0433083	-698.0242067	-698.2387628	-698.3711174	-698.0662340	-698.2806319	-698.4130259
p_1m5caC	1	1	-699.6356477	-699.5341491	-0.1014986	-698.4067503	-698.6176297	-698.7478558	-698.5084476	-698.7195556	-698.8498601

Table 3.3.1. The Boltzmann averaged **enthalpies** calculated at the (U)B3LYP-D3 and DLPNO-CCSD(T) level of theory for the systems **WITHOUT** the addition of explicit water. (**Quasi-Harmonic Approximation**)
(for 1 mol at 1 atm)

Molecule	Net Charge	Multipl	SMD/(U)B3LYP-D3/6-31+G(d,p)		DLPNO-CCSD(T)/BASIS // SMD/(U)B3LYP-D3/6-31+G(d,p)						
				Single Point Wihtout SMD		cc-pVTZ	cc-pVQZ	CBS	cc-pVTZ	cc-pVQZ	CBS
			solution	gas	solvation	gas	gas	gas	solution	solution	solution
			H ₂₉₈	H ₂₉₈	ΔH_{SOLV} = ΔE_{SOLV}	H ₂₉₈	H ₂₉₈	H ₂₉₈	H ₂₉₈ + ΔE_{SOLV}	H ₂₉₈ + ΔE_{SOLV}	H ₂₉₈ + ΔE_{SOLV}
d_U	-1	1	-414.3302851	-414.2305472	-0.0997379	-413.5342211	-413.6649952	-413.7449751	-413.6338620	-413.7645658	-413.8445978
U	0	1	-414.7864773	-414.7597206	-0.0267567	-414.0749408	-414.2002966	-414.2775394	-414.1016974	-414.2270532	-414.3042960
d_5mU	-1	1	-453.6242205	-453.5242098	-0.1000107	-452.7479646	-452.8899348	-452.9770540	-452.8478512	-452.9899794	-453.0773081
dr_5mU	-1	2	-452.9871219	-452.8933095	-0.0938124	-452.1131348	-452.2536052	-452.3397274	-452.2067898	-452.3472763	-452.4334975
5mU	0	1	-454.0822391	-454.0565933	-0.0256458	-453.2910403	-453.4278916	-453.5124007	-453.3166861	-453.4535374	-453.5380465
r_5mU	0	2	-453.4423096	-453.4191907	-0.0231189	-452.6509246	-452.7863003	-452.8698648	-452.6740434	-452.8094191	-452.8929836
d_5hmU	-1	1	-528.8462865	-528.7464771	-0.0998094	-527.8720926	-528.0389514	-528.1412151	-527.9718540	-528.1390391	-528.2415041
dr_5hmU	-1	2	-528.2234248	-528.1251554	-0.0982694	-527.2438983	-527.4086343	-527.5097383	-527.3404187	-527.5059678	-527.6073686
5hmU	0	1	-529.3010986	-529.2692072	-0.0318914	-528.4062670	-528.5678802	-528.6674695	-528.4387208	-528.6002476	-528.6997884
r_5hmU	0	2	-528.6731301	-528.6490765	-0.0240536	-527.7816625	-527.9411291	-528.0394298	-527.8057054	-527.9651688	-528.0634690
d_5fU	-1	1	-527.6652465	-527.5749671	-0.0902794	-526.7038296	-526.8672676	-526.9675542	-526.7949608	-526.9584859	-527.0586998
dr_5fU	-1	2	-527.0213802	-526.9332749	-0.0881052	-526.0618171	-526.2235889	-526.3227121	-526.1501925	-526.3120103	-526.4111237
5fU	0	1	-528.1109990	-528.0812198	-0.0297792	-527.2218447	-527.3802054	-527.4778449	-527.2530378	-527.4113322	-527.5088291
r_5fU	0	2	-527.4656240	-527.4350570	-0.0305670	-526.5759266	-526.7324818	-526.8288189	-526.6065636	-526.7631184	-526.8594524
d_5dhmU	-1	1	-604.0794988	-603.9651873	-0.1143115	-602.9964660	-603.1883838	-603.3058737	-603.1111220	-603.3028611	-603.4202683
dr_5dhmU	-1	2	-603.4669081	-603.3642873	-0.1026208	-602.3866879	-602.5766077	-602.6931029	-602.4891356	-602.6790110	-602.7954745
5dhmU	0	1	-604.5343668	-604.4965356	-0.0378312	-603.5380649	-603.7237970	-603.8382452	-603.5759197	-603.7615766	-603.8759492
r_5dhmU	0	2	-603.9101616	-603.8848621	-0.0252996	-602.9199055	-603.1039447	-603.2173557	-602.9452461	-603.1292794	-603.2426678
dd_5caU	-2	1	-602.4666676	-602.1558041	-0.3108635	-601.1754808	-601.3720381	-601.4915245	-601.4810899	-601.6788945	-601.7990454
d_5caU	-1	1	-602.9248548	-602.8357105	-0.0891443	-601.8713919	-602.0591596	-602.1744431	-601.9606827	-602.1482991	-602.2635053
5caU	0	1	-603.3699158	-603.3355081	-0.0344077	-602.3819889	-602.5647503	-602.6773400	-602.4164043	-602.5991654	-602.7117546

Table 3.3.2. The Boltzmann averaged **enthalpies** calculated at the (U)B3LYP-D3 and DLPNO-CCSD(T) level of theory for the systems **WITHOUT** the addition of explicit water. (**Quasi-Harmonic Approximation**)
(for 1 mol at 1 atm)

Molecule	Net Charge	Multipl	DLPNO-CCSD(T)/BASIS // SMD/(U)B3LYP-D3/6-31+G(d,p)								
			SMD/(U)B3LYP-D3/6-31+G(d,p)								
				Single Point Wihtout SMD		cc-pVTZ	cc-pVQZ	CBS	cc-pVTZ	cc-pVQZ	CBS
			solution H_{298}	gas H_{298}	solvation ΔH_{SOLV} = ΔE_{SOLV}	gas H_{298}	gas H_{298}	gas H_{298}	solution H_{298} + ΔE_{SOLV}	solution H_{298} + ΔE_{SOLV}	solution H_{298} + ΔE_{SOLV}
d_1mU	-1	1	-453.6090357	-453.4905081	-0.1185276	-452.7157914	-452.8584425	-452.9456590	-452.8343190	-452.9769701	-453.0641866
1mU	0	1	-454.0697788	-454.0456597	-0.0241191	-453.2629161	-453.4165035	-453.4838306	-453.2911537	-453.4406225	-453.5122603
d_1m5mU	-1	1	-492.9030190	-492.7858194	-0.1171996	-491.9316243	-492.0853931	-492.1797288	-492.0488239	-492.2025928	-492.2969285
dr_1m5mU	-1	2	-492.2656226	-492.1544902	-0.1111324	-491.2964336	-491.4486981	-491.5420425	-491.4075660	-491.5598305	-491.6531749
1m5mU	0	1	-493.3647614	-493.3421536	-0.0226078	-492.4957950	-492.6438314	-492.7353695	-492.5184028	-492.6664392	-492.7579773
r_1m5mU	0	2	-492.7253469	-492.7053748	-0.0199721	-491.8562154	-492.0028104	-492.0934183	-491.8761875	-492.0227825	-492.1133904
d_1m5hmU	-1	1	-568.1248431	-568.0114126	-0.1134304	-567.0594157	-567.2378106	-567.3471854	-567.1727954	-567.3511701	-567.4605404
dr_1m5hmU	-1	2	-567.5052927	-567.4084798	-0.0968129	-566.4451210	-566.6219313	-566.7304575	-566.5424904	-566.7188535	-566.8271609
1m5hmU	0	1	-568.5839058	-568.5549199	-0.0289859	-567.6110754	-567.7838892	-567.8905119	-567.6407342	-567.8134559	-567.9200324
r_1m5hmU	0	2	-567.9557329	-567.9350639	-0.0206690	-566.9867507	-567.1575122	-567.2629009	-567.0073922	-567.1783493	-567.2838701
d_1m5fU	-1	1	-566.9402439	-566.8323004	-0.1079435	-565.8814191	-566.0568917	-566.1644979	-565.9906179	-566.1660763	-566.2735195
dr_1m5fU	-1	2	-566.2971239	-566.1880636	-0.1090603	-565.2366686	-565.4103166	-565.5165803	-565.3457239	-565.5193701	-565.6256291
1m5fU	0	1	-567.3947807	-567.3681272	-0.0266536	-566.4275579	-566.5971494	-566.7018398	-566.4555113	-566.6250569	-566.7296194
r_1m5fU	0	2	-566.7493358	-566.7219185	-0.0274173	-565.7813798	-565.9491405	-566.0525071	-565.8089080	-565.9766694	-566.0800324
d_1m5dhmU	-1	1	-643.3610219	-643.2472046	-0.1138173	-642.1993575	-642.4018710	-642.5261223	-642.3133462	-642.5157907	-642.6399972
dr_1m5dhmU	-1	2	-642.7489352	-642.6483947	-0.1005405	-641.5907117	-641.7916211	-641.9150794	-641.6909511	-641.8919296	-642.0152896
1m5dhmU	0	1	-643.8179202	-643.7832937	-0.0346265	-642.7436965	-642.9406583	-643.0621544	-642.7782553	-642.9751516	-643.0965932
r_1m5dhmU	0	2	-643.1920155	-643.1699588	-0.0220567	-642.1258227	-642.3210711	-642.4414893	-642.1465430	-642.3418437	-642.4623053
dd_1m5caU	-2	1	-641.7428765	-641.4092049	-0.3336716	-640.3465100	-640.5554838	-640.6825624	-640.6801816	-640.8891554	-641.0162340
d_1m5caU	-1	1	-642.2051778	-642.1033062	-0.1018715	-641.0595058	-641.2588416	-641.3812199	-641.1612901	-641.3605782	-641.4829313
1m5caU	0	1	-642.6539236	-642.6228380	-0.0310856	-641.5881574	-641.7821900	-641.9018553	-641.6192513	-641.8132840	-641.9329493

Table 3.3.3. The Boltzmann averaged enthalpies calculated at the (U)B3LYP-D3 and DLPNO-CCSD(T) level of theory for the systems **WITH** the addition of explicit water. (**Quasi-Harmonic Approximation**) (for 1 mol at 1 atm)

Molecule	Net Charge	Multipl	DLPNO-CCSD(T)/BASIS // SMD/(U)B3LYP-D3/6-31+G(d,p)								
			SMD/(U)B3LYP-D3/6-31+G(d,p)			cc-pVTZ	cc-pVQZ	CBS	cc-pVTZ	cc-pVQZ	CBS
			Single Point Wihtout SMD			gas	gas	gas	solution	solution	solution
			solution H_{298}	gas H_{298}	solvation $\Delta H_{SOLV} = \Delta E_{SOLV}$	gas H_{298}	gas H_{298}	gas H_{298}	solution $H_{298} + \Delta E_{SOLV}$	solution $H_{298} + \Delta E_{SOLV}$	solution $H_{298} + \Delta E_{SOLV}$
d_1m5mU	-1	1	-569.3348997	-569.2219672	-0.1129324	-568.2632957	-568.4436454	-568.5542013	-568.3765561	-568.5569261	-568.6674824
dr_1m5mU	-1	2	-568.6970106	-568.5894231	-0.1075875	-567.6270007	-567.8059250	-567.9155107	-567.7350626	-567.9138751	-568.0234002
1m5mU	0	1	-569.7939381	-569.7627595	-0.0311786	-568.8126939	-568.9876531	-569.0956531	-568.8447766	-569.0196091	-569.1274253
r_1m5mU	0	2	-569.1538187	-569.1250783	-0.0287405	-568.1729792	-568.3460866	-568.4529187	-568.2022736	-568.3757141	-568.4825881
d_n1m5hmU	-1	1	-644.5572704	-644.4458597	-0.1114107	-643.3892885	-643.5944376	-643.7200997	-643.5024416	-643.7069231	-643.8323433
dr_1m5hmU	-1	2	-643.9372036	-643.8402962	-0.0969074	-642.7743373	-642.9774685	-643.1020951	-642.8719039	-643.0748741	-643.1994606
1m5hmU	0	1	-645.0149351	-644.9802946	-0.0346405	-643.9333504	-644.1323891	-644.2550638	-643.9690504	-644.1680957	-644.2907691
r_1m5hmU	0	2	-644.3864266	-644.3546353	-0.0317914	-643.2998748	-643.4972239	-643.6187826	-643.3361928	-643.5335344	-643.6550878
d_1m5fU	-1	1	-643.3712968	-643.2662239	-0.1050729	-642.2113012	-642.4134043	-642.5372039	-642.3180585	-642.5200915	-642.6437394
dr_1m5fU	-1	2	-642.7278177	-642.6206776	-0.1071401	-641.5656541	-641.7659462	-641.8884199	-641.6729242	-641.8732331	-641.9957408
1m5fU	0	1	-643.8235312	-643.7908247	-0.0327065	-642.7485889	-642.9443490	-643.0650163	-642.7813633	-642.9779151	-643.0988171
r_1m5fU	0	2	-643.1778808	-643.1436697	-0.0342112	-642.1004619	-642.2945100	-642.4138991	-642.1349118	-642.3292804	-642.4488595
d_1m5dhmU	-1	1	-719.7939418	-719.6814864	-0.1124554	-718.5299851	-718.7581544	-718.8982553	-718.6446181	-718.8728027	-719.0129127
dr_1m5dhmU	-1	2	-719.1797571	-719.0803975	-0.0993596	-717.9186100	-718.1460244	-718.2856456	-718.0191084	-718.2464727	-718.3860526
1m5dhmU	0	1	-720.2478560	-720.2070818	-0.0407743	-719.0638204	-719.2868344	-719.4242934	-719.1064785	-719.3295390	-719.4670096
r_1m5dhmU	0	2	-719.6252724	-719.5943447	-0.0309276	-718.4456930	-718.6671254	-718.8036029	-718.4768312	-718.6981965	-718.8346812
dd_1m5caU	-2	1	-718.1754864	-717.8586859	-0.3168004	-716.6926733	-716.9274261	-717.0704724	-717.0103045	-717.2450355	-717.3880003
d_1m5caU	-1	1	-718.6363203	-718.5340537	-0.1022665	-717.3630599	-717.5901115	-717.7293293	-717.4856701	-717.7128186	-717.8520714
1m5caU	0	1	-719.0824336	-719.0473340	-0.0350996	-717.9100384	-718.1302493	-718.2659196	-717.9454482	-718.1661159	-718.3020095

Table 3.4.1. The Boltzmann averaged enthalpies calculated at the (U)B3LYP-D3 and DLPNO-CCSD(T) level of theory for the systems **WITHOUT** the addition of explicit water. (**Quasi-Harmonic Approximation**) (for 1 mol at 1 atm)

Molecule	Net Charge	Multipl	DLPNO-CCSD(T)/BASIS// SMD/(U)B3LYP-D3/6-31+G(d,p)								
			SMD/(U)B3LYP-D3/6-31+G(d,p)								
				Single Point Wihtout SMD		cc-pVTZ	cc-pVQZ	CBS	cc-pVTZ	cc-pVQZ	CBS
			solution H_{298}	gas H_{298}	solvation ΔH_{SOLV} = ΔE_{SOLV}	gas H_{298}	gas H_{298}	gas H_{298}	solution H_{298} + ΔE_{SOLV}	solution H_{298} + ΔE_{SOLV}	solution H_{298} + ΔE_{SOLV}
G_5mC	0	1	-976.7341745	-976.6831386	-0.0510358	-975.0015105	-975.2944940	-975.4756601	-975.0525505	-975.3455323	-975.5266977
G_r5mC	0	2	-976.0928486	-976.0437996	-0.0490490	-974.3566246	-974.6481058	-974.8282631	-974.4056736	-974.6971547	-974.8773120
	1	1									
	1	2									
G_5hmC	0	1	-1051.9532312	-1051.8941581	-0.0590731	-1050.1156746	-1050.4331207	-1050.6292241	-1050.1747477	-1050.4921938	-1050.6882972
G_r5hmC	0	2	-1051.3197880	-1051.2640915	-0.0556965	-1049.4783334	-1049.7940234	-1049.9889830	-1049.5340300	-1049.8497199	-1050.0446795
	1	1									
	1	2									
G_5fC	0	1	-1050.7691449	-1050.7142501	-0.0548947	-1048.9385966	-1049.2531381	-1049.4473908	-1048.9934923	-1049.3080339	-1049.5022865
G_r5fC	0	2	-1050.1216451	-1050.0727206	-0.0489245	-1048.2940078	-1048.6066209	-1048.7995810	-1048.3429392	-1048.6555538	-1048.8485148
	1	1									
	1	2									
G_5dhmC	0	1	-1127.1867513	-1127.1260700	-0.0606813	-1125.2514788	-1125.5928592	-1125.8037810	-1125.3121604	-1125.6535406	-1125.8644624
G_r5dhmC	0	2	-1126.5638232	-1126.4956459	-0.0681772	-1124.6113561	-1124.9520900	-1125.1624145	-1124.6799228	-1125.0206631	-1125.2310013
	1	1									
	1	2									
	-1	1									
G_5caC	0	1	-1126.0215908	-1125.9664601	-0.0551307	-1124.0953731	-1124.4342919	-1124.6436063	-1124.1506462	-1124.4895635	-1124.6988755
	1	1									

Table 3.4.2. The Boltzmann averaged **enthalpies** calculated at the (U)B3LYP-D3 and DLPNO-CCSD(T) level of theory for the systems **WITHOUT** the addition of explicit water. (**Quasi-Harmonic Approximation**) (for 1 mol at 1 atm)

Molecule	Net Charge	Multipl	SMD/(U)B3LYP-D3/6-31+G(d,p)		DLPNO-CCSD(T)/BASIS// SMD/(U)B3LYP-D3/6-31+G(d,p)						
				Single Point Without SMD		cc-pVTZ	cc-pVQZ	CBS	cc-pVTZ	cc-pVQZ	CBS
			solution	gas	solvation	gas	gas	gas	solution	solution	solution
			H ₂₉₈	H ₂₉₈	ΔH_{SOLV} = ΔE_{SOLV}	H ₂₉₈	H ₂₉₈	H ₂₉₈	H ₂₉₈ + ΔE_{SOLV}	H ₂₉₈ + ΔE_{SOLV}	H ₂₉₈ + ΔE_{SOLV}
9mG_1m5mC	0	1	-1055.3009467	-1055.2560800	-0.0448667	-1053.4130116	-1053.7281926	-1053.9233484	-1053.4578783	-1053.7730593	-1053.9682151
9mG_1mr5mC	0	2	-1054.6600169	-1054.6171231	-0.0428938	-1052.7681072	-1053.0818261	-1053.2759935	-1052.8110010	-1053.1247199	-1053.3188873
	1	1									
	1	2									
9mG_1m5hmC	0	1	-1130.5208937	-1130.4686795	-0.0522143	-1128.5283412	-1128.8679885	-1129.0781160	-1128.5807377	-1128.9203706	-1129.1304829
9mG_1mr5hmC	0	2	-1129.8887011	-1129.8374166	-0.0512845	-1127.8900139	-1128.2284384	-1128.4375782	-1127.9413623	-1128.2798089	-1128.4889495
	1	1									
	1	2									
9mG_1m5fC	0	1	-1129.3369215	-1129.2881529	-0.0487686	-1127.3505999	-1127.6874995	-1127.8958386	-1127.3993684	-1127.7362680	-1127.9446071
9mG_1mr5fC	0	2	-1128.6898606	-1128.6471047	-0.0427559	-1126.7061209	-1127.0410529	-1127.2480704	-1126.7488768	-1127.0838088	-1127.2908263
	1	1									
	1	2									
9mG_1m5dhmC	0	1	-1205.7537640	-1205.6993945	-0.0543694	-1203.6630990	-1204.0267840	-1204.2517613	-1203.7176535	-1204.0812965	-1204.3062363
9mG_1mr5dhmC	0	2	-1205.1313186	-1205.0706569	-0.0606618	-1203.0213084	-1203.3846601	-1203.6092433	-1203.0851701	-1203.4483400	-1203.6727799
	1	1									
	1	2									
	-1	1									
9mG_1m5caC	0	1	-1204.5895406	-1204.5407208	-0.0488198	-1202.5077953	-1202.8690270	-1203.0923997	-1202.5567861	-1202.9180069	-1203.1413744
	1	1									

Table 3.5.1. The Boltzmann averaged **enthalpies** calculated at the (U)B3LYP-D3 and DLPNO-CCSD(T) level of theory for the systems **WITHOUT** the addition of explicit water. (**Quasi-Harmonic Approximation**)
(for 1 mol at 1 atm)

Molecule	Net Charge	Multipl	SMD/(U)B3LYP-D3/6-31+G(d,p)		DLPNO-CCSD(T)/BASIS// SMD/(U)B3LYP-D3/6-31+G(d,p)						
				Single Point Wihout SMD		cc-pVTZ	cc-pVQZ	CBS	cc-pVTZ	cc-pVQZ	CBS
			solution	gas	solvation	gas	gas	gas	solution	solution	solution
			H ₂₉₈	H ₂₉₈	ΔH_{SOLV} = ΔE_{SOLV}	H ₂₉₈	H ₂₉₈	H ₂₉₈	H ₂₉₈ + ΔE_{SOLV}	H ₂₉₈ + ΔE_{SOLV}	H ₂₉₈ + ΔE_{SOLV}
	-1	1									
	-1	2									
A_T	0	1	-921.3653902	-921.3252279	-0.0401623	-919.7352227	-920.0092200	-920.1787687	-919.7753877	-920.0493849	-920.2189334
A_r5mU	0	2	-920.7256811	-920.6879801	-0.0377010	-919.0934326	-919.3658493	-919.5343713	-919.1311408	-919.4035571	-919.5720788
	-1	1									
	-1	2									
A_5hmU	0	1	-996.5856637	-996.5389766	-0.0466871	-994.8516122	-995.1502773	-995.3348524	-994.8983059	-995.1969706	-995.3815453
A_r5hmU	0	2	-995.9568193	-995.9173163	-0.0395030	-994.2236198	-994.5201135	-994.7033791	-994.2631275	-994.5596186	-994.7428837
	-1	1									
	-1	2									
A_5fU	0	1	-995.3950643	-995.3512242	-0.0438402	-993.6670153	-993.9625799	-994.1452882	-993.7122353	-994.0077561	-994.1903128
A_r5fU	0	2	-994.7499143	-994.7056936	-0.0442207	-993.0198435	-993.3134985	-993.4948142	-993.0642518	-993.3578981	-993.5392024
	-1	1									
	-1	2									
A_5dhmU	0	1	-1071.8191427	-1071.7661888	-0.0529539	-1069.9834224	-1070.3061551	-1070.5055302	-1070.0363990	-1070.3591300	-1070.5585032
A_r5dhmU	0	2	-1071.1938224	-1071.1519910	-0.0418314	-1069.3607957	-1069.6818303	-1069.8801782	-1069.4023834	-1069.7234179	-1069.9217658
	-2	1									
	-1	1									
A_5caU	0	1	-1070.6545301	-1070.6061163	-0.0484138	-1068.8275199	-1069.1474484	-1069.3450985	-1068.8761504	-1069.1960453	-1069.3936675

Table 3.5.2. The Boltzmann averaged **enthalpies** calculated at the (U)B3LYP-D3 and DLPNO-CCSD(T) level of theory for the systems **WITHOUT** the addition of explicit water. (**Quasi-Harmonic Approximation**) (for 1 mol at 1 atm)

Molecule	Net Charge	Multipl	SMD/(U)B3LYP-D3/6-31+G(d,p)		DLPNO-CCSD(T)/BASIS// SMD/(U)B3LYP-D3/6-31+G(d,p)						
				Single Point Wihtout SMD		cc-pVTZ	cc-pVQZ	CBS	cc-pVTZ	cc-pVQZ	CBS
			solution	gas	solvation	gas	gas	gas	solution	solution	solution
			H ₂₉₈	H ₂₉₈	ΔH_{SOLV} = ΔE_{SOLV}	H ₂₉₈	H ₂₉₈	H ₂₉₈	H ₂₉₈ + ΔE_{SOLV}	H ₂₉₈ + ΔE_{SOLV}	H ₂₉₈ + ΔE_{SOLV}
	-1	1									
	-1	2									
9mA_1mT	0	1	-999.9325973	-999.8984216	-0.0341757	-998.1464665	-998.4428088	-998.6264134	-998.1806422	-998.4769845	-998.6605891
9mA_1mr5mU	0	2	-999.2930540	-999.2613811	-0.0316729	-997.5045858	-997.7993603	-997.9819359	-997.5362587	-997.8310332	-998.0136088
	-1	1									
	-1	2									
9mA_1m5hmU	0	1	-1075.1527932	-1075.1123445	-0.0404487	-1073.2629440	-1073.5839952	-1073.7826483	-1073.3033927	-1073.6244439	-1073.8230970
9mA_1mr5hmU	0	2	-1074.5242718	-1074.4909980	-0.0332738	-1072.6350663	-1072.9539559	-1073.1512910	-1072.6683403	-1072.9872301	-1073.1845653
	-1	1									
	-1	2									
9mA_1m5fU	0	1	-1073.9634709	-1073.9259778	-0.0374932	-1072.0794714	-1072.3974553	-1072.5942600	-1072.1183323	-1072.4362862	-1072.6329478
9mA_1mr5fU	0	2	-1073.3185498	-1073.2804296	-0.0381202	-1071.4318817	-1071.7478865	-1071.9432448	-1071.4700811	-1071.7860853	-1071.9814399
	-1	1									
	-1	2									
9mA_1m5dhmU	0	1	-1150.3869361	-1150.3405320	-0.0464041	-1148.3953454	-1148.7404759	-1148.9539482	-1148.4418448	-1148.7869777	-1149.0004468
9mA_1mr5dhmU	0	2	-1149.7616822	-1149.7253512	-0.0363310	-1147.7719723	-1148.1154290	-1148.3278605	-1147.8072899	-1148.1507466	-1148.3631781
	-2	1									
	-1	1									
9mA_1m5caU	0	1	-1149.2229189	-1149.1809583	-0.0419606	-1147.2400838	-1147.5824475	-1147.7941995	-1147.2820456	-1147.6244087	-1147.8361604

4. The pH-Dependence of the Hydration of 5-Formylcytosine: An Experimental and Theoretical Study

Fabian Zott, Vasily Korotenko, Hendrik Zipse

ChemBioChem, 2022, Wiley-VCH

Manuscript and SI: <https://doi.org/10.1002/cbic.202100651>

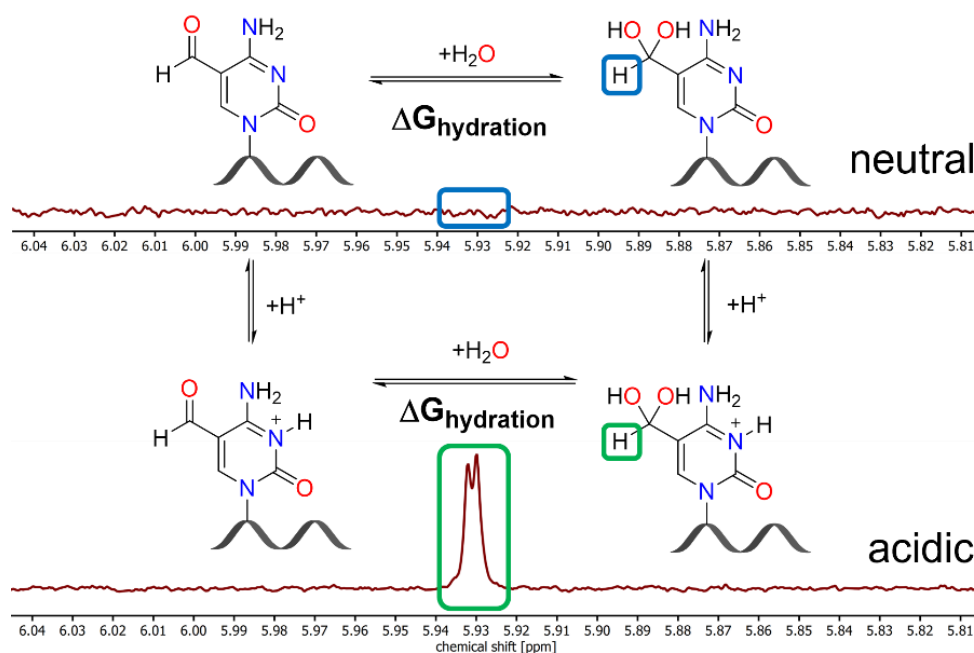
Author contributions:

The project was conceived by F.Z., V.K. and H.Z. The experimental study was performed by F.Z. The computational study was performed by V.K. The manuscript was jointly written by F.Z., V.K. and H.Z. The supplementary information was prepared by F.Z., V.K.

Copyright: Reprinted with permission from ChemBioChem, 2022

Copyright: 2022 Wiley-VCH

5-Formylcytosine is an important nucleobase in epigenetic regulation, whose hydrate form has been implicated in the formation of 5-carboxycytosine as well as oligonucleotide binding events. The hydrate content of 5-formylcytosine and its uracil derivative has now been quantified using a combination of NMR and mass spectroscopic measurements as well as theoretical studies. Small amounts of hydrate can be identified for the protonated form of 5-formylcytosine and for neutral 5-formyluracil. For neutral 5-formylcytosine, however, direct detection of the hydrate was not possible due to its very low abundance. This is in full agreement with theoretical estimates.



The pH-Dependence of the Hydration of 5-Formylcytosine: an Experimental and Theoretical Study

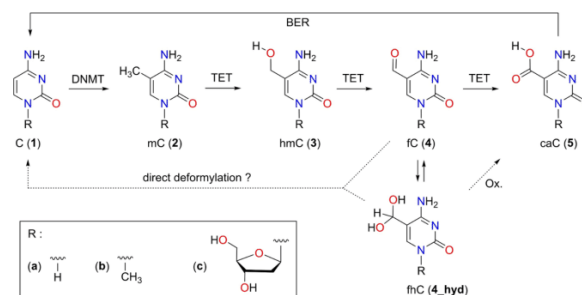
Fabian L. Zott⁺,^[a] Vasily Korotenko⁺,^[a] and Hendrik Zipse^{*[a]}

5-Formylcytosine is an important nucleobase in epigenetic regulation, whose hydrate form has been implicated in the formation of 5-carboxycytosine as well as oligonucleotide binding events. The hydrate content of 5-formylcytosine and its uracil derivative has now been quantified using a combination of NMR and mass spectroscopic measurements as well as

theoretical studies. Small amounts of hydrate can be identified for the protonated form of 5-formylcytosine and for neutral 5-formyluracil. For neutral 5-formylcytosine, however, direct detection of the hydrate was not possible due to its very low abundance. This is in full agreement with theoretical estimates.

Introduction

Epigenetic modifications add a further layer of information to the genetic code based on the linear sequencing of the four canonical DNA bases (A, C, G, T). This information may be encoded into the DNA by chemical modifications of the canonical nucleobases. For example, epigenetic modifications in the canonical nucleobase cytosine are known to control gene regulation in human cells and furthermore have implications in the development of cancer and other diseases.^[1–4] 5-Methylcytosine (mC, **2**) as the most common modification is generated by an enzyme-catalyzed methylation at the C5 position of the cytosine base (**1**) and accounts for approximately 1% of all DNA bases in the human genome (Scheme 1).^[5,6] The active removal of the methyl group from mC (demethylation) in the human genome is an active field of research. Since direct C–C bond cleavage in **2** is highly unfavorable from a thermochemical point of view, no known mammalian enzyme employs this pathway for the demethylation of mC.^[7,8] Instead, the active DNA demethylation pathway known today employs a sequential oxidation of mC to caC (**5**) via hmC (**3**) and fC (**4**), catalyzed by the ten-eleven translocation (TET) family of enzymes (Scheme 1).^[9–24] Many other pathways have been proposed, that lead to direct decarboxylation and deformylation of caC and fC, and evidence for the direct deformylation in mammalian cells has been reported recently.^[25–28] This deformylation pathway would elegantly avoid the possible damage of DNA strands by the base excision repair (BER, Scheme 1) mechanisms for the active



Scheme 1. Possible pathways for methylation and oxidative demethylation of cytosine (DNMT: DNA methyltransferases; TET: ten-eleven translocation enzymes; BER: base excision repair).

demethylation of caC and fC via the DNA repair protein thymidine DNA glycosylase (TDG).^[4,26,29] Since these oxidized cytosine derivatives have also been described as stable epigenetic markers, their susceptibility towards (spontaneous) oxidation is an important field of interest.^[30,31] Deaminated derivatives of fC such as 5-formyluracil (fU) can be formed by oxidative stress at thymine (T) sites via 5-hydroxymethyluracil (hmU), which is known to be toxic in mammalian cells.^[32–34] In mouse embryonic stem cells, it was found that deamination does not substantially contribute to hmU levels, and that TET enzymes facilitate the oxidation of thymine to hmU.^[35] During the discovery of fC in embryonic stem cell DNA, the authors reported evidence for the presence of its hydrated form fhC (**4_hyd**).^[10] This *gem*-diol was detected in positive ion MS experiments and quantified at approximately 0.5% at the single nucleotide level. Whether the hydrated form of 5-formylcytosine plays a role in structural or functional aspects of this base appears to depend on the specific system at hand.^[27–29] Burrows et al. reported on two unique formation events for fC-containing DNA duplexes when studying the dynamics of DNA mismatch kinetics. These two events have a ratio of 5:1 and led to the proposal that fC exists in equilibrium with its hydrate fhC, each of which having different base-flipping kinetics.^[36] Assuming the hydration reaction to be very slow, this implies

[a] F. L. Zott,⁺ V. Korotenko,⁺ H. Zipse
 Department of Chemistry, LMU München
 Butenandstrasse 5–13, 81377 München (Germany)
 E-mail: zipse@cup.uni-muenchen.de

[†] These authors contributed equally to this work.

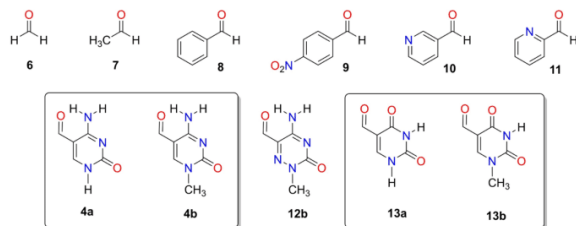
Supporting information for this article is available on the WWW under <https://doi.org/10.1002/cbic.202100651>

© 2022 The Authors. ChemBioChem published by Wiley-VCH GmbH. This is an open access article under the terms of the Creative Commons Attribution Non-Commercial License, which permits use, distribution and reproduction in any medium, provided the original work is properly cited and is not used for commercial purposes.

an equilibrium constant for the hydration (K_{hyd}) of 0.2. This value is similar to known hydration constants of aldehydes carrying electron-withdrawing substituents.^[39,40] Experimental studies may, in some cases, also be impacted by the known conformational *syn/anti* dynamics of **4**.^[41,42] In a recent NMR study on the melting kinetics of 5-formylcytosine in dsDNA no evidence for the respective geminal diol form was found in ^1H or ^{13}C NMR measurements.^[37] This does, of course, not exclude transient hydrate formation in TET2-mediated fC oxidation reactions.^[38] Direct measurements of the hydration equilibrium of fC have not yet been reported. Using a combined experimental/theoretical approach, we will show in the following that this may be difficult to achieve.

Results and Discussion

For selected aldehydes carrying aromatic substituents (Scheme 2) the relevant equilibrium data for the hydration reaction has been collected in Table 1. We also include formaldehyde (**6**) and acetaldehyde (**7**) here as two well studied small reference systems. Benzaldehyde (**8**) was employed as a prototype for aldehydes



Scheme 2. Structures of aldehydes studied in this work.

carrying aromatic substituents to verify the measurement strategy. 1-Methyl-5-formyluracil (**13b**), 5-formyluracil (**13a**), 5-formylcytosine (**4a**) and 1-methyl-5-formylcytosine (**4b**) have been synthesized and purified following modified procedures as described below. These model nucleobases retain the essential functionality of nucleotides while facilitating quantitative experimental and theoretical studies.^[42]

^{18}O Isotopic exchange experiment

In order to validate that the reversible addition of water to the aldehyde carbonyl group in **13b** leads to transient formation of the hydrate form **13b_hyd**, an ^{18}O isotope exchange experiment was performed under neutral conditions (Figure 1). The results show that the formyl group reacts readily with H_2^{18}O to yield the ^{18}O -labelled nucleobase ^{18}O -**13b**, most likely via the hydrated form **13b_hyd**. This latter conclusion is supported by analysis of the fragmentation patterns for **13b** and ^{18}O -**13b**, and oxygen exchange of the other carbonyl groups present in **13b** can be ruled out (see Supporting Information Figures S3 and S4). The ^{18}O isotope experiment for **4b** performed under the same conditions shows fast oxygen exchange, with the same results in fragmentation pattern analysis.

^1H NMR identification and quantification

The ^1H NMR spectrum of **13b** in D_2O measured at a concentration of $3.1 \times 10^{-3} \text{ mol L}^{-1}$ is shown in Figure 2. All ^1H resonances of aldehyde **13b** are accompanied by additional resonances for its hydrate **13b_hyd** at much lower intensities, which were also matched by NMR shift calculations. When measuring the same

Table 1. Equilibrium constants for the hydration of selected aldehydes (p_{-} for the protonated form).

System	K_w	K	T [°C]	$\Delta G_{(exp)}$ [kJ/mol]	Ref.
6	2.29×10^3	41.2	25	-9.2	[42]
	1.8×10^3	32.43	20	-8.5	[43]
7	1.06	0.0191	25	+9.8	[44]
	1.08	0.0194	25	+9.8	[45]
	1.50	0.0270	25	+8.9	[46]
	0.011	0.98×10^{-3}	25	+21.1	[47]
8	9.67×10^{-3}	1.74×10^{-4}	22	+21.3	this study
	0.25 ± 0.1	4.50×10^{-3}	25	+13.4	[48]
9	0.115	2.07×10^{-3}	20	+15.1	[49]
p_10	5.1	0.920	25	+5.9	[49]
11	0.66	0.012	25	+11.0	[46]
p_11	199	3.58	25	-3.2	[50]
4a	2.25×10^{-3}	4.05×10^{-5}	22	$> +24.8^{[c]}$	this study
	6.75×10^{-4}	1.22×10^{-5}	22	$< +27.8^{[h]}$	this study
4b^[c,d]	$< 4.50 \times 10^{-4}$	$< 8.11 \times 10^{-6}$	22	$> +28.8$	this study
p_4b^[a,b]	0.005	9.72×10^{-5}	22	+22.7	this study
	0.005	9.10×10^{-5}	30	+22.7	[14]
4c^[c]	$< 4.40 \times 10^{-4}$	$< 7.93 \times 10^{-6}$	22	$> +28.8$	this study
p_4c^[e]	0.007	1.23×10^{-4}	22	+22.1	this study
12b^[f]	0.25	0.0045	22	+13.3	[51]
13a^[g]	0.016	2.94×10^{-4}	22	+20.0	this study
13b^[g]	0.013	2.42×10^{-4}	22	+20.5	this study

[a] Protonated **4b**. [b] pH=2. [c] Derived from limit of detection (LOD, see Supporting Information, section S.5). [d] pH=7.7. [e] pH=2.6. [f] Presumably under neutral pH conditions. [g] pH=5.9. [h] Derived from limit of quantification (LOQ, see Supporting Information, section S.5).

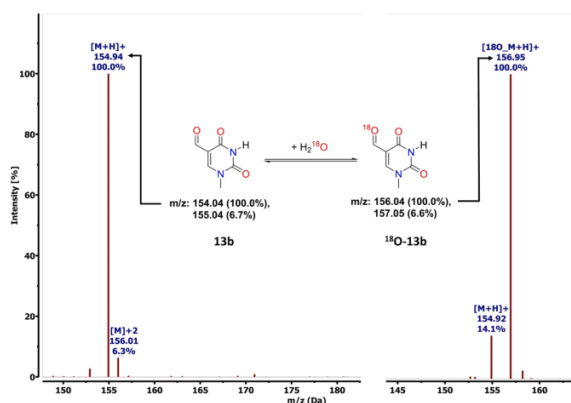


Figure 1. ^{18}O isotope exchange experiment with **13b** (left side: **13b** at natural abundance; right side: ^{18}O labelled **13b** after equilibration with H_2^{18}O ; only the $[\text{M}]^+$ peak region is shown).

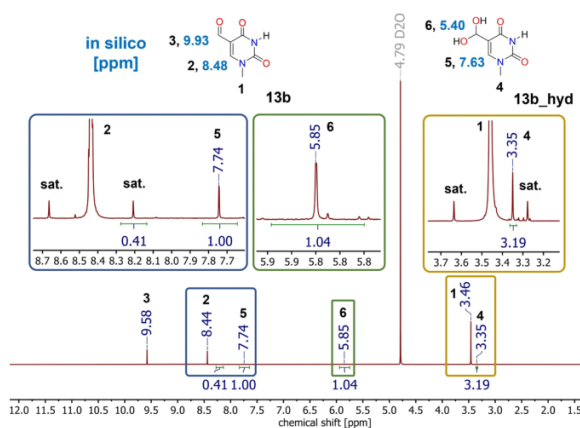


Figure 2. ^1H NMR spectra of **13b** and its hydrated form **13b_hyd** in D_2O at a concentration of $3.1 \times 10^{-3} \text{ mol L}^{-1}$ together with the relevant signal assignments and calculated chemical shifts (in light blue).

sample of **13b** in anhydrous $\text{DMSO-}d_6$, no signals for the hydrates can be observed (see Supporting Information Figure S12). Quantification of the formyl- and the hydrated forms was achieved by using the $^{13}\text{C}(^1\text{H})$ satellite signals of **13b** as a reference. Assuming that a single $^{13}\text{C}(^1\text{H})$ satellite signal corresponds to 0.535% of the intensity of the parent ^1H signal, we find a 100:1.3 ratio for aldehyde **13b** and its hydrate **13b_hyd** by a standardized procedure (see Supporting Information for details).^[52] At a reaction temperature of 23°C this corresponds to a free energy difference between the two forms of $\Delta G_{\text{exp}} = +20.5 \text{ kJ mol}^{-1}$ (Table 1).

Studying 1-methyl-5-formylcytosine (**4b**) under the same conditions, no ^1H NMR signals could be detected at the theoretically calculated shift region for hydrate **4b_hyd** at neutral pH. Still, the ^{18}O isotope experiment showed fast oxygen exchange under the same conditions. When acidifying the NMR sample to $\text{pH}=2$, distinct signals for the hydrate form (**p_4b_hyd**) arise at shift regions predicted *in silico* with an abundance of 0.5%

(Figure 3). This process is reversible upon neutralization excluding a kinetically controlled equilibrium, while deamination can be ruled out due to differences in chemical shifts (see Supporting Information). These observations are consistent with previous work by Carell et al., where levels of 0.5% **p_4c_hyd** have been detected by LC-MS measurements with water/acetonitrile (2 mM NH_4HCOO) under acidic conditions.^[14] Whether or not these conclusions are also valid at the full nucleoside level was subsequently studied for 5-formyl-2'-deoxycytidine (**4c**) through ^1H NMR measurements in D_2O . Under unbuffered conditions ($\text{pH}=8.3$) the hydrate signals proved too small for quantitative evaluation. Acidification to $\text{pH}=2.6$ leads to hydrate signals closely similar to those observed before for **4b_hyd**, and a free energy of hydration of $\Delta G_{\text{exp}} = +22.1 \text{ kJ mol}^{-1}$ was measured for protonated **4c** (**p_4c**). In contrast to **4b**, however, slow hydrolysis of nucleoside **4c** can be observed under acidic conditions, which also implies that the hydration energy for **4b** may be somewhat more reliable (see Supporting Information Figure S21). In any case we can conclude that protonation has a significant influence on the hydration equilibrium of 5-formylcytosine derivatives. In a more general sense this may also imply that the aldehyde/hydrate equilibrium of 5fC can be shifted through specific environmental effects. In Table 1 all experimentally determined free energies of hydration ΔG_{hyd} are listed along with important references for theoretical calculations. For systems where the ΔG_{hyd} value could not be determined experimentally, the limits of detection and quantification (LOD and LOQ, see Supporting Information section S.5) are stated.

Theoretical determination of ΔG_{hyd}

The hydration of aldehydes has been studied repeatedly using theoretical methods, but a reliable approach for the direct prediction of hydration energetics has not yet emerged.^[53] The performance of various theoretical approaches can be demon-

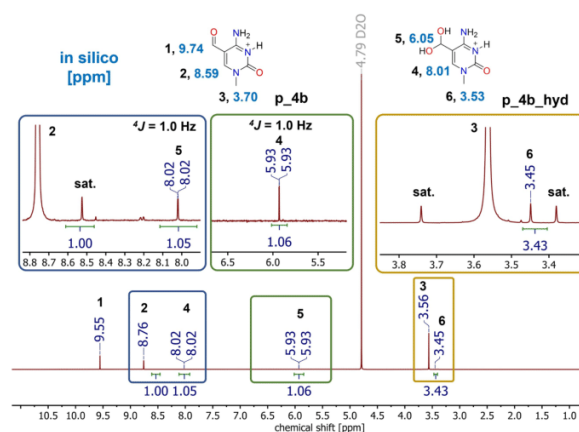


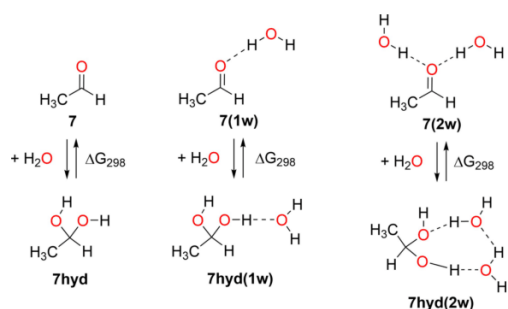
Figure 3. ^1H NMR spectra of the protonated form of **4b** and its hydrated form **p_4b_hyd** in D_2O at $\text{pH}=2$ and a concentration of $5.8 \times 10^{-3} \text{ mol L}^{-1}$ together with the relevant signal assignments and calculated chemical shifts (in light blue).

Table 2. Hydration Gibbs free energies (ΔG_{298} , in kJ mol^{-1}) for acetaldehyde (**7**) and benzaldehyde (**8**) in the gas phase and in aqueous solution.

	Gas phase			Water (SMD model)			Exp.
	DFT ^[a]	CCSD(T)/CBS ^[b,c]	G3B3	DFT ^[a]	CCSD(T)/CBS ^[b,c,d]	G3B3 ^[e]	
7	+17.5	+15.0	+15.8	+21.5	+16.2	+15.1	+9.8
7(w1)	+12.2	+12.6	+11.5	+20.9	+17.6	+13.5	+9.8
7(w2)	+0.5	+4.5	+1.5	+18.3	+14.7	+10.9	+9.8
8	+34.4	+27.3	+29.1	+44.1	+34.8	+32.4	+21.1
8(w1)	+29.8	+24.2	+25.2	+42.6	+35.9	+35.7	+21.1
8(w2)	+17.8	+13.9	+14.1	+37.8	+37.7	+32.5	+21.1

[a] B3LYP-D3/6-31+G(d,p). [b] Using gas phase B3LYP-D3/6-31+G(d,p) geometries. [c] Based on DLPNO-CCSD(T) single point calculations with the cc-pVTZ and cc-pVQZ basis sets. [d] SMD solvation energies calculated at SMD(H2O)/B3LYP-D3/6-31+G(d,p) level. [e] SMD solvation energies calculated at SMD(H2O)/B3LYP/6-31G(d) level.

strated for acetaldehyde (**7**) as a well-characterized small reference system (Table 2), the hydration reaction of this system being endergonic by $+9.8 \text{ kJ mol}^{-1}$ at 298.15 K.^[42,44] In order to address the effects of aqueous solvation appropriately, we employ a combination of continuum solvation models (here SMD) with different numbers of explicit water molecules (Figure 4). Analysis of the hydration energies of **7** with theoretical methods known to work well for the prediction of thermochemical data such as G3B3 or DLPNO-CCSD(T)/CBS shows this to be an endergonic process of around $\Delta G_{298} = +15 \text{ kJ mol}^{-1}$ (see Supporting Information for additional validation studies). The B3LYP-D3/6-31+G(d,p) hybrid DFT method employed here for geometry optimizations gives, in

**Figure 4.** The hydration of acetaldehyde (**7**) in the absence and presence of solvating water molecules.

this case, a closely similar value. The addition of explicit water molecules as in **7(1w)** or **7(2w)** makes the reaction systematically less endergonic, and leads to a basically thermoneutral process in the presence of two explicit water molecules. This finding indicates that the hydration equilibrium in non-aqueous (or non-homogeneous) environments may be altered by specific hydrogen bonding interactions and may also provide a rationalization for the comparatively high levels of 5-formylcytosine hydrate in DNA duplex systems reported by Burrows et al.^[36] The effects of bulk aqueous solvation have then been added with aid of the SMD continuum solvation model. This decreases the overall hydration energy and approaches the experimental value for the combination of the G3B3 compound scheme and two explicit water molecules. Similar validation steps have also been performed for benzaldehyde (**8**) as an aldehyde carrying an aromatic substituent and having a significantly less favorable hydration energy of $\Delta G_{298} = +21.1 \text{ kJ mol}^{-1}$. Again, the gas phase hydration energy becomes more favorable with each explicitly considered water molecule, while the additional consideration of bulk solvation with the SMD model leads to a notable increase. We note, however, that all theory combinations considered here predict the hydration reaction to be less favorable than observed experimentally by approximately 10 kJ mol^{-1} . Using the same theoretical methods and solvation strategies as before, hydration energies have been calculated for the aldehydes shown in Figure 2 (Table 3). In addition to neutral 1-methyl-5-formylcytosine (**4b**), this also includes its protonated form (**p_4b**) (Figure 5).

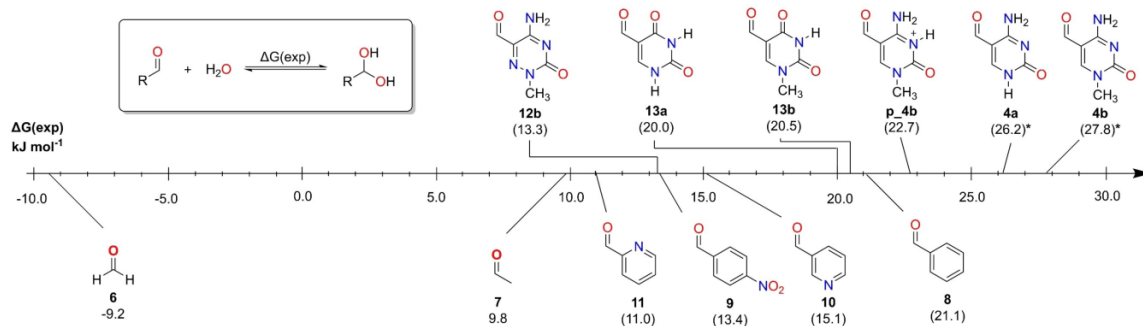
**Figure 5.** Experimental hydration free energies of selected aldehydes (* based on combination of the G3B3 $\Delta \Delta G_{298}$ values with the experimentally measured value for **p_4b**) as the reference).

Table 3. Hydration Gibbs free energies (ΔG_{298} , in kJ mol^{-1}) for the aldehydes shown in Figure 2.

	Water (SMD model)						Exp.
	No explicit water molecules			One explicit water molecule			
	DFT ^[a,d]	CCSD(T)/CBS ^[b,c,d]	G3B3 ^[e]	DFT ^[a,d]	CCSD(T)/CBS ^[b,c,d]	G3B3 ^[e]	
6	-3.7	-4.3	-2.4	-13.6	-12.0	-5.1	-9.2
7	21.5	16.2	15.1	20.9	17.6	13.5	9.8
8	44.1	34.8	32.4	42.6	35.9	35.7	21.1
9	32.9	26.2	23.6	27.2	23.0	23.8	13.4
10	38.9	29.9	27.7	37.4	31.4	26.5	15.1
11	28.0	22.3	24.8	31.1	27.1	20.1	11.0
4a	52.0	40.0	45.7	53.6	44.6	39.3	> 24.8/ < 27.8 ^[f]
4b	54.4	42.3	46.6	55.3	46.1	42.7	> 28.8
p_4b	42.3	36.3	36.3	42.5	35.8	36.1	22.7
12b	41.9	31.0	31.4	36.3	27.8	19.6	13.3
13a	38.5	34.3	29.0	39.1	35.6	31.3	20.0
13b	39.3	34.8	29.1	42.7	38.3	35.3	20.5

[a] B3LYP-D3/6-31+G(d,p). [b] Using gas phase B3LYP-D3/6-31+G(d,p) geometries. [c] Based on DLPNO-CCSD(T) single point calculations. [d] SMD solvation energies calculated at SMD(H₂O)/B3LYP-D3/6-31+G(d,p) level. [e] SMD solvation energies calculated at SMD(H₂O)/B3LYP/6-31G(d) level. [f] Calculated from LOQ and LOD.

For most aldehydes considered here, the calculated hydration energies are overestimated to a similar extent as already observed for benzaldehyde (**8**). Due to the systematic nature of this phenomenon, good linear correlations can be observed between experimentally measured and theoretically calculated hydration energies in aqueous solution at SMD(H₂O)/CCSD(T)/CBS or SMD(H₂O)/G3B3 level with $R^2=0.95-0.97$. These correlations can be employed for an accurate estimate of the hydration energy difference between **4b** and its protonated form **p_4b**. Based on the values reported in Table 3 at the CBS or G3B3 level, this difference falls into the range of $\Delta\Delta G_{298}=6.0-10.3\text{ kJ/mol}$. However, as already noted above, these values are generally somewhat too large and the correlations can be employed to scale these down to a more realistic value of $\Delta\Delta G_{298}=+5.1\text{ kJ mol}^{-1}$. Combination with the experimentally measured value of $\Delta G_{298}(\mathbf{p_4b})=+22.7\text{ kJ mol}^{-1}$, this then yields $\Delta G_{298}(\mathbf{4b})=+27.8\text{ kJ mol}^{-1}$, which is closely similar to the limiting value of $\Delta G_{298}(\mathbf{4b})>28.8\text{ kJ mol}^{-1}$ derived from the ¹H NMR measurements. The same approach yields a theoretically predicted value for the free base of $\Delta G_{298}(\mathbf{4a})=+26.2\text{ kJ mol}^{-1}$, being close to the experimental approximation derived from LOQ and LOD between +24.8–27.8 kJ mol^{-1} .

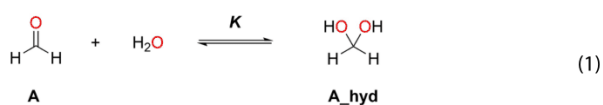
Conclusion

All experimental and theoretical studies presented here indicate that the hydrates of 5-formylcytosine (**4a**) and its N1-methylated derivative **4b** are just beyond the limit of what can be quantified reliably by ¹H NMR spectroscopy. The abundances of these species are expected to amount to less than 0.05% under unbuffered standard conditions in water at ambient temperature. Protonation at the N3 position under acidic conditions will increase hydrate formation such that its direct detection through ¹H NMR spectroscopy becomes feasible at an abundance of 0.53%. The hydrate form of 5-formyluridine as the formal deamination product of 5-formylcytosine is more abundant at 1.3% under

neutral aqueous conditions. Despite these seemingly low values, the aldehyde hydrate forms may nevertheless play an essential role in oxidation reactions to the respective 5-carboxy derivatives in a way well established for aldehyde oxidations mediated by chemical oxidants or dehydrogenase enzymes.^[38,54–56] In both areas evidence for the stabilization of hydrate intermediates through directed hydrogen bonding interactions has been found, which is in full support of the gas phase calculations with explicit water molecules in the current study. This may also provide a rational basis for the proposed high abundance of 5-formylcytosine hydrates reported by Burrows et al. in base-flipping kinetics studies.^[36] A potential TET-mediated oxidation of fc through the respective hydrate^[38] moves this process mechanistically closer to that of hmC, where recent theoretical studies have established similar reaction barriers for initial O–H vs. C–H hydrogen abstraction steps.^[19,57]

Experimental Section

Energy of hydration ΔG_{hyd} : The reaction of aldehydes (**A**) with water in aqueous solution yields the respective hydrate **A_{hyd}** according to Eq. (1). The position of this equilibrium is given through equilibrium constant K , which is defined through the equilibrium concentrations of reactants and products according to Eq. (2). In dilute solutions it is practical to consider the concentration of water as a constant with $[\text{H}_2\text{O}]=55.5\text{ mol l}^{-1}$ and combine this value with K into a new equilibrium constant K_w (sometimes also called K_{hyd}) according to Eq. (3). The true equilibrium constant K can then be obtained from experimentally measured K_w values according to Eq. (4). According to the law of mass action, the equilibrium constant K relates to the free energy of the reaction shown in Eq. (1) as defined in Eq. (5).



$$K = \frac{[A_{\text{hyd}}]}{[A] \times [\text{H}_2\text{O}]} \quad (2)$$

$$K \times [\text{H}_2\text{O}] = K_w = \frac{[A_{\text{hyd}}]}{[A]} \quad (3)$$

$$K = \frac{K_w}{[\text{H}_2\text{O}]} \quad (4)$$

$$\Delta G = -RT \ln(K) \quad (5)$$

¹⁸O Isotopic exchange experiments: Isotope exchange experiments were performed with an Advion ExpressionL compact mass spectrometer (CMS) by using the atmospheric solid analysis probe (ASAP) technique; 350 m/z, and acquisition speed 10000 m/z units per second. The ion source settings correspond to a capillary temperature of 250 °C, capillary voltage 110 V, source offset voltage 16 V, APCI source gas temperature 350 °C, and corona discharge voltage 4 μA. The obtained spectra were analyzed by using Advion CheMS Express software version 5.1.0.2. A trace amount of **13b** and **4b** was dissolved in 50 μL of ¹⁸O isotopically labeled water (97 atom %) under nitrogen atmosphere in an oven-dried GC vial and shaken for 1 h. The glass capillary of the ASAP probe was used quickly under hot conditions to exclude ambient moisture contamination. After background subtraction, the corresponding MS spectrum was obtained. For details see Supporting Information (S.3).

Quantum chemical calculations: Geometry optimization was performed at the B3LYP-D3/6-31+G(d,p) level of theory in gas phase.^[58–63] The solution state was modelled both through addition of explicit water molecules and through the implicit continuum solvation model (SMD).^[60] Free energies in solution are referenced to a standard state of 1 M through consideration of a standard state correction of $\Delta G_{0K \rightarrow 298K}^{\text{atm} \rightarrow 1M} = +7.91 \text{ kJ mol}^{-1}$. Single point energies were calculated for the optimized geometries using the DLPNO-CCSD(T) method.^[64–66] Two-point (cc-pVTZ and cc-pVQZ) extrapolation was employed at the DLPNO-CCSD(T) level of theory to estimate a result obtained using a complete (infinitely large) basis set.^[66] The isotropic chemical shielding values were calculated at the SMD(H₂O)/B3LYP/pcS-3//SMD(H₂O)/B3LYP-D3/6-31+G(d,p) level of theory.^[59] The ¹H chemical shifts were referenced relative to chemically and structurally similar molecules (see Supporting Information). All calculations were performed using Gaussian 09, Revision D.01.^[68] To identify the conformations of diol molecules, a relaxed potential energy surface scan on two dihedral angles H–O–C–C (two hydroxyl groups) was performed at the SMD(H₂O)/B3LYP-D3/6-31+G(d,p) level. The conformations with the lowest energies on the potential energy surface were then fully optimized at the SMD(H₂O)/B3LYP-D3/6-31+G(d,p) level. The optimized water-complexed geometries have been located by a stochastic search procedure. This procedure generates an ensemble of initial random arrangements of water molecules around the respective structure, whose optimization at B3LYP-D3/6-31+G(d,p) level then generates the minima used for all quantitative work.^[69,70]

Synthesis of 4b: A solution of 1-methyl-5-hydroxymethylcytosine (119 mg, 0.77 mmol) and activated MnO₂ (333 mg, 3.84 mmol, 5eq) in 12 ml of anhydrous acetonitrile was stirred at room temperature for 20 h. The reaction mixture was then diluted with methanol (10 mL) and filtered (washed with methanol). The crude product was purified by flash column chromatography over silica gel (12% to 15% MeOH/5% NH₄OH/DCM) to afford a clean white powder (35 mg, 0.23 mmol, 30%). R_f (15% MeOH/5% NH₄OH/DCM) = 0.54. ¹H-NMR (400 MHz, DMSO–D₆, ppm): δ = 9.41 (s, 1H, formyl-H), 8.64 (s, 1H, C₆-H), 7.98 (br-s, 1H, N-H₂), 7.79 (br-s, 1H, N-H₂), 3.37 (s, 1H,

–CH₃). ¹³C-NMR (100 MHz, DMSO–D₆, ppm): δ = 188.1, 162.7, 160.2, 153.9, 104.3, 37.7. ¹H-NMR (400 MHz, D₂O, ppm): δ = 9.45 (s, 1H, formyl-H), 8.46 (s, 1H, C₆-H), 3.49 (s, 1H, –CH₃). ¹³C-NMR (100 MHz, D₂O, ppm): δ = 189.9, 163.0, 160.4, 157.0, 105.4, 38.3. EA: Calculated [%]: C: 47.06 N: 27.44 H: 4.61; Found [%]: C: 47.90 N: 26.09 H: 4.36. HR-MS (EI, 70 eV, M⁺): [C₆H₇N₃O₂]⁺, calculated: 153.0533, found: 153.0533.

Synthesis of 13b: 1,5-Dimethyluracil (0.50 g, 3.57 mmol) was dissolved in 170 mL distilled water, then K₂S₂O₈ (1.93 g, 7.14 mmol, 2 eq) was added portion-wise over 1 h at 85 °C and the reaction mixture was stirred for 16 h. After the TLC showed complete conversion of the reactant, the reaction mixture was cooled down to room temperature and the solvent was removed under high vacuum. The crude product was purified by flash column chromatography over silica gel (3% MeOH/2% AcOH/DCM to 10% MeOH/2% AcOH/DCM) to afford a clean white powder (302.63 mg, 1.96 mmol, 55%). ¹H-NMR (400 MHz, DMSO–D₆, ppm): δ = 9.76 (s, 1H, formyl-H), 8.48 (s, 1H, C₅-H), 3.65 (br-s, 1H, N-H), 3.36 (s, 3H, –CH₃). ¹³C-NMR (100 MHz, DMSO–D₆, ppm): δ = 186.7, 163.0, 153.1, 151.0, 110.3, 36.8. ¹H-NMR (400 MHz, D₂O, ppm): δ = 9.58 (s, 1H, formyl-H), 8.44 (s, 1H, C₆-H), 3.46 (s, 3H, –CH₃). ¹³C-NMR (100 MHz, D₂O, ppm): δ = 186.7, 163.0, 153.1, 151.0, 110.3, 36.8. EA: Calculated [%]: C: 46.76 N: 18.18 H: 3.92; Found [%]: C: 48.49 N: 18.20 H: 3.98. HR-MS (EI, 70 eV, [M⁺]): [C₆H₆N₂O₃]⁺, calculated: 154.0373, found: 154.0372.

Acknowledgements

We thank the Deutsche Forschungsgemeinschaft (DFG, German Research Foundation) for financial support via SFB1309 (PID 325871075). We also thank Felix Müller and Sophie Gutenthaler for helping with the purification of compounds and Stella Marie Bauer for the assistance in compound synthesis, as well as the Daumann group for a sample of 5fdC (**4c**). Open Access funding enabled and organized by Projekt DEAL.

Conflict of Interest

The authors declare no conflict of interest.

Data Availability Statement

The data that support the findings of this study are available in the supplementary material of this article.

Keywords: aldehyde hydrates · computational chemistry · DNA methylation · epigenetics · modified nucleic acids · TET enzymes

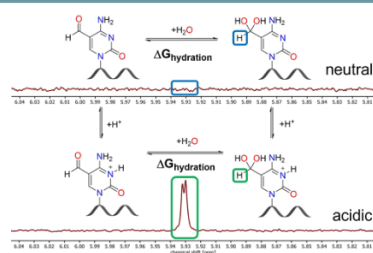
- [1] K. D. Robertson, *Nat. Rev. Genet.* **2005**, *6*, 597–610.
- [2] R. Lister, M. Pelizzola, R. H. Dowen, R. D. Hawkins, G. Hon, J. Tonti-Filippini, J. R. Nery, L. Lee, Z. Ye, Q.-M. Ngo, L. Edsall, J. Antosiewicz-Bourget, R. Stewart, V. Ruotti, A. H. Millar, J. A. Thomson, B. Ren, J. R. Ecker, *Nature* **2009**, *462*, 315–322.
- [3] A. M. Deaton, A. Bird, *Genes Dev.* **2011**, *25*, 1010–1022.
- [4] E.-A. Raiber, R. Hardisty, P. van Delft, S. Balasubramanian, *Nat. Chem. Rev.* **2017**, *1*, 0069.

- [5] A. Bird, *Genes Dev.* **2002**, *16*, 6–21.
- [6] M. G. Goll, T. H. Bestor, *Annu. Rev. Biochem.* **2005**, *74*, 481–514.
- [7] N. Bhutani, D. M. Burns, H. M. Blau, *Cell* **2011**, *146*, 866–872.
- [8] E. Kriukiene, V. Labrie, T. Khare, G. Urbanavičiūtė, A. Lapinaite, K. Koncevičius, D. Li, T. Wang, S. Pai, C. Ptak, J. Gordevičius, S.-C. Wang, A. Petronis, S. Klimašauskas, *Nat. Commun.* **2013**, *4*, 2190.
- [9] S. Kriaucionis, N. Heintz, *Science* **2009**, *324*, 929–930.
- [10] M. Tahiliani, K. P. Koh, Y. Shen, W. A. Pastor, H. Bandukwala, Y. Brudno, S. Agarwal, L. M. Iyer, D. R. Liu, L. Aravind, A. Rao, *Science* **2009**, *324*, 930–935.
- [11] S. Ito, A. C. D'Alessio, O. V. Taranova, K. Hong, L. C. Sowers, Y. Zhang, *Nature* **2010**, *466*, 1129–1133.
- [12] Y. F. He, B. Z. Li, Z. Li, P. Liu, Y. Wang, Q. Tang, J. Ding, Y. Jia, Z. Chen, L. Li, Y. Sun, X. Li, Q. Dai, C. X. Song, K. Zhang, C. He, G. L. Xu, *Science* **2011**, *333*, 1303–1307.
- [13] S. Ito, L. Shen, Q. Dai, S. C. Wu, L. B. Collins, J. A. Swenberg, C. He, Y. Zhang, *Science* **2011**, *333*, 1300–1303.
- [14] T. Pfaffeneder, B. Hackner, M. Truß, E. Münzel, M. Müller, C. A. Deiml, C. Hagemeyer, T. Carell, *Angew. Chem. Int. Ed.* **2011**, *50*, 7008–7012; *Angew. Chem.* **2011**, *123*, 7146–7150.
- [15] N. S. W. Jonasson, R. Janßen, A. Menke, F. L. Zott, H. Zipse, L. J. Daumann, *ChemBioChem* **2021**, *22*, 3333–3340.
- [16] R. M. Kohli, Y. Zhang, *Nature* **2013**, *502*, 472–479.
- [17] L. Hu, J. Lu, J. Cheng, Q. Rao, Z. Li, H. Hou, Z. Lou, L. Zhang, W. Li, W. Gong, M. Liu, C. Sun, X. Yin, J. Li, X. Tan, P. Wang, Y. Wang, D. Fang, Q. Cui, P. Yang, C. He, H. Jiang, C. Luo, Y. Xu, *Nature* **2015**, *527*, 118–122.
- [18] D. J. Crawford, M. Y. Liu, C. S. Nabel, X.-J. Cao, B. A. Garcia, R. M. Kohli, *J. Am. Chem. Soc.* **2016**, *138*, 730–733.
- [19] J. Lu, L. Hu, J. Cheng, D. Fang, C. Wang, K. Yu, H. Jiang, Q. Cui, Y. Xu, C. Luo, *Phys. Chem. Chem. Phys.* **2016**, *18*, 4728–4738.
- [20] M. Y. Liu, H. Torabifard, D. J. Crawford, J. E. DeNizio, X.-J. Cao, B. A. Garcia, G. A. Cisneros, R. M. Kohli, *Nat. Chem. Biol.* **2017**, *13*, 181–187.
- [21] J. E. DeNizio, M. Y. Liu, E. M. Leddin, G. A. Cisneros, R. M. Kohli, *Biochemistry* **2019**, *58*, 411–421.
- [22] S. O. Waheed, S. S. Chaturvedi, T. G. Karabencheva-Christova, C. Z. Christov, *ACS Catal.* **2021**, *11*, 3877–3890.
- [23] M. B. Berger, A. R. Walker, E. A. Vazquez-Montelongo, G. A. Cisneros, *Phys. Chem. Chem. Phys.* **2021**, *23*, 22227–22240.
- [24] B. A. Caldwell, M. Y. Liu, R. D. Prasasya, T. Wang, J. E. DeNizio, N. A. Leu, N. Y. A. Amoh, C. Krapp, Y. Lan, E. J. Shields, R. Bonasio, C. J. Lengner, R. M. Kohli, M. S. Bartolomei, *Mol. Cell* **2021**, *81*, 859–869.
- [25] D. Globisch, M. Münzel, M. Müller, S. Michalakis, M. Wagner, S. Koch, T. Brückl, M. Biel, T. Carell, *PLoS One* **2010**, *5*, e15367.
- [26] A. Maiti, A. C. Drohat, *J. Biol. Chem.* **2011**, *286*, 35334–35338.
- [27] S. Schiesser, T. Pfaffeneder, K. Sadeghian, B. Hackner, B. Steigenberger, A. S. Schröder, J. Steinbacher, G. Kashiwazaki, G. Höfner, K. T. Wanner, C. Ochsenfeld, T. Carell, *J. Am. Chem. Soc.* **2013**, *135*, 14593–14599.
- [28] K. Iwan, R. Rahimoff, A. Kirchner, F. Spada, A. S. Schröder, O. Kosmatchev, S. Ferizaj, J. Steinbacher, E. Parsa, M. Müller, T. Carell, *Nat. Chem. Biol.* **2018**, *14*, 72–78.
- [29] A. R. Weber, C. Krawczyk, A. B. Robertson, A. Kuśnierczyk, C. B. Vågbo, D. Schuermann, A. Klungland, P. Schär, *Nat. Commun.* **2016**, *7*, 10806.
- [30] M. Bachman, S. Uribe-Lewis, X. Yang, M. Williams, A. Murrell, S. Balasubramanian, *Nat. Chem.* **2014**, *6*, 1049–1055.
- [31] M. Bachman, S. Uribe-Lewis, X. Yang, H. E. Burgess, M. Iurlaro, W. Reik, A. Murrell, S. Balasubramanian, *Nat. Chem. Biol.* **2015**, *11*, 555–557.
- [32] S. Waschke, J. Reefschlager, D. Bärwolff, P. Langen, *Nature* **1975**, *255*, 629–630.
- [33] S. Bjelland, L. Eide, R. W. Time, R. Stote, I. Eftedal, G. Volden, E. Seeberg, *Biochemistry* **1995**, *34*, 14758–14764.
- [34] K. Kemmerich, F. A. Dingler, C. Rada, M. S. Neuberger, *Nucleic Acids Res.* **2012**, *40*, 6016–6025.
- [35] T. Pfaffeneder, F. Spada, M. Wagner, C. Brandmayr, S. K. Laube, D. Eisen, M. Truss, J. Steinbacher, B. Hackner, O. Kotljarova, D. Schuermann, S. Michalakis, O. Kosmatchev, S. Schiesser, B. Steigenberger, N. Raddaoui, G. Kashiwazaki, U. Müller, C. G. Spruijt, M. Vermeulen, H. Leonhardt, P. Schär, M. Müller, T. Carell, *Nat. Chem. Biol.* **2014**, *10*, 574–581.
- [36] R. P. Johnson, A. M. Fleming, R. T. Perera, C. J. Burrows, H. S. White, *J. Am. Chem. Soc.* **2017**, *139*, 2750–2756.
- [37] R. C. A. Dubini, A. Schön, M. Müller, T. Carell, P. Rovó, *Nucleic Acids Res.* **2020**, *48*, 8796–8807.
- [38] S. Sappa, D. Dey, B. Sudhamalla, K. Islam, *J. Am. Chem. Soc.* **2021**, *143*, 11891–11896.
- [39] S. H. Hilal, L. L. Bornander, L. A. Carreira, *QSAR Comb. Sci.* **2005**, *24*, 631–638.
- [40] S. Huang, A. K. Miller, W. Wu, *Tetrahedron Lett.* **2009**, *50*, 6584–6585.
- [41] D. K. Rogstad, J. Heo, N. Vaidehi, W. A. Goddard, A. Burdzy, L. C. Sowers, *Biochemistry* **2004**, *43*, 5688–5697.
- [42] R. E. Hardisty, F. Kawasaki, A. B. Sahakyan, S. Balasubramanian, *J. Am. Chem. Soc.* **2015**, *137*, 9270–9272.
- [43] J. P. Guthrie, *Can. J. Chem.* **1978**, *56*, 962–973.
- [44] R. P. Bell, in *Advances in Physical Organic Chemistry*, Vol. 4 (Ed.: V. Gold), Academic Press, **1966**, pp. 1–29.
- [45] J. L. Kurz, *J. Am. Chem. Soc.* **1967**, *89*, 3524–3528.
- [46] L. C. Gruen, P. T. McTigue, *J. Chem. Soc.* **1963**, 5217–5223.
- [47] E. Lombardi, P. B. Sogo, *J. Chem. Phys.* **1960**, *32*, 635–636.
- [48] P. Greenzaid, *J. Org. Chem.* **1973**, *38*, 3164–3167.
- [49] J. Sayer, *J. Org. Chem.* **1975**, *40*, 2545–2547.
- [50] S. Cabani, P. Gianni, E. Matteoli, *J. Phys. Chem.* **1972**, *76*, 2959–2966.
- [51] S. Barman, K. L. Diehl, E. V. Anslyn, *RSC Adv.* **2014**, *4*, 28893–28900.
- [52] A. Schön, E. Kaminska, F. Schelter, E. Ponkkonen, E. Korytiaková, S. Schiffers, T. Carell, *Angew. Chem. Int. Ed.* **2020**, *59*, 5591–5594; *Angew. Chem.* **2020**, *132*, 5639–5643.
- [53] K. J. R. Rosman, P. D. P. Taylor, *Pure Appl. Chem.* **1998**, *70*, 217–235.
- [54] R. Gómez-Bombarelli, M. González-Pérez, M. T. Pérez-Prior, E. Calle, J. Casado, *J. Phys. Chem. A* **2009**, *113*, 11423–11428.
- [55] L. P. Olson, J. Luo, Ö. Almarsson, T. C. Bruice, *Biochemistry* **1996**, *35*, 9782–9791.
- [56] A.-K. C. Schmidt, C. B. W. Stark, *Org. Lett.* **2011**, *13*, 4164–4167.
- [57] A. J. K. Roth, M. Tretbar, C. B. W. Stark, *Chem. Commun.* **2015**, *51*, 14175–14178.
- [58] H. Torabifard, G. A. Cisneros, *Chem. Sci.* **2018**, *9*, 8433–8445.
- [59] A. D. Becke, *J. Chem. Phys.* **1993**, *98*, 5648–5652.
- [60] F. Jensen, *J. Chem. Theory Comput.* **2008**, *4*, 719–727.
- [61] A. V. Marenich, C. J. Cramer, D. G. Truhlar, *J. Phys. Chem. B* **2009**, *113*, 6378–6396.
- [62] S. Grimme, J. Antony, S. Ehrlich, H. Krieg, *J. Chem. Phys.* **2010**, *132*, 154104.
- [63] T. J. Zuehlisdorff, C. M. Isborn, *J. Chem. Phys.* **2018**, *148*, 024110.
- [64] A. Nicolaidis, A. Rauk, M. N. Glukhovtsev, L. Radom, *J. Phys. Chem.* **1996**, *100*, 17460–17464.
- [65] F. Neese, E. F. Valeev, *J. Chem. Theory Comput.* **2011**, *7*, 33–43.
- [66] M. Saitow, U. Becker, C. Riplinger, E. F. Valeev, F. Neese, *J. Chem. Phys.* **2017**, *146*, 164105.
- [67] A. Altun, F. Neese, G. Bistoni, *J. Chem. Theory Comput.* **2019**, *15*, 215–228.
- [68] A. Altun, F. Neese, G. Bistoni, *Beilstein J. Org. Chem.* **2018**, *14*, 919–929.
- [69] M. J. Frisch, G. W. Trucks, H. B. Schlegel, G. E. Scuseria, M. A. Robb, J. R. Cheeseman, G. Scalmani, V. Barone, G. A. Petersson, H. Nakatsuji, X. Li, M. Caricato, A. V. Marenich, J. Bloino, B. G. Janesko, R. Gomperts, B. Mennucci, H. P. Hratchian, J. V. Ortiz, A. F. Izmaylov, J. L. Sonnenberg, Williams, F. Ding, F. Lipparini, F. Egidi, J. Goings, B. Peng, A. Petrone, T. Henderson, D. Ranasinghe, V. G. Zakrzewski, J. Gao, N. Rega, G. Zheng, W. Liang, M. Hada, M. Ehara, K. Toyota, R. Fukuda, J. Hasegawa, M. Ishida, T. Nakajima, Y. Honda, O. Kitao, H. Nakai, T. Vreven, K. Throssell, J. A. Montgomery Jr., J. E. Peralta, F. Ogliaro, M. J. Bearpark, J. J. Heyd, E. N. Brothers, K. N. Kudin, V. N. Staroverov, T. A. Keith, R. Kobayashi, J. Normand, K. Raghavachari, A. P. Rendell, J. C. Burant, S. S. Iyengar, J. Tomasi, M. Cossi, J. M. Millam, M. Klene, C. Adamo, R. Cammi, J. W. Ochterski, R. L. Martin, K. Morokuma, O. Farkas, J. B. Foresman, D. J. Fox, *Gaussian 09*, Rev. D.01, Wallingford, CT, **2009**.
- [70] M. Saunders, *J. Comb. Chem.* **2004**, *25*, 621–626.
- [71] D. Šakić, V. Vrček, *J. Phys. Chem. A* **2012**, *116*, 1298–1306.

Manuscript received: November 25, 2021
Revised manuscript received: January 24, 2022
Accepted manuscript online: January 27, 2022
Version of record online: ■■■, ■■■■

RESEARCH ARTICLE

The hydrate content of 5-formylcytosine and its uracil derivative has been identified and quantified using a combination of NMR and mass spectroscopic measurements as well as theoretical studies. We report a free energy of hydration for the hydration reactions of 5fC and 5fU. In case of 5fC, acidification leads to an increased hydrate content of up to 0.5% in aqueous solution.



*F. L. Zott, V. Korotenko, H. Zipse**

1 – 8

The pH-Dependence of the Hydration of 5-Formylcytosine: an Experimental and Theoretical Study



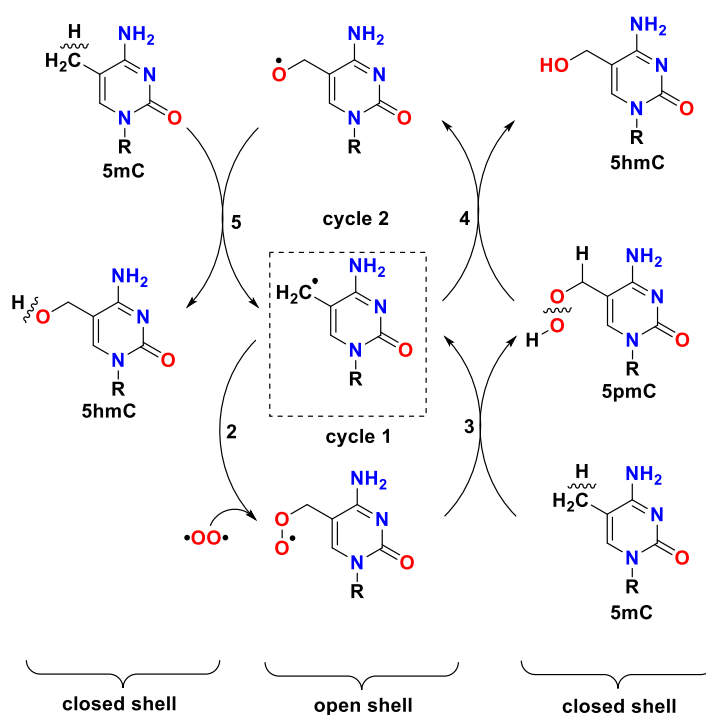
5. Autoxidation of 1,5-Dimethylcytosine: Computational Study

Vasily Korotenko, Hendrik Zipse

Unpublished results. Manuscript under preparation.

Author contributions: The project was conceived by V.K. and H.Z. The computational study was performed by V.K. The manuscript was written by V.K.

The (aut)oxidation reaction of 1,5-dimethylcytosine (1,5-dmC) was studied using DFT and DLPNO-CCSD(T) levels of theory. The autoxidation of 5mC is unlikely to occur through initiation by triplet oxygen or through unimolecular decomposition of hydroperoxides. All endergonic bimolecular chain reactions between neutral closed-shell compounds and free radicals involve the transfer of a hydrogen atom to form a product with a higher BDE value. The thermodynamics of the presented mechanism, in principle, agrees with the experimental kinetics. We assume that the protonation ($\text{pH} < 7$) of oxidizable nucleic acids inhibits the oxidation process by increasing the $\text{BDE}(\text{C-H})$ values.



Autoxidation of 1,5-Dimethylcytosine: Computational Study

V. Korotenko, H. Zipse*

Dept. Chemistry, LMU Munich, Butenandtstr. 5-13, D-81377 Munich, Germany

Oxidation, thermodynamic stability, radical stabilization energy, radicals, isodesmic equations, DFT, DLPNO-CCSD(T), nucleic base

The (aut)oxidation reaction of 1,5-dimethylcytosine (1,5-dmC) was studied using DFT and DLPNO-CCSD(T) levels of theory. The autoxidation of 5mC is unlikely to occur through initiation by triplet oxygen or through unimolecular decomposition of hydroperoxides. All endergonic bimolecular chain reactions between neutral closed-shell compounds and free radicals involve the transfer of a hydrogen atom to form a product with a higher BDE value. The thermodynamics of the presented mechanism, in principle, agrees with the experimental kinetics. We assume that the protonation ($\text{pH} < 7$) of oxidizable nucleic acids inhibits the oxidation process by increasing the BDE(C-H) values.

Introduction

Autoxidation reactions are defined as oxidations which can be brought about by oxygen gas at normal temperatures without the intervention of a visible flame or of an electric spark. Execution of a controlled hydrocarbon autoxidation is a challenge receiving increasing attention in both academic and industrial research.¹ This work is focusing on the calculated enthalpies and free energies of the autoxidation 1,5-dimethylcytosine. It has been observed experimentally that 5-methyl-2'-deoxycytidine (5mdC) can be sequentially oxidized by air to 5-hydroxymethyl-2'-deoxycytidine (5hmdC), 5-formyl-2'-deoxycytidine (5fdC), 5-carboxy-2'-deoxycytidine (5cadC).² (Figure 1) The mechanistic study of this reaction can help to better understand the chemical aspects of the oxidative epigenetic regulation of the DNA methylation.³ (Figure 2)

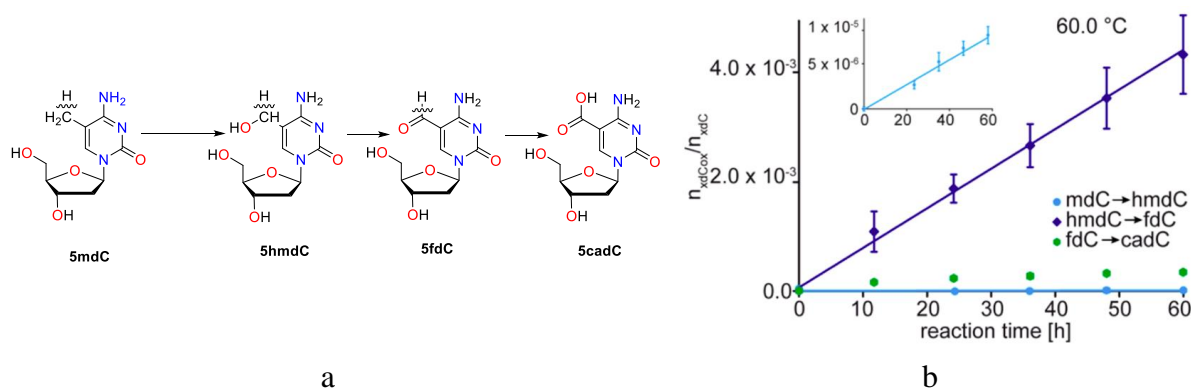


Figure 1. Experimental data reported in ref.²: a) oxidation products, and b) oxidation kinetics of 5mdC to 5hmdC (cyan), 5hmdC to 5fdC (blue), and 5fdC to 5cadC (green) at 60 °C and pH 7.4. While 5hmdC is efficiently oxidized to 5fdC, 5fdC gives only a little 5cadC. Depicted are the means of triplicate experiments; error bars reflect the standard deviations in the experiment.

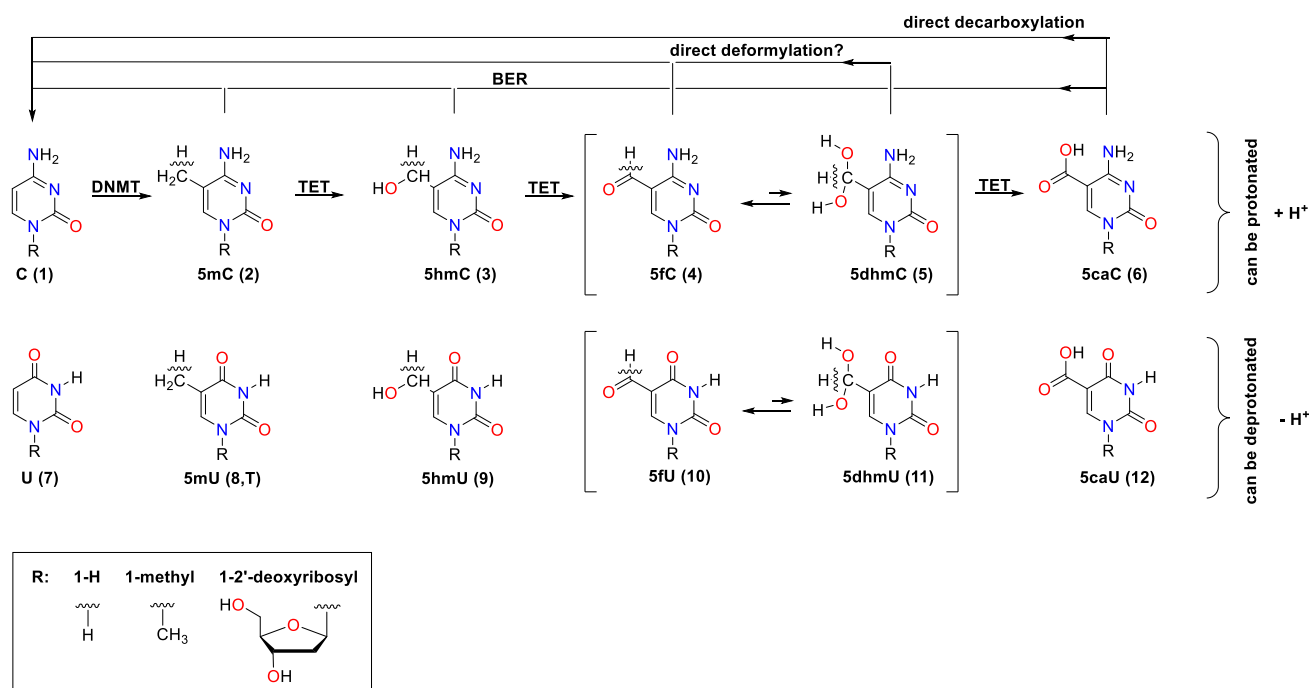


Figure 2. Cytosine derivatives formed during epigenetic gene regulation together with their deamination products. The wavy line indicates the C-H bonds for which the homolytic dissociation enthalpies (BDE) were calculated. DNMT - DNA methyltransferases, TET - ten-eleven translocation enzymes, BER - base excision repair.

Autoxidation reactions involve chain initiation reactions, chain propagation and chain termination reactions. While the last two reaction types seem to be quite well established, the primary chain initiation reactions remain hypothetical.⁴ Possible initiation reactions are: (a) the unimolecular dissociation of hydroperoxides into benzyloxy radical and hydroxyl radical, (b) the bimolecular hydroperoxide decomposition, in which benzyloxy radical, benzylperoxy radical and a water molecule are formed or the direct reaction of the hydrocarbon with either (c) triplet oxygen or (d) ozone.⁵ Zipse and Sandhiya have investigated the autoxidation initiation reactions (a), (b) and (c) on the example of toluene, which is comparable to 1,5-dimethylcytosine. They used CBS, QB3, G4 and G3B3 calculations to come to the conclusion that the autoxidation of hydrocarbons is unlikely to occur through initiation by triplet oxygen (c) or through unimolecular decomposition of hydroperoxides (a) due to a high positive enthalpy ($\Delta H_{298}(c)=+169.9\pm 2.0$ kJ mol⁻¹ and $\Delta H_{298}(a)=+202.0\pm 11.6$ kJ mol⁻¹). The bimolecular hydroperoxide decomposition (b) is the reaction with the lowest enthalpy ($\Delta H_{298}(b)=+65.8\pm 14.8$ kJ mol⁻¹) and therefore the most favorable out of these three reactions, even though the enthalpy is still higher than zero.⁵

Originally it was considered that autoxidation reaction chains are initiated by the thermal decomposition of hydroperoxides contained in the substrate.⁶ If that was true, then the thermal oxidation of the same organic material would be quite reproducible, which is not the case, as shown by Gugumus in 1998. He observed that the lifetime of polypropylene decreases at a higher ozone level and came to the conclusion that hydroperoxide initiated chain oxidation is determining only the rate of oxidation after the induction period. This is assumed to be valid also for other organic materials.⁴ Considering the research done by Zipse, Sandhiya and Gugumus that was mentioned before the direct reaction of the hydrocarbon with ozone it is most likely to substantially contribute to the chain initiation.

First, the thermodynamics of oxidation will depend on the stability of the oxidizing species, which in this reaction are oxygen-centered radicals. In chapter 2, it has been established, that in the presence of one explicit water molecule, the BDE(O-H) values in alcohols become higher, which means that the RSE(RO•) values of the corresponding radicals become less

negative: the radicals are less stable (Figure 3). This allows us (very careful) to make a hypothesis that the oxygen-centered radicals show more activity in water solution than in gas phase, even just because alcohol has one hydrogen atom more than its O-radical, and can form at least one more stabilizing intermolecular hydrogen bond.

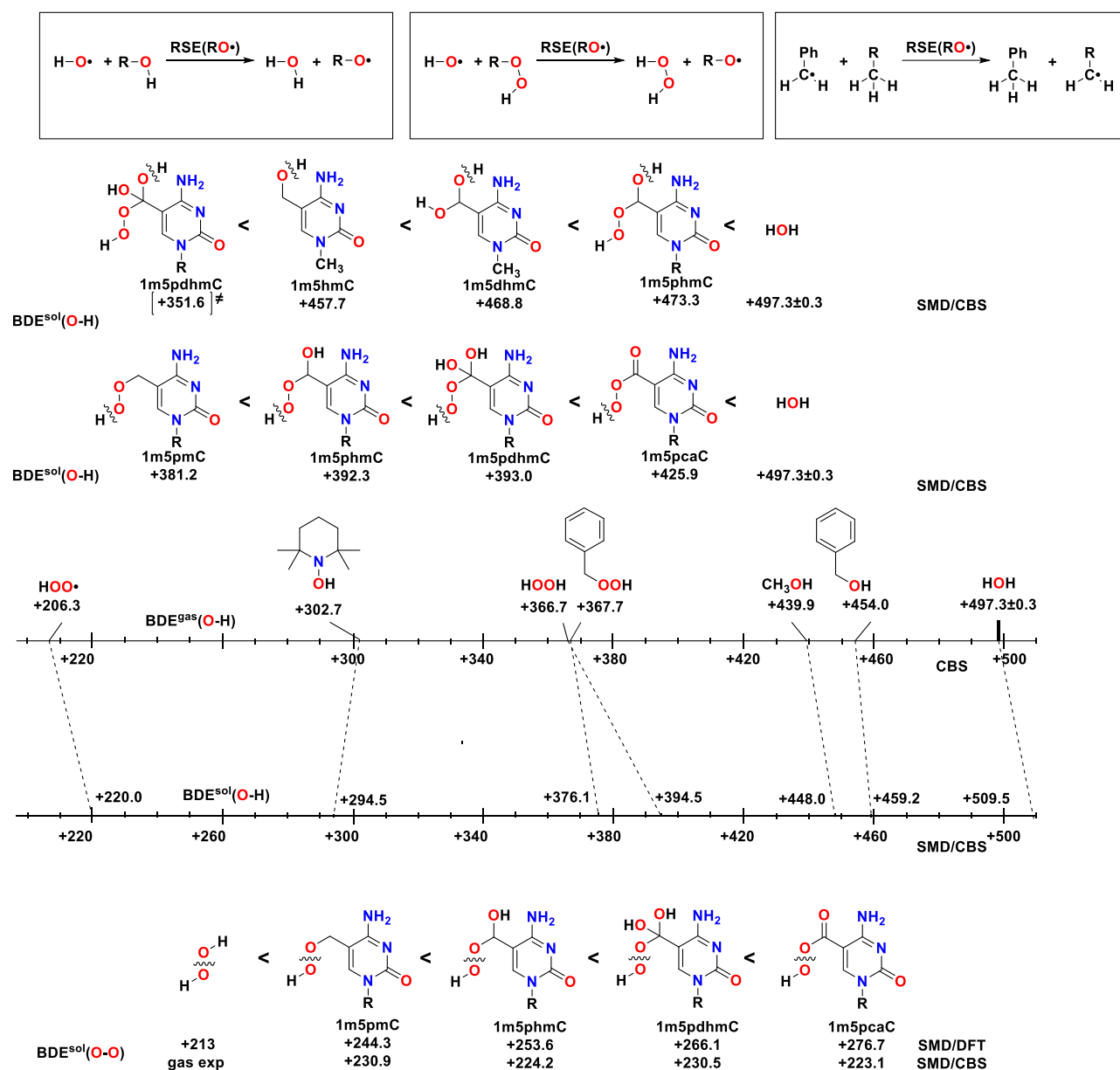


Figure 3. The calculated at the DLPNO-CCSD(T)/CBS level of theory BDE(O-O) values, BDE(O-H) values and the highest BDE-A(O-H)/BDE-D(O-H) values (best conformation by enthalpy) in kJ mol^{-1} .

Second, the thermodynamics of oxidation will depend on the BDE(C-H) values of the species being oxidized. In chapter 3 we showed, that in the derivatives of cytosine, among the substituent groups in the 5th position, the following trend in BDE(C-H) values is observed 5dhm- < 5hm- < 5m- < 5f- (where 5dhm- substituent is dihydroxymethyl, 5hm — hydroxymethyl, 5m — methyl, 5f — formyl). It has been also established that the charge will strongly affect the reactivity of studied molecules: protonation increases the calculated BDE(C-H) values in cytosine derivatives (Figure 4). Based on this knowledge about the oxidizing and reducing agents under consideration, it is possible to propose a mechanism for the autoxidation of 1,5-dimethylcytosine, which is presented in Figures 5-7.

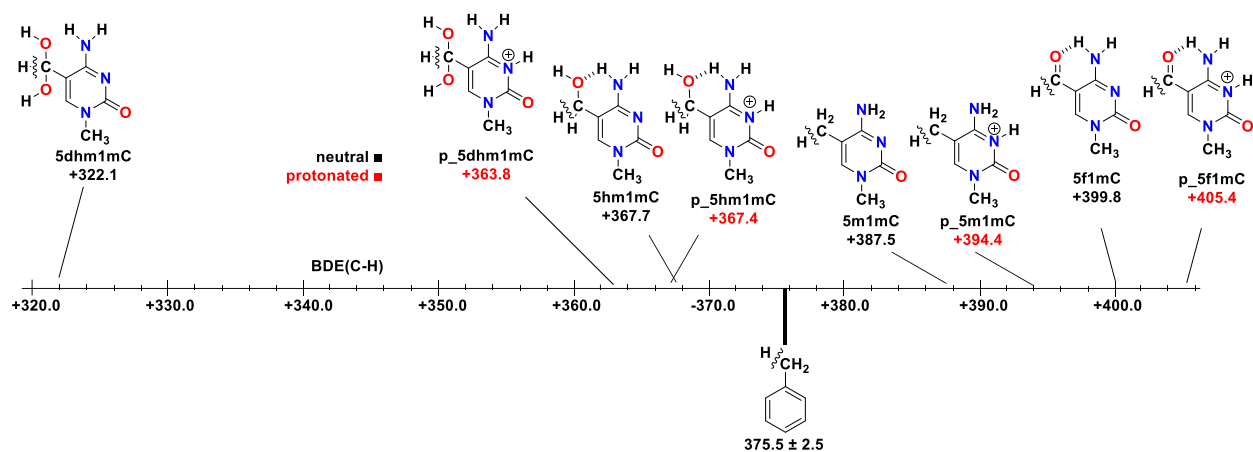


Figure 4. The calculated at the SMD(H₂O)/DLPNO-CCSD(T)/CBS level of theory BDE(C-H) values in kJ mol⁻¹.

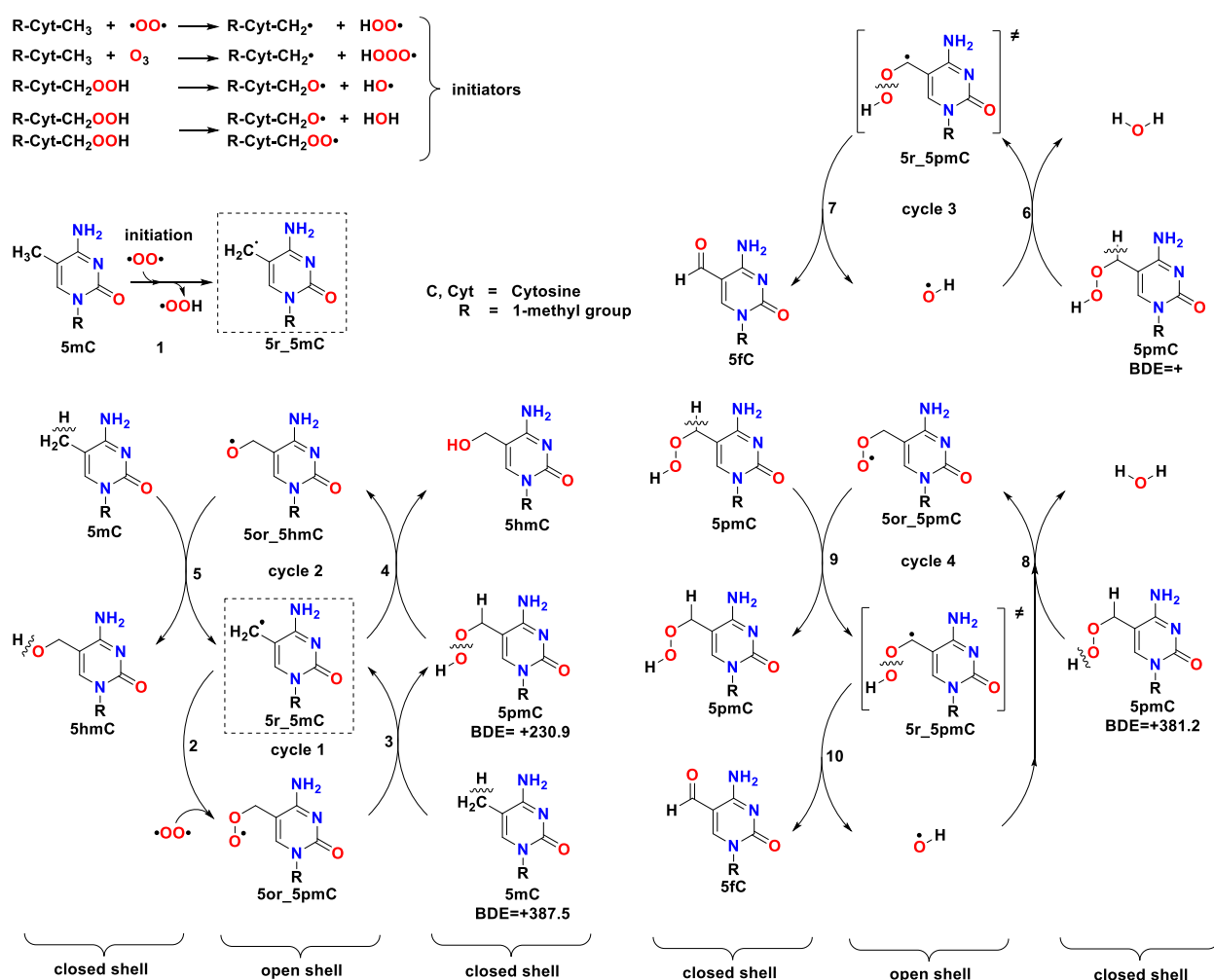


Figure 5. The proposal mechanism of (aut)oxidation reaction: initiation, cycles 1-4. Stable products: 5hm1mC, 5f1mC.

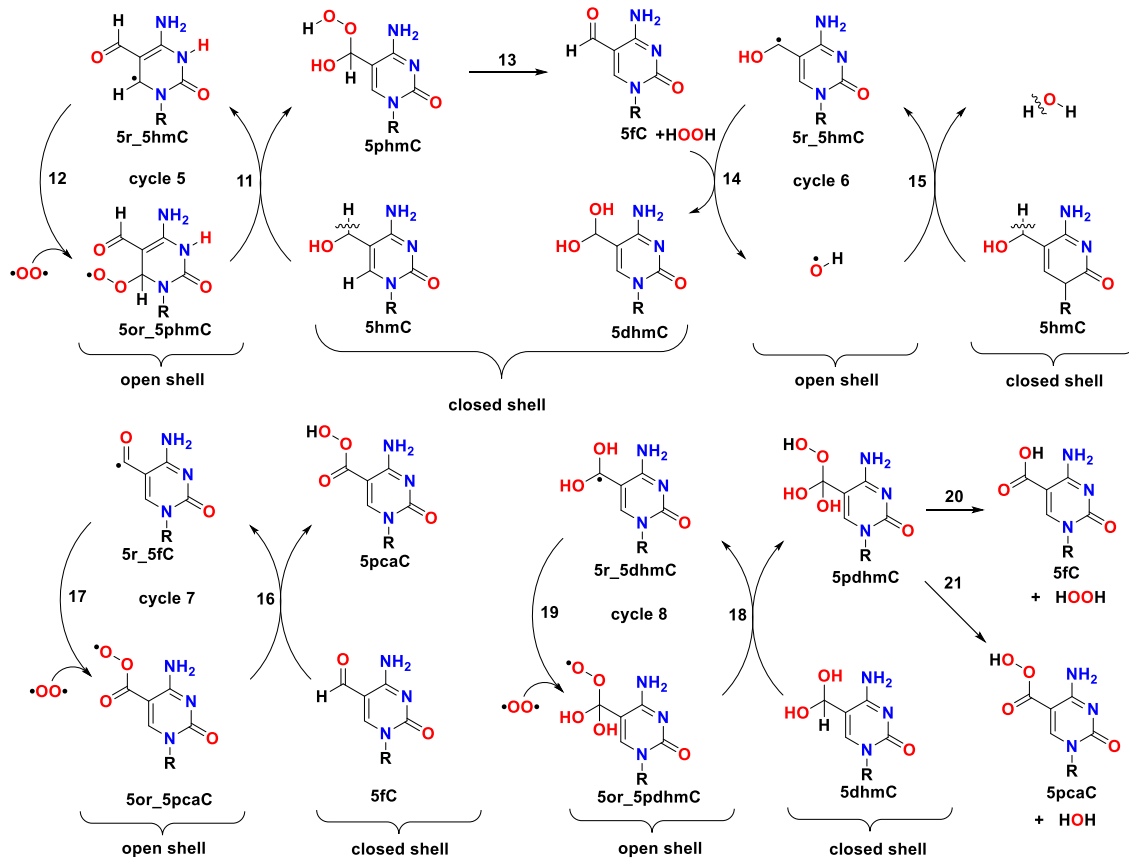


Figure 6. The proposal mechanism of (aut)oxidation reaction: cycles 5-8. Stable products: 5f1mC, 5ca1mC.

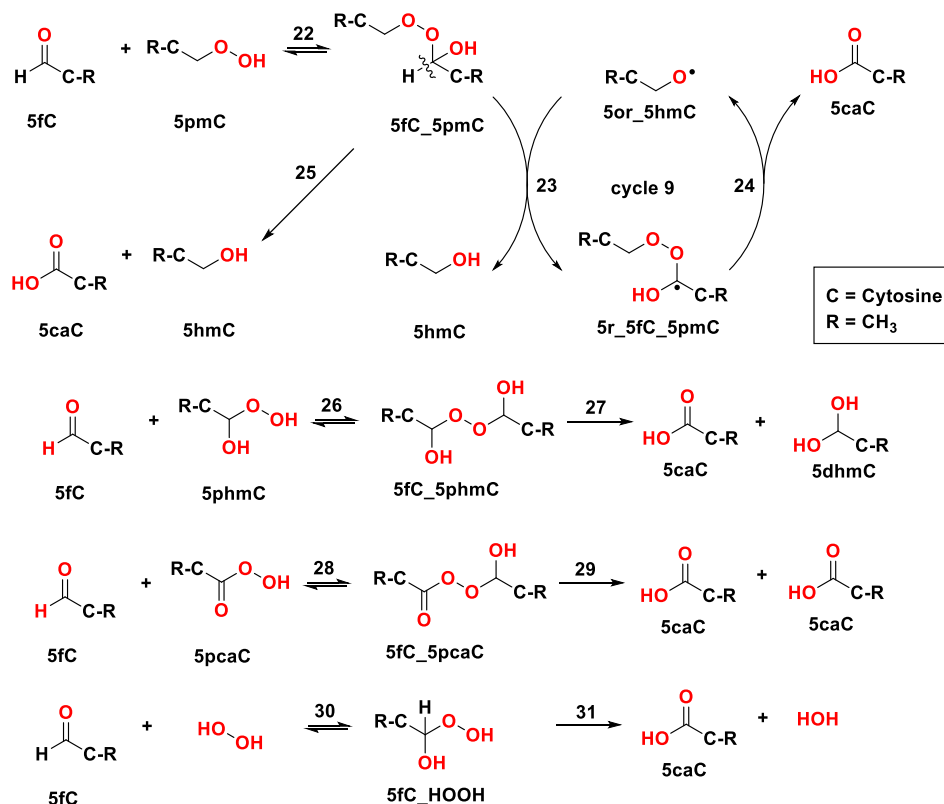


Figure 7. The proposal mechanism of (aut)oxidation reaction: cycle 9 and some possible reactions between peroxides and 5f1mC. Stable product: 5ca1mC.

Computational details

In this work, all geometries were optimized at the SMD(H₂O)/(U)B3LYP-D3/6-31+G(d,p) level of theory with the SMD implicit solvent model⁷ using Gaussian09, Revision D.01.⁸ D3 version of Grimme's dispersion was added to the method of optimization to account the dispersion interactions.^{9,10} Since the relative tautomeric stability of the studied molecules is not trivial and can be changed due to solvation effects, we tested all possible tautomers. Using the expression $C_n^k = \frac{n!}{(n-k)! \cdot k!}$, one can estimate the number of possible tautomers of an asymmetric molecule having n lone pairs and k acidic protons ($k \leq n$). The individuality of the found conformers/tautomers was confirmed using an energy criterion ($\Delta E_{\text{tot}} > 10^{-7}$ a.u.) and comparing geometries by distances between each atom and the centroid point.^{11,12} Frequency calculations have been carried out to verify that the optimized structures are real minima without any imaginary vibration frequency.

Frequency calculations have been carried out to verify that the optimized structures are true minima. Thermochemical corrections to H^{gas} and G^{gas} at 298.15 K were calculated with GoodVibes using the quasi-harmonic approximation.¹³ A «gas» symbol (^{gas}) denotes a standard state of 1 atm in the gas phase and «solution» (^{sol}) denotes 1 mol l⁻¹ in the solution phase. For each studied nucleobase, all the stable tautomers and conformers were taken into account when calculating the Boltzmann-weighted values of E_{tot} , H^{sol} , and G^{sol} . The single point energies were also calculated for the optimized geometries at the DLPNO-CCSD(T) level.¹⁴⁻¹⁶ Two-point (cc-pVTZ and cc-pVQZ) extrapolation was employed at the DLPNO-CCSD(T) level of theory to estimate a result obtained using a complete (infinitely large) basis set.^{15,17} Standard state solvation free energies ΔG^{solv} were computed as the difference between the solution phase free energy G^{sol} of the solution phase optimized molecule (SMD(H₂O)/(U)B3LYP-D3/6-31+G(d,p)), and the gas phase single point free energy G^{gas} ((U)B3LYP-D3/6-31+G(d,p)//SMD(H₂O)/(U)B3LYP-D3/6-31+G(d,p))

$$\Delta G^{\text{solv}} = G^{\text{sol}} - G^{\text{gas}}$$

The solution phase single-point free energies G^{sol} are computed by combining the gas phase free energies G^{gas} with the solvation free energies ΔG^{solv}

$$G^{\text{sol}} = E_{\text{tot}}^{\text{single-point}} + \text{ZPE}^{\text{SMD}/(\text{U})\text{B3LYP-D3}} + \Delta G_{0\text{K} \rightarrow 298\text{K}}^{\text{SMD}/(\text{U})\text{B3LYP-D3}} + \Delta G_{0\text{K} \rightarrow 298\text{K}}^{1\text{atm} \rightarrow 1\text{M}} + \Delta G^{\text{solv}}$$

$\Delta G_{0\text{K} \rightarrow 298\text{K}}^{1\text{atm} \rightarrow 1\text{M}} = +7.91$ kJ mol⁻¹ is the free energy difference for converting from the standard state concentration of 1 atm to the standard state concentration of 1 mol l⁻¹.

Results

The calculated results are presented in table 1. The calculations confirm that not only the enthalpy but also the free energy of the initiation reaction with triplet oxygen are highly positive making the reaction energetically not favorable (the most endothermic and endergonic reaction). This is due to the formation of a primary carbon radical from generally stable, biradical triplet oxygen. The enthalpy also matches very well with the enthalpy of reaction (c) found in the literature. If the depicted mechanism resembles the enzymatic cycle, TET enzymes likely increase reaction rates by stabilizing this highest-energy intermediate, which would also lower the activation energy according to the Bell-Evans-Polanyi principle. The highly reactive 5r_1,5-dmC is then oxidized by triplet oxygen in reaction 2. As the peroxy radical is more stable, this reaction is exothermic. But due to the reduction in moles and thus reduction of entropy, the liberated free energy is -7.91 kJ mol⁻¹ lower: this correction is included in all to all calculated free energies in this work for reactions with the increase (+7.91) or decrease (-7.91) of moles. It is noticeable that reaction 3 is also slightly endothermic and endergonic. The reason for this is that the corresponding BDE(C-H) value is significantly higher, than that of the ROO-H bond (the formation of primary doublet 5r_1,5-dmC is thermodynamically unfavorable). However, as the educt of reaction 3 is a doublet species as well, the reaction is much less endothermic and endergonic than the initiation. That would imply that the reverse reaction should dominate over the forward one. Since this reaction is just a small step in a larger

mechanism, there could still be a driving force through one of the following reactions making reaction 3 possible, for example if the formed hydroperoxide is rapidly consumed in reaction 4 or 5. That should be carefully considered from case to case and is not completely clear in this situation. According to Coote and co-workers reaction 3 is just not as relevant in autoxidation reactions as commonly assumed.¹⁸

Table 1. The calculated at the SMD(H₂O)/(U)B3LYP-D3/6-31+G(d,p) and SMD(H₂O)/DLPNO-CCSD(T)/CBS levels of theory ΔH^{sol} and ΔG^{sol} values of the studied reactions in kJ mol⁻¹.

Cycle	Reaction	Closed-shell		DFT		DLPNO	
		Educt	Product	ΔH^{sol}	ΔG^{sol}	ΔH^{sol}	ΔG^{sol}
	1	5mC		153.7	146.8	170.8	164.0
1	2			-107.2	-67.4	-113.5	-73.6
	3	5mC	5pmC	22.2	23.6	9.6	10.7
2	4	5pmC	5hmC	-171.6	-174.6	-172.0	-173.6
	5	5mC	5hmC	-54.3	-51.1	-66.9	-64.9
3	6	5pmC		-123.1	-129.3	-121.0	-126.8
	7		5fC	-156.8	-188.3	-165.2	-196.8
4	8	5pmC		-142.2	-146.5	-128.3	-132.3
	9	5pmC	5pmC	19.1	17.2	7.3	5.5
	10		5fC	-156.8	-188.3	-165.2	-196.8
5	11	5hmC	5phmC	4.2	0.2	-21.3	-24.0
	12			-116.8	-73.6	-115.5	-73.9
	13	5hpmC	5fC	7.7	-33.7	19.6	-21.6
6	14	5hmC		-147.7	-135.6	-172.0	-162.2
	15		5dhmC (5fC)	-145.5	-151.9	-138.4	-143.2
7	16	5fC		-2.7	-4.4	-22.8	-24.4
	17		5pcaC	-133.2	-93.1	-142.3	-102.0
8	18	5dhmC (5fC)		-62.8	-67.0	-5.2	-4.2
	19		5pdhmC	-56.0	-8.6	-137.8	-94.8
	20	5pdhmC	5caC	-42.3	-87.4	-27.7	-73.4
	21	5pdhmC	5pcaC	-37.9	-80.6	-31.6	-74.1
9	22	5hmC + 5fC	5fC_5pmC	-28.9	29.1	-41.6	17.5
	23	5fC_5pmC	5hmC	-333.8	-340.8	-316.2	-321.6
	24		5caC	47.4	-3.1	27.8	-25.6
	25		5hmC + 5caC	-286.4	-343.9	-288.4	-347.2
	26	5phmC + 5fC		-26.3	36.0	-	-
	27		5dhmC + 5caC	-294.6	-354.2	-	-
	28	5pcaC + 5fC		-18.3	38.2	-	-
	29		5caC + 5caC	-335.5	-388.3	-	-
	30	HOOH + 5fC		-7.8	33.6	-	-
	31		HOH + 5caC	-341.5	-376.9	-	-
Orange	Endergonic limiting reactions						
Yellow	Exergonic reactions dependent on limiting reactions						
Green	Exergonic reactions or cycles						

Reaction 4 is exothermic and exergonic as a methyl radical is oxidized to an oxo-methyl radical. Here, among the three bonds (BDE(C-H, O-O, O-H) = +370.5, +230.9, +381.2 kJ mol⁻¹) in the 5pm1mC molecule, the weakest O-O bond breaks. This reaction really influences the overall enthalpy and free energy change of the reaction mechanism. Reaction 5 completes the second cycle and thus replenishes the central radical intermediate.

Reaction 6 starts cycle 3, where the C-H bond in the 5pm1mC molecule is breaking, which leads to the formation of an unstable radical 5r_5pm1mC, which then decomposes into a hydroxyl radical HO• and 5f1mC in reaction 7.

Reaction 8 starts the more complicated cycle 4, where the OH bond in the 5pm1mC molecule is breaking. Reaction 9 is slightly endergonic, because in the 5pm1mC molecule the BDE(C-H) value is slightly higher than the BDE(O-H) value. Cycle 4 is finishing with the formation of hydroxyl radical HO• and 5f1mC in a highly exothermic manner.

Reactions 11-15 are exergonic and can be a good reason for both the increased 5f1mC (product) and decreased 5hm1mC (educt) concentrations observed in the kinetics measurements.² It should be noted that the resulting hydrate (~0.5%) in reaction 14 exergonic decomposes into 5f1mC (~99.5%) and HOH molecule.³

The percarboxylic acid 5pcaC that forms in cycles 7 and 8 can also serve as a source of the hydroxide radical HO• in cycle 1, in which case 5ca1mC will be one of the products of the cycle. Note that cycle 8 is generally exergonic, but it is thermodynamically limited by the positive free energy formation of the 5dhmC hydrate.³ The BDE(O-H, in the peroxy group) and BDE(O-O) scales in figure 3 show that among all the studied peroxides, 1m5pcaC has the strongest O-H and O-O bond. We hypothesize that this peroxide is the least active and can be seen in solution upon closer experimental examination.

Cycle 9 is exergonic; however, it is thermodynamically limited by the positive free energy formation of the 5f1mC_5pm1mC molecule (reaction 22). In this case, the 5f1mC_5pm1mC molecule will rather decompose into 5ca1mC and 5hm1mC than take part in cycle 9. In addition, we considered different variants of reaction 22: reactions 26, 28 and 30 - they are all endergonic and their products exergonic decompose with the formation of 5ca1mC (reactions 27, 29 and 31). Thus, the performed calculations show that the autoxidation of 1,5-dmC is thermodynamically probable. However, conclusions for biological systems should be made with caution, since the natural environment of cytosine has been completely ignored.

Conclusions

The current proposal mechanism is very similar with the toluene (aut)oxidation mechanism.⁵ The (aut)oxidation of 5mC is unlikely to occur through initiation by triplet oxygen or through unimolecular decomposition of hydroperoxides, rather, by ozone.

All endergonic bimolecular chain reactions between neural compounds and free radicals involve the transfer of a hydrogen atom to form a neural compound with a higher BDE value.

Absolutely most of the reactions in the considered (aut)oxidation mechanism is exergonic, with the exception of endergonic reactions that are thermodynamically limiting: 1 (initiation) > 22 > 3 > 9.

Based on the considered mechanism, it is possible to explain the results of the kinetic experiment² shown in figure 1, where the following trend in the oxidation rate of molecules can be seen **5fC** > **5caC** > **5hmC**:

5fC is readily formed in exergonic cycles **3**, **5** and **6** and not readily consumed in the slightly exergonic cycle 8 (ΔG^{sol} of the cycle start -4.2 kJ/mol), so 5fC may accumulate in solution

5caC is formed predominantly in the cycle **8**

5hmC is hardly produced in cycle **1** (ΔG^{sol} of the limiting reaction 3: +10.5 kJ/mol) and very easily consumed in exergonic cycles **5** and **6**

Lowering the pH value will likely slow down the oxidation process by protonating the nucleobases and increasing the BDE(C-H) values.

References

- [1] C. E. Frank, *Chemical Reviews* **1950**, *46*, 155.
- [2] S. Schiesser, T. Pfaffeneder, K. Sadeghian, B. Hackner, B. Steigenberger, A. S. Schröder, J. Steinbacher, G. Kashiwazaki, G. Höfner, K. T. Wanner, C. Ochsenfeld, T. Carell, *J. Am. Chem. Soc.* **2013**, *135*, 14593.
- [3] F. L. Zott, V. Korotenko, H. Zipse, *ChemBioChem* **2022**, *23*, e202100651.
- [4] F. Gugumus, *Polym. Degrad. Stab.* **1998**, *62*, 403.
- [5] L. Sandhiya, H. Zipse, *Chem. Eur. J.* **2015**, *21*, 14060.
- [6] J. Bolland, *Proc. Math. Phys. Eng. Sci.* **1946**, *186*, 218.
- [7] C. J. Cramer, D. G. Truhlar, *Chemical Reviews* **1999**, *99*, 2161.
- [8] M. Frisch, G. Trucks, H. B. Schlegel, G. E. Scuseria, M. A. Robb, J. R. Cheeseman, G. Scalmani, V. Barone, B. Mennucci, G. Petersson, *Inc., Wallingford CT* **2009**, 201.
- [9] S. Grimme, J. Antony, S. Ehrlich, H. Krieg, *J. Chem. Phys.* **2010**, *132*, 154104.
- [10] A. V. Marenich, C. J. Cramer, D. G. Truhlar, *J. Phys. Chem. B* **2009**, *113*, 6378.
- [11] V. Korotenko, <https://github.com/vnkorotenko/ess>.
- [12] V. Korotenko, <https://github.com/vnkorotenko/ccs>.
- [13] G. Luchini, J. V. Alegre-Requena, I. Funes-Ardoiz, R. S. Paton, *F1000Research* **2020**, *9*, 291.
- [14] A. Altun, F. Neese, G. Bistoni, *J. Chem. Theory Comput.* **2018**, *15*, 215.
- [15] F. Neese, E. F. Valeev, *J. Chem. Theory Comput.* **2011**, *7*, 33.
- [16] M. Saitow, U. Becker, C. Riplinger, E. F. Valeev, F. Neese, *J. Chem. Phys.* **2017**, *146*, 164105.
- [17] A. Altun, F. Neese, G. Bistoni, *Beilstein J. Org. Chem.* **2018**, *14*, 919.
- [18] G. Gryn'ova, J. L. Hodgson, M. L. Coote, *Org. Biomol. Chem.* **2011**, *9*, 480.

6. Appendix

6.1. Conformational Analysis Tools

Energy sorting script (ESS)

The Energy Sorting Script allows you to discard unnecessary calculation results, **possibly** containing repeating structures using energy criterion ($\Delta E_{\text{tot}} > 10^{-7}$ a.u. by default).

Options	
-7	Etot criterion 0.0000001 a.u. (by default)
-6	Etot criterion 0.000001 a.u.
-5	Etot criterion 0.00001 a.u.
-4	Etot criterion 0.0001 a.u.
-3	Etot criterion 0.001 a.u.
-z	Zero criterion 0 a.u.
-c	To enter your Etot criterion manually (0.0000001 a.u. by default)
-s	To enforce singlet output: $\langle S^2 \rangle = 0.0000$
-lm	Search for local minima (by default)
-ts	Search for transitional states
-a	You need all files in the list (without any exclusion)
-H298	Sort by H298
-G298	Sort by G298

The general algorithm of ESS includes the following steps¹

- 1) Extraction of the most important data from a list of Gaussian-log files: filename, ZPE1, $\delta H.1$, $\delta G.1$, E_{tot} , $\langle S^2 \rangle$, 1-st frequency. Check, if 1-st frequency > 0 .
- 2) Sorting the list of extracted data in ascending order of E_{tot} .
- 3) Comparison by E_{tot} . Each log-file will be compared with the previous one by E_{tot} using the following criterion: If $\Delta E_{\text{tot}} > 10^{-7}$ Hartree (by default) then it makes sense to consider this file. Otherwise: the current file is most likely a “replicant/duplicate”, **possibly** containing the same structure as in previous file.

Benefits:

- Allows you to reduce the number of conformers in the list quickly

Disadvantages:

- The “replicant” structures can still be presented in the list, because this analysis does not take into account geometry:

First example: Geometries can be almost the same, but have slightly different energies due to the difference in the number of geometry-convergence steps or in the number of SCF steps.

The second example: a radical particle with the same geometry can have two different wave functions that differ greatly in energy.

- Loss of structures (which is very rare, but possible) with a high conformational lability of the molecule: two different conformers can have almost the same energy (with a difference of less than ΔE_{tot} criterion). In this case, the structure will be eliminated from the list.

Centroid comparison script (CCS)

The analysis of certain interatomic distances and visualization of geometry is widely used by chemists all over the world. However, when it comes to a large number of structures and the search for individual conformations among them, "manual" methods take a lot of time and do not exclude human error.

The Centroid Comparison Script allows you to discard unnecessary xyz-files or Gaussian log-files, **possibly** containing repeating structures comparing geometries by distances between each atom and centroid point.² CCS is applicable only in chemistry, but wherever it comes to searching for individual geometries (just need to change the length units and criterion). (Figure 1 and 2)

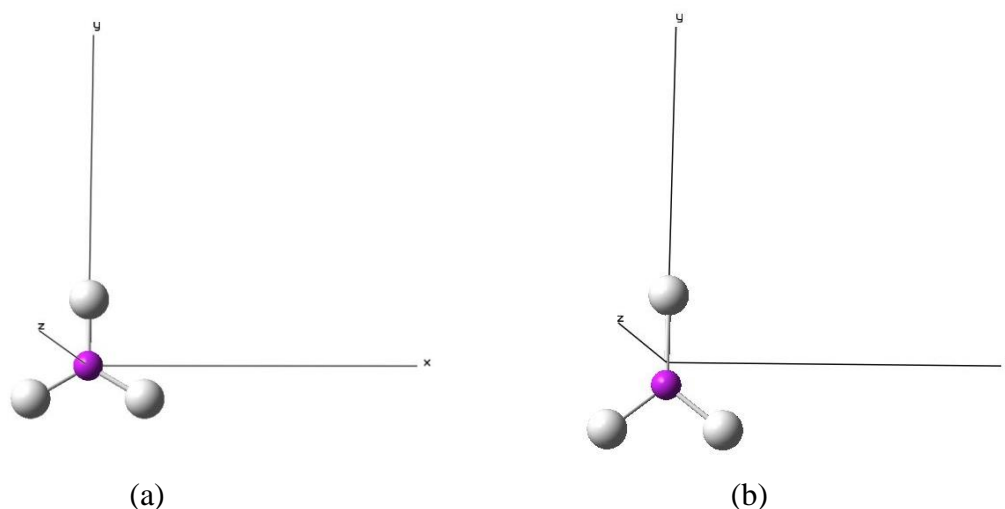


Figure 1. Equilateral (a) and Isosceles triangles (b). The lines correspond distances between triangle-vertices (gray points) and centroid (purple point).

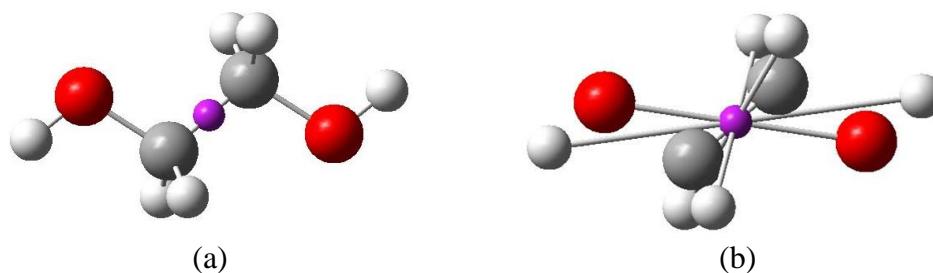


Figure 2. Ethylene glycol molecule. The lines correspond to (a) covalent bonds and (b) distances between atoms and centroid (purple point).

Algorithm/Principle	Data	General options:
Full Combinatoric Comparison	unsorted sorted	<u>xyz/log files:</u> ccs -f (Most accurate/expensive)
Restricted Combinatoric Comparison Based on Geometry Expansion	unsorted sorted	<u>xyz/log files:</u> ccs -r ccs -u ccs (default for unsorted) (Very accurate/less expensive)
Geometry Expansion Comparison	unsorted sorted	<u>xyz/log files:</u> ccs -e
Center of Mass vs. Centroid Comparison	unsorted sorted	<u>xyz/log files:</u> ccs -cmc ccs -schwerpunkt
Sorted Geometries Comparison	sorted	1) <u>xyz/log files:</u> create your own “.ccs” input-list file, where the geometries are sorted as you want (by any property). Each geometry will be compared to the previous one ccs ccs -s 2) <u>log files:</u> comparison of energy-neighboring geometries (just a special case). In this case, ESS will generate an input-list ess;ccs ess -(option);ccs -(option)

Other options:	
-nproc	number of parallel processes (1 by default; RCC,GEC)
-dl	enter your Δ -length criterion (0.015 Å by default)
-dlh	enter your Δ Expansion (Δ -lhash) criterion (0.001 Å by default per atom)
-rm	to remove relpicants after analysis! Be carefull
-symm	You have a symmetric molecule/system (at. num. is NOT important by default)
-nosymm	You have an asymmetric molecule/system (at. num. is important by default)
-num	(at. num. is important by default)
-nonum	(at. num. is NOT important by default)

Full combinatoric comparison

1) Reading of the Geometry from each xyz/log file (**G** - matrix). The number of atoms **n** must be the same in all files

$$\mathbf{G} = \begin{bmatrix} x_1 & y_1 & z_1 \\ \dots & \dots & \dots \\ x_i & y_i & z_i \\ x_n & y_n & z_n \end{bmatrix}$$

2) Calculation of Centroid point $C(x_c; y_c; z_c)$ for each geometry:

$$x_c = \frac{\sum_{i=0}^n x_i}{n}$$
$$y_c = \frac{\sum_{i=0}^n y_i}{n}$$
$$z_c = \frac{\sum_{i=0}^n z_i}{n}$$

and definition of **C** – matrix with **n** lines for each geometry:

$$\mathbf{C} = \begin{bmatrix} x_c & y_c & z_c \\ \dots & \dots & \dots \\ x_c & y_c & z_c \\ x_c & y_c & z_c \end{bmatrix}$$

3) Calculation of **L** – matrix for each geometry, which contains «xyz-components of the absolute distance l_i from i th atom to the C_{xyz} point ($i=1$ to n):

$$\mathbf{L} = \mathbf{G} - \mathbf{C} = \begin{bmatrix} x_1 & y_1 & z_1 \\ \dots & \dots & \dots \\ x_i & y_i & z_i \\ x_n & y_n & z_n \end{bmatrix} - \begin{bmatrix} x_c & y_c & z_c \\ \dots & \dots & \dots \\ x_c & y_c & z_c \\ x_c & y_c & z_c \end{bmatrix} = \begin{bmatrix} l_1^x & l_1^y & l_1^z \\ \dots & \dots & \dots \\ l_i^x & l_i^y & l_i^z \\ l_n^x & l_n^y & l_n^z \end{bmatrix}$$

This equation is equivalent to the translation of the molecule, leading to the alignment of the centroid with the origin $C_{xyz}(0;0;0)$

In other words, **L** – matrix contains the difference in the coordinates of each atom x_i, y_i, z_i ($i=1$ to n) and coordinates the C_{xyz} point:

$$l_i^x = x_i - x_c$$
$$l_i^y = y_i - y_c$$
$$l_i^z = z_i - z_c$$

Which is needed to calculate the distances between each atom and the centroid point

$$l_i = \sqrt{(l_i^x)^2 + (l_i^y)^2 + (l_i^z)^2}$$

And to define the **l** – column-matrix

$$\mathbf{l} = \begin{bmatrix} l_1 \\ \dots \\ l_i \\ l_n \end{bmatrix}$$

4) Calculation of $\Delta\mathbf{l}$ – column-matrices: $\Delta\mathbf{l}_j = |\mathbf{l}_j - \mathbf{l}_{ref}|$, where j is the geometry number ($j=2$ to N , N is the number of geometries). \mathbf{l}_{ref} corresponds to the first structure in the **list**, which is individual by default. This structure will be used as a reference, with which all the other $N-1$ structures will be compared

$$\Delta \mathbf{l}_j = \left| \begin{array}{c} [l_1] \\ \dots \\ [l_i] \\ [l_l]_j \end{array} - \begin{array}{c} [l_1] \\ \dots \\ [l_i] \\ [l_l]_{ref} \end{array} \right| = \begin{array}{c} [\Delta l_1] \\ \dots \\ [\Delta l_i] \\ [\Delta l_l]_j \end{array} \text{ (Lenght Change)}$$

$\Delta \mathbf{f}_j$ – column-matrices will be computed sequentially for $N - 1$ geometries in the **list**.

5) Geometry-individuality criterion. Each considered j-th geometry will be compared with the reference geometry using the following criterion: If at least one element of the $\Delta \mathbf{l}_j$ is > 0.02 Angström, then the j-th geometry can be considered different from the reference and it will be added to the **new list** for the **next iteration**) Otherwise: the j-th geometry is a “replicant” of the reference geometry. Start **next iteration** including steps 4 and 5 using **new list**. **Iterate** until the **new list** has >1 geometries. If only 1 **last** geometry is left in the **new list**, this is the **last individual**. Thus, the number of **iterations** will be equal to the number of individuals in total.

Restricted combinatoric comparison based on geometry expansion

1) See Full Combinatoric Comparison

2) See Full Combinatoric Comparison

3) **Modification:** Additionally, Geometric Expansion value will be calculated **for each geometry**

$$l_{hash} = \sum_{i=0}^n l_i$$

4) **Modification:** Structures in the **list** should be ranked in ascending order of their Geometric Expansion (l_{hash} value). $\Delta \mathbf{f}_j$

Calculation of $\Delta \mathbf{l}$ – column-matrices: $\Delta \mathbf{l}_j = |\mathbf{l}_j - \mathbf{l}_{ref}|$,

Only if $\Delta l_{hash_j} = |l_{hash_j} - l_{hash_{ref}}| < 0.01$ Angström (per atom); Otherwise: geometries are too different and no comparison is needed.

5) See Full Combinatoric Comparison

Restricted combinatoric comparison based on RMSD

Modification: Structures in the **list** should be ranked in ascending order of their RMSD value

Not robust to change of atomic numeration

Not robust/efficient for a symmetrical system or system which consists of symmetrical elements, for example:

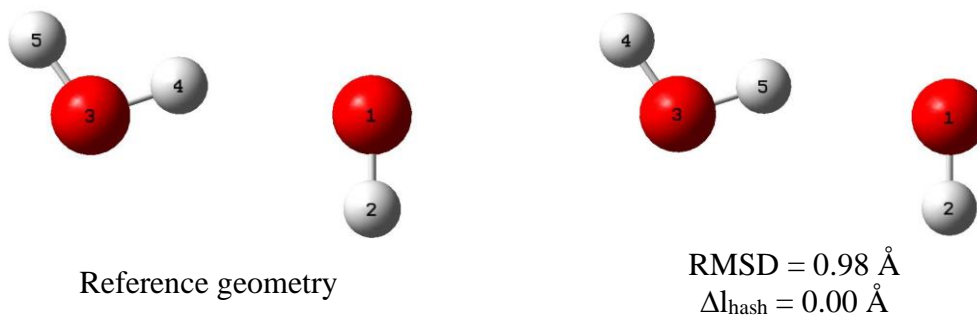


Figure 3. Comparison of RMSD and ΔI_{hash} : application to HO•..HOH complex.

Geometry expansion comparison

“Rearranging the positions of the terms does not change the sum”

Algebra

This option would be suitable if:

- you want to analyze xyz files (the energy is unknown)
- you want to analyze log files without the ESS analysis first.

In this case, CCS will compare geometries by the sum of all distances (l_{hash} value). The Algorithm of CCS includes the following steps²

- 1) Reading of the Geometry from each xyz/log file (**G** - matrix). The number of atoms **n** must be the same in all files
- 2) Calculation of Centroid point **C** ($x_c; y_c; z_c$) **for each geometry**
- 3) Calculation of the **I** – column-matrix and its l_{hash} value **for each geometry**

$$l_{hash} = \sum_{i=0}^n l_i$$

- 4) Calculation of Δl_{hash_j} – values: $\Delta l_{hash_j} = |l_{hash_j} - l_{hash_{j-1}}|$, where j is the geometry number ($j = 2$ to N , N is the number of geometries). Δl_{hash_j} –values will be computed sequentially for $(N - 1)$ geometries ranked in ascending order of their l_{hash} value.

- 5) Geometry-individuality criterion. Each considered j -th geometry will be compared with the previous one j -th geometry using the corresponding Δl_{hash_j} –value and the following criterion: If $\Delta l_{hash_j} > 0.001$ Angström (per atom), then the j -th geometry is considered different from the previous one and, therefore, “individual”. Otherwise: the j -th geometry is a “replicant” of j -th geometry.

Sorted geometries comparison

To start, you need to create a “.ccs” input-list file, where the geometries are sorted as you want (by any property). If you want to make a comparison of energy-neighboring geometries, you need a special input-list, where the geometries are sorted by energy. Such a list can be created using ESS.

In this case, the algorithm of CCS includes the following steps

- 1) Reading of the Geometry from each xyz/log file (**G** - matrix). The number of atoms **n** must be the same in all files
- 2) Calculation of **C** – matrix **for each geometry**
- 3) Calculation of **I** – column-matrices
- 4) Calculation of $\Delta \mathbf{I}$ – column-matrices: $\Delta \mathbf{I}_j = |\mathbf{I}_j - \mathbf{I}_{j-1}|$, where j is the geometry number ($j = 2$ to N , N is the number of geometries). Matrices will be computed sequentially for $(N - 1)$ geometries.
- 5) Geometry-individuality criterion. Each considered j -th geometry will be compared with the previous one j -th geometry using the following criterion: If at least one element of $\Delta \mathbf{I}_j$ is > 0.05 Angström, then the j -th geometry can be considered different from the previous one and, therefore, “individual”. Otherwise: the j -th geometry is a “replicant” of previous geometry.

Benchmark

If all the structures you are considering are individual, using formula $C_N^k = \frac{N!}{(N-k)! \cdot k!}$ known from combinatorics, one can estimate the number of geometry-comparisons that occur in the full method ($k=2$ and N is the number of files ($k \leq N$)).

Let's take a look at a set of geometries of the same system with the same number of atoms. A set of **random**-generated geometries usually contains 100% «individuals» and 0% «replicants». In practice, the percentage of «individuals» after geometry optimization, will decrease, but how much depends on the system (size; whether it is symmetrical or consists of symmetrical elements). In this example, the percentage in „**optimized**” of "individuals" \approx 40-50%, depending on the number of geometries considered.

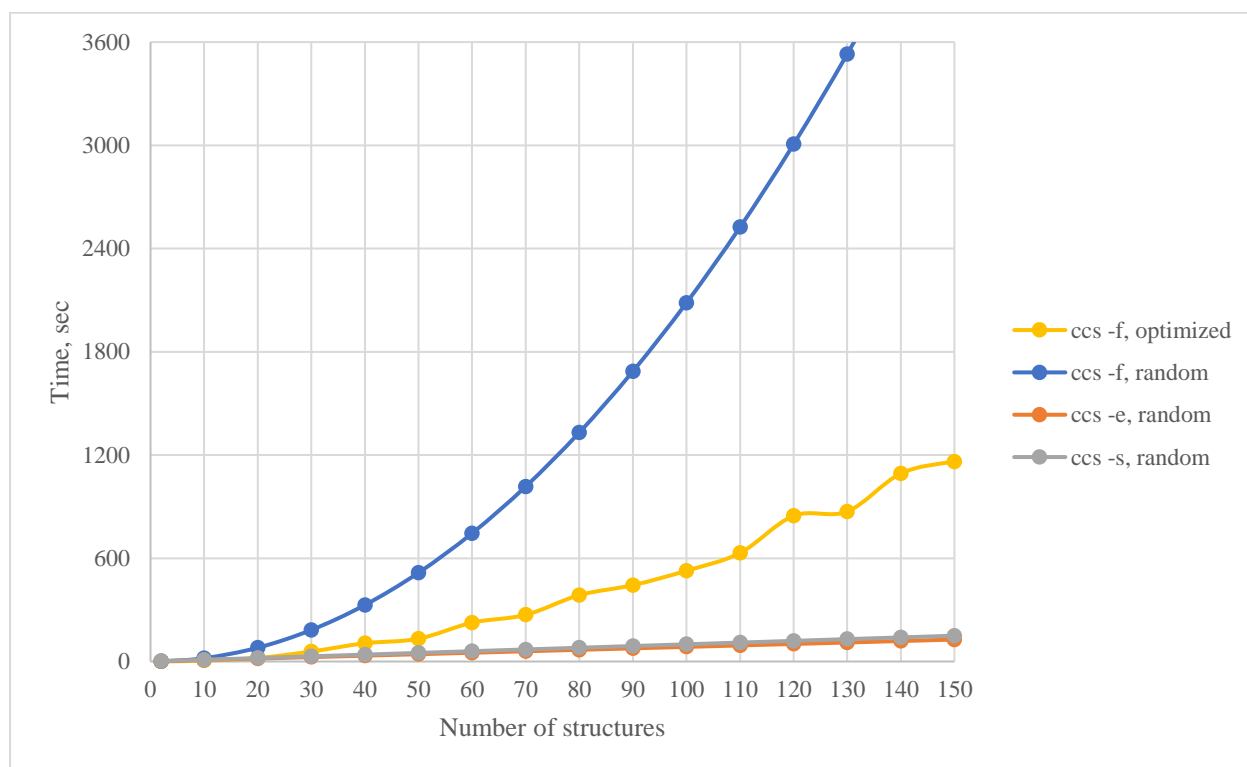


Figure 4. Benchmark for ccs. Time is proportional to:

Time (ccs -f) \propto number of atoms, number of geometry-comparisons.

Time (ccs -r) \propto number of atoms, number of geometry-comparisons.

Time (ccs -e) \propto number of atoms, number of geometries.

Time (ccs -s) \propto number of atoms, number of geometries.

In case of large molecules, to decrease the time of calculation it is recommended to decrease the the number of atoms: create a list of atoms which you want to analyze “any_name.atoms”

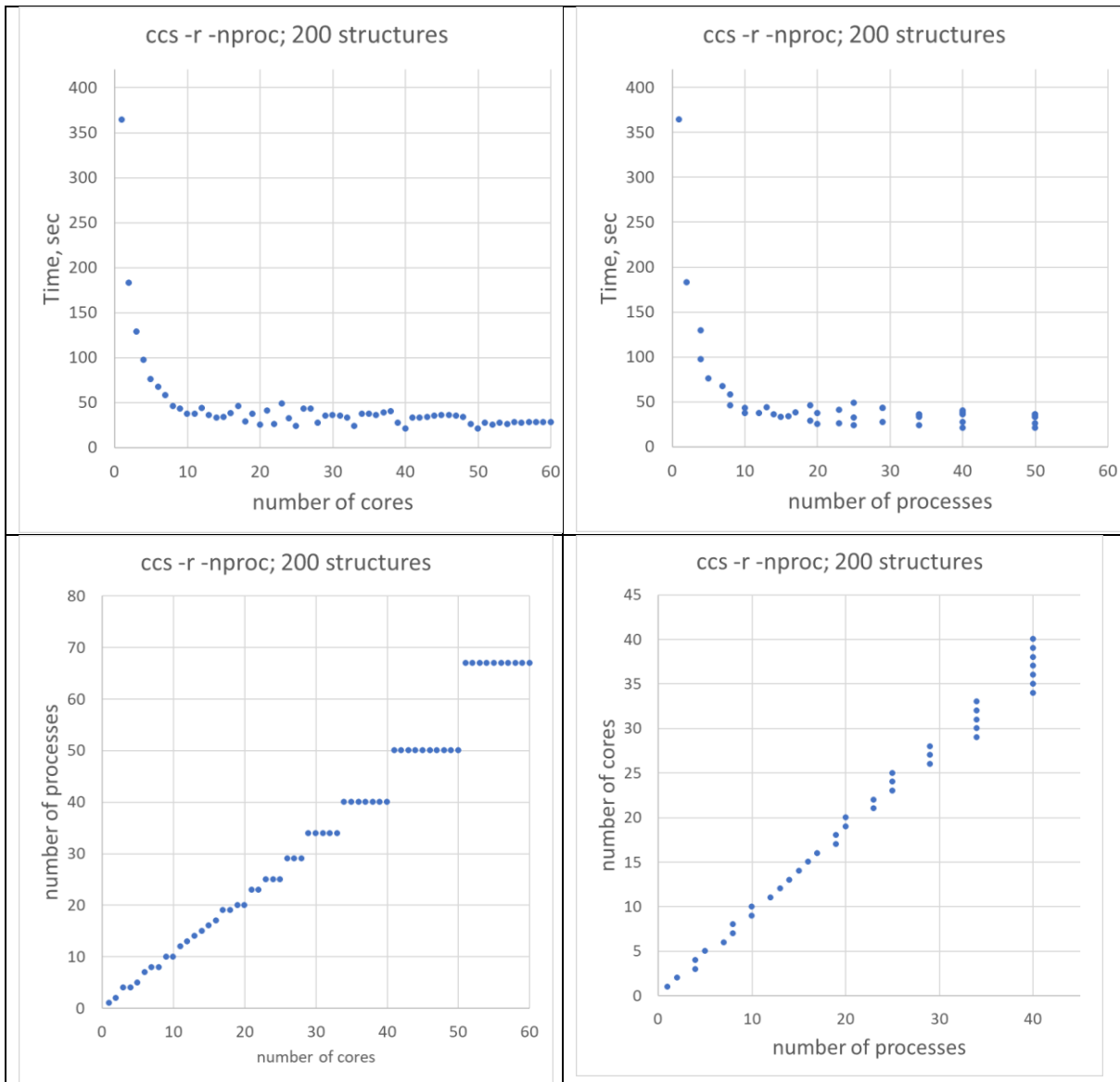


Figure 5. Multitasking Benchmark with 200 structures

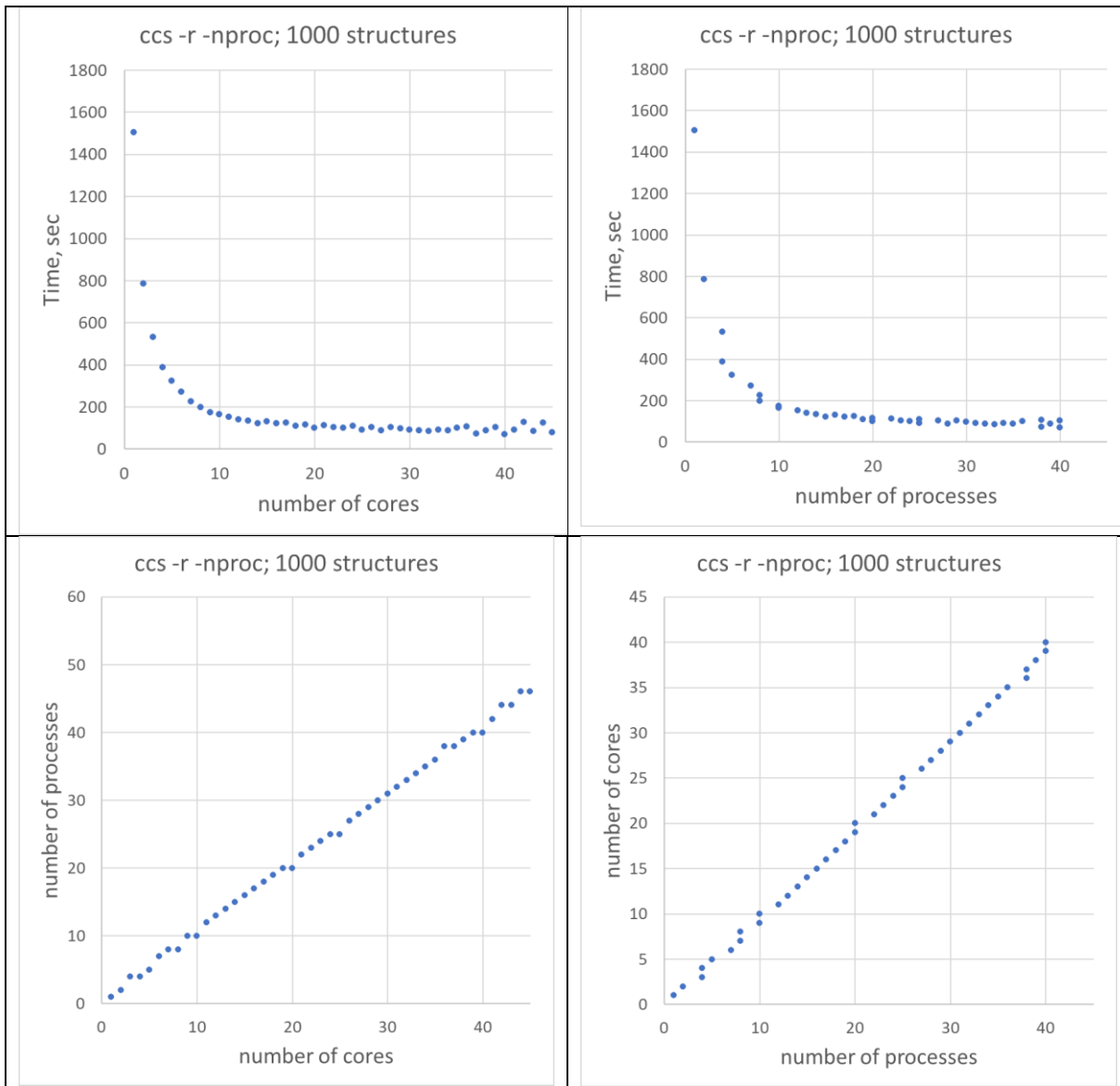


Figure 6. Multitasking Benchmark with 1000 structures

Strategy of stochastic conformational search

Sometimes we wonder how to generate random structures (intermolecular dimers, trimers, etc.) and make a stochastic conformational search.³⁻⁵ Here I will briefly describe the methodology of stochastic conformational search using a dimeric system (1 substrate molecule + 1 water molecule) as example

- 1) open or draw your molecule in GV5/GV6 and add one water molecule
- 2) save the geometry as example.com file
- 3) add "1" after coordinates of second atom
launch /scr7/vasily/scripts/kick/pre_kick_dimer
and enter the number of atoms in the second molecule: 3
- 4) open the generated example_kick file as text, select all, copy and past to "Input XYZ coordinates" WINDOW in the <https://kick.science/KICK.html> web-page
- 5) use these parameters:

DISTANCE PARAMETER:	2.4 (ANGSTROM)
NUMBER OF NEW FILES:	20
MINIMAL DISTANCE:	2.0 (ANGSTROM)
NUMBER OF FRAGMENTS:	1

- 6) click the " GENERATE " button
- 7) Save the generated kick.xyz file as example_kicked in the same folder as the example.com
- 8) Start DFT-optimization and frequencies calculation with
/scr7/vasily/scripts/kick/kick_b3lyp-D3_6-31+Gdp

Data analysis AFTER the calculations:

- 9) sep -n 2
- 10) cd normal
- 11) 'ess' command
- 12) 'ccs' command

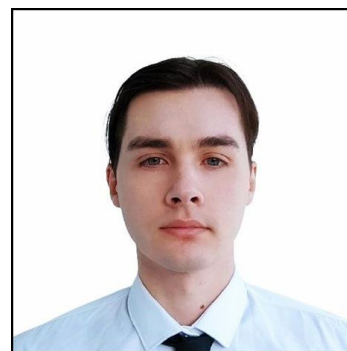
References

- [1] V. Korotenko. <https://github.com/vnkorotenko/ess>.
- [2] V. Korotenko. <https://github.com/vnkorotenko/ccs>.
- [3] D. Šakić, M. Hanževački, D. M. Smith, V. Vrček, *Org. Biomol. Chem.* **2015**, *13*, 11740.
- [4] D. Šakić. <https://kick.science/KICK.html>.
- [5] M. Saunders, *J. Comput. Chem.* **2004**, *25*, 621.

Curriculum Vitae

Personal Details

Name Vasilii Korotenko
Born 25 January 1994
ORCID iD 0000-0002-2045-2536
Mail (office) vakoch@cup.uni-muenchen.de
Tel. (office) +49 89 2180 77741



Education

- 01.2019–present** **Ph.D. in computational chemistry**
Ludwig-Maximilians-Universität München, Group Prof. Zipse, SFB 1309
Ph.D. thesis: «Oxidation of Modified DNA Nucleobases: Computational Study»
- 09.2016–08.2018** **Master of science in theoretical and experimental chemistry**
Mendeleev University Moscow, Group Prof. Tsirelson
Master thesis: «The electron gas pressure distribution in serine: neutral molecule, zwitterion, cluster, experimental crystal»
Grade point average: 1.5 (excellent)
- 09.2012–08.2016** **Bachelor of science in chemistry**
Mendeleev University Moscow, Group Prof. Tsirelson
Bachelor thesis: «Quantum chemical study of intramolecular non-covalent interactions in the conformers of neutral serine and its zwitterion»
Grade point average: 1.3 (excellent)

Professional Experience

- 09.2018–present** **Research Assistant**
Ludwig-Maximilians-Universität München, Group Prof. Zipse
Project SFB 1309: «Chemical Biology of Epigenetic Modifications»
HPC system administrator: support, management, hardware, software
Assistance in teaching activities (lab)
- 05.2015–08.2018** **Research Assistant**
Mendeleev University Moscow, Group Prof. Tsirelson
Project «Discrete structural model of a crystal with explicit representation of information on chemical bonding»
HPC system administrator: support, management, hardware, software
Assistance in teaching activities
- 04.2014–04.2015** **Research Assistant**
Mendeleev University Moscow, analytical chemistry department
Assistance in teaching activities (lab)

Further Education

- 04.2019** Course “BayBioMS meets SFB: proteomics for epigenetics”, TU Munich
- 11.2017–05.2018** B1-C1 German courses at the AStA Heinrich Heine University, Düsseldorf (Germany)
- 02.2018–03.2018** Practical workshop „Simulation von Biomolekülen“, Heinrich Heine University, Institut für Theoretische Chemie und Computerchemie, Düsseldorf (Germany)
- 09.2017–11.2017** Practical workshop „Molecular dynamics“, Moscow State University, Laboratory of chemical cybernetics, Moscow (Russia)

Skills

1. Languages Spoken: English, German, Russian, Ukrainian
2. Developer. Energy Sorting Script (ESS). 2020
<https://github.com/vnkorotenko/ess>
3. Developer. Centroid Comparison Script (CCS). 2020
<https://github.com/vnkorotenko/ccs>
4. Tester. “kick” script based on the stochastic search procedure. 2020
<https://kick.science/KICK.html>
5. Programming languages: Python, MATLAB, VBA, Java, C++.
6. Machine learning / neural networks: TensorFlow/Keras, PyTorch, SKLearn.
7. Python libraries: NumPy, Matplotlib, Seaborn, Pandas, RDKit, SciPy, MDAnalysis
8. Computational chemistry software: Gaussian, ORCA, Molpro, Psi4, GAMESS, Firefly, NAMD, VMD, GROMACS, CPMD, USPEX, Quantum ESPRESSO, WinXPRO, Multiwfn, HyperChem, Promolden, AIMAll, AIM2000.
9. Graphical Software: PyMOL, VMD, ChemCraft, Avogadro, Blender, Mercury, ChemDraw
10. Other: Linux, SLURM, Git, BitBucket, Jira, MS Office, LaTeX, SQL, MongoDB

Publications:

F. Zott, V. Korotenko, H. Zipse «The pH-Dependence of the Hydration of 5-Formylcytosine-an Experimental and Theoretical Study» *ChemBioChem* 2021

V. Korotenko, H. Zipse « The Stability of Oxygen-Centered Radicals and its Response to Hydrogen Bonding Interactions» *J. Comp. Chem.* 2023

V. Korotenko, F. Zott, H. Zipse «The Acid-Base Equilibrium and C-H Bond Dissociation Energies of Modified Pyrimidine DNA Bases: The Influence of the Hydrate Form of 5fC» *J. Phys. Chem.* 2023

A. Kastrati, A. Kremsmair, A. S. Sunagatullina, V. Korotenko, Y. C. Guersoy, S. K. Rout, F. Lima, C. E. Brocklehurst, K. Karaghiosoff, H. Zipse, P. Knochel «Calculation-Assisted Regioselective Functionalization of the Imidazo[1,2-a]pyrazine Scaffold via Zinc and Magnesium Organometallic Intermediates» *Chem. Sci.* 2023

Conference presentations:

1. 3rd International Conference on Hydrogen Atom Transfer iCHAT 2022
«The Stability of Oxygen-Centred Radicals and its Response to Hydrogen Bonding Interactions»
2. International Congress of Young Scientists in Chemistry and Chemical Technology 2018
«The features of atomic interactions in serine in terms of the components of local electron pressure»
3. International Congress of Young Scientists in Chemistry and Chemical Technology 2017
Topic 1: «Non-Covalent Interactions in the Glutamic Acid Diamide Molecule According to Quantum-Chemical Calculations».
Topic 2: «Intramolecular electron gas pressure in serine: zwitterion, cluster, crystal»
4. International Congress of Young Scientists in Chemistry and Chemical Technology 2016
«Noncovalent interactions in neutral serine conformers by quantum chemical methods»
5. International Congress of Young Scientists in Chemistry and Chemical Technology 2015
«Analysis of intramolecular noncovalent interactions in DL-serine crystal: combined application of quantum chemical calculations and accurate x-ray diffraction method»
6. International Congress of Young Scientists in Chemistry and Chemical Technology 2014
«Potential energy surface and intramolecular noncovalent interactions in serine molecule»
7. International Congress of Young Scientists in Chemistry and Chemical Technology 2013
«Quantum-chemical modelling of the solvated L-serine molecule»
8. Modern Methods in Theoretical and Experimental Electrochemistry: conference — Plyos 2013
«Chemical and phase composition of Fe-Mo sediments obtained by electrodeposition from ammonium citrate solutions»